2005

Molecular mechanisms of PKC[delta] in neurotoxin-induced apoptotic death of nigral dopaminergic neurons: relevance to the pathogenesis of Parkinson's disease

Yongjie Yang
Iowa State University

Molecular mechanisms of PKCδ in neurotoxin-induced apoptotic death of nigral dopaminergic neurons: Relevance to the pathogenesis of Parkinson's disease

by

Yongjie Yang

A dissertation submitted to the graduate faculty

in partial fulfillment of the requirements for the degree of

DOCTOR OF PHILOSOPHY

Co-majors: Neuroscience; Genetics

Program of Study Committee:
Anumantha G. Kanthasamy, Co-major Professor
Kristen Johansen, Co-major Professor
Donald S. Sakaguchi
Richard J. Martin
Susan Carpenter

Iowa State University

Ames, Iowa

2005

Graduate College

Iowa State University

This is to certify that the doctoral dissertation of

Yongjie Yang

has meet the dissertation requirements of Iowa State University

Signature was redacted for privacy.

Co-major Professor

Signature was redacted for privacy.

Co-major Professor

Signature was redacted for privacy.

For the Co-major Program

Signature was redacted for privacy.

For the Co-major Program

TABLE OF CONTENTS

ABSTRACT

We investigated the molecular role of the delta isoform of protein kinase C (PKCδ) in toxicity induced by the Parkinsonian toxin MPP^+. We also examined the role of PKCδ in apoptotic death induced by the potential Parkinson's disease (PD) risk factor dieldrin in rat mesencephalic dopaminergic neuronal (N27) cells and in the primary mesencephalic neuronal model. Both the protein and mRNA levels of PKCδ were selectively higher in the dopaminergic neurons in the substantia nigra (SN) region as compared to the cortex, brainstem, and striatum regions of rodent brains. PKCδ protein co-localized with tyrosine hydroxylase (TH), the rate-limiting enzyme responsible for dopamine synthesis in dopaminergic neurons. siRNA designed against PCKδ effectively silenced the expression of PKCδ and reduced dieldrin or MPP^+-induced apoptotic death of N27 cells and degeneration of primary dopaminergic neurons. Following dieldrin exposure in (N27) cells, we determined that the full-length PKCδ is first cleaved in the cytoplasm, and the activated PKCδ catalytic fragment subsequently translocates into the nucleus. The caspase-3 specific inhibitor (Z-DEVD-FMK), the cleavage resistant mutant of PKCδ (PKCδ-CRM), as well as the nuclear localization signal (NLS) deletion mutant of PKCδ (PKCδ-ΔNLS) all abolished the nuclear translocation of activated cleaved PKCδ. The proteolytic activation of full-length PKCδ and subsequent nuclear translocation of activated cleaved PKCδ are integral events required for PKCδ's pro-apoptotic function in apoptotic death of dopaminergic neuronal cells. Blockade of proteolytic activation of endogenous PKCδ by PKCδ-CRM also protected primary mesencephalic dopaminergic neurons from MPP^+-induced degeneration. Moreover, we demonstrated that activated cleaved PKCδ mediates Ser14 phosphorylation of histone

H2B followed by its nuclear translocation in apoptotic dopaminergic neuronal cells. Ser14 phosphorylation of H2B and apoptosis can also be directly induced by the catalytic fragment of PKCδ (PKCδ-CF), but not by the regulatory fragment of PKCδ (PKCδ-RF), PKCδ-CRM, PKCδ-ΔNLS, or the dominant-negative mutant of PKCδ (PKCδ-DN). Transfection of PKCδ-CF also directly induced degeneration of primary mesencephalic dopaminergic neurons while PKCδ-RF-transfected primary neurons remained intact. In addition, we also demonstrated that the N- and the C-terminals of PKCδ are in close proximity in the tertiary structure, as demonstrated by fluorescence resonance energy transfer (FRET). By employing the C1 or C2-like domain deletion mutant of PKCδ (PKCδ-ΔC1 or PKCδ-ΔC2), we showed that deletion of the C2-like domain, but not the C1 domain, induces strong nuclear localization of PKCδ. The exogenously expressed catalytic fragment of PKCδ (PKCδ-CF) also primarily localizes to the nucleus. Sequence analysis of the C2-like domain reveals a possible leucine-rich nuclear export signal (NES); however, the C2-like domain is not sensitive to the nuclear export inhibitor leptomycin B (LMB), suggesting that this leucine-rich motif is not a functional NES. Moreover, the C2-like domain alone was fused to the N-terminal of a NES mutated form of Rev protein, the RNA binding protein of Equine Infectious Anemia Virus (EIAV), to generate the Rev chimera. Interestingly, the Rev chimera with the C2-like domain is still primarily localized in the nucleus. Thus, the N-terminal C2-like domain apparently regulates the subcellular localization of PKCδ by masking the C-terminal NLS through the position obstacle in the tertiary structure, but not through NES or interaction with anchoring proteins. Taken together, our studies show that i) the novel PKC isoform family member PKCδ is highly expressed in nigral dopaminergic neurons, ii) PKCδ mainly

localizes in the cytoplasm by the position obstacle effect of the C2-like domain to the NLS, iii) neurotoxin exposure induces proteolytic activation of full-length PKCδ and subsequent nuclear translocation of the PKCδ cleaved fragment to cause histone H2B phosphorylation and apoptotic cell death, and iv) RNAi mediated suppression of PKCδ protects dopaminergic neurons against neurotoxic insults.

CHAPTER I: GENERAL INTRODUCTION

Dissertation Organization

This dissertation is written in an alternative dissertation format. It contains a general introduction, four research papers, a general conclusion, and an acknowledgement. The list of references cited is included at the end of each chapter. Chapter I, the general introduction, includes research objectives, background and literature review of my research subjects. Chapter II, "Suppression of caspase-3 dependent proteolytic activation of Protein Kinase C δ by small interfering RNA (siRNA) prevents MPP^+-induced dopaminergic degeneration," has been published in *Molecular and Cellular Neuroscience* (**25**: 406-421, 2004). Chapter III, "Proteolytically activated PKCδ translocates to the nucleus and mediates Ser14 phosphorylation of histone H2b in neurotoxin-induced apoptotic death of dopaminergic neuronal cells," Chapter IV, "Nuclear localization of PKCδ is regulated by proximity of N-terminal C2-like domain to the C-terminal nuclear localization signal (NLS)," and Chapter V, "Selectively high expression of oxidative-stress sensitive kinase Protein Kinase C delta (PKCδ) contributes to the vulnerability of nigral dopaminergic neurons to the MPP^+-induced degeneration," will be submitted for publication in *Cell Death and Differentiation*, the *Proceedings of National Academy of Sciences*, and the *Journal of Neuroscience*, respectively. Chapter VI contains the general conclusions.

This dissertation contains the experimental results obtained by the author during his graduate study under the supervision of his major professor, Dr. Anumantha G. Kanthasamy.

Research Objectives

Mechanisms of selective degeneration of nigral dopaminergic neurons in Parkinson's disease (PD) remain unsolved despite the many advances made during the past three decades. Environmental chemical exposure and genetic mutations have both been implicated in the pathogenesis of PD. Mutations in alpha-synuclein, Parkin and DJ genes are some key genetic defects associated with PD. Findings from *in vitro* and *in vivo* models of PD suggest that environmental neurotoxins-induced oxidative stress is one of the initial events that trigger the mitochondrial intrinsic apoptotic pathway in nigral dopaminergic neurons and apoptotic death (Beal, 2002; Dauer and Przedborski, 2003; Jenner, 2003; Olanow and Tatton, 1999). The deleterious nature of the metabolism of free cytosolic dopamine, the specific neurotransmitter employed by the dopaminergic neurons, potentially increases oxidative stress in dopaminergic neurons. The expression levels of several inherent factors involved in the regulation of free cytosolic dopamine levels have been implicated in the vulnerability of dopaminergic neurons (Hirsch et al., 1997; Uhl, 1998). Recent identification of genetic mutations of PTEN induced kinase 1 (PINK1) (Valente et al., 2004) and leucine-rich repeat kinase 2 (LRRK2) (Zimprich et al., 2004) in familial PD patients suggests that kinase might play an important role in the pathogenesis of PD. Our laboratory previously observed that neurotoxin exposure induces oxidative stress and activation of caspase-3 (Anantharam et al., 2002; Kanthasamy et al., 2003; Kitazawa et al., 2003; Yang et al., 2004). The activated caspase-3 further mediates proteolytic activation of protein kinase C delta (PKCδ) and promotes apoptotic death of rat pheochromocytoma (PC12) (Anantharam et al., 2002) and rat mesencephalic dopaminergic neuronal (N27) cells (Kaul et al., 2003; Kitazawa et al., 2003;

Yang et al., 2004). However, the expression level of PKCδ in nigral dopaminergic neurons and its detailed mechanisms in the apoptotic death of dopaminergic neuronal cells, including the localization change of activated PKCδ, downstream events following the activation of PKCδ, and the regulation of the nuclear localization of PCKδ, have not been investigated.

The major objectives of this dissertation are: 1) to determine the protein and RNA level of PKCδ, as well as other PKC isoforms in nigral dopaminergic neurons of rodent brains; 2) to investigate the localization change of the activated cleaved fragments of PKCδ and downstream events in the nucleus following the proteolytic activation of PKCδ; 3) to investigate the regulatory role of the N-terminal regulatory fragment in the nuclear localization of full-length PKCδ; and 4) to develop small interfering (siRNA) and small hairpin RNA (shRNA) against PKCδ as a novel neuroprotective strategy to prevent dopaminergic neurons from neurotoxin-induced degeneration. Taken together, these studies will provide detailed mechanisms for PKCδ's pro-apoptotic functions in the neurotoxin-induced degeneration of dopaminergic neurons and may provide useful insights about the role of kinase in the pathogenesis of Parkinson's disease.

Background and literature review

This section provides background information related to the studies described in the dissertation: (I) Parkinson's disease and its pathogenesis; (II) Vulnerability of Substantia nigra pars compacta (SNc) dopaminergic neurons in Parkinson's disease; (III) Apoptosis in Parkinson's disease; (IV) Involvement of Serine/Threonine protein kinases in the apoptotic

signaling and neurodegenerative diseases; (V) Proteolytic activation and nuclear translocation of serine/threonine protein kinases in apoptosis; (VI) RNA interference (RNAi) and its neuroprotective application in neurodegenerative diseases.

I. Parkinson's disease and its pathogenesis

I-1: Parkinson's disease

The clinical features of Parkinson's disease (PD) were first characterized by James Parkinson in his monograph, "An essay on the shaking palsy" in 1817 (Parkinson, 2002). Currently, Parkinson's disease is one of the most devastating neurodegenerative diseases among elders worldwide. In the U.S., about 2,000,000 individuals have been diagnosed with PD (Shastry, 2001). The incidence rate of PD is estimated at 0.3% among the general population and about 1-2% among the population over 65 in industrialized countries (de Rijk et al., 2000; Rajput, 1992). The prevalence of the disease increases up to 4-5% by the age of 85 (Giasson and Lee, 2001). The higher incidence rate in the elder population implies that aging itself contributes to the pathogenesis of PD. On the other hand, Parkinson's disease also occurs in young people. Rare young-onset PD (YOPD), developing between 21 and 40 years, or juvenile Parkinsonism (JP), with an onset age below 21 years, both have been reported (Paviour et al., 2004).

The major clinical symptoms of PD are characterized as resting tremor, muscular rigidity, bradykinesia, and postural instability. Although dysfunction involved in movement mainly defines this disorder, various non-motor features are also found, including cognitive and psychiatric changes, sleep disturbances, and autonomic dysfunction (Samii et al., 2004). A resting tremor, uncontrollable involuntary shaking of the hand or foot (less common) with

frequency of 3-5 Hz (Samii et al., 2004), is usually considered the first symptom in most PD patients. Tremor is usually asymmetric at disease onset and worsens with anxiety, contralateral motor activity, and during ambulation. Rigidity is the raised resistance noted during passive joint movement that is uniform throughout the range of motion of that joint. Rigidity usually correlates positively with resting tremor, as more pronounced rigidity is found in the more tremulous limb (Samii et al., 2004). Bradykinesia, the most disabling symptom of early Parkinson's disease, results in difficulty with fine motor tasks, such as closing buttons or handwriting, as well as reduced arm swing during walking (Martinez-Martin et al., 1994). Postural instability refers to the gradual development of poor balance, leading to an increased risk of falls. Postural instability is rarely seen in the early stage of PD.

After decades of effort, the underlying pathological changes in Parkinson's disease have been well characterized. Anatomically, the most affected portion of the brain in PD patients is the basal ganglia (Albin et al., 1989). The basal ganglia is a group of functionally related subcortical nuclei that includes the neostriatium (comprised of the caudate nucleus and the putamen), the ventral striatum, the Globus pallidus (GPe and GPi), the subthalamic nuclei (STN), and the substantia nigra pars reticulata or pars compacta (SNr and SNc). The dopaminergic neurons in the SNc normally project to the GABAergic neurons at the striatum (mainly the caudate nucleus and putamen) to form the nigrostriatal circuit. The nigrostriatal circuit and subsequent neuronal circuit among the striatum, thalamus, brain stem, and cortex are further organized into the corticobasal gangliathalamocortical circuits, which critically control voluntary movement (Alexander, 1990). The basal ganglia-thalamocortical circuitry under normal and PD conditions is shown in Figure 1. One of the output pathways of the striatum is the projection of the striatal neurons to the GPi (referred to as the direct pathway)

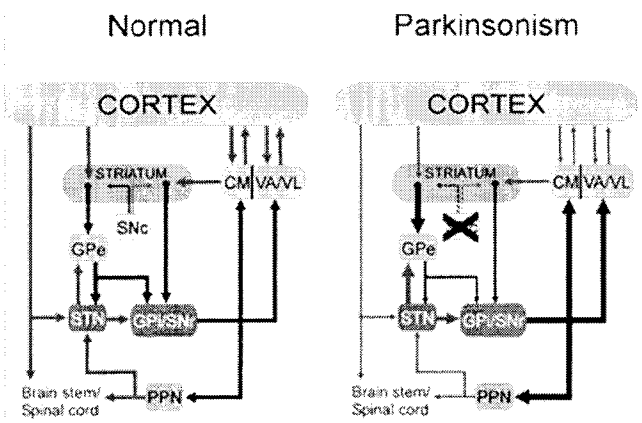

Figure 1. The basal ganglia-thalamocortical circuitry under normal condition and Parkinson's disease (Modified from Wichmann, 2003)

to inhibit GABA release from the GPi to the thalamus. On the other hand, striatial neurons also project to the GPe (referred to as the indirect pathway) to subsequently stimulate the release of GABA from the GPe to the subthalamic nucleus to inhibit glutamate release from the subthalamic nucleus to the SNr. The dopaminergic neurons projected from the SNc to the striatum normally release dopamine that is bound to the dopamine receptors in the postsynaptic GABAergic neurons. Because of the presence of two populations of striatal neurons that contain functionally distinct dopamine receptors, D1 or D2, dopamine apparently has dual roles in the modulation of the activity of basal ganglia output neurons. Dopamine released from SNc dopaminergic neurons excites GABAergic neurons in the striatum to either stimulate through the D1 receptor (in the direct pathway) or inhibit through the D2 receptor (in the indirect pathway) the release of the inhibitory neurotransmitter, GABA. The balance between direct and indirect pathways precisely controls the output of the basal ganglia and is critical to maintain normal motor function (Wichmann and DeLong, 2003).

In the early 1960s, Parkinson's disease was shown to result largely from the degeneration of dopaminergic neurons in the substantia nigra pars compacta (SNc) of basal ganglia (Albin et al., 1989). Later, many other studies consistently characterized the progressive and selective degeneration of dopaminergic neurons in the SNc and the resulting depletion of dopamine in the striatum in PD patients. The depletion of dopamine in the

striatum leads to increased activity in the indirect pathway and decreased activity in the direct pathway (Wichmann and DeLong, 2003). Both of these changes contribute to increased activity in the GPi, which results in the increased inhibition of subsequent thalamocortical and midbrain tegmental neurons and thus, the hypokinetic features of the disease (Kandel et al., 2000). The symptoms usually appear when the loss of dopaminergic neurons in the SNc reaches about 80% (Albin et al., 1989). In addition to the selective degeneration of the dopaminergic neurons in the SNc, formation of Lewy bodies, the intracellular inclusions of abnormal protein aggregation, is another pathological hallmark of Parkinson's disease (Hardy, 2003). Lewy bodies are widely found in many regions of the brain, particularly in the dopaminergic neurons of the SNc, the hypothalamus, the hippocampus, and the autonomic neurons of the esophagus and gastrointestinal tract and occasionally in the cortex (Dauer and Przedborski, 2003). Although the detailed mechanisms are still under intense investigation, the production of excessive misfolded proteins and the compromised ubiquitin-proteasome system are considered to play major roles in the formation of Lewy bodies (Dauer and Przedborski, 2003; Huang et al., 2004). Notably, the formation of the Lewy body is not unique in PD; in fact, Lewy bodies are also commonly found in the postmortem brains of Alzheimer's and several types of dementia patients (Dickson, 2002; Hardy, 2003; McKeith et al., 2003), suggesting that the abnormal protein aggregation in neurons is ubiquitously involved in the pathogenesis of various neurodegenerative diseases.

I-2: Pathogenesis of Parkinson's disease

Unlike the well-characterized pathological changes in PD, the pathogenesis of PD is still largely unclear, though great progress has been made in the past thirty years from studies

of MPTP-induced Parkinsonism and the genetic mutations identified in familial PD patients. Because the incidence rate of PD is higher in the elder population, aging itself has long been considered to play a role in the pathogenesis of PD. In the central nervous system, dopaminergic neurons are mainly distributed in the midbrain, particularly in the SNc region. At birth, the SNc contains approximately 400,000 dopaminergic neurons. As age increases, the number of dopaminergic neurons in the SNc declines, since dopaminergic neurons in the SNc normally degenerate at a rate of 2,400 neurons per year (Marsden, 1990). However, the number of remaining dopaminergic neurons in the SNc prevents the occurrence of PD symptoms when the degeneration process is not abnormally accelerated. Thus, normal aging is certainly associated with PD and is considered one of the risk factors for PD but does not cause this disorder alone (Samii et al., 2004).

I-2-1: Environmental factors in the pathogenesis of PD

The pathogenesis of PD was not understood until the early 1980s. In 1983, Langston and colleagues reported a series of patients who developed acute Parkinsonism after accidental exposure to 1-methyl-4-phenyl-1,2,5,6-tetrahydropyridine (MPTP), a toxic byproduct in the clandestine synthesis of a pethidine analogue (Langston et al., 1984). These patients also showed significant reduction in dopaminergic neuron activity in the basal ganglia, as normally seen in PD patients. Because MPTP-induced Parkinsonism in humans faithfully replicates the pathological features seen in PD patients, mechanisms of MPTP-induced dopaminergic neuron degeneration are under intense investigation. Numerous *in vitro* cell and *in vivo* animal models (including primate) have been created to study the mechanisms of MPTP-induced Parkinsonism (Przedborski and Vila, 2003). All these models

show that dopaminergic neurons are severely degenerated following MPTP exposure and hypokinetic symptoms develop in animals (Speciale, 2002; Vila and Przedborski, 2003).

MPTP itself is non-toxic but can cross the brain-blood barrier to enter the brain when administered to humans and mammals. In the brain, MPTP is converted into 1-methyl-4-phenyl-2,3-dihydropyridinium ($MPDP^+$) by monoamine oxidase (MAO-B) in astrocytes (Markey et al., 1984). The $MPDP^+$ is unstable and spontaneously oxidized to 1-methyl-4-phenylpyridinium (MPP^+) (Dauer and Przedborski, 2003). The MPP^+ is released from astrocytes and selectively taken into dopaminergic neurons in the SNc through dopamine transporter (DAT) due to its similar structure to dopamine (Mayer et al., 1986; Uhl et al., 1985).

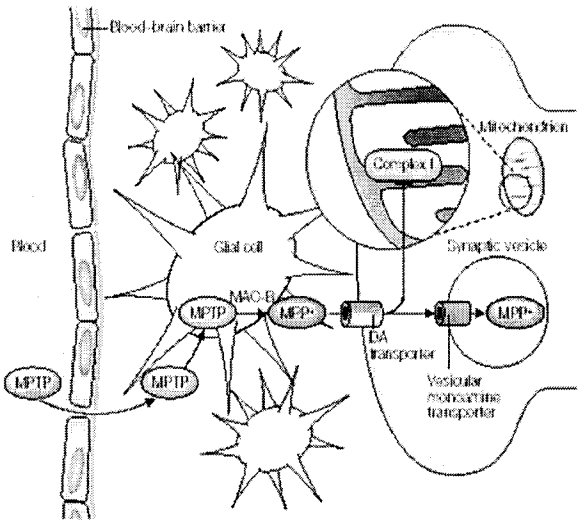

Figure 2. The MPTP model of Parkinson's disease (Modified from Vila, 2003)

Once inside the dopaminergic neuron, MPP^+ is concentrated within the mitochondria by a mechanism that relies on the mitochondrial transmembrane potential, though it can also be sequestered into synaptosomal vesicles by vesicular monoamine transporter 2 (VMAT2) (Liu et al., 1992). MPP^+ impairs oxidative phosphorylation by inhibiting the multi-enzyme complex I of the mitochondrial electron transport chain, which rapidly results in the low production of ATP in the neuron (Greenamyre et al., 2001; Ramsay et al., 1986; Vila and Przedborski, 2003). The decrease in ATP dramatically affects many processes in the neuron. Meanwhile, the MPP^+-induced inhibition of the complex I also induces oxidative stress by hampering the flow of electrons through complex I, which further triggers the mitochondria-

dependent apoptotic pathway (Cassarino et al., 1997; Kaul et al., 2003; Viswanath et al., 2001). MPP^+ can also directly interact with cytosolic enzymes (especially with those carrying negative charges) through its positive charges to interfere with their normal functions (Klaidman et al., 1993). Furthermore, perturbations in Ca^{2+} homeostasis are also observed within hours of MPTP administration in mice (Jackson-Lewis et al., 1995). After these initial events, multiple apoptotic responses are induced in the SNc dopaminergic neurons, including up-regulation of the Bcl-2 family protein Bax (Vila et al., 2001), activation of caspase-9 and -3 (Hartmann et al., 2000; Viswanath et al., 2001), and DNA oxidation-induced activation of pro-apoptic c-Jun N-terminal kinase (JNK) (Saporito et al., 2000; Xia et al., 2001), which eventually promotes the apoptotic death of SNc dopaminergic neurons.

Although studies of MPP^+-induced SNc dopaminergic neuronal degeneration in animal models (including primate) have significantly contributed to our knowledge about the pathogenesis of PD, humans are rarely exposed to MPP^+ (or MPTP), which are not found in the environment. In addition, the MPP^+-induced dopaminergic neuronal degeneration in primates and humans has some features that differ from those observed in PD patients. The most significant pathological difference is that formation of the Lewy body, one of the hallmarks in PD pathology, was not found in MPTP-treated animals (Forno et al., 1993). Nevertheless, the discovery that MPTP causes acute Parkinsonism in humans brings attention to other environmental chemicals possibly involved in the pathogenesis of PD. Because of the observation that MPP^+ strongly inhibits the complex I of mitochondria and induces the elevation of ROS, other complex I inhibitors become candidates of potential risk factors for PD. Interestingly, almost all these complex I inhibitors are also extensively used as herbicides or pesticides, like rotenone, paraquat, and diquat (Jenner, 2001). Animals exposed

to these chemicals all show SNc dopaminergic neuron degeneration and develop PD-like symptoms (Betarbet et al., 2000; Giasson and Lee, 2000; Jenner, 2001; McCormack et al., 2002). In rotenone-exposed rats, formation of the Lewy body in the SNc is also induced (Betarbet et al., 2000). Various case-control studies (Tanner and Ben-Shlomo, 1999; Tanner et al., 1989) also strongly suggest an association between exposure to pesticides and the development of PD. Currently, several other pesticides are also under investigation for their potential role in the pathogenesis of PD. One, dieldrin, is classified as one of the most persistent bioaccumulative and toxic (PBT) chemicals by the US EPA. It is not clear as to whether dieldrin also inhibits mitochondria complex I; however, several studies have indicated that dieldrin exposure is positively associated with the increased incidence of PD. The most supportive piece of evidence is that a significant level of dieldrin was detected in the postmortem brains of PD patients, whereas dieldrin was not found in age-matched control brains (Corrigan et al., 1996; Fleming et al., 1994). In addition, dieldrin exposure depletes dopamine in brains of ducks, rats and ring doves (Heinz et al., 1980; Wagner and Greene, 1978). Furthermore, previous studies from our laboratory and others also showed that dopaminergic cells are more sensitive to dieldrin-induced toxicity (Kitazawa et al., 2001; Sanchez-Ramos et al., 1998). The molecular/cellular mechanisms of dieldrin-induced dopaminergic neuronal degeneration are being investigated in our laboratory.

Besides pesticides, other chemicals are also suggested to be risk factors for PD. Heavy metals, like manganese, copper, iron, lead, and aluminum, have been reported to have a positive association with PD incidence in various etiological studies (Gorell et al., 1997; Kuhn et al., 1998; Paik et al., 1999). Interestingly, smoking, caffeine, and alcohol (not including wine) seem to protect against development of PD, based on case-control studies

(Gorell et al., 1999; Hellenbrand et al., 1996a; Hellenbrand et al., 1996b; Morens et al., 1995). The wide distribution of chemicals, the extensive interaction between different chemicals in the environment, and the exposure of humans to various sources of chemicals make tracking human exposure to environmental chemicals difficult. Furthermore, recognizing the risk of environmental chemicals and their distinct contributions to the pathogenesis of PD remain a challenge.

I-2-2: Genetic mutations in the pathogenesis of PD

Initially, genetic predisposition in the pathogenesis of PD was not fully recognized because most cases of PD are sporadic. An epidemiology study of 20,000 monozygote (MZ) and dizygote (DZ) twins showed that the concordance of PD incidence is similar between MZ and DZ twins, suggesting that genetic predisposition does not play a major role in the pathogenesis of PD (Tanner et al., 1999). However, recent identification of a number of genetic mutations in various genes in familial PD patients implicates a direct pathogenic role of genetic predisposition in PD (Huang et al., 2004). The genes found mutated in familial PD patients (Table 1) include α-synuclein, parkin, ubiquitin carboxyl-terminal hydrolase 1 (UCHL1), DJ-1, PTEN-induced kinase 1 (PINK1), leucine-rich repeat kinase 2 (LRRK2), and several others that have been mapped but not yet cloned (Dawson and Dawson, 2003; Shen, 2004). Among these genes, α-

Gene	Chromosome locus	Gene product	Mode of inheritance
PARK1	4q21.3	a-synuclein	Dominant
PARK2	6q25.2-q27	Parkin	Recessive
PARK3	2q13	Unknown	Dominant
PARK4	4q15	Unknown	Dominant
PARK5	4q14	UCHL1[a]	Dominant
PARK6	1p35-p36	PINK1[b]	Recessive
PARK7	1p36	DJ-1	Recessive
PARK8	12p11.2-q13.1	LRRK2[c]	Dominant
PARK10	1p32	Unknown	Dominant

a. Ubiquitin C-terminal hydrolase L1; b. PTEN-induced kinase 1; c. Leucine-rich repeat kinase 2

Table 1. Genes associated with familial Parkinson's disease patients

synuclein, parkin, and ubiquitin carboxyl-terminal hydrolase 1 (UCHL1) are mainly involved in protein aggregation and the ubiquitin-proteasome system. Other genes, like DJ-1 and PTEN-induced kinase 1 (PINK1), appear to be related to the oxidative stress response. The discovery of genetic mutations in these genes indicates a strong connection between the protein degradation system and oxidative stress in the pathogenesis of PD.

The first gene implicated in the pathogenesis of PD was α-synuclein. It was first identified in a large Italian-American family with autosomal dominant early-onset PD. The missense mutation A53T was found in exon 4 of the gene (Golbe et al., 1990). This mutation was also found in affected members of three Greek families with PD (Polymeropoulos et al., 1997). Since then, different mutations in α-synuclein genes have been identified in different families with PD, including A30P and E46K mutations (Kruger et al., 1998; Zarranz et al., 2004), and triplication of the α-synuclein gene (Singleton et al., 2003). Cellular studies reveal that α-synuclein is concentrated at pre-synaptic terminals, and is an important component of the Lewy body, the major PD pathological hallmark (Spillantini et al., 1997). Although tremendous efforts have been made to characterize α-synuclein's function, its exact physiological function remains unclear (Lotharius and Brundin, 2002). Recent studies with α-synuclein knock-out mice suggest that α-synuclein plays a role in synaptic vesicle cycling (Abeliovich et al., 2000). Cultured hippocampal neurons from these mice were found to have fewer synaptic vesicles than control mice, particularly in the reserve pool (Cabin et al., 2002). These mice also showed defects in synaptic transmission after prolonged, high-frequency stimulation. Other studies suggest that α-synuclein may function like a chaperone-

like protein (Recchia et al., 2004) or regulate gene expression (Baptista et al., 2003; Lindersson et al., 2004).

Yet, the pathogenic function of α-synuclein in PD is much better established. Full-length α-synuclein (140aa) normally is soluble in the cell, but at high concentrations, it can form protofibrils that are intermediate species in the fibrillization process from monomer to fibril (Lotharius and Brundin, 2002). The protofibrils further form the fibrils present in Lewy bodies in a nucleation-dependent manner. The A53T and A30P mutations identified in familial PD patients both increase the tendency for α-synucelin to form protofibrils (Conway et al., 2000a; Conway et al., 2000b); however, the A30P mutation inhibits the further formation of fibrils (Conway et al., 2000c). Along with evidence from other studies, the protofibrils are considered to be deleterious species and are highly toxic to the neurons (Bucciantini et al., 2002). Notably, various post-translational modifications, including phosphorylation (Fujiwara et al., 2002; Lee et al., 2004; Okochi et al., 2000), glycosylation (Munch et al., 2000), oxidation (Przedborski et al., 2001), nitration (Hodara et al., 2004; Souza et al., 2000), and ubiquitination (Shimura et al., 2001), have all been found in α-synuclein. In particular, α-synuclein deposited in the Lewy body is found to be ubiquitinated (Tofaris et al., 2003), suggesting these post-translational modifications are involved in the α-synuclein protofibril and fibril formation. Indeed, oxidative dimer formation has been demonstrated to be the critical rate-limiting step for α-synuclein fibrillogenesis in Parkinson's disease (Krishnan et al., 2003). Although the mechanisms by which α-synuclein-formed protofibrils lead to the degeneration of dopaminergic neurons are not clear, some evidence suggests that the desensitization of dopamine transporter (DAT) is inhibited when α-

synuclein becomes aggregated, resulting in massive uptake of dopamine from the synaptic cleft into the dopaminergic neurons and high production of oxidative species (Sidhu et al., 2004). The α-synuclein-formed protofibrils were also reported to permeabilize the synaptic vesicle, causing the increase in free dopamine in the cytosol and elevation of reactive oxygen species (Schulz et al., 2000). In contrast to the toxic effect of protofibrils, α-synuclein-formed fibrils are considered to be neuroprotective and neutralize the toxic effect of protofibrils by forming inclusion bodies (Lotharius and Brundin, 2002).

Besides α-synuclein, parkin and UCHL1 are two other genes mutated in familial PD patients. Genetic mutations of parkin are mainly identified in juvenile Parkinsonism and other early-onset PD patients (Lucking et al., 1998). Structurally, parkin is characterized as one of the members of ubiquitin E3 ligase, which attaches short ubiquitin peptide chains to proteins and tags them for degradation through the proteasome pathway. Although mutations in parkin are rarely found in sporadic PD patients, parkin is also found in Lewy bodies in sporadic PD patients, implicating its pathogenic role in both familial and sporadic PD (Vila and Przedborski, 2004). The direct link between loss of parkin function and dopaminergic neuron degeneration has not been established. Mutated parkin loses its E3 ligase activity, and thus is speculated to impair the neuron's ability to degrade the misfolded proteins, contributing to the abnormal protein aggregation. The E3 ligase activity of parkin was shown to modulate the sensitivity of cells to both proteasome inhibitor- and mutant α-synuclein-dependent cell death (Vila and Przedborski, 2004). Several studies have shown the functional interaction between α-synuclein and parkin. One report even showed that a 22-KDa glycosylated form of α-synuclein is a substrate of parkin (Shimura et al., 2001). Other than

glycosylated α-synuclein, several other substrates of parkin have also been identified, including cyclin E, synphilin-1, and parkin-associated endothelin receptor-like receptor (Chung et al., 2001; Imai et al., 2001; Zhang et al., 2000); however, none of these substrates shows enriched expression in dopaminergic neurons or plays a particularly important role in dopaminergic neurons. It remains unknown how the loss of parkin function selectively leads to the degeneration of the SNc dopaminergic neurons. UCHL1 is another enzyme involved in the proteasome system. This enzyme catalyzes the hydrolysis of C-terminal ubiquityl ester to release ubiquitin from degraded protein and recycle it in the proteasome system. Current studies on UCHL1's pathogenic role in PD are inconclusive (Vila and Przedborski, 2004). The I93M mutation identified in PD patients decreases the activity of UCHL1; however, UCHL1 knock-out mice do not display dopaminergic neuronal degeneration, suggesting that the loss of UCHL1 function can be compensated for *in vivo* (Saigoh et al., 1999). Recently, UCHL1 was demonstrated to also have ubiquitin ligase activity upon dimerization, which might be related to its pathogenic role in PD (Liu et al., 2002).

A number of other genes are being examined as genetic risk factors in PD, including genes involved in dopamine synthesis and metabolism, neurotrophic factors, genes involved in energy supply and oxidative stress response, genes involved in detoxification of metabolites, and genes involved in the maturation of dopaminergic neurons during development (Huang et al., 2004). It is highly likely that multiple mechanisms are present for the pathogenesis of PD as a result of the combinational effect of different genetic mutations and exposure to environmental chemicals. This complicates the development of a universal strategy to delay or cure PD, but could provide more targets for development of drugs which

specifically and effectively prevent degeneration of dopaminergic neurons involving different mechanisms and delay the further development of symptoms in PD patients.

II. Vulnerability of substantia nigra pars compacta (SNc) dopaminergic neurons in Parkinson's disease

In Parkinson's disease, dopaminergic neurons are most severely degenerated, though the degeneration of noradrenergic neurons (locus coeruleus), serotonergic neurons (raphe), and cholinergic neurons (nucleus basalis of meynert, dorsal motor nucleus of vagus, and cerebral cortex) is also observed (Dauer and Przedborski, 2003). In particular, the dopaminergic neurons in the SNc region are selectively degenerated, though dopaminergic neurons are predominantly localized not only in the SNc but also in the ventral tegmental area (VTA) and the retrorubral field of the midbrain (Korotkova et al., 2004; Riddle and Pollock, 2003). Within the SNc region, the degeneration of dopaminergic neurons is also not uniform. Dopaminergic neurons localized in the caudal, ventral, and lateral regions are more vulnerable than those in the rostral, dorsal, and medial regions (Gonzalez-Hernandez et al., 2004; Hirsch et al., 1997). It is clear that some groups of the SNc dopaminergic neurons are more vulnerable to the same level of environmental insults or same degree of comprise from genetic mutations. Different inherent factors in dopaminergic neurons have been implicated in selective vulnerability.

II-1: Dopamine metabolism and vulnerability of dopaminergic neurons

Dopamine, a catecholamine, is the specific neurotransmitter synthesized in and released from dopaminergic neurons. At the pre-synaptic terminal projected from

dopaminergic neurons, dopamine is synthesized from two steps of enzymatic reaction. Tyrosine is first converted to L-3,4-dihydroxyphenylalanine (L-dopa) by tyrosine hydroxylase (TH) and then to dopamine by aromatic amino acid decarboxylase (AADC) (Kandel et al., 2000). Synthesized dopamine is usually sequestered into vesicles for storage by vehicle membrane associated transporter 2 (VMAT2) and released to the synaptic cleft upon stimulation. The released dopamine is either bound by dopamine receptors residing on the membrane of post-synaptic neurons or reuptaken by dopamine transporter (DAT) on the pre-synaptic membrane.

Dopamine (DA) itself has been shown to be one of the inherent factors that contributes to the susceptibility of dopaminergic neurons in PD (Carlsson and Fornstedt, 1991; Hirsch et al., 1997). The metabolism of dopamine and generation of reactive oxygen species is illustrated in Figure 3. Free cytosolic dopamine can auto-oxidize at normal pH into toxic dopamine-quinone species ($SQ^{\cdot}$), superoxide radicals ($O_2^{\cdot -}$), and hydrogen peroxide (H_2O_2) (Graham, 1978; Lotharius and Brundin, 2002). Dopamine-quinone species can directly mediate modification of α-synuclein, which promotes its protofibril formation (Conway et al., 2001). Superoxide radicals are further converted into hydrogen peroxide by superoxide dismutase (SOD). Alternatively, dopamine is deaminated by monoamine oxidase (MAO) into 3, 4-dihydroxyphenylacetic acid (DOPAC) and hydrogen peroxide (Maker et al., 1981). Although hydrogen peroxide itself is innocuous and is usually converted into water while glutathione (GSH) is oxidized to glutathione disulfide (GSSG) by glutathione peroxidase, it can also be

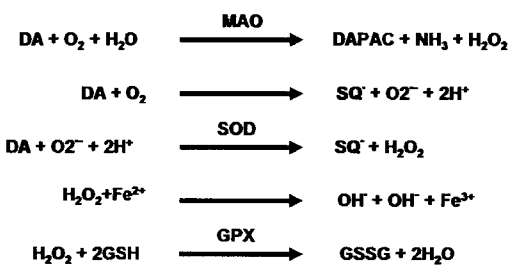

Figure 3. Dopamine metabolism and generation of reactive oxygen species (ROS)

broken down into cytotoxic hydroxyl radicals in a reaction involving Fe^{2+} (Halliwell, 1992). More vulnerable dopaminergic neurons have lower expression of glutathione peroxidase than neurons preserved in PD (Damier et al., 1993), which suggests that more cytotoxic hydroxyl radicals are generated in those neurons. All these reactive oxygen species directly cause lipid peroxidation and protein or DNA oxidation, which in turn leads to the loss of normal enzyme function or membrane integrity. Because of the deleterious nature of the metabolism of dopamine, SNc dopaminergic neurons are more exposed to oxidative stress. Indeed, several studies have demonstrated that oxidative stress is more severe in the SNc region of PD brains, as indicated by lipid peroxidation and protein or DNA oxidation (Dexter et al., 1989; Floor and Wetzel, 1998; Jenner, 1998).

The deleterious nature of the metabolism of dopamine necessitates tight control of the free dopamine level in the cytosol. The cytosolic level of dopamine depends on its synthesis and two transport processes mediated by DAT or VMAT2, respectively. Tyrosine hydroxylase (TH) is the key enzyme that catalyzes the rate-limiting reaction for catecholamine biosynthesis, including dopamine (Ramsey and Fitzpatrick, 2000). The activity of TH is regulated by its serine phosphorylation status and feedback inhibition of synthesized catecholamines in competition with tetrahydrobiopterin, the cofactor for TH (Nagatsu, 1995). The phosphorylation of different serine residues (Ser19, Ser31, and Ser40) on TH has been shown to increase its activity (Dunkley et al., 2004). Various Serine/Threonine kinases, including cAMP-dependent protein kinase A (PKA) (Lovenberg et al., 1975), cGMP-dependent protein kinase G (PKG) (Roskoski et al., 1987), protein kinase C (PKC) (Albert et al., 1984), Ca^{2+}-calmodulin dependent protein kinase II (CaMKII) (Vulliet et al., 1984), extracellular signal-related kinase (ERK1/2) (Sutherland et al., 1993),

and the recently identified cyclin-dependent protein kinase 5 (Cdk5) (Moy and Tsai, 2004) are responsible for mediating the phosphorylation of different serine residues on TH. However, none of these kinases were shown to selectively phosphorylate TH to increase its activity and subsequent dopamine synthesis in different groups of dopaminergic neurons in the brain. It is also unknown whether TH activity is dramatically changed during the pathogenesis of PD. Moreover, previous studies have shown that no expression change in TH was found in postmortem brains of age-matched control subjects and PD patients. Studies on the differentiation of dopaminergic neurons in rodent brain development also show that TH expression is uniform in different groups of dopaminergic neurons and constant from the time TH expression is induced through adulthood (Simon et al., 2003). In contrast, DAT and VMAT2, two transporters involved in the uptake of dopamine from the synaptic cleft into the neuron and in sequestration of free dopamine from the cytosol into the vesicle, respectively, show significantly different expression patterns in different groups of dopaminergic neurons.

DAT is only expressed in the dopaminergic neurons. It localizes on the plasma membrane to uptake released dopamine, thus regulating the intensity and duration of dopaminergic neurotransmission at the synapse. The expression pattern of DAT in different dopaminergic neurons is closely related to the neuronal vulnerability in PD. Immunostaining revealed that DAT has the highest expression in the caudal, ventral, and lateral regions of the SNc in monkey brains and postmortem brains of PD patients (Gonzalez-Hernandez et al., 2004; Hitri et al., 1994). Likewise, dopaminergic neurons in these regions have the most severe loss in PD. The intensity of DAT staining decreases dramatically in the dorsal region of SNc and the VTA region. A similar pattern was also shown by *in situ* hybridization in rat (Sanghera et al., 1997; Uhl, 1998). More DAT in the plasma membrane could uptake more

dopamine and cause increased production of cytotoxic metabolites of dopamine. In addition to its uptake of dopamine into the dopaminergic neurons, DAT can also selectively uptake some toxic chemicals into dopaminergic neurons, like MPP^+, 6-hydroxydopamine (6-OHDA), isoquinoline derivatives, and β-carboline derivatives because of their structural similarity to dopamine (Storch et al., 2004). Since humans are widely exposed to environmental chemicals, more DAT on the plasma membrane of dopaminergic neurons facilitates certain neurotoxin entry into dopaminergic neurons, thus increasing their susceptibility to degeneration. The expression of DAT in neurons that lack DAT confers these neurons susceptibility to MPP^+-induced toxicity (Gonzalez-Hernandez et al., 2004). The effect of DAT on the vulnerability of dopaminergic neurons has also been demonstrated in DAT knock-out or transgenic mice. In DAT heterozygous mice that express about one-half of the normal level of DAT, acute dopaminergic toxicity induced by MPTP is reduced to about one-half of that found in wild-type mice (Gainetdinov et al., 1997). In the DAT overexpressed mice, DAT expression is increased over 130%; however, dopaminergic neurons become more vulnerable and 70% more dopaminergic neuronal loss is observed in comparison to that in wild-type control mice following MPTP treatment (Uhl, 1998).

In contrast to the higher expression of DAT, vesicle membrane associated transporter 2 (VMAT2) has a lower expression level in the more vulnerable dopaminergic neurons. VMAT2 is expressed in the monoaminergic neurons. Immunoelectron microscopy reveals that VMAT2 protein is more abundant in the processes of neurons of the VTA than in those of the SNc (Nirenberg et al., 1996). This was also observed by *in situ* hybridization of VMAT2 (Peter et al., 1995). Because VMAT2 can sequestrate dopamine into vesicles so that less cytotoxic metabolites of dopamine are produced, higher expression of VMAT2 is

considered to be protective and reduces the susceptibility of dopaminergic neurons to oxidative stress. Like DAT, VMAT2 can also sequestrate not only dopamine but also other toxic chemicals structurally similar to dopamine, like MPP^+, into the vesicles. The neuroprotective effect of VMAT2 is supported by studies demonstrating that genetic or pharcological blockade of VMAT2 makes dopaminergic neurons more vulnerable to neurotoxins (Gainetdinov et al., 1998; Speciale et al., 1998). The heterozygous mice that express one-half the normal levels of VMAT2 show more than twice as much MPTP-induced dopaminergic neuronal loss than that in wild-type mice (Takahashi et al., 1997). Based on the relationship between the vulnerability of dopaminergic neurons and the expression level of DAT and VMAT2, the ratio between DAT and VMAT2 expression levels may determine the susceptibility of dopaminergic neurons to degeneration (Edwards, 1993; Miller et al., 1999; Uhl, 1998).

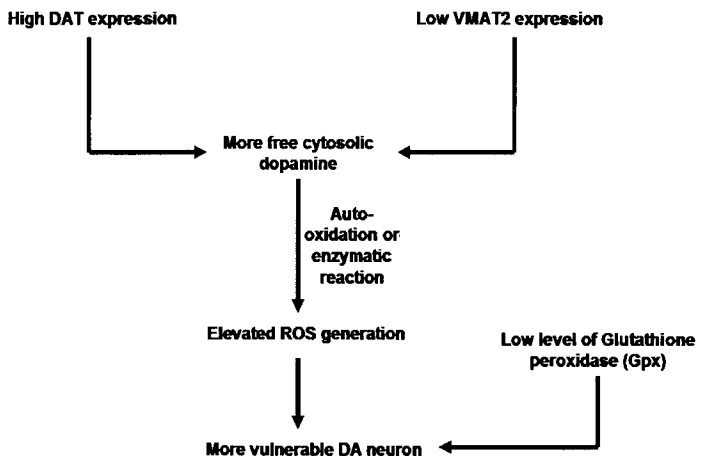

Figure 4. Regulation of free cytosolic dopamine level and the vulnerability of dopaminergic neurons

II-2: Neuromelanin, iron and the vulnerability of dopaminergic neurons

Dopaminergic neurons are the most highly pigmented cells in the human brain because of the preferential presence of neuromelanin (NM). Neuromelanin is an electron-dense substance that locates in the NM granules characterized as organelles surrounded by a double membrane in the neuronal perikaryon (Zecca et al., 2001). NM is only present in

primates, like the chimpanzee, gibbon and human. The proposed connection between NM and the vulnerability of dopaminergic neurons is based on the observation that melanized dopaminergic neurons are the most severely degenerated, whereas non-melanized dopaminergic neurons are preserved in PD (Hirsch et al., 1997).

Although it is not entirely clear, NM synthesis appears to be related to dopamine oxidation. Employing a chemical approach, a dopamine-NM compound was synthesized by the auto-oxidation of dopamine (Double et al., 2002). Alternatively, NM could be derived from quinones or semiquinones, the oxidized metabolite of dopamine with addition of a thiol group in mammalian brains (Fornstedt et al., 1986). NM synthesis was also experimentally induced in cultured rat substantial nigra neurons exposed to L-dopa (Sulzer et al., 2000). The experimental NM synthesis in rat neurons was blocked by overexpression of VMAT2, suggesting that an excess of cytosolic dopamine indeed contributes to the synthesis of NM (Liang et al., 2004). Although the pigmented dopaminergic neurons are consistently observed to be the most highly degenerated in PD, current knowledge about the effect of NM in the vulnerability of dopaminergic neurons is still contradictory.

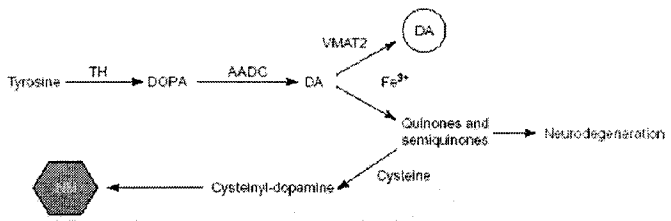

Figure 5. Synthesis of Neuromelanin (NM) (Modified from Zecca, 2003)

Because NM synthesis involves dopamine oxidation, more production of NM leads to the generation of a greater amount of free radicals during the oxidation of dopamine, which increases neuronal susceptibility (Double et al., 2002). Other evidence for its positive correlation with the vulnerability of dopaminergic neurons is that released NM from normally degenerated dopaminergic neurons during aging can stimulate release of the

neurotoxic mediators, including tumor-necrotic factor α (TNF-α), interleukin 6 (IL-6), and nitric oxide (NO) from microglia (Wilms et al., 2003). These factors potentially lead to a subsequent aggravation of neurodegeneration. Very recently, NM was shown to inhibit the enzymatic activity of 26S proteasome in human dopaminergic SH-SY5Y cells (Shamoto-Nagai et al., 2004). Since abnormal proteasome activity has been strongly implicated in the pathogenesis of PD, preferential localization of NM in dopaminergic neurons and its inhibition of 26S proteasome activity could significantly contribute to the vulnerability of dopaminergic neurons in PD.

On the other hand, the neuroprotective role of NM has also been suggested. The derivation of NM from quinones reduces the cytosolic level of quinones and prevents their potential damage to the neuron. In addition, NM can bind to toxins like MPP^+ and a variety of metals, including Zn, Cu, Mn, Cr, Co, Hg, Pb, Cd, and in particular, Fe (Zecca et al., 1994; Zecca et al., 1996). The accumulation of these metals and toxins in NM is considered to be protective, as the binding effectively inactivates their activity, thus significantly reducing their damage to the neuron. For example, the binding of NM to iron keeps it inactive and inhibits the production of hydroxyl radicals involving redox-active iron and hydrogen peroxide (Zareba et al., 1995). However, the protective NM can become cytotoxic depending on the cellular level of these metals and toxins, at least in the case of iron, as discussed below. With its binding ability to a variety of metals and toxic chemicals, NM is

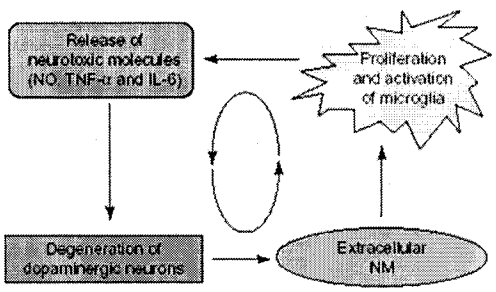

Figure 6. Possible role of NM in the pathogenesis of PD (Modified from Zecca, 2003)

speculated to act as a high capacity "waste handling center" to transport metals and toxins to lysosomes for their eventual degradation (Zecca et al., 2003).

Iron is another factor relevant to the vulnerability of dopaminergic neurons. The increase in iron content (30-35%) only in the SNc has consistently been found in both postmortem Parkinsonian brains and in living patients by imaging techniques (Good et al., 1992; Jellinger, 2000; Sofic et al., 1991). The regional increase in iron has also been reported in other neurodegenerative diseases, like Huntington's and Alzhemer's disease (Connor et al., 1992; Smith et al., 1997). Very interestingly, the topographical distribution of the increased iron matches well with the degenerated regions in these disorders, suggesting a ubiquitous role of iron in the vulnerability of different neurons in different disorders (Double et al., 2002). Although the mechanisms for the selective increase in iron in specific regions remain unclear, the increase in iron in the SNc is suggested to be partially due to the high amount of NM present in dopaminergic neurons, as iron accumulates in NM granules (Sofic et al., 1991).

Redox-active iron is potentially harmful to cells, as it is actively involved in the generation of hydroxyl radicals from superoxide or hydrogen peroxide. Thus, the selective elevation of iron in the SNc could promote the higher production of the hydroxyl radicals, making neurons more exposed to the oxidative stress. In addition, the effect of iron on the vulnerability of the SNc dopaminergic neurons is related to its cellular level and association with NM. When the cellular iron concentration is not high, NM can almost sequestrate all the iron into the granules, resulting in less free radical generation and an antioxidant effect; however, when the cellular iron concentration exceeds the threshold that NM can sequestrate, generation of free radicals is increased with increasing iron concentration (Zareba et al.,

1995). Interestingly, NM also appears to become a pro-oxidant in the presence of high iron concentrations, resulting in a measurably increased production of hydroxyl radicals measured with electron spin resonance (Pilas et al., 1988). Because of the dual effect of NM, when iron is selectively elevated in the SNc region due to unknown mechanisms, higher levels of cellular iron could be involved in the greater production of free radicals not only by itself but also by its modification of NM from neuroprotective to cytotoxic, resulting in the increased vulnerability of dopaminergic neurons. Still, many questions related to the effect of NM and iron on the vulnerability of SNc dopaminergic neurons remain unanswered. For example, are NM structure and properties modified in Parkinsonian brains (Lopiano et al., 2000)? How exactly does iron switch NM from anti-oxidant to pro-oxidant? What are the mechanisms responsible for the selective elevation of iron in the SNc? The development of new experimental tools and a model system are needed to answer these questions.

II-3: Calbindin D28K and the vulnerability of dopaminergic neurons

Calbindin-D28K (CB) is one of the Ca^{2+} binding proteins expressed in neurophils of the SNc and other regions of the brain (Andressen et al., 1993). The association between CB and the vulnerability of dopaminergic neurons is suggested from the observation that CB-rich dopaminergic neurons are much better preserved than CB-poor dopaminergic neurons in the SNc region in PD (Damier et al., 1999a, b). Based on the immunostaining pattern of CB, the SNc of the PD brain is subdivided into a CB-rich nigra matrix region and five CB-poor nigrosomes embedded in the matrix (Damier et al., 1999a). The examination of dopaminergic neuron loss by TH staining in these brains correspondingly reveals that the loss of dopaminergic neurons in the nigrosomes is significantly higher than the loss of dopaminergic

neurons in the matrix. Even within the five nigrosomes, the degree of dopaminergic neuron loss is not uniform. The mechanisms of CB's selectively high expression in some groups of dopaminergic neurons are unknown; however, neurotrophic factors have been suggested to increase CB expression in neurons and further reduce the vulnerability of these neurons to degeneration induced by various insults (Alexi and Hefti, 1996; Cheng and Mattson, 1991; Prehn et al., 1994). The up-regulation of CB and its protective role is also shown in the cadmium-adapted U937 cells. Up-regulation of CB by cadmium was suggested to maintain intracellular Ca^{2+} homeostasis and confer resistance to Ca^{2+} rise-induced apoptosis in U937 cells (Jeon et al., 2004). Although the protective role of CB has been characterized *in vitro*, the CB knock-out mice did not differ significantly in the MPTP-induced loss of dopaminergic neurons in comparison to the CB wild-type mice (Liang et al., 1996). It is still debatable as to whether the high expression of CB is directly related to the protective effect or is only a phenomenon observed simultaneously as other molecules are performing the real protective actions.

These studies indicate that the expression levels of molecules involved in the regulation of free cytosolic dopamine and dopamine-induced oxidative stress are closely associated with the vulnerability of dopaminergic neurons in PD. It is very likely that expression levels of other molecules sensitive to oxidative stress also contribute to the vulnerability of dopaminergic neurons. In addition to the oxidative stress, proteasome dysfunction, activation of microglia and inflammation, and glutamate excitatory toxicity are also implicated in the pathogenesis of PD (Mattson, 2000; Vila and Przedborski, 2003). The expression levels of molecules involved in these systems, for example, selectively high expression of a cytotoxic substrate for proteasome, could potentially contribute to the

vulnerability of dopaminergic neurons. Studies investigating the vulnerability of dopaminergic neurons will provide important insights into the distinct pathogenic mechanisms of PD and help to identify selective targets for the development of neuroprotective drugs.

III. Apoptosis in Parkinson's disease

Apoptosis is a genetically regulated form of cell death that critically controls embryonic development and maintains tissue homeostasis in adults (Meier et al., 2000). The machinery regulating apoptosis is evolutionarily conserved from lower organisms, like *C. elegans* and *Drosophila*, to higher mammalians, like mice and humans (Aravind et al., 2001). Dysfunctional regulation of apoptosis in development and tissue homeostasis has been implicated in many human diseases, including cancer, neurodegenerative diseases, and autoimmune disease, etc. (Nijhawan et al., 2000; Yuan and Yankner, 2000). For the past twenty years, many genes involved in the regulation and execution of apoptosis have been identified, and the biochemical mechanisms of apoptosis have been well characterized.

III-1: Signal transduction in apoptosis

Apoptotic signaling was first identified in studies of programmed cell death in *C. elegans*. In the early 1990s, three apoptosis related genes, CED-3, CED-4, and CED-9, were first cloned by H.R. Horvitz and colleagues from *C. elegans* (Metzstein et al., 1998). Since then, major groups of regulators and executioners of apoptosis have been cloned across different species, including ligands and death receptors, adaptors, cysteinyl aspartate-specific proteases (caspases, including initiator caspases and effector caspases), B cell leukemia (Bcl)

family proteins, non-caspase protease, etc. (Strasser et al., 2000). These regulators and executioners are coordinately involved in three major apoptotic signaling pathways: the extrinsic (receptor-mediated) or intrinsic (mitochondria-mediated) pathways and the caspase-independent pathway (see Figure 7) (Orrenius et al., 2003).

The extrinsic pathway mainly mediates apoptotic signals from the extracellular environment. The ligands, like Fas or TNF-related apoptosis-inducing ligand (TRAIL), bind to the death receptor and form the death-inducible signaling complex (DISC), resulting in the activation of pro-caspase-8, one of the initiator caspases (Chinnaiyan et al., 1995; Medema et al., 1997). The pro-caspase-8 directly activates pro-casapse-3 by cleavage, which subsequently cleaves target proteins in the cell, leading to cell death. The intrinsic apoptotic pathway is triggered by damage inside the cell and is mainly mitochondria centered (Wang, 2001). Specific damage sensors located on different organelles detect the damage caused by either the external agents or internal dysfunction of physiological processes in the cells. Such damage includes toxins-induced loss of mitochondrial membrane integrity or elevation of reactive oxidative species, DNA-damaging agents or irradiation-induced DNA damage in the nucleus, abnormal protein folding or perturbations of calcium homeostasis in the endoplasmic reticulum (ER), etc. (Ferri and Kroemer, 2001). After the detection of damage by organelle-specific sensors, apoptotic signals are transmitted to the mitochondria and trigger the intrinsic pathway. The initial and most important steps in the intrinsic pathways are the release of cytochrome C. Cytochrome C normally resides in the inner membrane space of the mitochondria and is involved in oxidation phosphorylation, but becomes an apoptosome recruiting molecule in apoptosis (Li et al., 1997). Although not entirely clear, several models have been proposed to explain the release of cytochrome C from

mitochondria. Among these models, oligomerization of pro-apoptotic and anti-apoptotic members in the Bcl-2 family and their translocation to the outer membrane of mitochondria play critical regulatory roles (Vander Heiden and Thompson, 1999). The released cytochrome C recruits apoptosis protease activating factor 1 (Apaf-1) and pro-caspase-9 to form apoptosome, causing the activation of pro-caspase-9 and subsequent activation of pro-caspase-3 by activated caspase-9 mediated cleavage (Li et al., 1997).

Besides Bcl-2 family proteins, many other apoptosis regulators and regulatory roles in this pathway have also been characterized, including inhibitor of apoptosis proteins (IAP) as inhibitors of caspases (Srinivasula et al., 2001), and second mitochondrial activator of caspases (Smac) and Omi as negative regulators of IAPs (Du et al., 2000; Hegde et al., 2002), pro-thymosin-α (Pro-T) and the tumor suppressor putative HLA-DR-associated protein (PHAP) as regulators of apoptosome (Jiang et al., 2003). Moreover, caspase-independent mechanisms are also present in the intrinsic pathway. At least two proteins, apoptosis inducing factor (AIF) (Susin et al., 1996) and endonuclease G (EndoG) (Li et al., 2001) are released from mitochondria and translocate to the nucleus, inducing the appearance of chromatin condensation and DNA fragmentation, hallmarks of apoptosis.

The extrinsic and intrinsic apoptotic pathways are connected. In the extrinsic pathway, as an alternative to caspase-8 mediated activation of caspase-3, caspase-8 can cleave Bid and induce its oligomerization with anti-apoptotic Bcl-2/xl followed by its translocation to the mitochondria, allowing oligomerization and insertion of pro-apoptotic Bax/Bak into the mitochondrial outer membrane to induce pore formation at the mitochondria and subsequent release of cytochrome C (Schmitz et al., 1999). Moreover, extensive cross-talks are present among different organelle-specific apoptotic pathways,

which allow different organelles to coordinately respond to apoptotic signals (Ferri and Kroemer, 2001). Caspase-3 activation is the central step in both the extrinsic and intrinsic apoptotic pathways. Activated caspase-3 cleaves various substrates that contain the DXXD tetrapeptide motif (Grutter, 2000; Nicholson and Thornberry, 1997). Cleavage of these substrates leads to the release of activated DNase (Enari et al., 1998), inactivation of enzymes for cell survival (Itoh and Horio, 2001), collapse of nuclear envelope structure (Buendia et al., 1999), and amplification of apoptotic signals (Leverrier et al., 2002), which globally accelerates the death process.

In addition to the extrinsic and intrinsic pathways that exert caspase-3 as the major

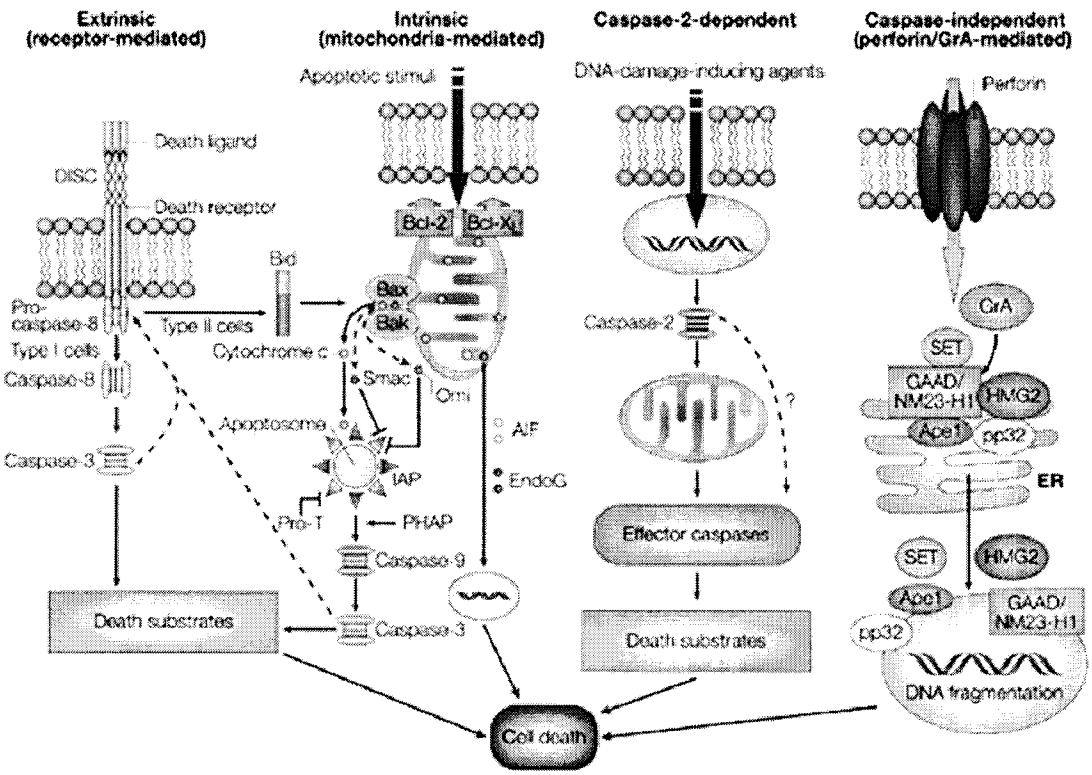

Figure 7. Major signal transduction pathways in apoptosis (Modified from Orrenius, 2003)

executioner, the noncaspase protease-mediated apoptotic pathway has also been described in

some cells. Noncaspase proteases characterized so far include cathepsins, calpains, and granzymes (Johnson, 2000). The Granzyme A (GrA)-mediated apoptotic pathway in the target cells, as employed by cytotoxic T lymphocytes (CTLs) and natural killer cells to defend against viruses and parasitic agents, has been well characterized (Beresford et al., 2001; Fan et al., 2003). In this pathway, serine protease Granzyme A and the membrane pore formation protein perforin are secreted from CTLs or natural killer cells and enter into target cells through the perforin formed membrane pore (Liu et al., 1995). After entering the target cells, Granzyme A starts to cleave the inhibitor of GrA-activated DNase (IGAAD) protein complex that normally inhibits the endonuclease involved in the formation of single-stranded DNA nicks in the target cells. The GrA-mediated cleavage of the IGAAD complex releases GrA-activated DNase (GAAD), which further translocates to the nucleus and induces DNA strand break (Beresford et al., 2001; Fan et al., 2003).

III-2: Apoptosis of nigral dopaminergic neurons in Parkinson's disease

Apoptosis is not only a physiologically important process in neurogenesis; the aberrations in apoptosis control also contribute to the pathogenesis of a variety of neurological disorders, including Parkinson's disease (Mattson, 2000; Yuan and Yankner, 2000). To demonstrate that dopaminergic neurons undergo apoptosis in PD, the apoptotic hallmarks were detected in postmortem brains of PD patients. By using the TdT-mediated dUTP digoxigenin nick end labeling (TUNEL) technique, apoptotic dopaminergic neurons were found in some Parkinsonian brains (Mochizuki et al., 1996). Subsequent studies, using other apoptotic characteristics, either succeeded or failed to detect apoptotic dopaminergic neurons in postmortem PD brain samples (Vila and Przedborski, 2003). In addition to the

apoptotic hallmarks, expression changes in key regulators or activation of key executioners in apoptotic pathways have also been observed. For example, a higher expression level of Bax, one of the pro-apoptotic Bcl-2 family proteins, was found in the SNc dopaminergic neurons of postmortem PD brains as compared to control brains (Hartmann et al., 2001a); increased activity of both initiator caspases, caspase-8, -9, and the effector caspase, caspase-3, have been observed in postmortem PD brains (Hartmann et al., 2000; Hartmann et al., 2001b). Because most SNc dopaminergic neurons in postmortem PD brains are usually degenerated at the time of pathological evaluation, the direct detection of apoptotic dopaminergic neurons in the postmortem PD brains is difficult and hard to reproduce.

Numerous *in vivo* and *in vitro* models have been developed to investigate the mechanisms of MPP^+-induced degeneration of dopaminergic neurons after MPP^+ was found to cause degeneration of the SNc dopaminergic neurons and to induce acute Parkinsonism in humans. The establishment of these models also facilitates the investigation of the involvement of apoptosis in SNc dopaminergic neuron degeneration. In MPTP-administered mice, alteration of energy metabolism, generation of reactive oxygen species (Zarranz et al.), and perturbations in Ca^{2+} homeostasis were observed and suggested as upstream events to trigger various downstream apoptotic pathways (Vila and Przedborski, 2003). In this model, the pro-apoptotic Bax is strongly up-regulated (Vila et al., 2001), whereas anti-apoptotic Bcl-2 is down-regulated (Sharma and Ebadi, 2003). The recruitment of the intrinsic apoptotic pathway and subsequent activation of caspase-9 and caspase-3 are also characterized (Viswanath et al., 2001). In addition to the intrinsic apoptotic pathway, the extrinsic apoptotic pathway is also recruited in the degeneration of SNc dopaminergic neurons, as caspase-8 is activated in MPTP-administered mice (Hartmann et al., 2001b; Viswanath et al.,

2001). The activation of both intrinsic and extrinsic apoptotic pathways is also observed in PD models developed using other neurotoxins or genes involved in familial PD, suggesting apoptosis is a fundamental mode of cell death in the degeneration of SNc dopaminergic neurons in PD (Lev et al., 2003; Tatton et al., 2003).

IV. Involvement of serine/threonine protein kinases in apoptotic signaling and neurodegenerative diseases

Serine/threonine phosphorylation of a wide range of apoptotic components, including major apoptotic regulators (Bcl-2 family proteins), executioners (caspases), organelle-specific stress sensors, various effectors downstream of caspase activation, and apoptosis-involved transcriptional factors, have been found in different systems. The serine/threonine phosphorylation of apoptotic components dramatically modulates their pro- or anti-apoptotic property to either promote or inhibit the apoptotic process (Cross et al., 2000b).

IV-1: Survival and apoptotic serine/threonine kinases in the apoptotic signaling

Many upstream serine/threoine protein kinases responsible for phosphorylation have been identified and categorized as either survival or apoptotic kinases based upon the effect of phosphorylation on these apoptotic components. Survival kinases mainly include protein kinase B (PKB, also known as Akt), full-length P21-activated protein kinase 2 (PAK-2), extracellular signal-related kinase (ERK), pp90 ribosome S6 kinase (Rsk), and α, βI, ε isoforms of protein kinase C (PKCα, PKCβI, PKCε). PKB, PAK-2, ERK, and Rsk all can phosphorylate Bad, one of the pro-apoptotic members in the Bcl-2 family, causing its binding to chaperone protein 14-3-3 and blocking its translocation to mitochondria and induction of

cytochrome C release (Bonni et al., 1999; Scheid and Duronio, 1998; Yuan and Yankner, 2000). ERK and Rsk also phosphorylate transcription factor cAMP response element binding protein (CREB) to further induce expression of survival genes (Bonni et al., 1999; Yuan and Yankner, 2000). In addition, PKB can phosphorylate caspase-9 to reduce its activity (Cardone et al., 1998). It also can phosphorylate Forklhead transcription factor (FKHRL) to inhibit transcription of death-inducing genes like Fas ligand (Brunet et al., 1999). Besides the mitochondrial apoptotic pathway, phosphorylation of the elongation factor 2α (eIF2α) by ER-resident type I transmembrane protein kinase (PERK) in the ER, in response to the accumulation of unfolded proteins in the ER, shuts down the translation before the degradation of all unfolded proteins and protects cells against unfolded proteins-induced apoptosis (Ferri and Kroemer, 2001; Kadowaki et al., 2004).

Apoptotic kinases promoting apoptosis mainly include C-Jun N-terminal kinases (JNKs), p38 mitogen-activated protein (MAP) kinase, apoptosis signal-regulating kinase 1 (ASK1), mammalian sterile 20-like kinase (Mst), and δ, θ isoforms of protein kinase C (PKCδ, PKC0). In particular, JNK/p38 MAP kinase and ASK1 all belong to the MAP kinase family and are major kinases involved in the stress-induced apoptotic signaling (Davis, 2000; Matsuzawa and Ichijo, 2005). ASK1 is one of the very upstream kinases in the MAP kinase family that mediates activation of JNK and p38 after its activation by oxidative stress, the extracellular death signal TNF or Fas ligand, or ER stress (Matsukawa et al., 2004; Takeda et al., 2003). JNK is involved in both the mitochondrial-mediated intrinsic and death-receptor-mediated extrinsic apoptotic pathways. In the intrinsic pathway, activation of JNK is required for stress-induced release of cytochrome C, but the exact mechanism is not yet clear (Tournier et al., 2000). However, both Bcl-2 and Bcl-xl, two anti-apoptotic members in the

Bcl-2 family, have been found to be phosphorylated by JNK *in vitro,* and the phosphorylation inhibits their anti-apoptotic property (Maundrell et al., 1997; Yamamoto et al., 1999), which might be one of the mechanisms for JNK's function in the induction of stress-induced release of cytochrome C. JNK's involvement in the extrinsic pathway is linked to the ER unfolded protein-induced apoptotic signaling. Unfolded proteins in the ER bind to the ER chaperone Bip/Grp78, resulting in the dissociation of Bip to the Ire1-α, a transmembrane ER serine/threonine kinase, and its auto-activation (Katayama et al., 1999). The activation of Ire1-α recruits the cytosolic adapter protein TRAF2, leading to activation of the upstream kinase ASK1 and subsequent activation of JNK (Urano et al., 2000). MAP kinase p38 is usually activated along with JNK and also mediates stress-induced apoptotic signaling (Takeda et al., 2003).

Mst kinase is in another apoptotic kinase family. The pro-apoptotic function of Mst is related to the JNK/p38 MAP pathway, as different genetic analyses have suggested that Mst acts upstream of JNK/p38 MAP kinase to directly activate JNK/p38 MAP kinase (de Souza and Lindsay, 2004). In addition, Mst can also be proteolytically activated by activated caspase-3 and translocate to the nucleus, mediating phosphorylation of histone H2B and facilitating chromatin condensation (Cheung et al., 2003; Lee et al., 2001; Lee and Yonehara, 2002). The pro-apoptotic function of apoptotic kinases has been extensively demonstrated by genetic analysis in cells or knock-out mice; however, biochemical mechanisms of these apoptotic kinases in apoptotic signaling have not been well characterized, largely due to the failure to identify their specific substrates in the apoptotic signaling pathways. So far, only several transcription factors, AP-1, p53, and NF-κB and possibly members of the Bcl-2 family, have been suggested to be the substrates for these apoptotic kinases (Cross et al.,

2000b; Ferri and Kroemer, 2001). More efforts are needed to identify substrates and to better elucidate the regulation of apoptotic kinases in the signal transduction of apoptosis.

IV-2: Activation of protein kinase C delta (PKCδ) and its function in apoptosis

Protein kinase C delta (PKCδ) is one of the novel PKC members. So far, more than 11 isoforms have been categorized in the PKC family and subdivided into three major subfamilies, i.e., conventional PKC (α, βI, βII, γ), novel PKC (δ, ε, η, θ), and atypical PKC (τ/λ, ζ) (Newton, 2003; Spitaler and Cantrell, 2004). A conserved structural property of the PKC family, PKCδ contains N-terminal regulatory and C-terminal catalytic fragments that are connected by a hinge region harboring the caspase-3 recognition and cleavage motif (Kikkawa et al., 2002). The regulatory fragment contains a C1 domain that confers the binding for lipid molecules (diacylglycerol, DAG or phorbol 12-myristate 13-acetate, PMA) and a C2-like domain that lacks the Ca^{2+} binding capacity. The regulatory fragment also contains a pseudosubstrate that binds to the catalytic site in the tertiary structure and keeps the kinase inactivated. PKCδ is ubiquitously expressed in most tissues and cell types (Leibersperger et al., 1991; Wetsel et al., 1992). In murine tissue, a high expression level of PKCδ was found in the epidermis, placenta, uterus, brain, lung, and kidney (Leibersperger et al., 1991). In the central nervous system, PKCδ is highly expressed

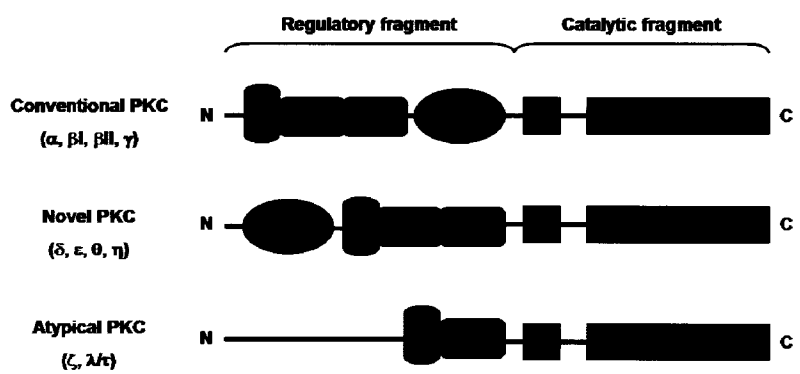

Figure 8. Classification and primary structure of PKC isoforms

in the thalamus, septal nuclei, and purkinje cells in the posterior cerebellum (Barmack et al., 2000; Naik et al., 2000); however, the expression of PKCδ in the SNc dopaminergic neurons has not been investigated.

Diverse functions of PKCδ have been described in different cells. The function of PKCδ appears to be closely related to its activation mechanism (Gschwendt, 1999; Kikkawa et al., 2002). Three mechanisms for the activation of PKCδ have been suggested: the first is membrane translocation. The translocated PKCδ either binds to the phosphatidylserine (PS) on the plasma membrane or diacylglycerol (DAG) generated from phosphatidylinositol 4,5 - bisphosphate (PIP2) by phospholipase C (PLC) or the exogenously added lipid molecule PMA. The binding of lipid molecules changes the conformation of PKCδ, releasing the pseudosubstrate from the catalytic site and activating the kinase (Nishizuka, 1992; Toker, 1998). The lipid-mediated activation of PKCδ is mostly involved in its normal physiological function as downstream effector of the G-protein coupled receptor (GPCR) or other receptors (Nishizuka, 1992). The second mechanism of activation of PKCδ is proteolytic cleavage. Caspase-3-mediated proteolytic cleavage of PKCδ removes the pseudosubstrate along with the whole regulatory domain to persistently activate the kinase (Emoto et al., 1996; Emoto et al., 1995). The proteolytic activation of PKCδ mainly responds to apoptotic stimuli and promotes the cell death process (Brodie and Blumberg, 2003). The

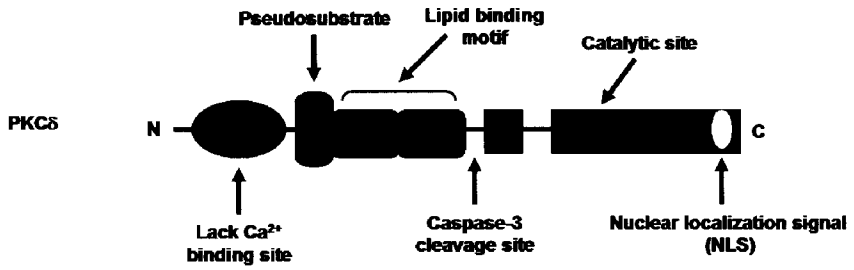

Figure 9. Functional domains of PKCδ

third mechanism of activation of PKCδ is phosphorylation. Both serine/threonine and tyrosine phosphorylation activate PKCδ (Blass et al., 2002; Konishi et al., 2001; Toker, 1998). The activation loop at the terminal of the catalytic domain contains threonine 505 and serine 643 and 662 (Newton, 2003). The phosphorylation of these serine/threonines possibly by 3-phosphoinositide-dependent kinase 1 (PDK-1) facilitates the conformational change for the removal of pseudosubstrate from the catalytic site and is sufficient for activation of the kinase (Hodgkinson and Sale, 2002; Le Good et al., 1998). Extensive tyrosine phoshphorylation has been found at various tyrosine sites (Blass et al., 2002; Konishi et al., 2001). The effect of tyrosine phosphorylation on the activity of PKCδ depends on the individual tyrosine sites; in particular, Y311 and Y332 phosphorylated PKCδ recovered from H_2O_2-treated cells has been found to be constitutively active and independent of DAG (Konishi et al., 1997; Konishi et al., 2001).

The involvement of PKCδ in apoptosis has been well demonstrated in different cells (Brodie and Blumberg, 2003). In most of cases, PKCδ is pro-apoptotic, though some studies suggest that it is anti-apoptotic. Depending on the apoptotic stimuli and cell types, PKCδ can translocate to the mitochondria, nucleus, endoplasmic reticulum (ER), golgi, as well as the plasma membrane in apoptotic cells (Brodie and Blumberg, 2003). Translocation of PKCδ to the mitochondria was shown to facilitate the mitochondrial pore formation, promote cytochrome C release, and induce the redistribution of Bcl-2 family proteins (Majumder et al., 2000; Murriel et al., 2004; Sitailo et al., 2004). The translocation of PKCδ to the nucleus was linked to nuclear events that either regulate the mitochondrial apoptotic pathway or facilitate the collapse of nuclear structure in apoptotic cells (Cross et al., 2000a; DeVries et al., 2002).

A potential feedback mechanism between PKCδ and caspase-3 at either the nucleic or mitochondrial level has been suggested to amplify apoptotic signals by increasing caspase-3 activity (DeVries et al., 2002; Leitges et al., 2001; Leverrier et al., 2002). Although PKCδ has been found to undergo caspase-3-dependent proteolytic activation and promote neurotoxin-induced apoptotic death of dopaminergic neuronal cells (Kaul et al., 2003; Kitazawa et al., 2003), the detailed mechanisms, including the localization change of activated PKCδ and downstream events following the activation of PKCδ, have not been investigated in dopaminergic neuronal cells.

IV-3: Involvement of serine/threonine kinases in neurodegenerative diseases

Abnormality of serine/theroine protein kinases is also implicated in the neurodegenerative diseases (Wagey and Krieger, 1998). In Parkinson's disease, recent studies have identified mutations in the PTEN-induced kinase 1 (PINK1) or leucine-rich repeat kinase 2 (LRRK2) from familial PD patients. Both PINK1 and LRRK2 appear to be involved in Ras/MAP kinase signaling, as suggested by preliminary studies (Shen, 2004). A mutation in PKCγ was also shown to cause Parkinsonian syndrome in the rat (Craig et al., 2001). In MPTP-administered mice, JNK was activated and promoted the apoptotic death of dopaminergic neurons (Saporito et al., 2000; Xia et al., 2001). Moreover, casein kinase-1 and -2 (CK-1 and -2) were found to phosphorylate α-synuclein which was mutated in familial PD patients (Lee et al., 2004; Okochi et al., 2000). The phosphorylation regulates α-synuclein and synphilin-1 interaction and inclusion body formation (Lee et al., 2004). In Alzheimer's disease, several kinases, like glycogen synthase kinase-3 (GSK3) and cyclin-dependent

kinase 5 (Cdk5), cause hyperphosphorylation of the microtubule associated protein Tau (Jope and Johnson, 2004; Stoothoff and Johnson, 2005). Hyperphosphorylation of Tau prevents the normal assembly of Tau with microtubules and the orderly polymerization of microtubules, to promote the formation of intracellular neurofibrillary tangle (NFT) (Stoothoff and Johnson, 2005). GSK3 also facilitates the production of β-amyloid (Aβ) peptide (Phiel et al., 2003). Activation of GSK3 was also observed in the neurons exposed to Aβ, and inhibition of GSK3 activity protects neurons from Aβ-induced neurotoxicity (Jope and Johnson, 2004). In Huntington's disease, PKCδ associates with intranuclear inclusions in a transgenic model of Huntington's disease (Zemskov et al., 2003). The extensive involvement of serine/threonine protein kinases in various neurological disorders demonstrates the importance of fully understanding their exact roles, especially their regulation or mediation roles in the pathogenesis of these neurological disorders.

V. Proteolytic activation and nuclear translocation of serine/threonine protein kinases in apoptosis

V-1: Proteolytic activation of serine/threonine kinases and their function in apoptosis

Serine/threonine protein kinases have emerged as one main category of substrates of activated caspase-3. Serine/threonine protein kinases identified as substrates of caspase-3 include focal adhesion kinase (FAK) (Wen et al., 1997), mutated in ataxia telangiectasia kinase (ATM) (Tong et al., 2000), DNA dependent protein kinase catalytic subunit (DNA-PKcs) (Itoh and Horio, 2001), p21-activated protein kinase 2 (PAR2) (Jakobi et al., 2003), LIM-kinase 1 (LIMK1) (Tomiyoshi et al., 2004), first level mitogen-activated kinase 1 (MEKK1) (Cardone et al., 1997), mammalian sterile 20-like (Mst) kinase family (de Souza

and Lindsay, 2004; Lee et al., 2001), Rho associated kinases I ROCKI (Coleman et al., 2001), protein kinase N (PKN) (Takahashi et al., 1998), sterile 20-related kinase (SLK) (Sabourin et al., 2000), hematopoietic progenitor kinase 1 (HPK1) (Chen et al., 1999), and two isoforms of protein kinase C (PKCδ and PKCθ) (Datta et al., 1997; Emoto et al., 1995). Most of these kinases, except for FAK, ATM, and DNA-PKcs, are normally inactivated due to the binding of the auto-inhibitory motif located on the regulatory domain of the catalytic site in their tertiary structure. Therefore, caspase-3-mediated proteolytic cleavage removes the auto-inhibitory domain and leads to the constitutive activation of kinases. However, caspase-3-mediated cleavage inactivates ATM, DNA-PKcs, and FAK activity. Inactivation of ATM and DNA-PKcs abolishes their phosphorylation to the downstream kinase DNA-damage-induced kinases (Chk) and inhibits the phosphorylation of transcriptional factor p53 and its degradation, resulting in down-regulation of anti-apoptotic Bcl-2 and up-regulation of pro-apoptotic proteins, Bax, Noxa, and PUMA (Ferri and Kroemer, 2001). The inactivation of FAK disrupts the intergin-mediated cell attachment to the extracellular matrix or other cells and promotes cell death (Wen et al., 1997).

The proteolytically activated kinases all promote apoptosis as the overexpression of the catalytic domain is sufficient to induce apoptosis, and the dominant-negative form of kinases inhibits their pro-apoptotic function. Some of them, MEKK1, HPK1, Mst, and SLK, are suggested to amplify apoptotic signals by forming nuclear or mitochondrial feedback loops as caspase activity increased along with the proteolytic activation of these kinases (de Souza and Lindsay, 2004; Widmann et al., 1998). Indeed, the JNK pathway has been ubiquitously found to be activated by these kinases after their proteolytic activation in different cell lines (Chen et al., 1999). In addition, proteolytically activated kinases more

often serve as effectors to directly mediate the morphological and biochemical changes in apoptotic cells, which eventually accelerate the apoptotic process. Proteolytic activation of ROCK1, LIMK 1, PAK2, PKN, SLK, MST, HPAK65 is involved in the appearance of different apoptotic morphology and biochemical changes, including formation of membrane blebbing and the apoptotic body, cell and nucleus shrinkage, collapse of the nuclear envelope, chromatin condensation, etc. (Chen et al., 1999; Coleman et al., 2001; Cross et al., 2000a; Rudel and Bokoch, 1997; Sabourin et al., 2000; Tomiyoshi et al., 2004).

The ectopic expression of cleaved active hPAK65 was found to associate with cellular and nuclear shrinkage in apoptosis (Lee et al., 1997). The proteolytic cleavage of SLK releases not only an activated kinase domain, but also an actin-dissembling domain, which efficiently promotes the cytoskeleton fiber disassembly in apoptosis (Sabourin et al., 2000). ROCKI, the Rho-associated kinase, after its proteolytic activation, plays an essential role in membrane blebbing in the apoptotic cells by phosphorylating myosin light chain to induce actomyosin contractility (Coleman et al., 2001; Sebbagh et al., 2001). Proteolytically activated LIMK1 is another kinase involved in the membrane blebbing of apoptotic cells (Tomiyoshi et al., 2004). Activated LIMK1 can stabilize ROCK-induced actomyosin contractile structures and phosphorylate cofinlin to inactivate it. As cofinlin is an actin-binding protein that stimulates depolymerization of actin filament, its inactivation thus promotes actin filament assembly in the blebbing process of apoptotic cells (Tomiyoshi et al., 2004). PAR2 is another kinase that can be proteolytically activated and contributes to the morphological and cytoskeletal changes in apoptosis (Rudel and Bokoch, 1997), though the exact mechanism is not yet clear. PKCδ, one of the novel PKC isoforms, can also be proteolytically activated by caspase-3. Activated PKCδ mediates phosphorylation of lamin B

and increases its susceptibility to caspase-3-mediated cleavage, thus facilitating the collapse of the nuclear envelope in apoptotic cells (Cross et al., 2000a). Major biochemical changes in the apoptotic cells include DNA fragmentation and chromatin condensation. The fragmentation of chromatin is due to the action of caspase-activated DNase (CAD) or several other DNases, like endonuclease G (Endo G) and Granzyme A-activated DNase (GAAD) (Orrenius et al., 2003). However, the mechanisms of chromatin condensation are still unclear. It has been suggested that post-translational modification of histones may play an essential role in the condensation of chromatin in apoptosis, as histone phosphorylation has been associated with chromatin condensation in mitosis (Ajiro, 2000; Cheung et al., 2000; Nowak and Corces, 2004). Recently, proteolytically activated Mst1 was shown to translocate to the nucleus and mediate phosphorylation of histone H2B which is associated with chromatin condensation in apoptotic cells (Cheung et al., 2003).

Protein kinases that can be proteolytically activated are normally regulated by other signaling molecules and are involved in other cellular processes. For example, full-length MEKK1 and PAK2 are normally activated by p21 GTP-binding protein Ras or Cdc42/Rac (Knaus and Bokoch, 1998). The activated full-length MEKK1 and PAK2 promote cell survival (Jakobi, 2004). ROCK1 is normally regulated by Rho GTPase and LIMK is activated by Rho-ROCK and Rac/Cdc42-PAK, regulating actin cytoskeleton reorganization (Coleman et al., 2001; Tomiyoshi et al., 2004). However, proteolytic activation of protein kinases in apoptosis and their extensive mediation roles in the apoptotic morphological and biochemical changes suggest that proteolytic cleavage serves as an important switch that converts these kinases from their normal function to pro-apoptotic function. Knowledge of the proteolytic activation of these serine/threonine kinases provides a target for drug

development to specifically inhibit the proteolytic cleavage instead of inhibiting the normal kinase activity, which could block the apoptotic morphological and biochemical changes and rescue the cells from death or delay the death process.

V-2: Mechanisms of nuclear/cytoplasmic transport

Subcellular localization and trafficking of protein kinases are important, as kinases need to be in close proximity to their activators or substrates for rapid transmission of signals and fulfillment of their effector function (Teruel and Meyer, 2000). The nucleocytoplasmic transport of kinases is particularly important because the cytoplasm and nucleus are two major compartments for all activities in the cell. Although molecules smaller than 40KDa can passively diffuse into the nucleus, nucleocytoplasmic transport is mainly regulated by the nuclear import and export machinery that includes nuclear localization signal (NLS)/nuclear export signal (NES), importin/exportin, and Ran GTPase (Moroianu, 1999). For nuclear import, proteins bearing the nuclear localization signal (NLS) are bound to the import receptor, importin. The protein-

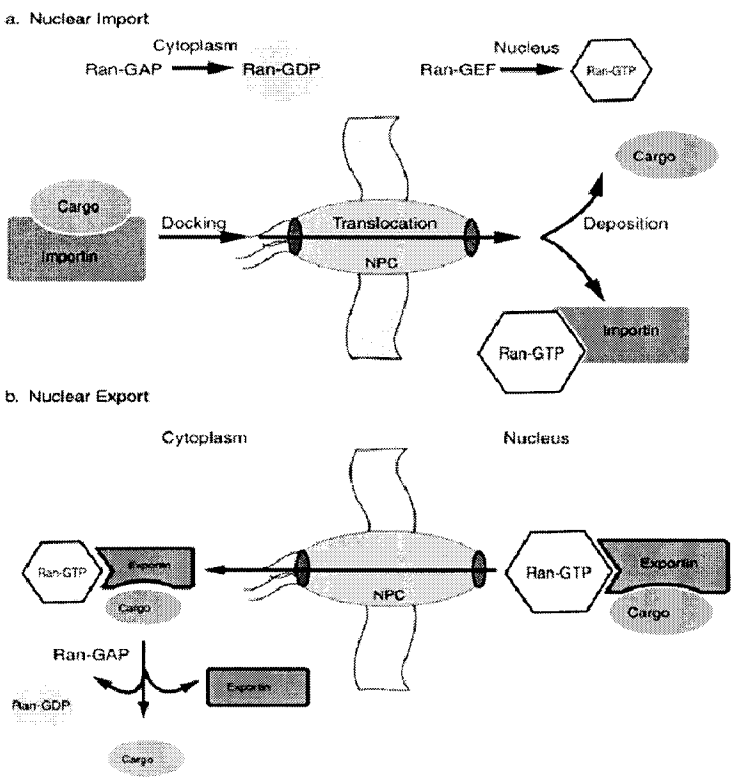

Figure 10. NLS/NES mediated Nuclear import/export (Modified from Kaffman, 1999)

importin complex is then targeted to the nuclear pore complex (NPC) and translocates into the nucleus. In the nucleus, proteins are dissociated from importin as importin binds to the Ran-GTP. For nuclear export, the export receptor exportin only binds to NES containing proteins in the presence of Ran-GTP. The protein-exportin-Ran-GTP complex is transported out of the nucleus and proteins are disassociated when Ran-GTP undergoes hydrolysis induced by Ran-GTPase activating protein (Ran-GAP) and Ran-binding protein 1 (Kaffman and O'Shea, 1999).

V-3: Regulation of nuclear localization of serine/threonine kinases by proteolytic cleavage in apoptosis

In apoptosis, many kinases undergo NLS or NES dependent transport between the nucleus and the cytoplasm. For example, ERK translocates to the nucleus and phosphorylates transcriptional factor CREB in response to neurotrophic factors induced cell survival (Ajenjo et al., 2004; Yuan and Yankner, 2000). Interestingly, proteolytic cleavage of kinases by caspase-3 closely regulates their nucleocytoplasmic localization, which further regulates their distinct function in apoptosis (Jakobi, 2004). The regulatory role of proteolytic cleavage in kinase subcellular localization and function is based on the observation that full-length PAR2 is predominantly localized in the cytoplasm and is involved in cell survival, whereas the cleaved PAR2p34 translocates to the nucleus and promotes apoptosis (Jakobi et al., 2003; Knaus and Bokoch, 1998). Full-length PAR2 contains an N-terminal regulatory and a C-terminal catalytic domain. Although the regulatory domain contains a functional NES motif and the hinge region contains a functional NLS motif, the nuclear export seems dominant over the nuclear import, and thus full-length PAR2 predominantly localizes in the cytoplasm.

After the cleavage, however, the NES is removed along with the regulatory domain; the nuclear import mediated by the NLS in the hinge region becomes dominant and leads to the nuclear localization of cleaved PAR2p34 (Jakobi et al., 2003). Similar to the PAR2, two functional NES are found in the C-terminal regulatory domain of Mst1 to keep full-length MSt1 in the cytoplasm (Lee and Yonehara, 2002; Ura et al., 2001). The proteolytic cleavage removes both NES along with C-terminal regulatory domain and induces nuclear translocation of cleaved Mst1p36 (Ura et al., 2001). PKCδ is another kinase that the cleaved catalytic domain trnaslocates to the nucleus (Brodie and Blumberg, 2003). Functional NLS has been found in the C-terminal catalytic domain and no functional NES has been found yet (DeVries et al., 2002). Intriguingly, although it contains only functional NLS, but not functional NES, PKCδ is primarily localized in the cytoplasm, though a small fraction is localized in the nucleus. It is likely that the NLS in PKCδ is normally kept, possibly by the N-terminal regulatory domain, in the incompetent status, and the proteolytic cleavage could convert the NLS from incompetent status into competent status by removing the regulatory domain, thus promoting its nuclear translocation.

VI. RNA interference (RNAi) and its neuroprotective application in neurodegenerative diseases

RNA interference (RNAi) is a new form of post-transcriptional gene silencing (PTGS) discovered within the past 10 years. The endogenous process down-regulates gene expression by either inducing the sequence-specific degradation of complementary mRNA or by inhibiting translation, or possibly by promoting DNA methylation or formation of heterochromatin (Hannon, 2002). After its initial discovery in *C. elegans*, the RNAi

phenomenon has been observed in many other systems, including *Arabidopsis* (also called co-suppression or virus induced gene silencing, VIGS), fungi, *Drosophila*, various mammalian cells and animals (Fire et al., 1998; Hammond et al., 2001; Schwarz et al., 2002). Meanwhile, endogenous micro RNA (miRNA) encoding genes are being rapidly and widely identified in different species, including humans, and are implicated in regulation of various physiological processes (Bartel, 2004).

VI-1: Mechanisms of RNA interference

The machinery and mechanisms of RNAi are being rapidly revealed after the intense studies conducted during the past several years. The mechanisms of RNAi have been conserved across different species, though specific adjustments are present in different species. For example, in *C. elegans* and plants, RNAi is heritable and shows a systematic (spreading throughout the whole organism) nature of silencing; in *Drosophila* and mammals, it shows cell-autonomous, non-heritable silencing (Hannon, 2002). All species have a Dicer enzyme that belongs to the RNase III ribonuclease family and catalyzes the conversion of exogenous long (300-500bp) double-strand RNA (dsRNA) to

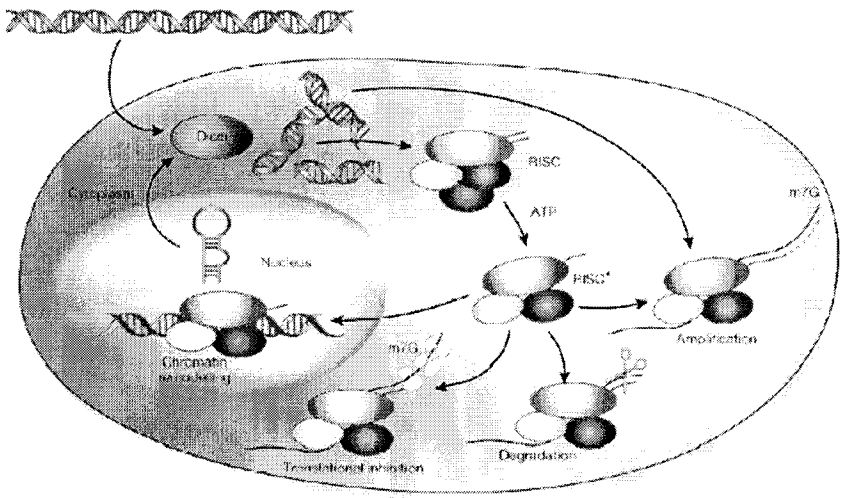

Figure 11. General mechanisms of RNAi (Modified from Hannon, 2002)

21-23bp small interfering RNA (siRNA) (Bernstein et al., 2001). The generated siRNA usually contains 5' phosphates and 2 nt 3' overhangs, as characteristic of RNase III cleavage products (Elbashir et al., 2001b). The double-strand siRNA is then separated by helicase so that only one strand is incorporated into a nuclease complex, RNA induced silencing complex (RISC) (Nykanen et al., 2001; Zamore et al., 2000). This complex, after binding to siRNA, is activated in an ATP dependent manner and leads to the degradation of target mRNA that is complementary to the siRNA (Nykanen et al., 2001; Zamore et al., 2000). In addition to the degradation of target mRNA, the RISC-siRNA complex can also down-regulate gene expression by translational inhibition or by promoting chromatin remodeling, including DNA methylation, heterochromatin formation, and DNA rearrangements (Bartel, 2004; Schramke and Allshire, 2004). In mammals, however, exogenously introduced long dsRNA is recognized as viral RNA by mammalian cellular defense systems, which activates RNA-dependent protein kinase (PKR). Activated PKR subsequently phosphorylates protein synthesis initiation factor EIF-2α and leads to the inhibition of all protein synthesis in the cells (Gil and Esteban, 2000). Therefore, in mammals, siRNA, instead of dsRNA, is directly used for induction of specific silencing effects (Elbashir et al., 2001a).

The observation that very small amounts of dsRNA can induce strong RNAi effects which spread throughout the organism in plants and *C. elegans* suggests that RNAi in these organisms may have specific mechanisms to amplify and spread RNAi signals (Hannon, 2002). The dsRNA-induced silencing effect in these organisms requires proteins similar in sequence to a tomato RNA-directed RNA polymerase (RdRP) (Schiebel et al., 1998). Genetic studies in *Arabidopsis* and *C. elegans* have identified several mutants that might act as RdRP to produce extra dsRNA using initially generated siRNA as the primer (Dalmay et

al., 2000; Mourrain et al., 2000). The additionally produced dsRNA can be further cleaved by Dicer enzyme to produce more siRNA, thus increasing the silencing effect. It has also been speculated that the RISC-siRNA complex may induce chromatin structure alteration and produce aberrant mRNA, which can also be employed by RdRP to produce extra dsRNA (Hannon, 2002). For systemic RNAi effects, a transitive RNAi phenomenon has been observed in which the silencing signal moved along a particular gene from 3'-5' (in *C. elegans*) or in both directions (in plants) (Baulcombe, 2002a, b). In addition, it has also been speculated in plants that silencing signals could be passed to adjacent cells through cell-cell junctions (movement of RNA and proteins via cell-cell junctions is well characterized), or even further through the vasculature (Hannon, 2002; Voinnet et al., 1998). Indeed, the sid-1 gene is required for a systemic silencing effect in *C. elegans*. This gene encodes a transmembrane protein that may act as a channel for import of the silencing signal in *C. elegans* (Winston et al., 2002). Interestingly, SID-1 homologues are absent in *Drosophila*, consistent with the lack of systemic spreading of the silencing effect in flies (Hannon, 2002).

VI-2: Design of siRNA for mammalian systems

RNAi provides a powerful tool for characterization of gene function as the loss-of-function phenotype can be quickly linked to a specific gene. Indeed, genome-wide RNAi screening has been carried out in several plants and invertebrates (Dykxhoorn et al., 2003; Hammond et al., 2001). In mammals, though long dsRNA fails to induce specific silencing effects because it triggers cellular defense systems, specific silencing effects have been successfully achieved by an alternative short siRNA strategy (Elbashir et al., 2001a; Mittal, 2004). Although the short siRNA sequence is mainly based on the target mRNA sequence,

the selection of exact target sites on the target mRNA is still difficult and thus not every designed siRNA is effective. Basically, short siRNA (21bp) needs to have a phosphorylation group at the 5' end and 2nt UU overhang at the 3' end, so a typical siRNA would be 5'P-(N19)UU-3', where N is any of four nucleotides (Mittal, 2004).

In addition, several empirical criteria based on the biochemical mechanisms of RNAi have been suggested in the selection of target sites and structural requirements of siRNA sequences (Mittal, 2004; Reynolds et al., 2004). These criteria include: 1) the target sequence has overall low to medium GC content (30-50%) that facilitates its interaction with RISC complex and its unwinding; 2) the internal stability should be lower in the 5' antisense strand but higher in the 5' sense strand to promote the incorporation of antisense but not the sense strand into the RISC complex, i.e., choose A or U instead of G or C at the 3' end of the sense strand that forms weaker hydrogen bonds (Schwarz et al., 2003); 3) no internal repeats or palindromes are present in the siRNA that reduce liklihood of formation of an siRNA dimer; 4) the presence of a U at position 10 of the sense strand that promotes RISC mediated cleavage of mRNA and dissociation of the RISC-siRNA complex. These criteria significantly improve the efficiency of designed siRNA, though all designed siRNAs still need to be tested. Designed siRNA can be either chemically synthesized or generated via *in vitro* transcription (Holle et al., 2004; Yu et al., 2002). For *in vitro* transcription, the DNA template for siRNA is usually linked to a T7 promoter so that both sense and antisense strands can be transcribed *in vitro* by T7 RNA polymerase and annealed to generate the functional double strand siRNA.

Recently, expression of vector-based small hairpin RNA (shRNA) has become preferred, as it can consistently induce a silencing effect for the observation of some late phenotypes and allows establishment of a stable cell line. The design of shRNA is based on

the recent progress made in the natural production and maturation of micro RNA (miRNA) in cells (Bartel, 2004). The miRNA is maturated from pri-miRNA transcribed from miRNA genes. The cleavage of pri-miRNA by Drosha RNase III endonuclease in the nucleus releases a 60-70nt stem loop intermediate, known as the miRNA precursor (pre-miRNA) (Lee et al., 2002; Zeng and Cullen, 2003; Zeng et al., 2003). The stem loop shaped pre-miRNA is then exported out of the nucleus and cleaved by Dicer endonuclease to generate the mature double strand miRNA (Lee et al., 2003). Based on this model, small DNA oligonucleotide that contains sense and antisense strands complementary to the target mRNA and interspaced by loop nucleotides is cloned into an expression vector driven by RNA polymerase III promoter, like small nuclear RNA (snRNA) U6 or H1 RNA (Paddison et al., 2002; Paul et al., 2002; Sui et al., 2002). Similar stem loop structure, like pre-miRNA, would be formed after the DNA oligonucleotide is transcribed in the cell. This expressed stem loop "pre-siRNA" can then be cleaved by Dicer to generate functional siRNA in the cells. This strategy of producing siRNA and induction of a silencing effect has become a choice method, especially for *in vivo* experiments in which delivery of siRNA is usually very inefficient.

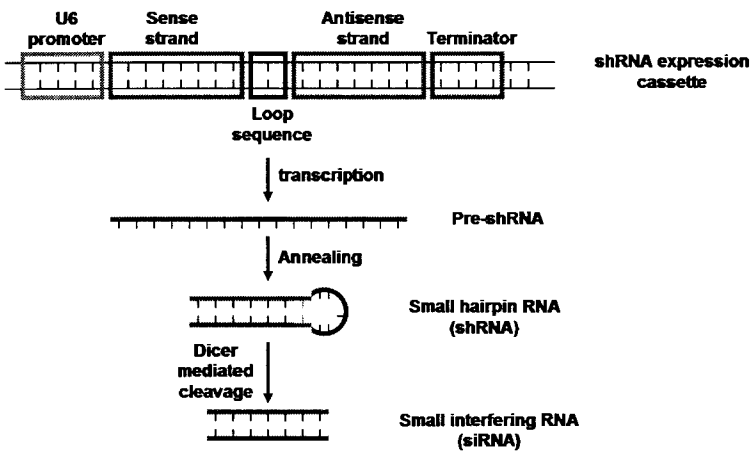

Figure 12. Schematic diagram of shRNA expression cassette and the generation of siRNA from expressed shRNA

VI-3: Application of RNAi-mediated neuroprotective strategy in neurodegenerative diseases

The high efficiency of siRNA in mammalian cells, along with its target specificity and easy handling, has provided a new neuroprotective strategy for neurodegenerative diseases. Because RNAi can specifically down-regulate specific genes, dominant mutated alleles implicated in the pathogenesis of different neurodegenerative diseases are potentially good targets for therapeutic gene silencing (Mittal, 2004). The selective RNAi targeting of only the dominant mutated allele is critical, as the normal allele can still produce proteins for its normal function in the cells. This approach has been recently demonstrated in the selective silencing of mutated ataxia-3, contributing to the polyglutamine (polyQ) toxicity in spinocerebellar ataxia type 3 (SCA3) (Xia et al., 2004). In the polyglutamine disorders, the expansion of the CAG repeat in the genes causes the additional incorporation of glutamine that changes the protein's conformation and promotes the abnormal aggregation. In this study, effective siRNA targeting the CAG repeat was first designed, but down-regulated both the mutant and wild-type genes. Instead, other siRNAs targeting a single nucleotide polymorphism (SNP) located immediately 3' to the CAG repeat, which is in linkage disequilibrium with the disease-causing CAG expansion and segregates with the disease allele in most families, were designed and effectively silenced only the expression of the mutated allele and not the wild type allele (Xia et al., 2004). Similar strategies have also been successfully applied to other dominant disease-causing alleles, including the missense mutation Tau V337M underlying the disorder frontotemporal dementia with Parkinsonism (Miller et al., 2003), the TorsinA gene underlying a form of dystonia, a missense mutation of muscle acetylcholine receptor (AchR) α subunit S226F that causes the slow channel

congenital myasthenic syndrome (SCCMS) (Gonzalez-Alegre et al., 2003), and a tandem missense mutation of the amyloid precursor protein APPsw underlying Alzheimer's disease (Miller et al., 2004). Such technologies show promise for application in other neurodegenerative diseases in which mutated disease-causing dominant alleles are implicated.

For the more common sporadic form of neurodegenerative diseases, progress in the investigation of apoptotic death of neurons will likely lead to identification of cytotoxic proteins that underlie the pathogenesis of diseases as potential targets for RNAi. In our laboratory, we have demonstrated that down-regulation of the oxidative stress sensitive kinase PKCδ by siRNA effectively protects dopaminergic neurons from MPP^+-induced toxicity (Yang et al., 2004). The down-regulation of prostate apoptosis response-4 (Par-4) by siRNA protects against cell death in a Cu/Zn superoxide dismutase (Cu/Zn-SOD) transgenic mouse model of Amyotrophic lateral sclerosis (ALS) (Xie et al., 2005). The many enzymes and kinases shown to facilitate the production of free radicals or cell death may be good targets for RNAi. However, because many of these molecules are involved in both physiological and pathological processes, the effect of the down-regulation of these targets on normal physiological process must be considered and be autonomously or artificially compensated for in the cells.

Most of the successful siRNA-mediated neurprotective strategies have been demonstrated in cells by direct transfection of siRNA or introduction of vector expressing shRNA. In some cell lines, chemically synthesized or *in vitro* transcribed siRNA can be easily introduced into the cells by electroporation or lipophilic reagents (Mittal, 2004). However, these approaches are limited by their transient nature, as introduced siRNAs are usually degraded in several days (Dykxhoorn and Lieberman, 2005). Although the

expression of shRNA partially solves this problem by facilitating the establishment of a stable cell line, both the synthetic siRNA and vector-based shRNA often fail to efficiently deliver siRNA into neuronal cells or non-dividing primary neurons due to the very low transfection efficiency in these cells (Mittal, 2004). In addition, an *in vivo* mammalian animal model demonstrating the neuroprotective effect of siRNA is required to really demonstrate that siRNA could be a good therapeutic reagent. Also, new tools for the efficient introduction and long term expression of siRNA in neurons *in vivo* are required.

Numerous viral vectors have been developed from adenovirus, recombinant adeno-associated virus (AAV), retrovirus, and lentivirus to solve the siRNA delivery problem *in vivo* (Brenner and Malech, 2003; Kirik and Bjorklund, 2003; Rubinson et al., 2003). Among these viral vectors, the replication-deficient lentiviral vector is most desirable because lentivirus can infect not only the dividing cells but also the non-dividing cells, and can integrate its genome efficiently into the genome of host cells (Blomer et al., 1997; Kafri et al., 1997; Mittal, 2004; Miyoshi et al., 1997). To deliver the siRNA into the neuron, a shRNA cassette that contains the RNA polymerase III promoter, shRNA template, and RNA polymerase III terminator is first cloned into the replication-deficient lentiviral vector, and then lentivirus is produced by infection of the 293FT cells. The produced lentivirus, after concentration, can be directly injected into the brain to infect certain groups of neurons. Lentiviral vector mediated delivery of shRNA has been successful in mice and inhibits the expression of co-transfected reported plasmids (Lewis et al., 2002; McCaffrey et al., 2002), of the endogenous pro-apoptotic Fas receptor (Song et al., 2003), and of the tyrosine hydroxylase (TH) gene in the brain (Hommel et al., 2003). Recently, inducible lentiviral vectors have also been developed, which provide more flexibility to create animal disease

models and to test the neuroprotective effect of specific siRNA (Wiznerowicz and Trono, 2003). By using the inducible lentiviral vector, in principle, shRNA targeting any genes can be transduced into the mice and inducibly expressed to allow the observation of some late phenotypes (Mittal, 2004). This approach, compared to the large scale ethylnitrosurea (ENU) mutagenesis, is much less laborious and more effective.

CHAPTER II: SUPPRESSION OF CASPASE-3 DEPENDENT PROTEOLYTIC ACTIVATION OF PROTEIN KINASE Cδ BY SMALL INTERFERING RNA (SiRNA) PREVENTS MPP^+-INDUCED DOPAMINERGIC DEGENERATION

A paper published in *Molecular and Cellular Neuroscience*

Yongjie Yang, Siddharth Kaul, Danhui Zhang, Vellareddy Anantharam,

Anumantha G. Kanthasamy

ABSTRACT

The cellular mechanisms underlying the neurodegenerative process in Parkinson's disease are not well understood. Using RNA interference (RNAi), we demonstrate that caspase-3 dependent proteolytic activation of protein kinase C δ (PKCδ) contributes to the degenerative process in dopaminergic neurons. The Parkinsonian toxin MPP^+ activated caspase-3 and proteolytically cleaved PKCδ into catalytic and regulatory subunits, resulting in persistent kinase activation in mesencephalic dopaminergic neuronal cells. The caspase-3 inhibitor Z-DEVD-FMK and the caspase-9 inhibitor Z-LEHD-FMK effectively blocked MPP^+-induced PKCδ proteolytic activation. To characterize the functional role of PKCδ activation in MPP^+-induced dopaminergic cell death, RNAi mediated gene knock-down was performed. Among four siRNAs designed against PKCδ, two specifically suppressed PKCδ expression. The application of siRNA abolished the MPP^+-induced PKCδ activation, DNA

fragmentation, and TH positive neuronal loss. Together, these results suggest that proteolytic activation of PKCδ may be a critical downstream event in the degenerative process of Parkinson's disease.

INTRODUCTION

Understanding the cellular mechanisms involved in the selective loss of nigral dopaminergic neurons in Parkinson's disease (PD) remains a formidable challenge. Apoptosis has recently been recognized as an important mode of cell death in PD, mainly by the identification of key markers of apoptotic cell death including mitochondrial cytochrome c release, caspases activation and DNA fragmentation in PD pathology (Dodel et al., 1998; Hartmann et al., 2000; Mizuno et al., 1998; Viswanath et al., 2001). Major insights into the neurodegenerative process in PD have been gained from the use of the mitochondrial toxin MPTP (1-methyl-4-phenyl-1,2,3,6-tetrahydropyridine), which faithfully replicates the salient Parkinsonian symptoms and pathology (Albanese et al., 1993; Betarbet et al., 2002; Langston et al., 1984). MPTP is converted to its ionic metabolite MPP^+ (1-methyl-4-phenylpyridinium) in the brain, which induces a series of apoptotic signaling events including reactive oxygen species (ROS) generation, mitochondrial dysfunction, cytochrome c release, caspases activation, and DNA fragmentation in cell culture and animal PD models (Cassarino et al., 1997; Cassarino et al., 1999; Hartmann et al., 2000; Lee et al., 2000; Lotharius and O'Malley, 2000; Viswanath et al., 2001; Wu et al., 2003). Furthermore, ROS is one of the major contributors to apoptotic cell death in dopaminergic neurons (Beal, 2002; Ischiropoulos and Beckman, 2003; Lotharius and Brundin, 2002; Olanow and Tatton, 1999). However, little is

known about the molecules and mechanisms that act downstream of caspases during MPP^+-induced apoptotic cell death in dopaminergic neurons.

Phosphorylation is a major cellular signaling mechanism by which many critical neuronal functions including cell survival, differentiation, and death are regulated. One of the key members of phosphorylation signaling is protein kinase C (PKC) family. It includes 13 isoforms, which are classified mainly into three subgroups based on their dependence upon diacylglycerol (DAG) and Ca^{2+} for activation (Dempsey et al., 2000; Gschwendt, 1999; Maher, 2001). The conventional PKC isoforms (PKC α, βI, βII, and γ) require DAG and Ca^{2+} for activation, the novel PKC isoforms (PKC δ, ε, η, θ, and μ) require only DAG but not Ca^{2+} for activation and the atypical PKCs (PKC ζ, λ and ι) require neither Ca^{2+} nor DAG for activation. Kinase activation involves autophosphorylation followed by translocation to the cell membrane and other organelles (Brodie and Blumberg, 2003; Gschwendt, 1999; Kikkawa et al., 2002). Recent studies have shown that PKCδ can be proteolytically activated by caspase-3 during apoptotic cell death in non-neuronal cells (Emoto et al., 1996; Mandil et al., 2001; Meinhardt et al., 1999; Pongracz et al., 1999; Reyland et al., 1999). These studies characterized the function of PKCδ activation in apoptotic cell death mainly by utilizing the pharmacological inhibitor rottlerin or dominant-negative mutants. The non-specific nature of this pharmacological inhibitor (Davies et al., 2000) and the inherent problems with overexpression (Buchner, 2000; Gschwendt, 1999) warrant use of a more powerful tool to investigate the function of PKCδ in dopaminergic cell death.

Double-strand RNA (dsRNA)-mediated RNA interference (RNAi) is emerging as a powerful tool to characterize gene function by genetic loss-of-function analysis. This novel

post-transcriptional gene silencing mechanism was first demonstrated with great success in plants, *C. elegans, Drosophila* (Barstead, 2001; Carmell et al., 2002; Elbashir et al., 2001a; Hammond et al., 2001; Hasuwa et al., 2002; Morel and Vaucheret, 2000; Shi, 2003; Sorensen et al., 2003; Vaucheret et al., 2001; Vaucheret and Fagard, 2001; Xia et al., 2002) and more recently in cultured mammalian cells as well as in animal models (Carmell et al., 2002; Elbashir et al., 2001a; Hasuwa et al., 2002; Shi, 2003; Sorensen et al., 2003; Xia et al., 2002). Small interfering RNA (siRNA), usually 21 bp, is widely applied in mammalian cell cultures as compared to 300-500 bp dsRNA in non-mammalian systems (Donze and Picard, 2002; Krichevsky and Kosik, 2002; Paddison et al., 2002). Because of its high efficacy, selectivity and ease of application, RNAi is now a preferred method over pharmacological inhibitor studies, the antisense technique, and overexpression analysis (Jen and Gewirtz, 2000; Opalinska and Gewirtz, 2002). In the present study, we demonstrate that proteolytic activation of PKCδ by caspase-3 facilitates apoptotic cell death in an *in vitro* model of Parkinson's disease and suppression of PKCδ expression using siRNA rescues dopaminergic neuronal cells from MPP^+-induced cell death.

RESULTS

MPP^+ exposure induces caspase-3 mediated proteolytic activation of PKCδ

Activity of the key effector cysteine protease caspase-3 was measured in rat mesencephalic clonal dopaminergic neuronal (N27) cells treated with the Parkinsonian toxin MPP^+ (300 μM). Maximal caspase-3 activation of 228% over untreated control cells was observed 36 hr following MPP^+ treatment (Fig 1A). Activation of caspases by MPP^+ was also

confirmed by *in situ* caspase staining (Fig 1B). All the MPP^+-treated cells showed intense green florescence indicative of caspase activation, while untreated cells showed very low levels of caspase activation.

Interestingly, MPP^+ exposure for 36 hr also induced the proteolytic cleavage of native PKCδ (72-74 kDa) to yield catalytically active (41/38 kDa) fragments (Fig 2A). Co-treatment with the caspase-3-specific inhibitor Z-DEVD-FMK almost significantly reduced MPP^+-induced proteolytic cleavage of PKCδ, indicating that caspase-3 mediated the cleavage of PKCδ (Fig 2A). Densitometric analysis revealed an 81% inhibition of PKCδ cleavage by Z-DEVD-FMK. Moreover, we sought to determine whether caspase-9, the upstream initiator of the mitochondrial-mediated caspase cascade, contributes to the caspase-3-dependent proteolytic cleavage of PKCδ. The caspase-9-specific inhibitor Z-LEHD-FMK significantly blocked MPP^+-induced PKCδ cleavage (Fig 2B). Thus, caspase-9 might be the upstream initiator caspase that proteolytically activates caspase-3, which subsequently cleaves PKCδ.

Caspase-3-mediated proteolytic cleavage of PKCδ results in the permanent dissociation of the regulatory subunit from the catalytic subunit, resulting in the persistently active catalytic fragment. Therefore, we performed immunoprecipitation kinase assays to determine if caspase-3-dependent proteolytic cleavage of PKCδ increased its kinase activity during MPP^+ treatment. A 36hr exposure to 300 μM MPP^+ increased PKCδ enzymatic activity 239% in comparison to untreated control cells (Fig 2C). Co-treatment with the caspase-3 specific inhibitor Z-DEVD-FMK completely blocked MPP^+-induced increases in PKCδ enzyme activity, suggesting that caspase-3 mediated proteolytic activation of PKCδ

contributed to the increases in kinase activity. To further determine whether MPP^+ treatment alters PKCδ gene expression in dopaminergic neuronal cells, we conducted RT-PCR analysis. As shown Figure 2D, the PKCδ mRNA level remained unchanged after MPP^+ treatment. PKCδ translocation was also examined by extraction of membrane and cytosolic fractions and by Western blot analysis. PKCδ did not translocate to the membrane during MPP^+ treatment (Fig 3A). Cleavage of the other major PKC isoform, PKCα (Fig 3B), was not detected either, suggesting that the PKCδ isoform is mainly activated by proteolytic cleavage during MPP^+ treatment.

Design and generation of siRNAs

To determine the functional role of proteolytic activation of PKCδ in apoptotic cell death, genetic loss-of-function analysis was performed using siRNA. Four siRNAs were designed: three targeted different positions within the coding region (siRNA-δ-1, 2 and 4) and one (siRNA-δ-3) targeted the 3'UTR of PKCδ mRNA (Fig 4A). Choice of target sites was based on previous empirical criteria (Elbashir et al., 2001b). A non-specific siRNA (siRNA-NS) was also designed to serve as a negative control. For each siRNA, sense and antisense templates were designed based on each target sequence and partial T7 promoter sequence (Fig 4B). siRNAs were prepared using an *in vitro* transcription method employing Ambion's silencer siRNA construction kit (Ambion,Austin, TX). Synthesized double stranded siRNAs were examined for transcriptional efficacy and purity in the native PAGE gel as shown in Fig 4C. All the siRNAs except siRNA-δ-3 were transcribed efficiently, as depicted by the single band of expected size. siRNAs were also labeled with Cy3-fluorescent

dye using the Ambion's silencer siRNA labeling kit (Ambion,Austin, TX) to determine the transfection efficiency as well as to identify the siRNA-transfected cells. The transfection efficiency determined by counting the number of Cy3 positive cells at 24 hr post-transfection was about 80%.

Selective suppression of PKCδ expression by siRNA

We next examined the ability of siRNAs to suppress endogenous PKCδ expression. N27 cells were transfected with 5-25 nM of siRNA-δ-1, 2, 3, 4 and siRNA-NS using the *Trans*IT-TKO transfection reagent (Mirus, Madison, WI). Cell lysates were extracted at 24 and 48 hrs post transfection and the levels of PKCδ protein expression were determined by Western blotting. siRNA-δ-1 and siRNA-δ-4 significantly suppressed PKCδ expression in a time- and dose-dependent manner (Fig 5 A&B). Densitometric analysis revealed 12%, 26%, and 66% reduction in endogenous PKCδ protein expression following transfection with 5 nM, 10 nM, and 25 nM siRNA-δ-4 for 24 hr, respectively. Unlike siRNA-δ-4, PKCδ expression was significantly reduced in siRNA-δ-1-transfected cells only at 48 hr post-transfection and densitometric analysis revealed 69% reduction following transfection with 25 nM siRNA-δ-1. On the other hand, PKCδ expression was not significantly suppressed in siRNA-δ-2- and siRNA-δ-3-transfected N27 cells at either 24 hr or 48 hr (data not shown). siRNA-NS had no silencing effect on PKCδ expression at either 24 hr or 48 hr post-transfection (Fig 5 A&B). Notably, siRNA-δ-4 and siRNA-δ-1 did not alter the expression level of the closely related novel PKC isoform PKCε, indicating their high selectivity for PKCδ (Fig 5 A&B). Moreover, temporal analysis of PKCδ expression in cells transfected with siRNA-δ-4 revealed that the

suppression of PKCδ expression by siRNA-δ-4 was maximal at 24 hr post-transfection (Fig 5C). RT-PCR analysis of PKCδ mRNA also revealed a 50% reduction in PKCδ mRNA level with siRNA-δ-4 treatment as compared to siRNA-NS treatment (Fig 5D), indicating that siRNA-δ-4 effectively degrades PKCδ transcripts, which subsequently reduces PKCδ protein expression.

In situ localization of siRNA and PKCδ immunohistochemistry

We next performed siRNA labeling and immunostaining studies to determine if PKCδ expression was specifically suppressed in siRNA-δ-4-transfected cells. After transfecting N27 cells with Cy3-labeled siRNA-δ-4, PKCδ immunostaining and Hoechst 33342 counterstaining were used to identify PKCδ protein and nucleus, respectively. PKCδ immunofluorescence revealed a strong and equal distribution of the kinase in the cytoplasm of normal N27 cells (Fig 6C). In siRNA-δ-4-transfected cells, Cy3-labeled siRNA accumulated largely in the cytoplasm at the same time PKCδ protein expression was significantly reduced, indicating that siRNA-δ-4 transfection indeed suppressed the expression of PKCδ (Fig 6A). In siRNA-NS transfected cells, merged yellow fluorescence was clearly observed, suggesting that Cy3-labeled siRNA-NS still accumulated but PKCδ protein expression was not altered at all (Fig 6B). The fluorescence intensity of PKCδ immunoreactivity was also quantified using Metamorph image analysis software. As shown in Figure 6D, siRNA-δ-4-transfected cells showed an approximate 71% reduction in PKCδ expression as compared to control cells, whereas PKCδ expression was not significantly changed in siRNA-NS-transfected cells compared to controls cells. Furthermore, cellular

morphology and integrity were not changed in siRNA-transfected N27 cells as compared to normal N27 cells, indicating that the cells tolerate siRNA treatment.

Suppression of MPP^+-induced PKCδ kinase activity and DNA fragmentation by siRNA-δ-4

To determine if siRNA-δ-4 blocks MPP^+-induced PKCδ activity, we performed an *in vitro* kinase assay following immunoprecipitation of PKCδ in control and siRNA-δ-4-transfected cells after MPP^+ exposure. PKCδ kinase activity was significantly increased by 215% in cells exposed to MPP^+ (300 μM) for 36 hr as compared to untreated control cells (Fig 7A). MPP^+ did not induce PKCδ activity in siRNA-δ-4-transfected cells, demonstrating that siRNA-δ-4 effectively suppressed PKCδ expression and thereby attenuated MPP^+-induced proteolytic activation of PKCδ. To further characterize the functional role of PKCδ activation in apoptotic cell death, we examined the effect of siRNA-δ-4 on MPP^+-induced DNA fragmentation. DNA fragmentation was increased 2-fold in N27 cells following MPP^+ treatment and was almost completely blocked in siRNA-δ-4 transfected cells (Fig 7B), demonstrating the key proapoptotic function of PKCδ in MPP^+-induced dopaminergic cell death.

Suppression of PKCδ expression by siRNA-δ-4 in primary mesencephalic neuronal cultures

The efficiency of siRNA-δ-4 at suppressing PCKδ expression was further examined in primary dopaminergic neurons. Cy3-labeled siRNAs were transfected into primary

mesencephalic cultures isolated from rat E17 embryos. Tyrosine hydroxylase (TH) and PKCδ immunostaining were performed 24 hr post-transfection to determine the efficiency of siRNA incorporation in dopaminergic neurons and to measure PKCδ expression, respectively. As depicted in Figure 8A, Cy3-labeled siRNA-δ-4 effectively incorporated in TH positive neurons and the siRNAs localized mainly in the cytoplasm. Quantitative analysis of PKCδ expression, as measured by the fluorescence intensity of PKCδ immunoreactivity, in siRNA-δ-4- or siRNA-NS-transfected TH positive neurons revealed a 42% reduction in PKCδ expression (Fig 8B). Collectively, these results demonstrate that siRNA-δ-4 efficiently incorporates in primary dopaminergic neurons and suppresses PKCδ expression.

Neuroprotective effect of siRNA-δ-4 against MPP^+-induced dopaminergic toxicity in primary mesencephalic neurons

We further examined whether or not siRNA-δ-4 protects against MPP^+-induced neurotoxicity in nigral dopaminergic neurons. TUNEL staining and nuclei counterstaining with Hoechst 33342 were employed to detect *in situ* DNA fragmentation induced by MPP^+ treatment. TUNEL and TH dual staining is complicated by MPP^+ treatment, which results in significant loss of TH positive cells. However, dopaminergic neurons in primary mesencephalic cultures can be readily identified by their large cell bodies and extensive neuronal processes as compared to other cell types. After selecting a field that contains these neurons, we performed TUNEL imaging. As shown in Figure 9A, Cy3-labeled si-RNA-δ-4 and siRNA-NS were found in the cytoplasm and around nuclei. TUNEL staining showed that MPP^+ treatment induces apoptosis in siRNA-NS treated cells. The TUNEL positive cells also

showed chromatin condensation, as observed by Hoechst 33342 staining. However, siRNA-δ-4-transfected neurons showed no TUNEL staining and the nuclei remained intact during MPP^+ treatment. These results indicate that siRNA-δ-4 prevents MPP^+-induced DNA fragmentation in primary mesencephalic neurons. To further demonstrate siRNA's protective effect in dopaminergic neurons, the number of TH positive neurons was counted; quantification of TH positive neurons is considered to be a reliable method of determining MPP^+-induced dopaminergic toxicity in primary mesencephalic cultures (Callier et al., 2002; Choi et al., 1999). Treatment with 10 μM MPP^+ for 48 hr substantially decreased the number of dopaminergic neurons by over 87% as compared to untreated control cells (Fig 9B). However, MPP^+-induced TH^+ neuronal loss was dramatically reduced to 33% in the siRNA-δ-4-transfected primary neurons, demonstrating a significant neuroprotective effect of siRNA-δ-4. siRNA-NS-transfected primary neurons were not significantly protected following MPP^+ exposure (Fig 9B). Figure 9C summarizes the actual number of TH positive neurons in each treatment group. Together, these results demonstrate that suppression of PKCδ expression by siRNA protects against dopaminergic degeneration induced by MPP^+.

Cytotoxicity testing following siRNA-δ-4 treatment

In conventional gene silencing methods such as antisense mediated knock-down, cytotoxicity is always a major concern because of the high concentration of antisense oligonucleotides introduced into cells and/or the nucleotide modifications made to the antisense probes. To investigate whether siRNA suppresses gene expression without causing significant toxicity to cells, we monitored lactate dehydrogenase (LDH) release in the

extracellular media as a marker of cytotoxicity (Kanthasamy et al., 1995). As shown in Figure 10, LDH levels in the extracellular medium of either siRNA-δ-4- or siRNA-NS-transfected cells were not significantly different from untreated control cells, indicating that siRNA treatment is not significantly toxic to mesencephalic neuronal cells.

DISCUSSION

The present study demonstrates that MPP^+ induces proteolytic activation of PKCδ in a caspase-3 dependent manner, which subsequently contributes to apoptotic cell death in mesencephalic dopaminergic cells. Notably, siRNA against rat PKCδ mRNA effectively blocked MPP^+-induced PKCδ activation and DNA fragmentation in dopaminergic neuronal cells, suggesting that PKCδ is an important proapoptotic molecule in dopaminergic degeneration. To our knowledge, this is the first report demonstrating a siRNA based neuroprotective strategy in a cell culture model of Parkinson's disease.

Oxidative stress is considered a key mediator of neurodegenerative processes in Parkinson's disease because of the extreme sensitivity of nigral dopaminergic neurons to oxidative insults (Ischiropoulos and Beckman, 2003; Jenner, 2003; Lotharius and Brundin, 2002). The Parkinsonian neurotoxin MPP^+ induced cell death model serves as an useful model to delineate the cellular mechanisms underlying degenerative process in Parkinson's disease (Kaul et al., 2003; Kaur et al., 2003; Lotharius et al., 1999). Recent studies have demonstrated that reactive oxygen species (ROS) generated from mitochondrial and/or non-mitochondrial sources (Lotharius and O'Malley, 2000) appear to contribute to MPP^+-induced

neurodegeneration (Kaur et al., 2003; Lee et al., 2000; Lotharius et al., 1999; Wu et al., 2003). MPP^+-induced ROS generation has been previously shown to promote mitochondrial cytochrome c release, caspase-9 activation and subsequently caspase-3 dependent apoptotic cell death (Jackson-Lewis et al., 1995; Viswanath et al., 2001). However, caspase-8 mediated apoptotic cascade does not seem to be critical to MPP^+-induced apoptotic cell death (Kaul et al., 2003; Vila and Przedborski, 2003). In this study, we showed that MPP^+ induces activation of caspase-3 within 36 hr of MPP^+ treatment. Our result is in agreement with recent reports which identified caspase-3 as a critical factor in the selective apoptotic cell death of dopaminergic neurons in the MPTP mouse model and in post mortem brains of patients with PD (Dodel et al., 1998; Hartmann et al., 2000). Recently, we showed that ROS scavengers and a caspase-9 inhibitor block MPP^+ induced capase-3 activation (Kaul et al., 2003). In the present study, we further demonstrate that caspase-9 inhibitor Z-LEHD-FMK significantly inhibit MPP^+ -induced PKCδ proteolytic cleavage. Taken together, these results suggest that mitochondrial mediated caspase cascade involving cytochrome c release and activation of caspase-9 and caspase-3 may be important upstream events in the proteolytic activation of PKCδ.

The downstream cellular events initiated by caspase-3 have not been clearly defined in dopaminergic cell death following exposure to MPP^+. Although the DNA repair enzymes Poly (ADP-ribose) polymerase (PARP) (Earnshaw et al., 1999; Tewari et al., 1995), DNA-PK (Itoh and Horio, 2001), and several nuclear envelope proteins (Martelli et al., 2001) are characterized as substrates of caspase-3 in non-neuronal cells, their contribution to dopaminergic neuronal cell death is unclear. Since phosphorylation is a key regulatory mechanism in apoptotic signaling, we focused our attention on the PKC isoforms in the

present study. The majority of studies have shown that activation of PKC isoforms mainly suppresses apoptosis in a variety of non-neuronal cell types (Brodie and Blumberg, 2003; Dempsey et al., 2000; Gschwendt, 1999; Kikkawa et al., 2002; Maher, 2001). However, accumulating evidence indicates that apoptotic stimuli and oxidative insults induce activation of the novel PKC isoform PKCδ (Ha et al., 2001; Kikkawa et al., 2002; Majumder et al., 2001; Otieno and Kensler, 2000; Sun et al., 2000) PKCδ can be activated through at least three different mechanisms: (i) translocation to the plasma membrane, (ii) phosphorylation at tyrosine, serine or threonine, and (iii) caspase-3-mediated proteolytic cleavage (Kikkawa et al., 2002). Our data demonstrate a persistent activation of PKCδ during MPP^+ treatment resulting from proteolytic cleavage mediated by caspase-3 that leads to permanent dissociation of the catalytic subunit of PKCδ from the regulatory subunits. The caspase-3 inhibitor Z-DEVD-FMK blocked 81% of PKCδ cleavage as determined by the densitometric analysis of Western blot data whereas a complete inhibition was observed with Z-DEVD-FMK on PKCδ activity (Fig 2C). This difference may be due to the residual effect of the cleaved fragments detected in the Western blot or may due to effectiveness of a newly prepared caspase-3 inhibitor used in the kinase assay. Furthermore, PKCδ did not translocate to the membrane, indicating that proteolytic activation is the major form of activation of PKCδ during MPP^+ treatment.

Our findings clearly demonstrate that siRNA inhibits PKCδ in an isoform specific manner, which has never been possible with the use of pharmacological inhibitors. For example, rottlerin has been widely used as an inhibitor of PKCδ (Basu et al., 2001; Reyland et al., 1999), but recent reports indicate that rottlerin can inhibit other kinases including MAP

kinases (Davies et al., 2000). The mechanisms of action of siRNA in the present study may be due to translational suppression of PKCδ because siRNA-δ-4 effectively inhibited both PKCδ mRNA (Fig. 5D) and the protein expression (Fig. 5A). Previous studies have shown the suppression of mRNA and protein levels following siRNA treatments (Hannon, 2002; Irie et al., 2002; Nagy et al., 2003). Recently, Kaasinen et al reported that PKCδ expression was induced following a kainate lesion or in ischemic brain damage (Kaasinen et al., 2002). However, we did not find any significant induction of PKCδ mRNA expression up to 36 hr of MPP^+ treatment. The induction of PKCδ expression in kainate and ischemic cell death may be related to the neuronal excitation associated with excitotoxicity. In this regard, neuronal excitation due to glutamate treatment found to increase PKCδ activation which is independent of cleavage (Ahlemeyer et al., 2002). Blockade of MPP^+-induced proteolytic activation PKCδ and DNA fragmentation by siRNA-δ-4 in N27 cells clearly establishes proapoptotic function for PKCδ in neuronal apoptosis. Tunnel staining in MPP^+-treated primary mesencephalic dopaminergic neurons further extends the apoptotic function of PKCδ in dopaminergic neuronal degeneration. In primary mesencephalic cultures, the effect of siRNA on PKCδ protein suppression (42%) and dopaminergic neuronal survival (54%) showed a reasonable correlation, further supporting the proapoptotic role of PKCδ in dopaminergic neuronal cell death.

We also found that siRNA transfected cells were phenotypically similar to control cells, suggesting that siRNA treatments are well tolerated by neuronal cells. Thus, siRNA-mediated knock-down of PKCδ appears to be an extremely effective method of gene inactivation that does not induce significant toxicity. Because of the high specificity and low

toxicity of siRNAs, the therapeutic application of this technique has recently been explored (Caplen, 2003; O'Neil et al., 2001). Xia et al., 2002 demonstrated as proof of principle that siRNA technology could attenuate neurodegeneration in an animal model of Huntington's disease.

Although the cellular events downstream of PKCδ responsible for cell death are not well understood, PKCδ has been shown to regulate a number of molecules that are associated with the cell death process including scrambalase (Frasch et al., 2000), DNA protein kinase (DNA-PK) (Bharti et al., 1998), heat-shock proteins-25/27 (Maizels et al., 1998), lamin B (Cross, 2000 #14), human RAD9 (Yoshida et al., 2003) and the redox sensitive transcription factor NF-κB (Page et al., 2003). Recently, PKCδ was also shown to translocate to the nucleus upon activation (DeVries et al., 2002). Thus, PKCδ may exert its proapoptotic function by interacting with the one or more of the downstream effectors. Studies are underway to identify key PKCδ interacting proteins that might contribute to apoptotic cell death in dopaminergic neurons.

In conclusion, we demonstrated that proteolytic activation of PKCδ facilitates dopaminergic cell death in cell culture models of PD and selective targeting of the proapoptotic kinase PKCδ by siRNA could rescue dopaminergic neurons. The proapoptotic function PKCδ in dopaminergic degeneration may have therapeutic implications in Parkinson's disease.

MATERIALS AND METHODS

Reagents

MPP^+ (1-Methyl-4-phenylpyridinium), protease cocktail, ATP, protein-A-sepharose, and anti-β-actin antibody were obtained from Sigma-Aldrich (St. Louis, MO); CaspACE® kit was purchased from Promega; Z-DEVD-FMK was obtained from Alexis Biochemicals (San Diego, CA); Z-LEHD-FMK was purchased from BD Biosciences (San Diego, CA). Ac-DEVD-AMC (Acetyl-Asp-Glu-Val-Asp-7-Amino-4-Methyl-Coumarin) and the rabbit polyclonal antibody for tyrosine hydroxylase were obtained from Calbiochem Bioscience, Inc. (King of Prussia, PA); antibodies to PKCδ, PKCα, and PKCε were purchased from Santa Cruz Biotechnology, Inc. (Santa Cruz, CA). Anti-rabbit and anti-mouse secondary antibodies and the ECL chemiluminescence kit were purchased from Amersham Pharmacia Biotech. (Piscataway, NJ). Alexa 488 conjugated anti-rabbit antibody and Hoechst 33342 were purchased from Molecular Probes, Inc. (Eugene, OR). The Cell Death Detection ELISA plus Assay Kit was purchased from Roche Molecular Biochemicals (Indianapolis, IN). [γ-^{32}P] ATP was purchased from Perkin Elmer Life Science Products (Boston, MA). The Bradford protein assay kit was purchased from Bio-Rad Laboratories (Hercules, CA). RPMI, fetal bovine serum, L-glutamine, penicillin, and streptomycin were purchased from Invitrogen (Gaithesburg, MD). The siRNA silencer construction kit and labeling kit were purchased from Ambion, Inc (Austin, TX). *Trans*IT-TKO Reagent was purchased from Mirus (Madison, WI). Oligonucleotides were synthesized and PAGE purified with Integrated DNA Technology (Iowa City, IA). Quantity One 4.2.0 software was purchased from Bio-Rad (Hercules, CA) and Vector NTI software was purchased from InforMax Inc., (Frederick,

MD). TUNEL kit was purchased from Upstate Biotechnology (Lake Placid, NY). cDNA synthesis kit and Taq enzyme were purchased from Invitrogen, Inc., (Carlsbad, CA).

Cell culture

The immortalized rat mesencephalic dopaminergic neuronal cell line (N27) was a kind gift from Dr. Kedar N. Prasad, University of Colorado Health Sciences Center (Denver, CO). N27 cells were grown in RPMI 1640 medium containing 10% fetal bovine serum, 2 mM L-glutamine, 50 units penicillin, and 50 μg/ml streptomycin. Cells were grown in a humidified atmosphere of 5% CO_2 at 37^0C as previously described (Anantharam et al., 2002; Kitazawa et al., 2003), and 4-5 days old cells were used for the experiments.

Primary mesencephalic neuronal culture

Primary mesencephalic neuronal cultures were prepared from the ventral mesencephalon of gestational 16-17 day old rat embryos as described in detail elsewhere (Madhavan et al., 2003; Wang et al., 1995). Briefly, dissected tissues were maintained on ice cold calcium free EBSS supplemented with gentomycin (50 mg/ml) and penicillin/streptomycin (200units/ml) and then dissociated in EBSS solution containing trypsin (0.25%) for 15 min. The dissociated cells were plated at equal density (0.5×10^6 cells) in 30 mm diameter tissue culture wells pre-coated with poly-L-lysine (1 mg/ml). Cultures were maintained in a chemically defined, serum-free medium consisting of neurobasal medium fortified with B-27 supplements, L-Glutamine (500 μM), penicillin (100 IU/ml) and streptomycin (100 μg/ml) (Life Technologies). The cells were maintained in a humidified CO_2 incubator (5% CO_2, 37°C) for 24 hr and then treated with cytosine

arabinoside (10 μM) for 24 hr to inhibit glial cell proliferation. Half of the culture medium was replaced every 2 days. Approximately 6-7 day old cultures were used for experiments.

Treatment paradigm

Transfected and untransfected N27 cells were treated with 300 μM MPP^+ for 36 to 42 hr at 37°C. Primary neuron was exposed to 10μM MPP^+ for 48hr. MPP^+ was added to siRNA transfected cells 24 hr post-transfection. In caspase-3 and caspase-9 inhibitor studies, cells were co-treated with Z-DEVD-FMK or Z-LEHD-FMK and MPP^+. Untreated cells were used as a negative control.

Design and preparation of siRNAs

siRNAs were prepared by an *in vitro* transcription method. Target sites were selected based on previously established empirical criteria (Elbashir et al., 2001b) Initially, four siRNA (siRNA-δ-1, δ-2, δ-3, and δ-4) target sites specific to rat PKCδ mRNA (gi: 18959249), as determined by blast analysis, were chosen. One non-specific siRNA (siRNA-NS) was also chosen based on random sequence. For each siRNA, sense and antisense templates were designed based on each target sequence and partial T7 promoter sequence (Donze and Picard, 2002). All template oligonucleotides were chemically synthesized and PAGE purified. *In vitro* transcription, annealing, and purification of siRNA duplexes were performed using the protocol supplied with the silencer siRNA construction kit (Ambion, Inc. Austin, TX). Briefly, ~ 2 μg of each single-strand (ss) transcription template was first annealed with the T7 promoter and filled in by Klenow DNA polymerase to form double-strand transcription templates. For preparation of each siRNA duplex, transcription reactions

were first performed with separated antisense and sense templates using the T7 RNA polymerase provided with the kit and then annealed to form siRNA duplexes. Then the siRNA duplex was treated with DNase and RNase to remove the extra nucleotides of transcribed siRNA to meet the structural 3'UU overhang and 5'phosphate requirement (Elbashir et al., 2001b).

siRNA transfection

N27 Cells (50-70% confluency) and primary mesencephalic neurons were transfected with siRNA duplexes using the protocol supplied with the *Trans*IT-TKO Reagent (Mirus Corp, Madison, WI). Briefly, the TKO reagent was first diluted (1:100) into RPMI 1640 medium for about 15 min, and then the siRNA duplex was added to the medium to form a lipid-siRNA complex. Following additional 15 min incubation, transfection was initiated by adding the lipid-siRNA complex to 24-well or 6-well plates. The final concentration of siRNA varied from 5 to 25 nM.

Cy3 labeling of siRNAs

Purified siRNA duplexes were labeled using the silencer siRNA labeling kit (Ambion, Austin, TX). Briefly, ~5 μg siRNA duplex was added to the Cy3 labeling reagent and the reaction mixture was then incubated at 37°C in the dark for 1 hr. The unlabeled Cy3 was removed by ethanol precipitation. The labeled siRNAs were then delivered to cells by transfection. Cy3 labeled siRNAs in transfected cells were visualized using a Nikon inverted fluorescence microscope (Model TE-2000U) and pictures were captured with a SPOT digital camera (Diagnostic Instruments, Sterling Heights, MI).

Isolation of cytoplasmic fractions

Cytoplasmic fractions were isolated as described previously (Anantharam et al., 2002). Briefly, after treatment, the N27 cells were harvested with trypsin/EDTA solution and spun at 200 x g for 5 min. Cell pellets were then washed twice with ice-cold PBS (1 mM sodium phosphate, 15 mM NaCl, and pH 7.4) and resuspended in 200 μl of hypotonic buffer (10 mM HEPES, pH 7.9, 1.5 mM $MgCl_2$, 10 mM KCl, 1 mM DTT, and protease inhibitor cocktail diluted 1:100). Triton-X 100 (final concentration 0.5%) was then added to the homogenization and vortexed vigorously for 15 sec. Cell lysates were centrifuged for 30 min at 14,000 rpm and supernatants were collected. Protein concentrations were determined using a Bradford protein assay kit.

Western blotting

Equal amounts of cytoplasmic protein (10-20μg) were loaded in each lane and separated on a 10% SDS-polyacrylamide gel as described previously (Anantharam et al., 2002). Proteins were then transferred to nitrocellulose membrane by electro-blotting overnight (4°C, 25 V). Non-specific binding sites were blocked by treating the nitrocellulose membranes with 5% non-fat dry milk TBST solution (10 mM Tris, 150 mM NaCl, and 0.1% Tween 20) for 1 hr. The nitrocellulose membranes were then incubated with primary antibodies for 1 hr at RT (anti-PKCα, δ or ε antibodies, 1:2000). The primary antibody treatment was followed by treatment with secondary HRP-conjugated anti-rabbit or anti-mouse IgG (1:2000) for 1 hr at RT. Secondary antibody-bound proteins were detected using an ECL chemiluminescence kit (Amersham). To confirm equal protein loading, blots were

reprobed with β-actin antibody (1:5000). Gel photographs and densitometric analysis were performed with a Kodak image station (Model 1000R, Rochester, New York).

RT-PCR

After treatment, cells were lysed in 1 ml TRIZOL reagent and total RNA was isolated by chloroform extraction and precipitated by ethanol. First, total RNA was treated with DNase I to remove DNA contamination and then reversely transcribed into first strand cDNA using the SuperScript III first-strand synthesis system (Invitrogen, Inc, Carlsbad, CA) as described in the kit instructions. Quantitative PCR was performed with PKCδ primers and control GAPDH primers as previously described (Suzuki et al., 2000). The primer sequences used were as follows: rat PKCδ – forward: 5' gggctacgttttatgcagct 3'; reverse: 5' agcaggtctgggagctcact 3'; rat GAPDH - forward: 5' atgggaagctggtcatcaac 3'; reverse: 5' tgtagcccaggatgccctt 3'. The PCR reaction was performed in DNA thermal cycler. The amplified products were visualized on agarose gel impregnated with ethidium bromide and the intensity of amplified products was measured with a Kodak image station.

Immunocytochemistry

Immunostaining of PKCδ was performed 24 hr post-transfection in untransfected, Cy3-siRNA-δ-4, and Cy3-siRNA-NS transfected N27 cells. Cells grown on poly L-lysine coated glass cover slips were gently washed with PBS twice, fixed in 4% paraformaldehyde, washed 3 X 7 min with PBS, permeabilized, and blocked with blocking reagent (0.4% BSA, 5% goat serum, and 0.2% Triton-X 100 in PBS) for 20 min. Cells were then incubated with

anti-PKCδ rabbit polyclonal antibody (1:200 in blocking reagent) overnight at 4°C and then washed 4 X 8 min with PBS. PKCδ was visualized by incubation with Alexa 488-conjugated goat anti-rabbit secondary antibody (1:200 in PBS) at RT for 90 min. After another 4 X 8 min PBS wash, Hoechst 33342 (final concentration of 10 μg/ml in PBS) was added to stain the cell nuclei at RT for 3 min. Finally, cells were washed once in PBS and mounted on a slide with Antifade mounting medium. The cells were observed under a Nikon inverted fluorescence microscope (Model TE-2000U) and pictures were captured with a SPOT digital camera (Diagnostic Instruments, Sterling Heights, MI). For primary neurons, immunostaining of TH was performed using rabbit polyclonal TH antibody (1:200). Quantitative analysis of immuno fluorescence was measured by defining the region of interest (RO1) in Metamorph image analysis software and plotted in Prism software.

Immunoprecipitation kinase assay

PKCδ enzymatic activity was assayed using an immunoprecipitation kinase assay as previously described (Anantharam et al., 2002). After treatment with MPP^+, N27 cells were washed twice with PBS and resuspended in 200 μl of PKC lysis buffer (25 mM HEPES, pH 7.5, 20 mM β-glycerophosphate, 0.1 mM sodium orthovanadate, 0.1% Triton X 100, 0.3 M NaCl, 1.5 mM $MgCl_2$, 0.2 mM EDTA, 0.5 mM DTT, 10 mM NaF, and 4 μg/ml each of aprotonin and leupeptin). The cells were homogenized by sonication for 15 sec under ice-cold conditions. The cytoplasmic factions were collected by centrifuging the cell lysates at 14,000 x g for 30 min. Protein concentrations were determined by Bradford protein assay. Cytoplasmic protein (0.2-0.4 mg) was immunoprecipitated overnight at 4°C using 4 μg of

anti-PKCδ antibody. The immunoprecipitates were then incubated with protein-A–sepharose for 1 hr at 4°C. The protein-A bound antigen-antibody complexes were then washed 3 times with PKC lysis buffer, 3 times with kinase buffer (40 mM Tris, pH 7.4, 20 mM $MgCl_2$, 20 μM ATP, and 2.5 mM $CaCl_2$), and resuspended in 20 μl of kinase buffer. Reactions were started by adding 20 μl of reaction buffer containing 0.4 mg Histone H1 and 5 μCi of [γ-^{32}P] ATP (3,000 Ci/mM) to the immunoprecipitated samples and incubated for 10 min at 30°C. SDS gel loading buffer (2X) was then added to terminate the reaction, the samples were boiled for 5 min, and the products were separated on a 12% SDS-PAGE gel. The phosphorylated H1 histone bands were detected using a Personal Molecular Imager (FX model, Bio-Rad) and quantified using Quantity One 4.2.0 software (Bio-Rad, Hercules, CA).

Enzymatic assay for caspase-3

Caspase-3 activity was measured as previously described (Yoshimura et al., 1998). Briefly, cells were spun down after treatment and the pellets were lysed with Tris buffer (pH 7.4, 50 mM Tris HCl, 1 mM EDTA, and 10 mM EGTA) containing 10 μM digitonin for 15 min at 37°C. Lysates were centrifuged at 900 x g for 3 min and the resulting supernatants were incubated with a specific fluorogenic caspase-3 substrate (Ac-DEVD-AMC, 10 μM) at 37°C for 1 hr. Cleaved substrate was monitored at excitation λ 380 nm and emission λ 460 nm using a multiwell fluorescence plate reader (Model: Gemini XS, Molecular Devices, Sunnyvale, CA). Caspase-3 activity was calculated as fluorescence units per mg protein per hour and expressed as percentage of control.

In situ analysis of caspase activity

A cell-permeable fluorescent probe FITC-VAD-FMK was used in this assay. The experimental procedure was performed according to Promega's CaspACE® kit, with some minor modifications. N27 cells were grown on poly-L lysine (0.1 mg/ml) coated cover slips for 24 hrs. After exposure to MPP^+, the cells were treated with 10 μM FITC-VAD-FMK for 20 min at 37°C in the dark. Cells were then rinsed once with PBS and fixed with 10% buffered formalin for 30 min at room temperature in the dark. After fixation, the cells were washed twice and observed under a Nikon Diaphot microscope. Pictures were captured with a SPOT digital camera (Diagnostic Instruments, Sterling Heights, MI).

Quantification assay for DNA fragmentation

DNA fragmentation was measured using a recently developed Cell Death Detection ELISA plus Assay Kit (Molecular Biochemicals, Indianapolis, IN) (Anantharam et al., 2002; Reyland et al., 1999). Briefly, cells were spun down at 200 x g for 5 min and washed twice with 1X PBS. Cells were then incubated with a lysis buffer (supplied with the kit) at RT. After 30 min, samples were centrifuged and 20 μl aliquots of the supernatant were then dispensed into streptavidin-coated 96 well microtiter plates followed by addition of 80 μl of HRP-conjugated antibody cocktail, and incubated for 2 hr at RT with mild shaking. After incubation, unbound components were removed by washing with the incubation buffer supplied with the kit. The nucleosomes retained by the antibody cocktail in the immunocomplex were quantified spectrophotometrically with ABTS as an HRP substrate. Measurements were made at 405 nm and 490 nm using a SpectroMax 190 spectrophotometer

(Molecular Devices, Sunnyvale, CA). The difference of absorbance between OD 405 and OD 490 nm was used to measure the actual DNA fragmentation level.

TUNEL staining

Primary neurons were cultured on coverslip in 6-well plates. After siRNA transfection and MPP^+ treatment, cells were washed by 1X PBS and fixed with 4% paraformaldehyde for 15min and permeabolized with 0.2% Triton-X containing 0.2% BSA in PBS for another 15 min. Cells were then incubated in TdT end-labeling cocktail (50μl/coverslip) containing Biotin-dUTP, TdT buffer and TdT for 60 min at RT and reaction was stopped by immersing cells in 1X TB buffer. After the wash, the neurons were incubated in blocking reagent containing avidin-FITC for 30 min at RT and then washed with 1X PBS. Nucleus counterstaining was then performed by incubating cells with Hoechst 33342 for 3 min. Cells were washed with 1X PBS and mounted on slides. The cells were observed and pictures captured as described in the immunocytochemistry section. Quantitative analysis of fluorescence immunoreactivity was measured by defining the region of interests (ROI) in Metamorph software and plotted in Prism software.

Lactate Dehydrogenase (LDH) Assay

LDH activity in the cell-free extracellular supernatant was quantified as an index of cell death (Kanthasamy et al., 1995). We modified the original method to a 96-well format (Kitazawa et al., 2001). Briefly, both untransfected and siRNA transfected N27 cells were plated in 96-well plate and 24 hr after transfection 10 μl of the extracellular supernatant was added to 200 μl of 0.08 M Tris buffer (pH 7.2) containing 0.2 M NaCl, 0.2 mM NADH, and

1.6 mM sodium pyruvate. LDH activity was measured continuously by monitoring the decrease in the rate of absorbance at 339 nm using a microplate reader (Molecular Devices, Sunnyvale, CA) and the temperature was maintained at 37°C during reading. Changes in absorbance per minute ($\delta A/\delta T$) were used to calculate LDH activity (U/I), using the following equation: $U/I = (\delta A/\delta T) \times 9682 \times 0.66$, where 9682 was a coefficient factor, and 0.66 was a correction factor at 37°C.

Data analysis

Data analysis was performed using Prism 3.0 software (GraphPad Software, San Diego, CA). Data from PKCδ kinase, DNA fragmentation and LDH assays were first analyzed using one-way ANOVA. Bonferroni's post-test was then performed to compare all groups and differences with $p<0.05$ were considered significant. To analyze the caspase-3 enzymatic activity results, the paired t-test was used.

ACKNOWLEDGEMENTS

This study was supported by the National Institute of Health (NIH) grants NS38644 and ES10586.

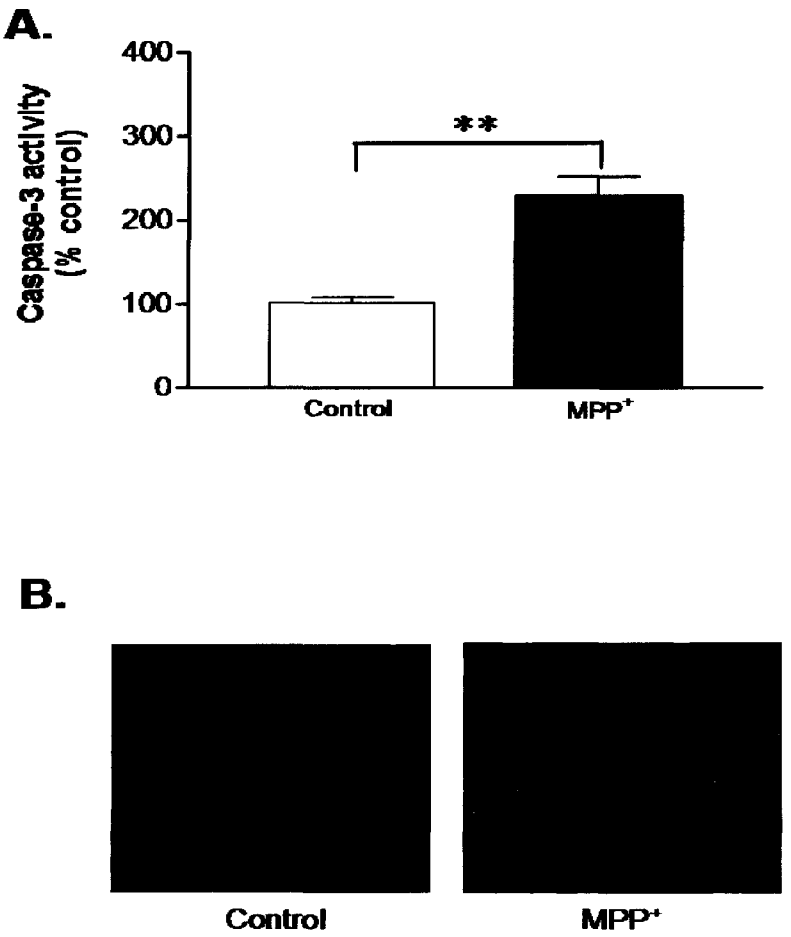

Figure1: MPP^+ treatment activates caspase-3 in rat mesencephalic dopaminergic neuronal (N27) cells.

(A) Caspase-3 enzyme activity increases significantly after MPP^+ (300 μM) exposure for 36 hr. Caspase-3 activity was assayed using a specific fluorogenic substrate, Ac-DEVD-AMC (10 μM), as described in the Methods. The data represent the mean ± SEM from two separate experiments in triplicate (**, $p<0.01$; N=6). (B) MPP^+ (300 μM) treatment for 36 hr also induces caspase activation as observed by in situ staining using FITC-VAD-FMK as a substrate.

Figure 2: Caspase-3 and Caspase-9 cascade mediate MPP^+-induced proteolytic activation of PKCδ in N27 cells.

A) Co-treatment with Z-DEVD-FMK (50 μM) blocks the MPP^+ (300 μM) induced proteolytic cleavage of PKCδ cleavage (38-41 kDa), *(B)* Caspase-9 inhibitor Z-LEHD-FMK (50μM) also blocks proteolytic cleavage of PKCδ, (C) MPP^+ induced PKCδ kinase activity is suppressed by caspase-3 inhibitor with Z-DEVD-FMK (50 μM), and *(D)* No change in PKCδ mRNA level during MPP^+ treatment as measured by RT-PCR. Cells were treated with 300 μM MPP^+ for 36 hr in the presence or absence of caspase inhibitors. Cells were then lysed and the lysate was used for Western blot analysis and kinase assay. To confirm equal protein loading in Western blot, the membranes were reprobed with β-actin antibody. For RT-PCR analysis, total mRNA was isolated from MPP^+ (300 μM for 36 hr) treated cells and then reverse transcription was performed with the use of Superscript III first-strand synthesis system (Invitrogen, Carlsbad, CA). GAPDH was used as internal control. Images are representative from three separate experiments. The kinase assay data represent the mean ± SEM from two separate experiments in triplicate (***, $p<0.001$; N=6).

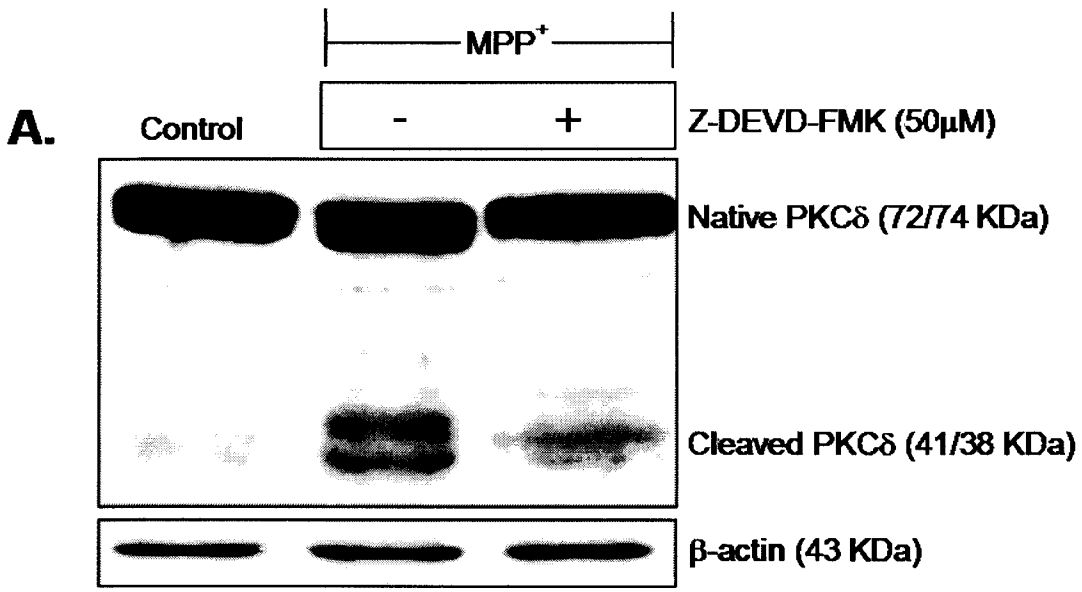
A.
MPP+
Control
-
+
Z-DEVD-FMK (50μM)
Native PKCδ (72/74 KDa)
Cleaved PKCδ (41/38 KDa)
β-actin (43 KDa)

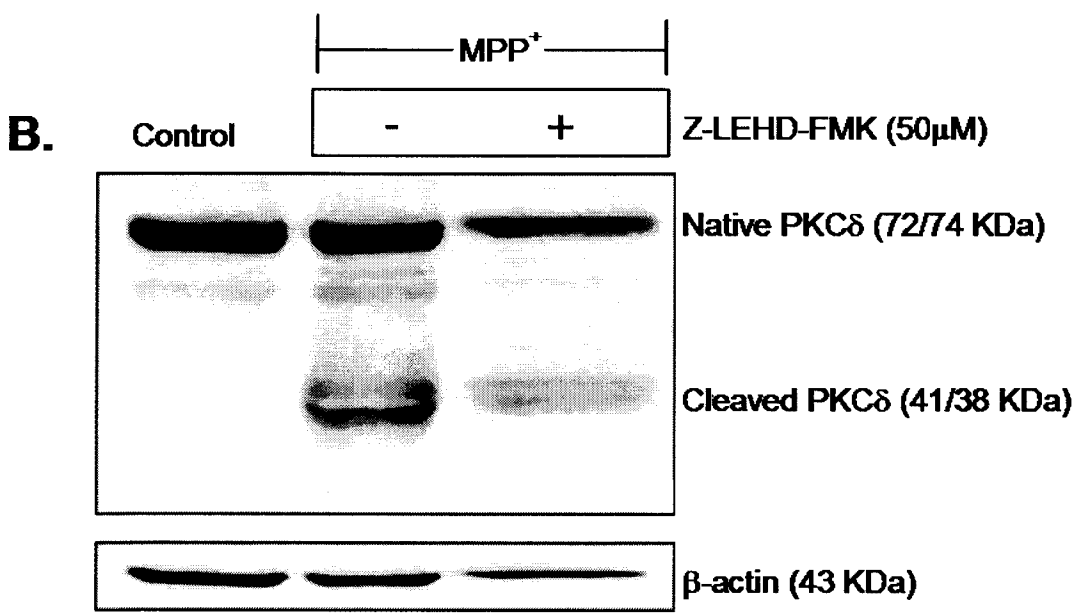
B.
MPP+
Control
-
+
Z-LEHD-FMK (50μM)
Native PKCδ (72/74 KDa)
Cleaved PKCδ (41/38 KDa)
β-actin (43 KDa)

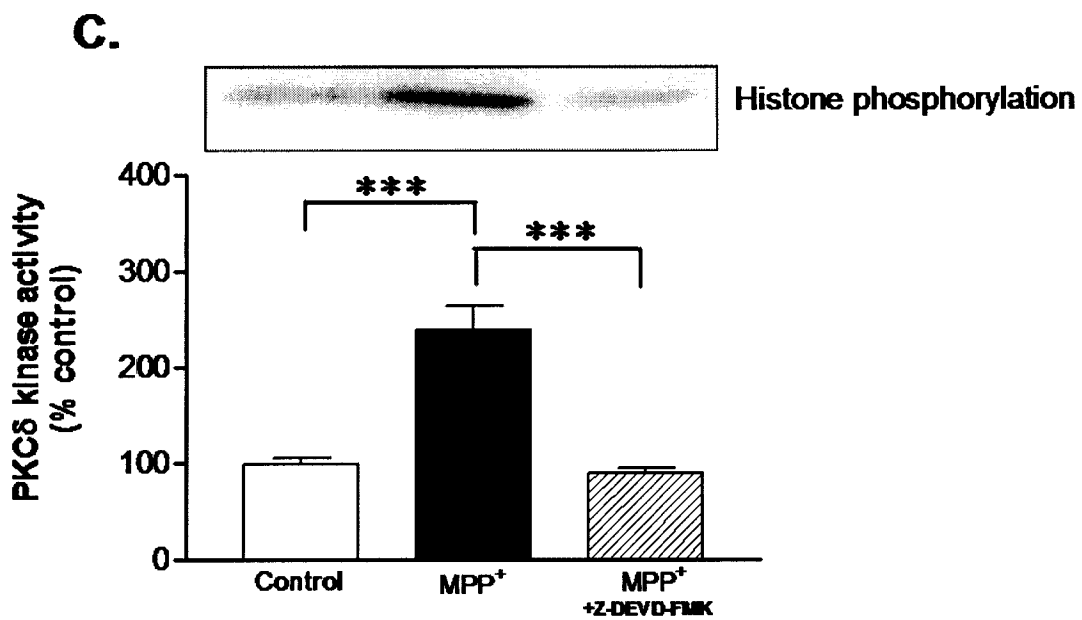
C.
Histone phosphorylation
PKCδ kinase activity
(% control)
400
300
200
100
0
***
***
Control
MPP+
MPP+
+Z-DEVD-FMK

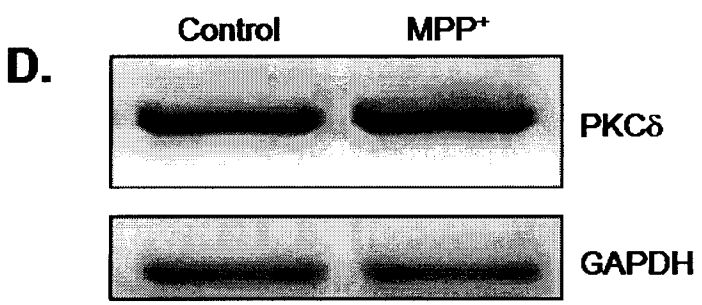
D.
Control
MPP+
PKCδ
GAPDH

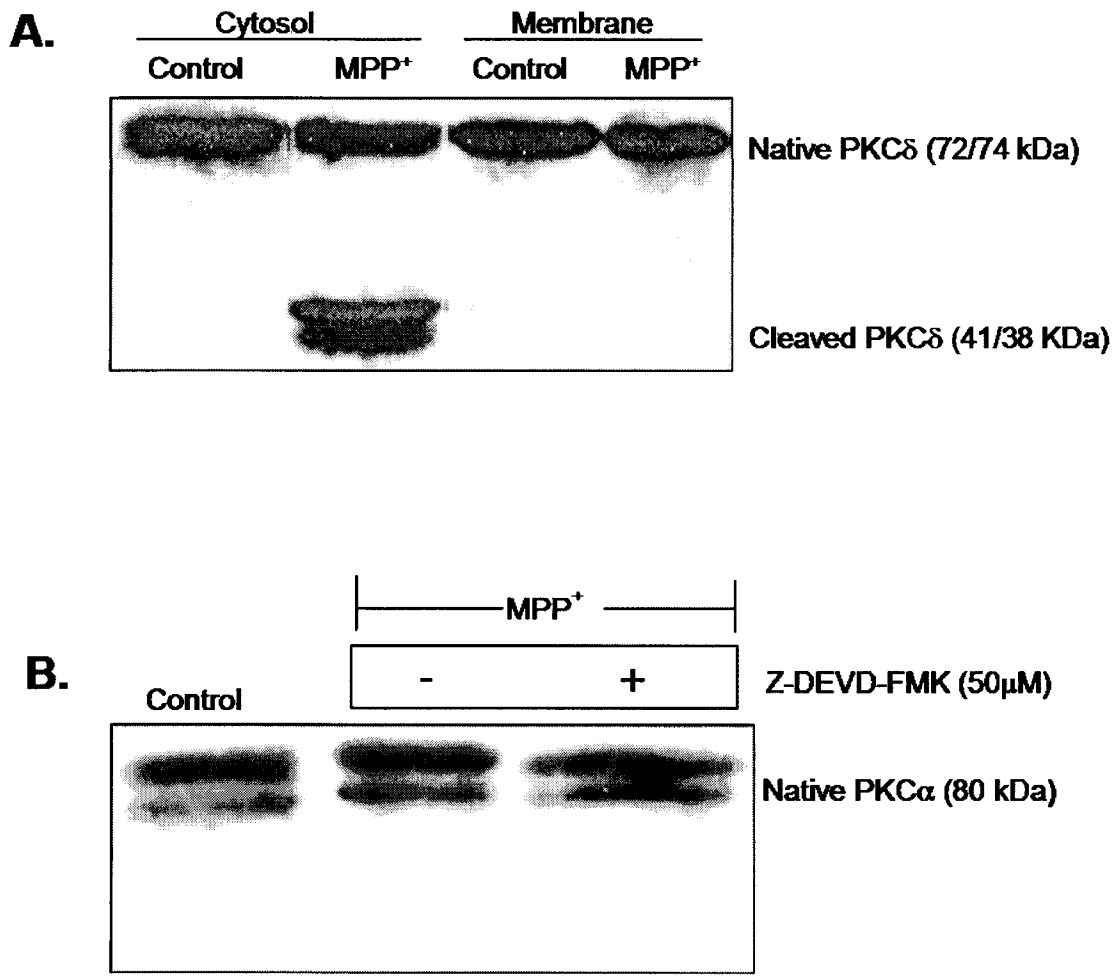

Figure 3: Specificity of proteolytic activation of PKCδ during MPP^+ treatment

(A) No membrane translocation of PKCδ following MPP^+ treatment. After treatment with 300 μM MPP^+ for 36 hr, cytosol and membrane fractions were separated and used for determining PKCδ translocation. (B) No proteolytic activation of PKCα during MPP^+ treatment. Whole cell lysates were prepared after MPP^+ (300 μM) treatment for determining PKCα cleavage. All experiments were repeated three times and representative images are presented.

Figure 4: Design and Synthesis of siRNAs against PKCδ.

(A) Schematic representation of the primary structure of rat PKCδ mRNA (gi: 18959249) and four target sites of siRNA. The exact position of each target site was shown in the diagram and GC% was calculated with Vector NTI software (InforMax Inc., Frederick, MD). (B) Template sequences of siRNA duplexes. A pair of sense and antisense templates was designed to generate siRNA duplexes. The partial T7 promoter sequence (underlined) was also included in each template. All oligonucleotides were synthesized and PAGE purified by Integrated DNA Technology (Iowa City, IA). (C) In vitro transcription of siRNA. In vitro transcription, annealing, and purification of siRNA duplexes were performed using the protocol supplied with the silencer siRNA kit (Ambion Inc, Austin, TX). The siRNAs were separated on 12% PAGE and visualized by ethidium bromide staining. All siRNAs except siRNA-δ-3 showed the specific transcription products of expected size.

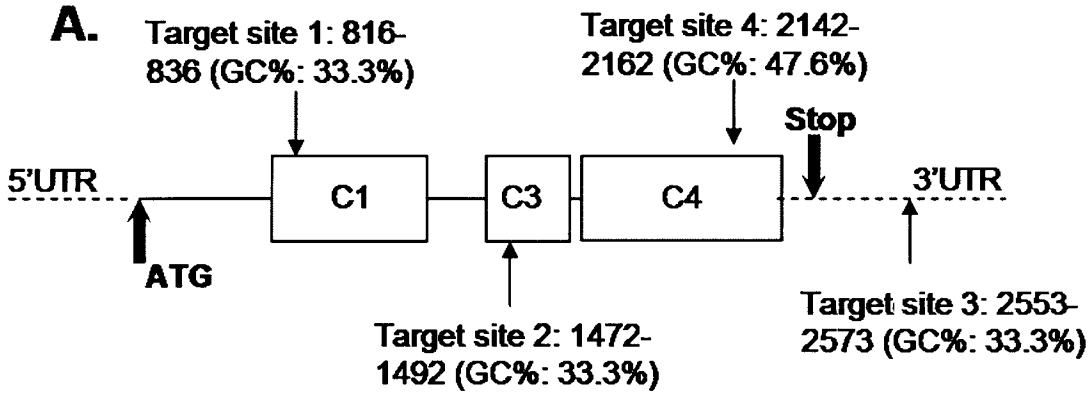

B.

siRNA-δ-1:
Antisense: 5′-AAGATTCACTACATCAAGAACCCTGTCTC-3′
Sense: 5′-AAGTTCTTGATGTAGTGAATCCCTGTCTC-3′

siRNA-δ-2:
Antisense: 5′-AAGGTACTTTGCAATCAAGTACCTGTCTC-3′
Sense: 5′-AATACTTGATTGCAAAGTACCCCTGTCTC-3′

siRNA-δ-3:
Antisense: 5′-AACATCAGGCTTCACCCCTTTCCTGTCTC-3′
Sense: 5′-AAAAAGGGGTGAAGCCTGATGCCTGTCTC-3′

siRNA-δ-4
Antisense: 5′-AACTGTTTGTGAATTTGCCTTCCTGTCTC-3′
Sense: 5′-AAAAGGCAAATTCACAAACAGCCTGTCTC-3′

siRNA-NS (non-specific control):
Antisense: 5′-AATTCTCACACTTCGGAGAACCCTGTCTC-3′
Sense: 5′-AAGTTCTCCGAAGTGTGAGAACCTGTCTC-3′

C.

Figure 5: Suppression of PKCδ expression in N27 cells transfected with siRNA-δ-1 and siRNA-δ-4.

(A) Isoform specific suppression of PKCδ expression at 24hr post-transfection with siRNA-δ-4, (B) Isoform specific suppression of PKCδ expression at 48hr post-transfection with siRNA-δ-1, (C) Time course analysis of PKCδ expression in cells transfected with siRNA-δ-4. (D) RT-PCR analysis of PKCδ mRNA expression in siRNA-δ-4 and siRNA-NS transfected N27 cells. PKCδ expression in N27 cells transfected with different siRNAs was determined by immunoblotting at 24 hr and 48hr post transfection. Final concentrations of siRNAs varied from 5 nM to 25 nM. To examine the specificity of siRNAs and verify equal protein loading, the membranes were reprobed with PKCε (90 kDa), one of the closest isoforms of PKCδ, and β-actin (43 kDa) antibodies, respectively. For RT-PCR analysis, total mRNA was extracted 24 hr after siRNA transfection. All experiments were repeated three times and representative images are presented.

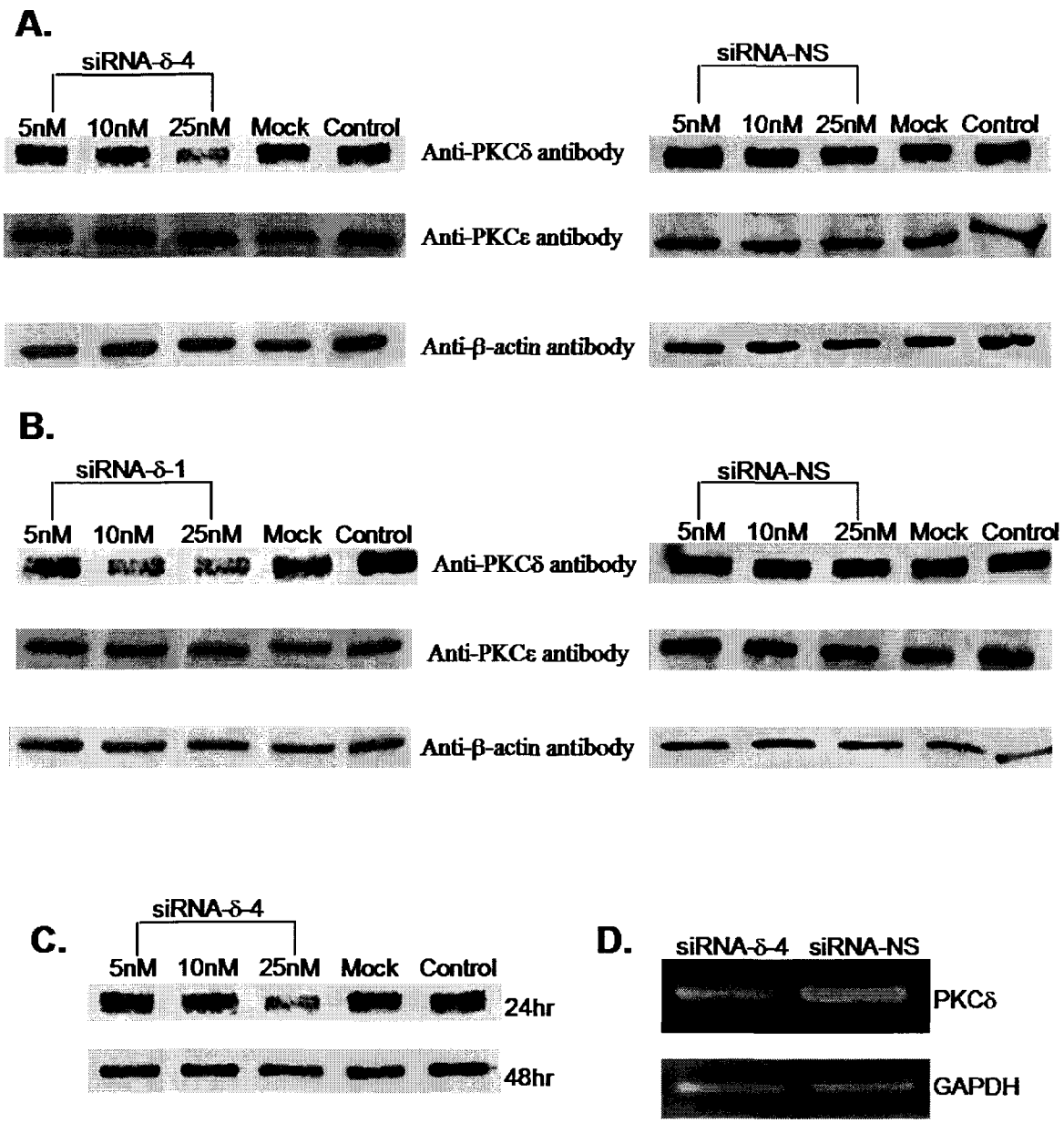
A.
siRNA-δ-4
5nM 10nM 25nM Mock Control
siRNA-NS
5nM 10nM 25nM Mock Control
Anti-PKCδ antibody
Anti-PKCε antibody
Anti-β-actin antibody
B.
siRNA-δ-1
5nM 10nM 25nM Mock Control
siRNA-NS
5nM 10nM 25nM Mock Control
Anti-PKCδ antibody
Anti-PKCε antibody
Anti-β-actin antibody
C.
siRNA-δ-4
5nM 10nM 25nM Mock Control
24hr
48hr
D.
siRNA-δ-4 siRNA-NS
PKCδ
GAPDH

Figure 6: *In situ* localization of siRNA and immunochemistry of PKCδ in siRNA transfected N27 cells.

(A) Cells transfected with Cy3-labeled siRNA-δ-4 (25 nM) showing greatly reduced PKCδ expression. (B) Cells transfected with Cy3-labeled siRNA-NS (25 nM) showing no change in PKCδ expression. (C) Untransfected N27 cells showing normal PKCδ expression. (D) Quantitiative analysis of in situ suppression of PKCδ expression by siRNA-δ-4 in N27 cells. For PKCδ immunostaining, cells were permeablized and incubated with PKCδ antibody 24 hr post-transfection and then visualized with Alexa 488 (green) conjugated anti-rabbit antibody. siRNA was visualized by labeled Cy3 (red) fluorescence. The nuclei were visualized by Hoechst 33342 counterstaining (blue). Cy3-labeled siRNAs were prepared prior to transfection according to the silencer siRNA labeling kit (Ambion Inc, Austin, TX). Cells were observed under a Nikon inverted fluorescence microscope and pictures were captured with a SPOT digital camera (Diagnostic Instruments, Sterling Heights, MI). For in situ quantitative analysis of PKCδ expression, fluorescence immunoreactivity of PKCδ was measured in each group using Metamorph image software and data plotted in Prism software. Experiments were repeated three times and representative images are presented.

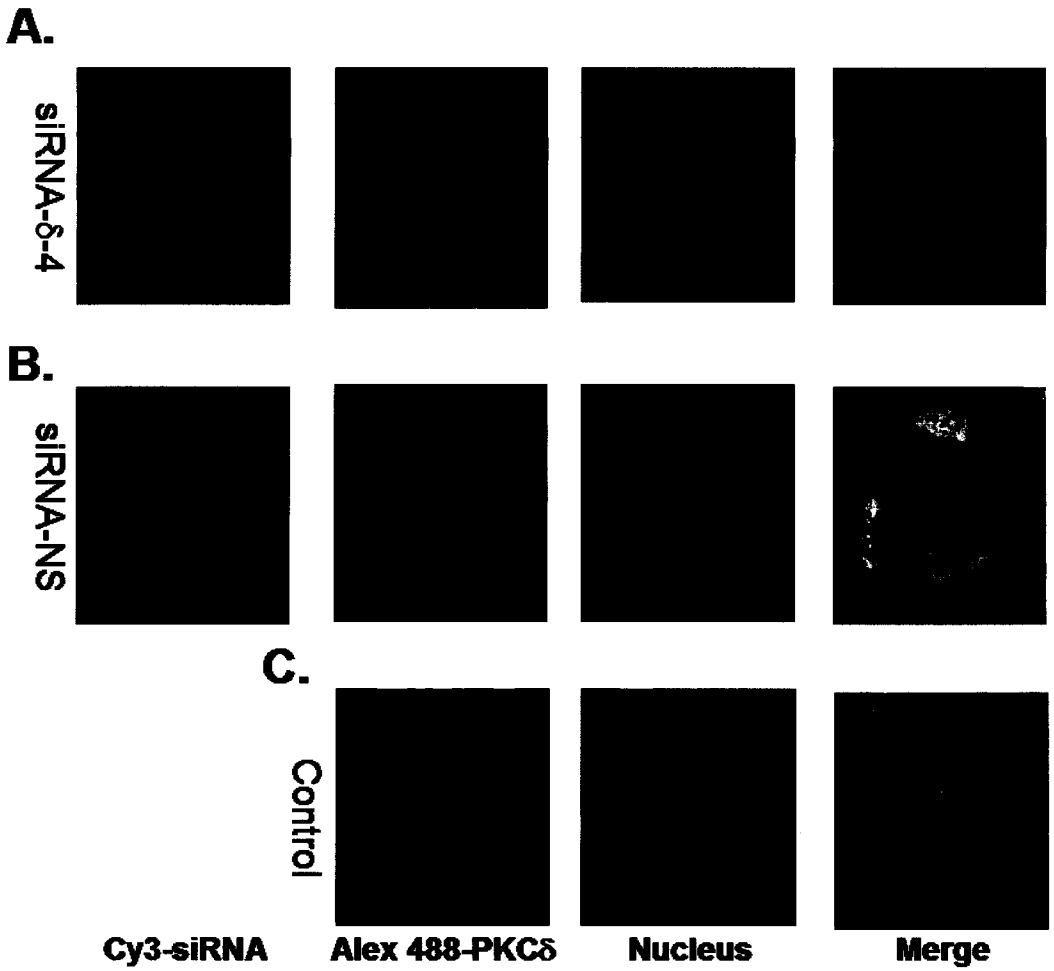
A.
siRNA-δ-4
B.
siRNA-NS
C.
Control
Cy3-siRNA
Alex 488-PKCδ
Nucleus
Merge

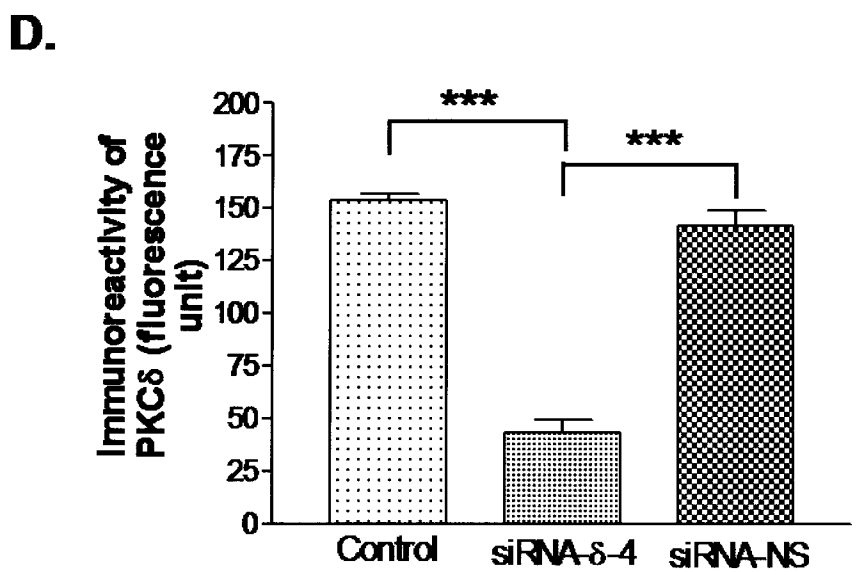
D.
Immunoreactivity of PKCδ (fluorescence unit)
200
175
150
125
100
75
50
25
0
***
***
Control
siRNA-δ-4
siRNA-NS

Figure 7: Ablation of MPP^+-induced PKCδ kinase activity and DNA fragmentation by siRNA-δ-4 in mesencephalic dopaminergic neuronal cells.

(A) Transfection of siRNA-δ-4 prior to MPP^+ exposure (300 μM for 36 hr) reduces PKCδ kinase activity to the control level. (B) Transfection of siRNA-δ-4 almost completely protects cells against MPP^+-induced DNA fragmentation. Sub-confluent cultures of N27 cells were transfected with siRNA-δ-4 (25 nM) for 24 hr and the cells were treated with MPP^+ for 42 hr. After exposure to MPP^+, the N27 cells were harvested, lysed, and analyzed. Untransfected N27 cells not exposed to MPP^+ were used as controls. The data represent the mean ± SEM from two separate experiments in triplicate (*, $p<0.05$; **, $p<0.01$ and ***, $p<0.001$; N=6).

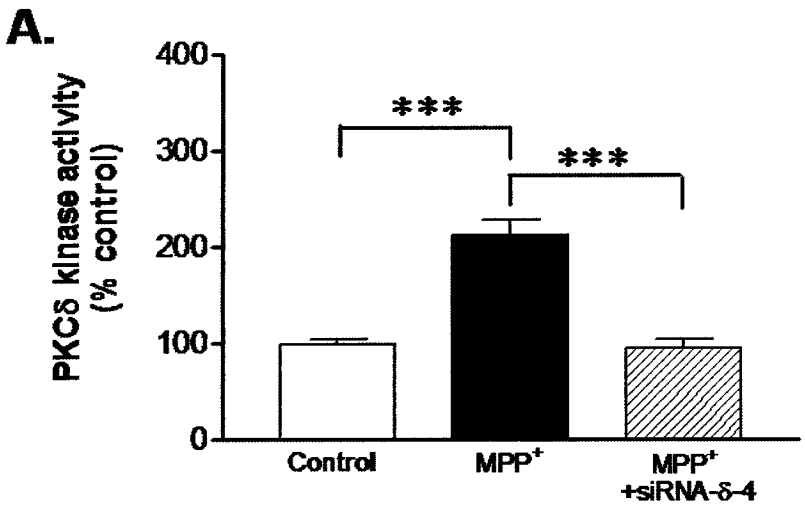
A.
PKCδ kinase activity
(% control)
400
300
200
100
0
***
***
Control
MPP+
MPP+
+siRNA-δ-4

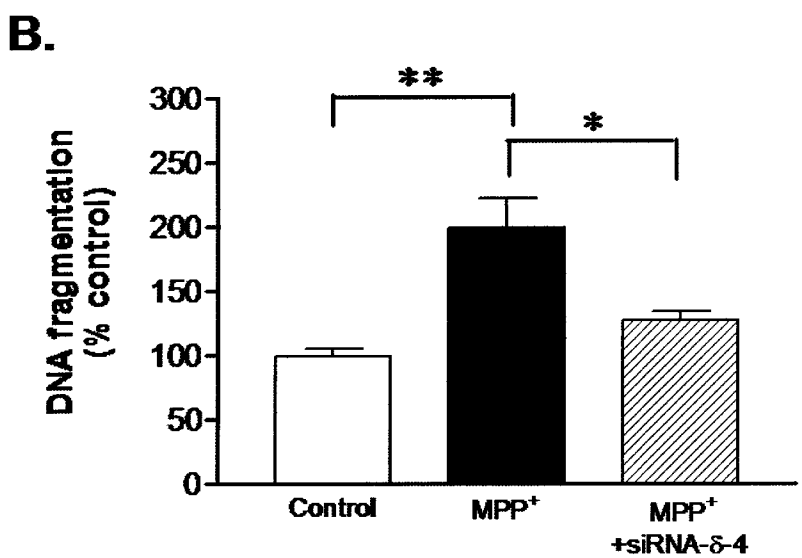
B.
DNA fragmentation
(% control)
300
250
200
150
100
50
0
**
*
Control
MPP+
MPP+
+siRNA-δ-4

Figure 8: *In situ* suppression of PKCδ expression by siRNA-δ-4 in primary mesencephalic cultures.

(A) Localization of siRNA-δ-4 in TH positive neuron. (B) Quantitative analysis of in situ suppression of PKCδ by siRNA-δ-4 in primary mesencephalic cells. Primary mesencephalic neurons were cultured from E15 rat embryo midbrain and then transfected with Cy3-labelled siRNA (red). PKCδ or TH immunostaining was performed 24hr post-transfection of siRNA, by using PKCδ or TH antibodies and then visualized separately with Alexa 488 (green) conjugated anti-rabbit antibody. The nuclei were counterstained by Hoechst 33342 (blue). Stained primary neurons were observed under a Nikon inverted fluorescence microscope and pictures were captured with a SPOT digital camera (Diagnostic Instruments, Sterling Heights, MI). For in situ quantitative analysis of PKCδ expression, fluorescence immunoreactivity of PKCδ was measured from neurons in each group using Metamorph software and the data plotted in Prism software. The data represent the mean $\pm$ SEM from two separate experiments in triplicate (*, $p<0.05$; N=6).

A.

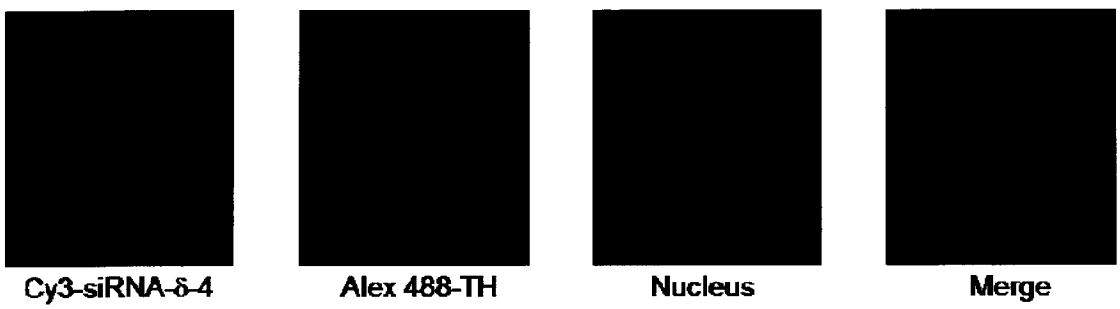
Cy3-siRNA-δ-4
Alex 488-TH
Nucleus
Merge

B.

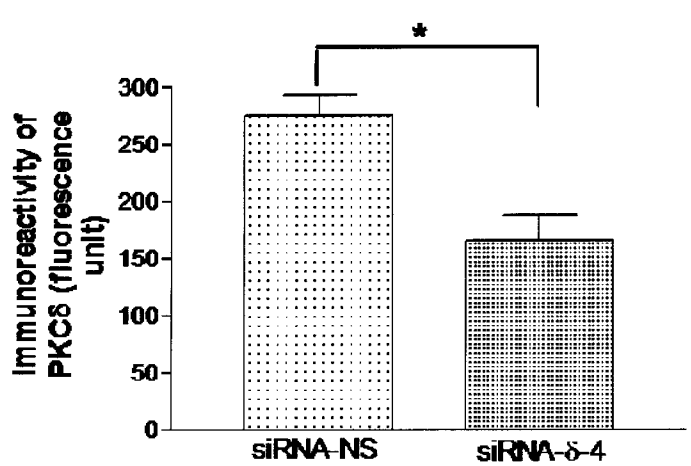
*
Immunoreactivity of PKCδ (fluorescence unit)
300
250
200
150
100
50
0
siRNA-NS
siRNA-δ-4

Figure 9: siRNA-δ-4 prevents MPP^+-induced apoptotic death in primary mesencephalic TH positive neurons.

(A) TUNEL staining in MPP^+ treated rat primary mesencephalic neurons. Primary mesencephalic cultures were transfected with Cy3 labeled siRNAs and then exposed to 10 μM MPP^+ for an additional 48 hr. FITC-TUNEL staining and Hoechst 33342 nuclear staining were performed. (B) Quantitative analysis of TH positive neurons following siRNA-δ-4 transfection and MPP^+ treatment. After siRNAs transfection, cells were exposed to 10 μM MPP^+ for 48 hr and then TH positive neurons were identified using anti-TH antibody exposure. Data represent the mean ± SEM from two separate experiments in triplicates (*, $p<0.05$; N=6). (C) Total number of TH^+ neurons per 5000 mesencephalic primary cells counted in each group.

A.

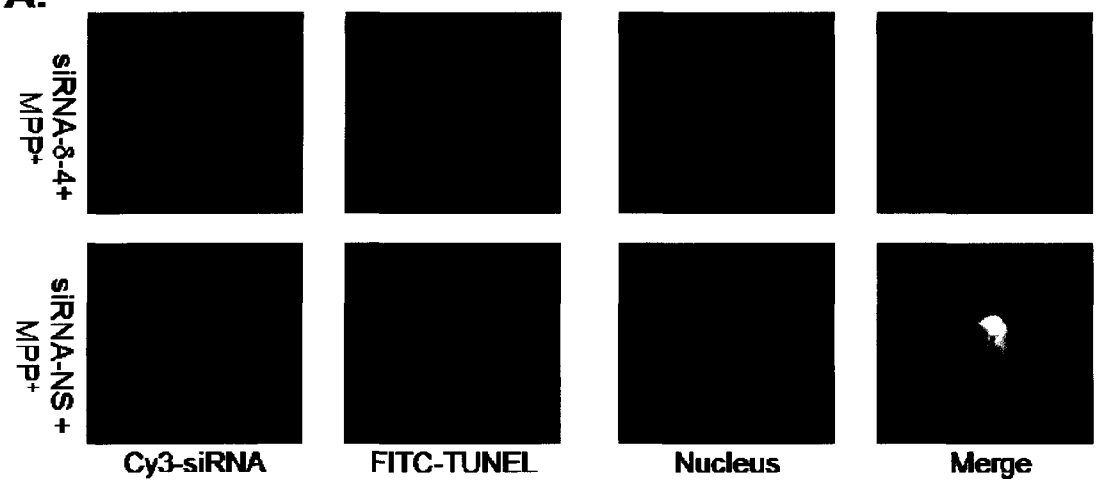

B.

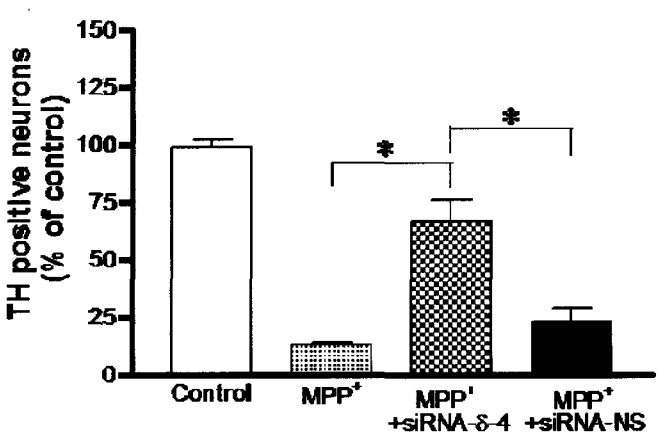

C.

	Control	MPP+	siRNA-δ-4 +MPP+	siRNA-NS +MPP+
# of TH positive neurons (Mean ± SEM)	57.0±10.0	7.3±0.3	38.0 ± 5.5	13.3 ± 3.2

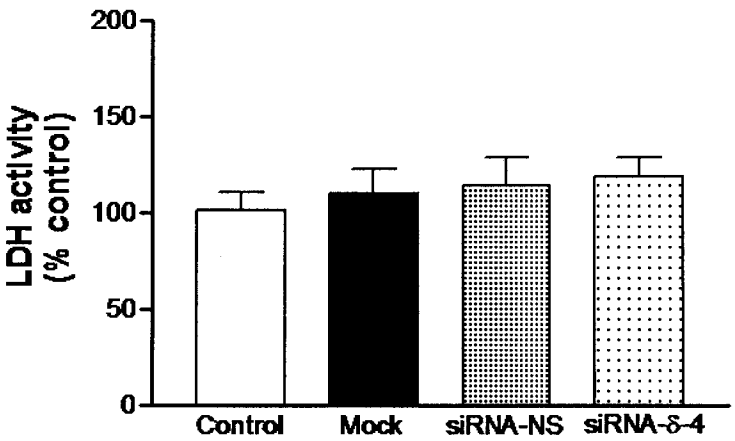

Figure 10: siRNAs are non-toxic to mesencephalic dopaminergic neuronal cells.

siRNA-δ-4 and siRNA-NS (25 nM) were transfected into N27 cells. Following the 24 hr transfection, cell free culture medium was collected, and LDH activity was measured spectrophotometrically. Values represent mean ± SEM for two separate experiments in triplicate (*, $p<0.05$; N=6).

REFERENCES

Ahlemeyer, B., Kolker, S., Zhu, Y., Hoffmann, G.F., Krieglstein, J., 2002. Increase in glutamate-induced neurotoxicity by activated astrocytes involves stimulation of protein kinase C. J Neurochem. 82,504-15.

Albanese, A., Granata, R., Gregori, B., Piccardi, M.P., Colosimo, C., Tonali, P., 1993. Chronic administration of 1-methyl-4-phenyl-1,2,3,6-tetrahydropyridine to monkeys: behavioural, morphological and biochemical correlates. Neuroscience. 55,823-32.

Anantharam, V., Kitazawa, M., Wagner, J., Kaul, S., Kanthasamy, A.G., 2002. Caspase-3-dependent proteolytic cleavage of protein kinase Cdelta is essential for oxidative stress-mediated dopaminergic cell death after exposure to methylcyclopentadienyl manganese tricarbonyl. J Neurosci. 22,1738-51.

Barstead, R., 2001. Genome-wide RNAi. Curr Opin Chem Biol. 5,63-6.

Basu, A., Woolard, M.D., Johnson, C.L., 2001. Involvement of protein kinase C-delta in DNA damage-induced apoptosis. Cell Death Differ. 8,899-908.

Beal, M.F., 2002. Oxidatively modified proteins in aging and disease. Free Radic Biol Med. 32,797-803.

Betarbet, R., Sherer, T.B., Greenamyre, J.T., 2002. Animal models of Parkinson's disease. Bioessays. 24,308-18.

Bharti, A., Kraeft, S.K., Gounder, M., Pandey, P., Jin, S., Yuan, Z.M., Lees-Miller, S.P., Weichselbaum, R., Weaver, D., Chen, L.B., Kufe, D., Kharbanda, S., 1998. Inactivation of DNA-dependent protein kinase by protein kinase Cdelta: implications for apoptosis. Mol Cell Biol. 18,6719-28.

Brodie, C., Blumberg, P.M., 2003. Regulation of cell apoptosis by protein kinase c delta. Apoptosis. 8,19-27.

Buchner, K., 2000. The role of protein kinase C in the regulation of cell growth and in signalling to the cell nucleus. J Cancer Res Clin Oncol. 126,1-11.

Callier, S., Le Saux, M., Lhiaubet, A.M., Di Paolo, T., Rostene, W., Pelaprat, D., 2002. Evaluation of the protective effect of oestradiol against toxicity induced by 6-hydroxydopamine and 1-methyl-4-phenylpyridinium ion (Mpp+) towards dopaminergic mesencephalic neurones in primary culture. J Neurochem. 80,307-16.

Caplen, N.J., 2003. RNAi as a gene therapy approach. Expert Opin Biol Ther. 3,575-86.

Carmell, M.A., Xuan, Z., Zhang, M.Q., Hannon, G.J., 2002. The Argonaute family: tentacles that reach into RNAi, developmental control, stem cell maintenance, and tumorigenesis. Genes Dev. 16,2733-42.

Cassarino, D.S., Fall, C.P., Swerdlow, R.H., Smith, T.S., Halvorsen, E.M., Miller, S.W., Parks, J.P., Parker, W.D., Jr., Bennett, J.P., Jr., 1997. Elevated reactive oxygen species and antioxidant enzyme activities in animal and cellular models of Parkinson's disease. Biochim Biophys Acta. 1362,77-86.

Cassarino, D.S., Parks, J.K., Parker, W.D., Jr., Bennett, J.P., Jr., 1999. The parkinsonian neurotoxin MPP+ opens the mitochondrial permeability transition pore and releases cytochrome c in isolated mitochondria via an oxidative mechanism. Biochim Biophys Acta. 1453,49-62.

Choi, W.S., Canzoniero, L.M., Sensi, S.L., O'Malley, K.L., Gwag, B.J., Sohn, S., Kim, J.E., Oh, T.H., Lee, E.B., Oh, Y.J., 1999. Characterization of MPP(+)-induced cell death in

a dopaminergic neuronal cell line: role of macromolecule synthesis, cytosolic calcium, caspase, and Bcl-2-related proteins. Exp Neurol. 159,274-82.

Davies, S.P., Reddy, H., Caivano, M., Cohen, P., 2000. Specificity and mechanism of action of some commonly used protein kinase inhibitors. Biochem J. 351,95-105.

Dempsey, E.C., Newton, A.C., Mochly-Rosen, D., Fields, A.P., Reyland, M.E., Insel, P.A., Messing, R.O., 2000. Protein kinase C isozymes and the regulation of diverse cell responses. Am J Physiol Lung Cell Mol Physiol. 279,L429-38.

DeVries, T.A., Neville, M.C., Reyland, M.E., 2002. Nuclear import of PKCdelta is required for apoptosis: identification of a novel nuclear import sequence. Embo J. 21,6050-60.

Dodel, R.C., Du, Y., Bales, K.R., Ling, Z.D., Carvey, P.M., Paul, S.M., 1998. Peptide inhibitors of caspase-3-like proteases attenuate 1-methyl-4- phenylpyridinum-induced toxicity of cultured fetal rat mesencephalic dopamine neurons. Neuroscience. 86,701-7.

Donze, O., Picard, D., 2002. RNA interference in mammalian cells using siRNAs synthesized with T7 RNA polymerase. Nucleic Acids Res. 30,e46.

Earnshaw, W.C., Martins, L.M., Kaufmann, S.H., 1999. Mammalian caspases: structure, activation, substrates, and functions during apoptosis. Annu Rev Biochem. 68,383-424.

Elbashir, S.M., Harborth, J., Lendeckel, W., Yalcin, A., Weber, K., Tuschl, T., 2001a. Duplexes of 21-nucleotide RNAs mediate RNA interference in cultured mammalian cells. Nature. 411,494-8.

Elbashir, S.M., Lendeckel, W., Tuschl, T., 2001b. RNA interference is mediated by 21- and 22-nucleotide RNAs. Genes Dev. 15,188-200.

Emoto, Y., Kisaki, H., Manome, Y., Kharbanda, S., Kufe, D., 1996. Activation of protein kinase Cdelta in human myeloid leukemia cells treated with 1-beta-D-arabinofuranosylcytosine. Blood. 87,1990-6.

Frasch, S.C., Henson, P.M., Kailey, J.M., Richter, D.A., Janes, M.S., Fadok, V.A., Bratton, D.L., 2000. Regulation of phospholipid scramblase activity during apoptosis and cell activation by protein kinase Cdelta. J Biol Chem. 275,23065-73.

Gschwendt, M., 1999. Protein kinase C delta. Eur J Biochem. 259,555-64.

Ha, H., Yu, M.R., Choi, Y.J., Lee, H.B., 2001. Activation of protein kinase c-delta and c-epsilon by oxidative stress in early diabetic rat kidney. Am J Kidney Dis. 38,S204-7.

Hammond, S.M., Caudy, A.A., Hannon, G.J., 2001. Post-transcriptional gene silencing by double-stranded RNA. Nat Rev Genet. 2,110-9.

Hannon, G.J., 2002. RNA interference. Nature. 418,244-51.

Hartmann, A., Hunot, S., Michel, P.P., Muriel, M.P., Vyas, S., Faucheux, B.A., Mouatt-Prigent, A., Turmel, H., Srinivasan, A., Ruberg, M., Evan, G.I., Agid, Y., Hirsch, E.C., 2000. Caspase-3: A vulnerability factor and final effector in apoptotic death of dopaminergic neurons in Parkinson's disease. Proc Natl Acad Sci U S A. 97,2875-80.

Hasuwa, H., Kaseda, K., Einarsdottir, T., Okabe, M., 2002. Small interfering RNA and gene silencing in transgenic mice and rats. FEBS Lett. 532,227-30.

Irie, N., Sakai, N., Ueyama, T., Kajimoto, T., Shirai, Y., Saito, N., 2002. Subtype- and species-specific knockdown of PKC using short interfering RNA. Biochem Biophys Res Commun. 298,738-43.

Ischiropoulos, H., Beckman, J.S., 2003. Oxidative stress and nitration in neurodegeneration: cause, effect, or association? J Clin Invest. 111,163-9.

Itoh, T., Horio, T., 2001. DNA-dependent protein kinase catalytic subunit is cleaved during UV-induced apoptosis. J Dermatol Sci. 25,72-7.

Jackson-Lewis, V., Jakowec, M., Burke, R.E., Przedborski, S., 1995. Time course and morphology of dopaminergic neuronal death caused by the neurotoxin 1-methyl-4-phenyl-1,2,3,6-tetrahydropyridine. Neurodegeneration. 4,257-69.

Jen, K.Y., Gewirtz, A.M., 2000. Suppression of gene expression by targeted disruption of messenger RNA: available options and current strategies. Stem Cells. 18,307-19.

Jenner, P., 2003. Oxidative stress in Parkinson's disease. Ann Neurol. 53 Suppl 3,S26-36; discussion S36-8.

Kaasinen, S.K., Goldsteins, G., Alhonen, L., Janne, J., Koistinaho, J., 2002. Induction and activation of protein kinase C delta in hippocampus and cortex after kainic acid treatment. Exp Neurol. 176,203-12.

Kanthasamy, A.G., Matsumoto, R.R., Gunasekar, P.G., Trunong, D.D., 1995. Excitoprotective effect of felbamate in cultured cortical neurons. Brain Res. 705,97-104.

Kaul, S., Kanthasamy, A., Kitazawa, M., Anantharam, V., Kanthasamy, A.G., 2003. Caspase-3 dependent proteolytic activation of protein kinase C delta mediates and regulates 1-methyl-4-phenylpyridinium (MPP+)-induced apoptotic cell death in dopaminergic cells: relevance to oxidative stress in dopaminergic degeneration. Eur J Neurosci. 18,1387-401.

Kaur, D., Yantiri, F., Rajagopalan, S., Kumar, J., Mo, J.Q., Boonplueang, R., Viswanath, V., Jacobs, R., Yang, L., Beal, M.F., DiMonte, D., Volitaskis, I., Ellerby, L., Cherny, R.A., Bush, A.I., Andersen, J.K., 2003. Genetic or pharmacological iron chelation

prevents MPTP-induced neurotoxicity in vivo: a novel therapy for Parkinson's disease. Neuron. 37,899-909.

Kikkawa, U., Matsuzaki, H., Yamamoto, T., 2002. Protein Kinase Cdelta (PKCdelta): Activation Mechanisms and Functions. J Biochem (Tokyo). 132,831-9.

Kitazawa, M., Anantharam, V., Kanthasamy, A.G., 2003. Dieldrin induces apoptosis by promoting caspase-3-dependent proteolytic cleavage of protein kinase Cdelta in dopaminergic cells: relevance to oxidative stress and dopaminergic degeneration. Neuroscience. 119,945-964.

Krichevsky, A.M., Kosik, K.S., 2002. RNAi functions in cultured mammalian neurons. Proc Natl Acad Sci U S A. 99,11926-9.

Langston, J.W., Langston, E.B., Irwin, I., 1984. MPTP-induced parkinsonism in human and non-human primates--clinical and experimental aspects. Acta Neurol Scand Suppl. 100,49-54.

Lee, H.S., Park, C.W., Kim, Y.S., 2000. MPP(+) increases the vulnerability to oxidative stress rather than directly mediating oxidative damage in human neuroblastoma cells. Exp Neurol. 165,164-71.

Lotharius, J., Brundin, P., 2002. Pathogenesis of Parkinson's disease: dopamine, vesicles and alpha-synuclein. Nat Rev Neurosci. 3,932-42.

Lotharius, J., Dugan, L.L., O'Malley, K.L., 1999. Distinct mechanisms underlie neurotoxin-mediated cell death in cultured dopaminergic neurons. J Neurosci. 19,1284-93.

Lotharius, J., O'Malley, K.L., 2000. The parkinsonism-inducing drug 1-methyl-4-phenylpyridinium triggers intracellular dopamine oxidation. A novel mechanism of toxicity. J Biol Chem. 275,38581-8.

Madhavan, L., Freed, W.J., Anantharam, V., Kanthasamy, A.G., 2003. 5-hydroxytryptamine 1A receptor activation protects against N-methyl-D-aspartate-induced apoptotic cell death in striatal and mesencephalic cultures. J Pharmacol Exp Ther. 304,913-23.

Maher, P., 2001. How protein kinase C activation protects nerve cells from oxidative stress-induced cell death. J Neurosci. 21,2929-38.

Maizels, E.T., Peters, C.A., Kline, M., Cutler, R.E., Jr., Shanmugam, M., Hunzicker-Dunn, M., 1998. Heat-shock protein-25/27 phosphorylation by the delta isoform of protein kinase C. Biochem J. 332,703-12.

Majumder, P.K., Mishra, N.C., Sun, X., Bharti, A., Kharbanda, S., Saxena, S., Kufe, D., 2001. Targeting of protein kinase C delta to mitochondria in the oxidative stress response. Cell Growth Differ. 12,465-70.

Mandil, R., Ashkenazi, E., Blass, M., Kronfeld, I., Kazimirsky, G., Rosenthal, G., Umansky, F., Lorenzo, P.S., Blumberg, P.M., Brodie, C., 2001. Protein kinase Calpha and protein kinase Cdelta play opposite roles in the proliferation and apoptosis of glioma cells. Cancer Res. 61,4612-9.

Martelli, A.M., Zweyer, M., Ochs, R.L., Tazzari, P.L., Tabellini, G., Narducci, P., Bortul, R., 2001. Nuclear apoptotic changes: an overview. J Cell Biochem. 82,634-46.

Meinhardt, G., Roth, J., Totok, G., Auner, H., Emmerich, B., Hass, R., 1999. Signaling defect in the activation of caspase-3 and PKCdelta in human TUR leukemia cells is associated with resistance to apoptosis. Exp Cell Res. 247,534-42.

Mizuno, Y., Mochizuki, H., Sugita, Y., Goto, K., 1998. Apoptosis in neurodegenerative disorders. Intern Med. 37,192-3.

Morel, J.B., Vaucheret, H., 2000. Post-transcriptional gene silencing mutants. Plant Mol Biol. 43,275-84.

Nagy, P., Arndt-Jovin, D.J., Jovin, T.M., 2003. Small interfering RNAs suppress the expression of endogenous and GFP-fused epidermal growth factor receptor (erbB1) and induce apoptosis in erbB1-overexpressing cells. Exp Cell Res. 285,39-49.

Olanow, C.W., Tatton, W.G., 1999. Etiology and pathogenesis of Parkinson's disease. Annu Rev Neurosci. 22,123-44.

O'Neil, N.J., Martin, R.L., Tomlinson, M.L., Jones, M.R., Coulson, A., Kuwabara, P.E., 2001. RNA-mediated interference as a tool for identifying drug targets. Am J Pharmacogenomics. 1,45-53.

Opalinska, J.B., Gewirtz, A.M., 2002. Nucleic-acid therapeutics: basic principles and recent applications. Nat Rev Drug Discov. 1,503-14.

Otieno, M.A., Kensler, T.W., 2000. A role for protein kinase C-delta in the regulation of ornithine decarboxylase expression by oxidative stress. Cancer Res. 60,4391-6.

Paddison, P.J., Caudy, A.A., Hannon, G.J., 2002. Stable suppression of gene expression by RNAi in mammalian cells. Proc Natl Acad Sci U S A. 99,1443-8.

Page, K., Li, J., Zhou, L., Iasvoyskaia, S., Corbit, K.C., Soh, J.W., Weinstein, I.B., Brasier, A.R., Lin, A., Hershenson, M.B., 2003. Regulation of airway epithelial cell NF-kappa B-dependent gene expression by protein kinase C delta. J Immunol. 170,5681-9.

Pongracz, J., Webb, P., Wang, K., Deacon, E., Lunn, O.J., Lord, J.M., 1999. Spontaneous neutrophil apoptosis involves caspase 3-mediated activation of protein kinase C-delta. J Biol Chem. 274,37329-34.

Reyland, M.E., Anderson, S.M., Matassa, A.A., Barzen, K.A., Quissell, D.O., 1999. Protein kinase C delta is essential for etoposide-induced apoptosis in salivary gland acinar cells. J Biol Chem. 274,19115-23.

Shi, Y., 2003. Mammalian RNAi for the masses. Trends Genet. 19,9-12.

Sorensen, D.R., Leirdal, M., Sioud, M., 2003. Gene silencing by systemic delivery of synthetic siRNAs in adult mice. J Mol Biol. 327,761-6.

Sun, X., Wu, F., Datta, R., Kharbanda, S., Kufe, D., 2000. Interaction between protein kinase C delta and the c-Abl tyrosine kinase in the cellular response to oxidative stress. J Biol Chem. 275,7470-3.

Suzuki, T., Higgins, P.J., Crawford, D.R., 2000. Control selection for RNA quantitation. Biotechniques. 29,332-7.

Tewari, M., Quan, L.T., O'Rourke, K., Desnoyers, S., Zeng, Z., Beidler, D.R., Poirier, G.G., Salvesen, G.S., Dixit, V.M., 1995. Yama/CPP32 beta, a mammalian homolog of CED-3, is a CrmA-inhibitable protease that cleaves the death substrate poly(ADP-ribose) polymerase. Cell. 81,801-9.

Vaucheret, H., Beclin, C., Fagard, M., 2001. Post-transcriptional gene silencing in plants. J Cell Sci. 114,3083-91.

Vaucheret, H., Fagard, M., 2001. Transcriptional gene silencing in plants: targets, inducers and regulators. Trends Genet. 17,29-35.

Vila, M., Przedborski, S., 2003. Targeting programmed cell death in neurodegenerative diseases. Nat Rev Neurosci. 4,365-75.

Viswanath, V., Wu, Y., Boonplueang, R., Chen, S., Stevenson, F.F., Yantiri, F., Yang, L., Beal, M.F., Andersen, J.K., 2001. Caspase-9 activation results in downstream

caspase-8 activation and bid cleavage in 1-methyl-4-phenyl-1,2,3,6-tetrahydropyridine-induced Parkinson's disease. J Neurosci. 21,9519-28.

Wang, M.Z., Jin, P., Bumcrot, D.A., Marigo, V., McMahon, A.P., Wang, E.A., Woolf, T., Pang, K., 1995. Induction of dopaminergic neuron phenotype in the midbrain by Sonic hedgehog protein. Nat Med. 1,1184-8.

Wu, D.C., Teismann, P., Tieu, K., Vila, M., Jackson-Lewis, V., Ischiropoulos, H., Przedborski, S., 2003. NADPH oxidase mediates oxidative stress in the 1-methyl-4-phenyl-1,2,3,6-tetrahydropyridine model of Parkinson's disease. Proc Natl Acad Sci U S A. 100,6145-50.

Xia, H., Mao, Q., Paulson, H.L., Davidson, B.L., 2002. siRNA-mediated gene silencing in vitro and in vivo. Nat Biotechnol. 20,1006-10.

Yoshida, K., Wang, H.G., Miki, Y., Kufe, D., 2003. Protein kinase Cdelta is responsible for constitutive and DNA damage-induced phosphorylation of Rad9. Embo J. 22,1431-41.

Yoshimura, S., Banno, Y., Nakashima, S., Takenaka, K., Sakai, H., Nishimura, Y., Sakai, N., Shimizu, S., Eguchi, Y., Tsujimoto, Y., Nozawa, Y., 1998. Ceramide formation leads to caspase-3 activation during hypoxic PC12 cell death. Inhibitory effects of Bcl-2 on ceramide formation and caspase-3 activation. J Biol Chem. 273,6921-7.

CHAPTER III: PROTEOLYTICALLY ACTIVATED PKCδ TRANSLOCATES TO THE NUCLEUS AND MEDIATES SER14 PHOSPHORYLATION OF HISTONE H2B IN APOPTOTIC DEATH OF DOPAMINERGIC NEURONAL CELLS

A paper submitted to Cell Death and Differentiation

Yongjie Yang, Vellareddy Anantharam, Anumantha Kanthasamy

ABSTRACT

We previously showed that oxidative stress sensitive kinase PKCδ promotes apoptotic death in dopaminergic neurons following neurotoxin exposures (Kitazawa et al., 2003; Yang et al., 2004). However, its mechanism has not been well understood. In the present study, we determined that the full-length PKCδ is first cleaved in the cytoplasm and the activated cleaved PKCδ subsequently translocates into the nucleus. The caspase-3 specific inhibitor Z-DEVD-FMK, the cleavage resistant mutant of PKCδ (PKCδ-CRM), as well as the nuclear localization signal (NLS) deletion mutant of PKCδ (PKCδ-ΔNLS) abolishes the nuclear translocation of activated cleaved PKCδ. Our study showed that proteolytic activation of full-length PKCδ and subsequent nuclear translocation of activated cleaved PKCδ are integral events required for PKCδ's pro-apoptotic function in apoptosis of dopaminergic neuronal cells. Moreover, we demonstrated that activated cleaved PKCδ, after its nuclear translocation, mediates Ser14 phosphorylation of histone H2B in apoptotic

dopaminergic neuronal cells. Ser14 phosphorylation of H2B and apoptosis can also be directly induced by the catalytic fragment of PKCδ (PKCδ-CF), but not by the regulatory fragment of PKCδ (PKCδ-RF), dominant-negative mutant of PKCδ (PKCδ-DN), PKCδ-CRM, or PKCδ-ΔNLS. Taken together, our study suggests that proteolytically activated PKCδ translocates into the nucleus and mediates Ser14 phosphorylation of H2B to promote neurotoxin-induced apoptosis of dopaminergic neuronal cells.

INTRODUCTION

Mechanisms of selective degeneration of midbrain dopaminergic neurons in Parkinson's disease (PD) remain elusive despite intensive studies into the pathogenesis of PD. Although the recent identification of a number of genetic mutations that cause several groups of familial PD shed light on the understanding of the mechanisms of dopaminergic neuron degeneration (Dawson and Dawson, 2003; Greenamyre and Hastings, 2004; Shen, 2004), exact causes of sporadic PD cases, which account for over 90% of total PD patients, are still not clear. On the other hand, the discovery that mitochondria complex I inhibitor 1-methyl-4-phenyl-1,2,3,6,-tetrahydropyridine (MPTP) induces Parkinsonism in humans (Langston et al., 1984) suggests that exposure to environmental neurotoxins can contribute to dopaminergic neuron degeneration in sporadic PD patients (Dauer and Przedborski, 2003; Langston et al., 1984; Vila and Przedborski, 2003; Wichmann and DeLong, 2003). Mouse and primate models exposed to MPTP or other mitochondria complex I inhibitors have been developed and exhibit degeneration of midbrain dopaminergic neurons and PD-like symptoms (Betarbet et al., 2002; Betarbet et al., 2000; Dauer and Przedborski, 2003; McCormack et al., 2002).

Interestingly, most of these mitochondria complex I inhibitors (paraquat, rotenone) are also commonly used pesticides, which implicates the potential pathogenic role of pesticides in PD (Betarbet et al., 2002; Giasson and Lee, 2000; Greenamyre et al., 2001; Jenner, 2001). As supportive evidence, epidemiological studies have also found that incidence rate of sporadic PD is higher among farming communities (Jenner, 1998; Seidler et al., 1996; Tanner and Langston, 1990).

Dieldrin is an organochlorine pesticide that was widely used decades ago for the control of soil pests. Although it has been banned for about thirty years, the wide exposure of humans to dieldrin still exists through its persistent accumulation in the environment (Kitazawa et al., 2001, 2003). It is not clear as to whether dieldrin also inhibits mitochondria complex I; however, several studies have indicated that dieldrin exposure is positively associated with the increased incidence of PD. In fact, significant levels of dieldrin were detected in postmortem brains of PD patients, whereas no dieldrin was found in age-matched control brains (Corrigan et al., 1998; Fleming et al., 1994). Also, dieldrin exposure depletes dopamine in brains of ducks, ring doves and rats (Heinz et al., 1980; Sharma et al., 1976; Wagner and Greene, 1978). Furthermore, our previous studies also show that dopaminergic cells are highly sensitive to dieldrin induced toxicity (Kitazawa et al., 2001; Kitazawa et al., 2002).

By employing the well-developed MPTP (as well as other neurotoxin) cell and animal models of PD, it has been demonstrated that neurotoxin induced oxidative stress is one of the earliest events that triggers diverse downstream apoptotic pathways and induces the activation of executioner caspases in dopaminergic neurons (Beal, 2002; Greenamyre et al., 2001; Hartmann et al., 2000; Hartmann et al., 2001; Jenner, 2003). Activated executioner

caspases directly mediate cleavage of a wide range of downstream substrates and lead to cell death. Protein kinases, one of the major signal transducers in the cell, have emerged as one major category of substrates for activated caspases. Kinases in different families, including Raf-1 and AKT (Widmann et al., 1998b), ATM, MEKK-1 (Widmann et al., 1998a), hPAK2/hPAK65 (Jakobi et al., 2003; Lee et al., 1997), PKC isoform δ and θ (Datta et al., 1997; Emoto et al., 1995), PKN (Takahashi et al., 1998), ROCK1 (Coleman et al., 2001), SLK (Sabourin et al., 2000), HPK1 (Chen et al., 1999), LIMK1 (Tomiyoshi et al., 2004), and Mst (de Souza and Lindsay, 2004; Huang et al., 2002), have been identified as substrates of activated caspases. Cleavage of these kinases not only regulates their activity (activation or inactivation), but also induces their relocation inside the cell, which moves kinases proximal to their specific substrates and transduces specific apoptotic signals (Jakobi, 2004; Teruel and Meyer, 2000). The proteolytic cleavage of ATM, for example, inactivates the protein, further impairing the DNA repair mechanism of cells in response to DNA damage (Smith et al., 1999). In other cases, caspases mediated cleavage activates certain kinases, like Mst, and induces its nuclear translocation to facilitate apoptosis (Cheung et al., 2003; Huang et al., 2002).

Protein kinase C delta (PKCδ), a member of the novel PKC family, is one of the kinases identified as a downstream target of caspase-3 in many different cell types, including dopaminergic neuronal cells, in response to apoptotic stimuli (Anantharam et al., 2002; Brodie and Blumberg, 2003; Kitazawa et al., 2003; Reyland et al., 1999). As a member of the novel PKC family, PKCδ contains a lipid-sensitive C1 domain and a Ca^{2+} binding deficient C2 domain. The binding of lipid molecules (diacylglycerol or 4-phorbol 12-myristate 13-acetate) induces rapid translocation of PKCδ to the plasma membrane and activates the

kinase through conformational change that removes the pseudosubstrate from the catalytic site (Newton, 2003). The lipid-mediated activation allows PKCδ to send normal transducing signals from receptors (Nishizuka, 1992). Moreover, the serine/threonine phosphorylation of its activation loop at its C-terminal by PDK-1 also contributes to PKCδ's activation (Newton, 2003; Toker, 1998). In apoptotic cells, caspase-3 mediated proteolytic cleavage of PKCδ removes its regulatory fragment containing the pseudosubstrate and leads to persistent activation of the kinase (Kanthasamy et al., 2003; Kikkawa et al., 2002). The diverse mechanisms for the activation of PKCδ raise an interesting question as to whether the proteolytic activation of full-length PKCδ is necessary and specific for its function in apoptosis. Simultaneous with the activation, PKCδ also relocates to the mitochondria, nucleus, endoplasmic reticulum (ER), golgi, as well as plasma membrane in apoptotic cells (Brodie and Blumberg, 2003). Translocation of PKCδ to the mitochondria was shown to facilitate the mitochondrial pore formation, promoting cytochrome C release (Majumder et al., 2000) and inducing the redistribution of Bcl-2 family proteins (Murriel et al., 2004; Sitailo et al., 2004). The translocation of PKCδ to the nucleus was linked to nuclear events that either regulate the mitochondrial apoptotic pathway or facilitate the collapse of nuclear structure in apoptotic cells (Cross et al., 2000; DeVries et al., 2002).

We previously demonstrated that PKCδ is a downstream target of activated caspase-3 and its proteolytic activation is associated with a wide range of neurotoxins induced apoptosis in dopaminergic neuronal cells (Kaul et al., 2003; Kitazawa et al., 2003; Yang et al., 2004). However, very little is known about the downstream actions of PKCδ following its proteolytic activation. In the present study, we investigate the downstream events following

proteolytic activation of PKCδ and determine the correlation between proteolytic cleavage and nuclear translocation of PKCδ in dopaminergic neuronal cells. Furthermore, we also investigate the function of the activated cleaved PKCδ in the nucleus of dieldrin induced apoptotic dopaminergic neuronal cells.

MATERIALS AND METHODS

Reagents

Anti-cleaved caspase-3 antibody was obtained from Cell Signaling Technology, Inc. (Beverly, MA). Anti-LDH antibody was obtained from Research Diagnostics, Inc. (Flanders, NJ). Anti-lamin B antibody was obtained from Abcam, Inc (Cambridge, MA). Dieldrin, protease cocktail, purified Histone H2B, ATP, protein-A-sepharose, and anti-β-actin antibody were obtained from Sigma-Aldrich (St. Louis, MO); Z-DEVD-FMK was obtained from Alexis Biochemicals (San Diego, CA); antibodies to PKCδ and PARP were purchased from Santa Cruz Biotechnology, Inc. (Santa Cruz, CA). Anti-phospho-Histone H2B (Ser14) antibody was purchased from Upstate Biotechnology (Waltham, MA). TaqMan Rat PKCδ and 18s ribosome RNA assay kit and PCR master mix was purchased from Applied Biosystems (Foster City, CA). Anti-rabbit and anti-mouse secondary antibodies and the ECL chemiluminescence kit were purchased from Amersham Pharmacia Biotech (Piscataway, NJ). NE-PER^{TM} nuclear and cytoplasmic extraction reagent was obtained from Pierce Biotechnology, Inc (Rockford, IL). Alexa 488 conjugated anti-rabbit secondary antibody and Hoechst 33342 were purchased from Molecular Probes, Inc. (Eugene, OR). Cy3 conjugated

anti-mouse secondary antibody was obtained from Jackson Laboratory (Bar Harbor, Maine). The Cell Death Detection ELISA plus Assay Kit was purchased from Roche Molecular Biochemicals (Indianapolis, IN). [γ-^{32}P] ATP was purchased from Perkin Elmer Life Science Products (Boston, MA). The Bradford protein assay kit was purchased from Bio-Rad Laboratories (Hercules, CA). *Pfu* DNA polymerase was purchased from Stratagene (La Jolla, CA). SuperScript III first-strand synthesis system, TRIZOL reagent, ViraPower^{TM} lentiviral expresson system, RPMI, Opti-MEM, fetal bovine serum, L-glutamine, blasticidin, penicillin, and streptomycin were purchased from Invitrogen, Inc. (Carlsbad, CA).

Cell culture and treatment

The immortalized rat mesencephalic dopaminergic neuronal (N27) cell line was a kind gift from Dr. Kedar N. Prasad, University of Colorado Health Sciences Center (Denver, CO) (Adams et al., 1996; Prasad et al., 1998). N27 cells were grown in RPMI 1640 medium containing 10% fetal bovine serum, 2 mM L-glutamine, 50 units penicillin, and 50 μg/ml streptomycin. Cells were grown in a humidified atmosphere of 5% CO_2 at 37^{0}C. For dieldrin treatment, N27 cells were treated with 60μM dieldrin in serum-free medium for up to 3hr at 37°C. In caspase-3 inhibitor studies, cells were co-treated with 50 -100μM Z-DEVD-FMK and dieldrin. Untreated cells were used as negative control.

Construction of plasmids

A series of PKCδ-related constructs was prepared, including PKCδ-WT (wild type), PKCδ-CRM (cleavage resistant mutant), PKCδ-ΔNLS (deletion of nuclear localization

signal), PKCδ-DN (dominant negative mutant), PKCδ-CF (catalytic fragment), and PKCδ-RF (regulatory fragment). To prepare PKCδ-CF, PKCδ-RF, PKCδ-ΔNLS or PKCδ-WT fragments, 995-2035bp, 14-982bp, 14-1843bp or full-length of mouse PKCδ (gi: 6755081) cDNA were first amplified from pGFP-PKCδ (kind gift of Dr. Reyland at University of Colorado) (DeVries et al., 2002) with the following primer pairs, respectively. For PKCδ-CF, forward primer: 5' caccatgaacaacgggacctatggcaa 3'; reverse primer: 5' aatgtccaggaattgctcaaac 3'; for PKCδ-RF, forward primer: 5' caccatggcacccttcctgcgc 3'; reverse primer: 5' actcccagagacttctggctt 3'; for PKCδ-ΔNLS, forward primer: 5'caccatggcacccttcctgcgc 3'; reverse primer: 5'ctccaggagggaccagtt 3'; for PKCδ-WT, forward primer: 5' caccatggcacccttcctgcgc 3'; reverse primer: 5' aatgtccaggaattgctcaaac 3'. To prepare PKCδ-CRM, full-length mouse PKCδ cDNA with a point mutation at 993 (A to C) that abolishes the caspase-3 cleavage site of PKCδ was amplified with pGFP-PKCδ^{D327A} (kind gift of Dr. Reyland at University of Colorado) (DeVries et al., 2002) as template and the same primer pairs used for amplification of PKCδ-WT. To prepare PKCδ-DN, full-length mouse PKCδ cDNA with a point mutation at 1489 (A to G) that abolishes the ATP binding site of PKCδ was amplified with pPKCδ^{K376R}-EGFP (kind gift of Dr. Reyland at University of Colorado) as template and the same primer pairs used for amplification of PKCδ-WT. All PCR reactions were performed with *Pfu* DNA polymerase to maintain the fidelity of the sequence. All PCR products were directly cloned in-frame into a V5-tagged expression vector (at the C terminal) pLenti/TOPO from Invitrogen, to get pLenti/PKCδ-CF, pLenti/PKCδ-RF, pLenti/PKCδ-ΔNLS, pLenti/PKCδ-WT, pLenti/PKCδ-DN, and pLenti/PKCδ-CRM. All positive clones were confirmed by sequencing.

Generation of PKCδ-CRM, PKCδ-ΔNLS, PKCδ-DN, and PKCδ-WT stably expressing dopaminergic neuronal (N27) cell line

ViraPower Lentiviral gene expression system from Invitrogen (Carlsbad, CA) was employed for the establishment of a stable cell line. To produce lentiviral particles containing different constructs, pLenti/PKCδ-CRM, pLenti/PKCδ-ΔNLS, pLenti/PKCδ-DN, or pLenti/PKCδ-WT, as well as supporting plasmids (provided with the kit) were co-transfected into human 293FT cells with the use of lipofectamine 2000, respectively, as described in the instruction of the kit. The lentiviral particles in the medium were then collected by centrifuging at 3000 rpm for 15 min at 48-72 hr post-transfection. To generate stably expressing cell lines, lentiviral particles containing different PKCδ constructs were added into cultured N27 cells ($2x10^5$) followed by polybrene (6 μg/ml), cells were incubated for 24 hr, and fresh medium was added and old medium was removed. Positive N27 cells were selected by keeping blasticidin (10 μg/ml) in medium for up to 2 weeks. N27 cells stably expressing lacZ (pLenti/lacZ was supplied with the kit) were also established to serve as a vector control. PKCδ-CRM, PKCδ-ΔNLS, or PKCδ-WT stably expressing N27 cells were identified by immunostaining of the C-terminal V5 epitope.

Transient transfection of N27 cells

Transient transfection of N27 cells was performed with the use of lipofectomine 2000 from Invitrogen, Inc (Carlsbad, CA). Briefly, cells ($0.7\text{-}0.8x10^6$) were pre-plated in poly L-lysine coated glass cover slips in a 6-well plate. After 16-24 hr, 4 μg plasmid (PKCδ-CF or PKCδ-RF) and 10 μl lipofectomine 2000 were first diluted in 250 μl Opti-MEM medium,

separately. After a 5 min incubation at RT, diluted plasmid was mixed with diluted lipofectomine 2000 and incubated for another 20 min for the formation of DNA-lipid complex. The DNA-lipid complex was then added to the cells in a 6-well plate and incubated for 16-24 hr at 37^0C.

Preparation of nuclear and cytosolic fractions

Nuclear and cytosolic fractions were prepared by employing NE-PER™ nuclear and cytosolic extraction reagent from Pierce Biotechnology, Inc (Rockford, IL). Briefly, the N27 cells ($10x10^6$) were harvested with trypsin/EDTA and spun at 200xg for 5 min. Cell pellets were then washed twice with ice-cold PBS and resuspended in 200 µl of CERI buffer (pH7.5, 10 mM HEPES, 10 mM KCl, 1.5 mM $MgCl_2$ and 1:100 dilution of protease inhibitor). To lyse the cells, 0.1% Nonide P-40 (NP-40) was added into the sample and incubated for 3 min on ice. The lysates were then centrifuged for 30 min at 14,000xg at 4^0C and supernatants were collected as cytosolic fraction. The nuclei pellets were further resuspended in 50 µl NER buffer (420 nM NaCl, 20 mM HEPES, 1.5 mM $MgCl_2$, 0.2 mM EDTA, and 25% glycerol, pH7.9) for 40 min on ice. The nuclear suspension was centrifuged for 10 min at 14,000xg at 4^0C and supernatants were collected as nuclear fraction. The relative purity of cytosolic and nuclear fractions was examined by the corresponding marker proteins lactase dehydroxylase (LDH) and lamin B.

Preparation of whole cell homogenates

After treatment, the N27 cells ($10x10^6$) were harvested with trypsin/EDTA and spun at 200xg for 5 min. Cell pellets were then washed twice with ice-cold PBS and resuspended

in 200 μl of homogenization buffer (pH8.0, 20 mM Tris, 10 mM EGTA, 2 mM EDTA, 2 mM DTT, 0.5% Triton X-100 and 1:100 dilution of protease inhibitor). After incubation on ice for 5 min, the cell lysates were centrifuged for 30 min at 14,000xg at 4^0C and supernatants were collected as whole cell lysates.

Western blotting

Equal amount of protein was loaded in each lane and separated on SDS-polyacrylamide gel as described previously. Proteins were then transferred to nitrocellulose membrane by electro-blotting overnight (4°C, 25V). Non-specific binding sites were blocked by treating the nitrocellulose membranes with 5% non-fat dry milk TBST solution (10 mM Tris, 150 mM NaCl, and 0.1% Tween 20) for 1 hr. The nitrocellulose membranes were then incubated with primary antibodies (1:1000) for 1 hr at RT. The primary antibody treatment was followed by treatment with secondary HRP-conjugated anti-rabbit or anti-mouse IgG (1:2000) for 1 hr at RT. Secondary antibody-bound proteins were detected using an ECL chemiluminescence kit (Amersham). To confirm equal protein loading, blots were reprobed with β-actin antibody (1:5000). Gel photographs and densitometric analysis were performed with a Kodak image station (Model 1000R, Rochester, New York).

Quantitative real time RT-PCR

After treatment, cells were lysed in 1 ml TRIZOL reagent and total RNA was isolated by chloroform extraction and precipitated by ethanol. Total RNA was first treated with DNase I to degrade contaminated DNA and then reversely transcribed into first strand cDNA using the SuperScript III first-strand synthesis system (Invitrogen, Inc, Carlsbad, CA) as

described in the kit instructions. To detect the abundance of PKCδ mRNA in the sample, quantitative real time PCR was performed with TaqMan rat PKCδ and control 18s ribosome RNA (rRNA) assay kits. Briefly, about 50 ng cDNA was mixed with primers, TaqMan probe, as well as 2x PCR master mix to set up the reaction. For each sample, triplicates were run on the same plate. The PCR reaction was performed and data were analyzed in a Mx4000 multiplex Quantitative PCR system (stratagene, La Jolla, CA).

Immunocytochemistry

Cells grown on poly L-lysine coated glass cover slips were first fixed in 4% paraformaldehyde, then permeabilized and blocked with blocking reagent (0.4% BSA, 5% goat serum, and 0.2% Triton-X 100 in PBS) for 20 min. Cells were then incubated with primary antibody (1:1000 in blocking reagent) overnight at 4°C and then washed for 4x8 min with PBS. Endogenous PKCδ, cleaved caspase-3, Ser 14 phosphorylated histone H2B, or overexpressed PKCδ-WT, PCKδ-CRM, or PKCδ-ΔNLS was visualized by incubation with Alexa 488-conjugated goat anti-rabbit secondary antibody or Cy3-conjugated goat anti-mouse secondary antibody (1:2000 in PBS) at RT for 90 min. After another 4x8 min PBS wash, Hoechst 33342 (final concentration of 10 μg/ml in PBS) was added to stain the cell nuclei at RT for 3 min. Finally, cells were mounted on a slide with antifade mounting medium. The cells were observed under regular fluorescence or confocal microscopy. For regular fluorescence microscopy, a Nikon inverted fluorescence microscope (Model TE-2000U) was used and pictures were captured with a SPOT digital camera (Diagnostic Instruments, Sterling Heights, MI). For confocal microscopy, a TCS/NT confocal

microscopy system (Leica, Bannockburn, IL) was employed. All images were processed in MetaMorph 5.07 from Universal imaging (Downingtown, PA).

Immunoprecipitation kinase assay

PKCδ enzymatic activity was assayed using an immunoprecipitation kinase assay as previously described (Anantharam et al., 2002; Reyland et al., 1999). After treatment with dieldrin, nuclear lysates of N27 cells ($20x10^6$) were first prepared as described above. About 0.1-0.2 mg protein was immunoprecipitated overnight at 4°C using 2 μg of anti-PKCδ antibody. The immunoprecipitates were then incubated with protein-A–sepharose for 1 hr at 4°C. The protein-A bound antigen-antibody complexes were then washed 3 times with 1x PBS, 3 times with kinase buffer (40 mM Tris, pH7.4, 20 mM $MgCl_2$, 20 μM ATP, and 2.5 mM $CaCl_2$), and resuspended in 20 μl of kinase buffer. Reactions were started by adding 20 μl of reaction buffer containing 0.4 mg purified histone H2B and 5μCi of [γ-^{32}P] ATP (3,000 Ci/mM) to the immunoprecipitated samples and incubated for 10 min at 30°C. 2xSDS gel loading buffer was then added to terminate the reaction, the samples were boiled for 5 min, and the products were separated on a 12% SDS-PAGE gel. The phosphorylated histone bands were detected using a Personal Molecular Imager (FX model, Bio-Rad) and quantified using Quantity One 4.2.0 software (Bio-Rad, Hercules, CA).

Acid extraction of histone mixtures

Briefly, the N27 cells ($10x10^6$) were harvested with trypsin/EDTA and spun at 200xg for 5 min. Cell pellets were then washed twice with ice-cold PBS and resuspended in 200 μl

of homogenization buffer (pH7.5, 10 mM HEPES, 10 mM KCl, 1.5 mM $MgCl_2$ and 1:100 dilution of protease inhibitor). To lyse the cells, 0.5% Triton-X-100 was added into the sample and incubated for 5 min on ice. The lysates were then centrifuged for 5 min at 14,000xg to collect the nuclei pellets. To extract the histones, nuclei pellets were resuspended with 100 µl 0.2 M HCl and shaken at 4^0C for 3 hr. Nuclear lysates were then centrifuged at 14,000xg at 4^0C for 10 min and histone mixtures were collected from the supernatant.

Quantification assay for DNA fragmentation

DNA fragmentation was measured using a recently developed Cell Death Detection ELISA plus Assay Kit (Molecular Biochemicals, Indianapolis, IN). Briefly, cells were spun down at 200xg for 5 min and washed twice with 1X PBS. Cells were then incubated with lysis buffer (supplied with the kit) at RT. After 30 min, samples were centrifuged and 20 µl aliquots of the supernatant were then dispensed into streptavidin-coated 96 well microtiter plates followed by addition of 80 µl of HRP-conjugated antibody cocktail, and incubated for 2 hr at RT with mild shaking. After incubation, unbound components were removed by washing with the incubation buffer supplied with the kit. The nucleosomes retained by the antibody cocktail in the immunocomplex were quantified spectrophotometrically with ABTS as an HRP substrate. Measurements were made at 405nm and 490nm using a SpectroMax 190 spectrophotometer (Molecular Devices, Sunnyvale, CA). The difference of absorbance between OD 405 and OD 490 nm was used to measure the actual DNA fragmentation level.

Data analysis

Data analysis was performed using Prism 3.0 software (GraphPad Software, San Diego, CA). Data from PKCδ kinase, DNA fragmentation, and QRT-PCR were first analyzed using one-way ANOVA. Bonferroni's post-test was then performed to compare all groups and differences with $p<0.05$ were considered significant.

RESULTS

Caspase-3 is primarily activated and remains in the cytoplasm of dopaminergic neuronal (N27) cells following dieldrin exposure

Activation of key apoptotic protease caspase-3 following dieldrin exposure was first determined by monitoring the production of cleaved (activated) caspase-3 on immunoblots with the use of specific anti-cleaved caspase-3 antibody. Also, to determine the subcellular localization of activated caspase-3, the cytosolic and nuclear fractions of N27 cells following dieldrin exposure were prepared and separated by 15% SDS-PAGE. As shown in Figure 1A, cleaved caspase-3 can be detected starting at 0.5 hr in the cytosolic fraction and the maximum intensity of cleaved caspase-3 on immunoblot of the cytosolic fraction is reached at the 1 hr time point. However, cleaved caspase-3 is barely detected at the 0.5 hr time point on immunoblot of the nuclear fraction, and there is only a weak increase in the intensity of cleaved caspase-3 at the 1 hr time point. To show the relative purity of the cytosolic and nuclear fractions, cytosolic and nuclear fractions were separated again by SDS-PAGE and immunobloted by the cytosolic fraction marker Lactase dehydroxylase (LDH) or nuclear fraction marker lamin B. As shown in Figure 1A, only very little LDH was detected in the

nuclear fraction and no clear lamin B was detected in the cytosolic fraction. To visualize the localization of activated caspase-3 *in situ*, immunostaining of cleaved caspase-3 and counterstaining of nuclei was performed in N27 cells at 1 hr following dieldrin exposure. As shown in Figure 1B, the immunoreactivity of cleaved caspase-3 was significantly elevated following dieldrin exposure for 1 hr. The increased immunoreactivity was also predominantly localized in cytoplasm as seen in Figure 1Bf. Taken together, this result suggests that caspase-3 was primarily activated and retained in the cytoplasm; only a very small fraction of activated caspase-3 translocated to the nucleus at the later time point.

Dieldrin exposure induces PKCδ cleavage without changing its expression level in dopaminergic neuronal (N27) cells

PKCδ was recently identified as one of the downstream targets of caspase-3 that can be proteolytically activated in apoptotic cells (Brodie and Blumberg, 2003; Kikkawa et al., 2002). Here, we examine the cleavage of PKCδ induced by dieldrin exposure in dopaminergic neuronal cells. Anti-PKCδ antibody from Santa Cruz Biotechnology (Santa Cruz, CA), which recognizes the C-terminal epitope of PKCδ, was employed. As shown in Figure 2A, cleaved PKCδ fragments (41/38KDa) were detected from whole cell lysates of N27 cells starting at 1 hr after dieldrin exposure and decreased at the 3 hr time point, which matches the time for caspase-3 activation shown in Figure 1A. To demonstrate that the activated caspase-3 indeed starts to cleave its substrates, cleavage of the classical substrate of activated caspase-3, poly (ADP-ribose) polymerase (PARP) (Tewari et al., 1995), was also examined. The whole cell lysates of N27 cells after dieldrin treatment were separated by

7.5% SDS-PAGE and immunobloted with anti-PARP antibody. As shown in Figure 2B, the cleaved PARP (85KDa) was detected as early as 0.5 hr and the intensity of cleaved PARP on immunoblot increased over time up to 3 hr after dieldrin treatment. Both membranes were reprobed with anti-β-actin antibody and the results showed that equal amounts of proteins were loaded on the gel.

To examine whether dieldrin exposure induces transcriptional change in PKCδ mRNA in N27 cells, the relative abundance of PKCδ mRNA copies in control and dieldrin-treated N27 cells was determined by quantitative real-time RT-PCR assay. After dieldrin treatment of 1 and 3 hr, total RNA from control and dieldrin-treated N27 cells was isolated and reversely transcribed into cDNA. Equal amounts of cDNAs were then used to perform real-time PCR with the use of a TaqMan rat PKCδ probe. The 18s ribosome RNA (rRNA) probe was employed to serve as endogenous control to equalize the RNA used in the real-time PCR assay. The real-time amplification plots from control and dieldrin-treated samples were shown in Figure 2C and the fluorescence intensity generated as the result of the amplification of PKCδ cDNA was nearly identical, suggesting that the same amount of PKCδ between control and dieldrin-treated N27 cells was amplified during PCR. The relative quantity of PKCδ mRNA in control and dieldrin-treated N27 cells converted by the formula $2^{-(\Delta Ct\ PKC\delta - \Delta Ct\ 18s\ rRNA)}$ (Ct: threshold of cycle) (Bustin, 2000, 2002) is presented in Figure 2D; no significant difference was found. This result indicates that short exposures to dieldrin induce no transcriptional change in PKCδ in N27 cells.

Nuclear accumulation of cleaved fragments of PCKδ in N27 cells following dieldrin exposure

Subcellular localization of PKCδ after its proteolytic activation in neurotoxin-induced apoptotic dopaminergic neuronal cells has not been determined. We first examined the localization of PKCδ by immunostaining in N27 cells following dieldrin exposure. The immunostaining of PKCδ was performed at 1 hr following dieldrin exposure. The immunoreactivity of PKCδ was predominantly found in the cytoplasm rather than in the nucleus in control N27 cells (Figure 3Ac). However, in dieldrin-treated N27 cells, a dramatic shift of immunoreactivity of PKCδ from the cytoplasm to the nucleus was observed (Figure 3Af). To determine the dieldrin-induced subcellular localization change of both full-length and cleaved PCKδ, nuclear and cytosolic fractions from N27 cells following dieldrin exposure up to 3 hr were prepared, separated by 10% SDS-PAGE and immunoblotted with anti-PKCδ antibody. As shown in Figure 3B, full-length PKCδ was largely found in the cytosolic fraction and dieldrin exposure did not induce the elevation of PKCδ protein level, which is consistent with the quantitative RT-PCR result shown in Figure 2D. In addition, no significant localization change between the cytoplasm and the nucleus for full-length PKCδ in N27 cells following dieldrin exposure was observed. On the other hand, the cleaved fragments of PKCδ can be detected in the cytosolic fraction of N27 cells as early as 0.5 hr after dieldrin exposure, while cleaved fragments of PKCδ in the nuclear fraction of N27 cells only appeared after the1 hr time point following dieldrin exposure.

Since caspase-3 was primarily activated and retained in the cytoplasm as shown in Figure 1, and the cleaved fragments of PKCδ in the cytosolic fraction appeared at an earlier

time point as compared to the nuclear fraction of N27 cells following dieldrin exposure, this result suggests that the full-length PKCδ is first cleaved in the cytoplasm and then the cleaved fragments of PCKδ are translocated to the nucleus. To investigate whether the nuclear accumulation of cleaved fragments of PKCδ was caspase-3 dependent, N27 cells were co-treated with dieldrin and the caspase-3 specific inhibitor Z-DEVD-FMK. As shown in Figure 3C, cleaved fragments of PKCδ appeared in both cytosolic and nuclear fractions following dieldrin exposure. Following co-treatment with Z-DEVD-FMK and dieldrin, cleaved fragments of PKCδ were dramatically decreased in the cytosolic fraction. Similarly, the cleaved fragments in the nuclear fraction were also reduced. Notably, however, the reduction in cleaved fragments of PKCδ in the nuclear fraction was not as significant as that observed in the cytosolic fraction. Possibly a small fraction of cleaved fragments of PKCδ was still generated in the cytoplasm due to the incomplete inhibition of Z-DEVD-FMK; therefore, these cleaved fragments of PCKδ continued to translocate and accumulate in the nucleus. This result matched our previous observation that the cleaved fragments of PKCδ appeared at an earlier time point in the cytosolic fraction compared to the nuclear fraction, reinforcing the model that the full-length PKCδ is first cleaved in the cytoplasm and the cleaved fragments of PKCδ subsequently translocate to the nucleus in N27 cell following dieldrin exposure.

We also tried to directly determine the localization change of the catalytic fragment of PKCδ in N27 cells following dieldrin exposure. Because antibody specifically detecting the catalytic fragment of PCKδ is currently unavailable, we then transiently transfected PKCδ-CF into N27 cells to examine the localization of the catalytic fragment of PKCδ

(PKCδ-CF). Immunostaining of the V5 tag and counterstaining of the nucleus were performed at 24 hr post-transfection. As shown in Figure 3D, PKCδ-CF, revealed by V5 immunoreactivity, primarily localizes in the nucleus, further indicating that cleaved fragments of PKCδ translocate to the nucleus.

Cleavage resistant mutant of PKCδ (PKCδ-CRM) abolishes dieldrin induced proteolytic activation of PKCδ in N27 cells and protects cells from dieldrin induced apoptosis

In order to investigate the necessity of caspase-3 mediated proteolytic activation of PKCδ in dieldrin induced apoptosis of N27 cells, the PKCδ-CRM stably expressing N27 cell line was generated via the ViraPower^{TM} lentiviral expression system (Invitrogen). Figure 4A shows that about 80% of N27 cells in this cell line were PKCδ-CRM expressing cells, as identified by immunostaining of the V5 tag. PKCδ-CRM contains a point mutation (D327A) in its caspase-3 recognition and cleavage motif, which abolishes the cleavage of PKCδ by activated caspase-3 (DeVries et al., 2002; Ghayur et al., 1996). As shown in Figure 4B, in the control (no transfection) cells, PKCδ cleavage was induced at the 1 hr time point following dieldrin exposure and was abolished by co-treatment with Z-DEVD-FMK and dieldrin; however, in the PKCδ-CRM expressing N27 cells, cleaved fragments of PKCδ were barely detected at the 1 hr time point following dieldrin exposure.

The detailed mechanism of the inhibition of PKCδ-CRM in dieldrin induced cleavage of endogenous PKCδ is under investigation. Some preliminary results from our lab suggest that overexpressed PKCδ down-regulates the expression of endogenous PKCδ. The

overexpressed PKCδ-CRM might also inhibit the feedback loop between PKCδ and caspase-3 (Leverrier et al., 2002), resulting in the inhibition of continuous activation of caspase-3. It is also possible that the overexpressed PKCδ-CRM simply out-competes endogenous PKCδ for activated caspase-3, thus leaving endogenous PKCδ intact. With the co-treatment of Z-DEVD-FMK and dieldrin in PKCδ-CRM cells, dieldrin induced cleavage of PKCδ was completely blocked. Meanwhile, the PKCδ kinase activity was also examined in PKCδ-CRM expressing cells. As shown in Figure 4C, dieldrin treatment for 1 hr in the control (no transfection) cells increased PKCδ kinase activity to 220% in comparison to untreated control cells. However, in PKCδ-CRM expressing cells, dieldrin exposure for 1 hr increased PKCδ kinase activity by only 20% compared to untreated PKCδ-CRM cells.

We next examined whether abolishment of caspase-3 mediated proteolytic activation of PKCδ by PKCδ-CRM protects N27 cells against dieldrin induced apoptotic cell death. In control cells, dieldrin exposure for 1 hr induced about 520% increase in the DNA fragmentation level compared to untreated control cells; however, in the PKCδ-CRM expressing N27 cells, only 50% increase in the DNA fragmentation level was induced following dieldrin exposure for 1 hr in comparison to untreated PKCδ-CRM expressing cells (Figure 4D). These results clearly suggest that the caspase-3 mediated proteolytic activation of PKCδ following dieldrin exposure is required for PKCδ's pro-apoptotic function in dieldrin induced apoptotic cell death in dopaminergic neuronal cells.

Lipid-mediated activation of full-length PKCδ induces neuronal differentiation but not apoptosis in N27 cells

Other than proteolytic activation, PKCδ can also be activated through the binding of lipid (diacylglycerol, phorbol esters) to its C1 domain, resulting in subsequent translocation to the plasma membrane (Newton, 2003). To investigate whether the lipid-mediated activation of full-length PKCδ also contributes to apoptosis of dopaminergic neuronal cells, N27 cells were treated with either 100 nM bistratene A, the specific PKCδ activator (Frey et al., 2000; Frey et al., 2001) or 100 nM TPA, the classical pan-PKC activator, for 30 min. The immunostaining of PKCδ was performed after treatment and observed under confocal microscopy. As shown in Figure 5Ai, PKCδ showed uniform cytoplasmic distribution, and no clear neurites were observed in the untreated N27 cells. After treatment with bistratene A for 30 min, PKCδ was translocated to the plasma membrane (Figure 5Ad) and differentiation of N27 cells were observed (Figure 5Af). Multiple elongated neurites were induced, and the cell body became more compact. N27 cells were also treated with TPA. As shown in Figure 5Aa, plasma membrane translocation of PKCδ and differentiation of N27 cells were induced following TPA exposure. No PKCδ cleavage was induced in N27 cells following either TPA or bistratene A exposure for 30 min, as shown in Figure 5B. Following bistratene A or TPA exposure, the DNA fragmentation level in N27 cells was also determined. As shown in Figure 5C, no significant difference was found in DNA fragmentation levels in N27 cells treated with bistratene A or TPA compared to the untreated cells. Taken together, these results clearly suggest that although full-length PKCδ can be activated through lipid molecules, the activated full-length PCKδ contributes to neuronal differentiation, but not the apoptotic death of dopaminergic neuronal cells.

Blockade of the nuclear localization of cleaved fragments of PKCδ protects N27 cells from apoptosis

As shown above, dieldrin exposure induces not only caspase-3 mediated proteolytic activation of PKCδ, but also the nuclear translocation of activated cleaved PKCδ. It has been recently reported that the C-terminal of PKCδ contains a functional nuclear localization signal (NLS) (DeVries et al., 2002). Point mutation of this NLS abolishes the nuclear translocation of PKCδ in rat parotid salivary cells (DeVries et al., 2002). To investigate whether the nuclear translocation of activated cleaved PCKδ is essential for its function in apoptosis, we first prepared PKCδ-ΔNLS with the deletion of the complete nuclear localization signal (NLS) and generated the N27 cell line stably expressing PKCδ-ΔNLS and PKCδ-WT with the use of the ViraPower^{TM} lentiviral expresson system (Invitrogen).

The schematic representation of the primary structure of PCKδ-WT, PKCδ-ΔNLS, and PKCδ-CRM is shown in Figure 6A. An N27 cell line stably expressing β-galactosidase (LacZ, supplied with the kit) was also generated as a vector control. Expressed PKCδ-ΔNLS or PKCδ-WT could be identified by immunostaining of the V5 tag at the C terminal. Because the V5 tag is located at the C-terminal, immunostaining of the V5 tag identified both the full-length and cleaved catalytic fragment of PKCδ. In the PKCδ-WT expressing cells, PKCδ-WT, revealed by V5 immunoreactivity, was primarily localized in the cytoplasm in the untreated cells (Figure 6Ba). At 1 hr following dieldrin exposure, V5 immunoreactivity accumulated in the nucleus, as shown in Figure 6Bd, which is consistent with our observation of the endogenous PKCδ (Figure 3A). In the PKCδ-ΔNLS expressing cells, PKCδ-ΔNLS, revealed by V5 immunoreactivity, localized only in the cytoplasm regardless of the treatment

with dieldrin (Figure 6Bb&e). The subcellular localization of PKCδ-CRM was also examined. As shown in Figure 6Bc&f, PKCδ-CRM, revealed by V5 immunoreactivity, also showed predominant localization in the cytoplasm with or without treatment with dieldrin, which suggests again that only cleaved fragments of PKCδ, not the full-length PKCδ, translocates to the nucleus.

We next examined the DNA fragmentation level in PKCδ-WT and PKCδ-ΔNLS expressing cells following dieldrin exposure. As shown in Figure 6C, DNA fragmentation levels following dieldrin exposure only increased by 60% in PKCδ-ΔNLS expressing cells when compared to untreated PKCδ-ΔNLS cells; however, an approximate 210% DNA fragmentation level was induced following dieldrin exposure in both PKCδ-WT expressing and vector control cells. Together with the DNA fragmentation result from Figure 4D, our study clearly indicates that not only the proteolytic activation of full-length PKCδ, but also the subsequent nuclear translocation of activated cleaved PCKδ, are both necessary for PKCδ's pro-apoptotic function in dieldrin-induced apoptosis of dopaminergic neuronal (N27) cells.

Activated cleaved PKCδ mediates Ser14 phosphorylation of histone H2B following its nuclear translocation in dieldrin induced apoptotic N27 cells

Phosphorylation of histones has been suggested to play a role in the formation of chromatin condensation in apoptotic cells (Ajiro, 2000). In particular, histone H2B phosphorylation at Ser14 has been ubiquitously found in apoptotic cells (Cheung et al., 2003). To investigate whether activated cleaved fragments of PKCδ mediate H2B phosphorylation

following nuclear translocation, we first examined the Ser14 phosphorylation in dieldrin-induced apoptotic N27 cells. The immunostaining of phosphorylated H2B was performed with the use of anti-phospho-Histone H2B (Ser14) antibody in N27 cells at the 1 hr time point following dieldrin exposure. As shown in Figure 7Aa, Ser14 phosphorylated H2B was clearly detected in dieldrin-induced apoptotic cells. To ensure that it occurred inside the nucleus, nuclei were also counterstained with Hoechst 33342. As shown in Figure 7Ab, a condensed nucleus was also observed in the same apoptotic cell and the merged image (Figure 7Ac) confirms the co-staining. Histone mixtures were also extracted from the nuclei of N27 cells following dieldrin treatment alone or after co-treatment with Z-DEVD-FMK and dieldrin, separated by 15% SDS-PAGE, and immunobloted with anti-phospho-Histone H2B (Ser14) antibody. As shown in Figure 7B, Z-DEVD-FMK co-treatment reduced dieldrin-induced Ser14 phosphorylation of H2B, indicating that Ser14 phosphorylation of H2B is caspase-3 dependent.

To directly examine whether PKCδ mediated the phosphorylation of H2B, PKCδ was immunoprecipitated from N27 cells following co-treatment of Z-DEVD-FMK and dieldrin or dieldrin treatment alone. Immunoprecipitated PKCδ was then performed with an *in vitro* kinase assay with purified H2B as substrate in the presence of ^{32}P. As shown in Figure 7C, PKCδ immunoprecipitated from cells treated only with dieldrin showed a significant increase in phosphorylation of H2B over time (from 1 hr to 3 hr) compared to untreated cells, however, Z-DEVD-FMK co-treatment reduced dieldrin-induced phosphorylation of H2B by immunoprecipitated PKCδ.

PKCδ-CRM and PCKδ-ΔNLS have been shown above to inhibit the nuclear translocation of activated cleaved PKCδ. To investigate whether PKCδ-CRM and PKCδ-ΔNLS also block dieldrin-induced Ser14 phosphorylation of H2B, double immunostaining of V5 and Ser14 phosphorylated H2B was performed in PKCδ-CRM and PKCδ-ΔNLS stably expressing N27 cells following dieldrin exposure. In addition, double staining of V5 and Ser14 phosphorylated H2B was also performed in dieldrin treated PKCδ-WT and PKCδ-DN stably expressing N27 cells to determine whether PKCδ indeed mediates Ser14 phosphorylation of H2B. As shown in Figure 7Da-d, Ser14 phosphorylated H2B was clearly detected in PKCδ-WT expressing N27 cells, and fragmentation of the nucleus was also observed after dieldrin treatment. However, Ser14 phosphorylated H2B staining could not be detected in PKCδ-DN (Figure 7Df), PKCδ-CRM (Figure 7Dj) and PKCδ-ΔNLS (Figure 7Dn) expressing cells. Nuclei of these cells are also intact after dieldrin treatment. The effective inhibition of PKCδ-DN, PKCδ-CRM, and PKCδ-NLS indicates that the cleaved, kinase-active fragments of PKCδ, after nuclear translocation, mediate Ser14 phosphorylation of H2B and promote dieldrin induced apoptotic death of dopaminergic neuronal cells.

Catalytic fragment of PKCδ directly induces Ser14 phosphorylation of histone H2B and apoptosis in dopaminergic neuronal cells

Next, we directly introduced the catalytic fragment of PKCδ (PKCδ-CF) in the N27 cells to investigate whether PKCδ-CF itself can induce Ser14 phosphorylation of H2B and apoptosis in N27 cells. PKCδ-CF was introduced into the N27 cells through lipofectamine-mediated transfection. PKCδ-RF was also introduced into the N27 cells to serve as a control.

About 48 hr after transfection, double immunostaining of Ser14 phosphorylated H2B and the V5 tag as well as counterstaining of nuclei were performed to visualize the localization of PKCδ-CF and phosphorylation of H2B. As shown in Figure 8a, PKCδ-CF, revealed by V5 immunoreactivity, only localizes in the nucleus, and strong staining of Ser14 phosphorylated H2B was also observed in the same cell (Figure 8b). Nucleus counterstaining showed that the nucleus was also broken apart and chromatin became condensed (Figure 8c), confirming that this cell indeed underwent apoptosis. In contrast, the nucleus of a PKCδ-RF positive N27 cell is still intact (Figure 8g) and no clear staining of Ser14 phosphorylated H2B could be observed (Figure 8f). The direct induction of Ser14 phosphorylation of H2B and apoptosis by the nuclear localized PKCδ-CF is consistent with our results above that proteolytically activated cleaved PKCδ mediates neurotoxin-induced Ser14 phosphorylation of H2B and apoptosis of dopaminergic neuronal cells. Interestingly, we first tried to generate PKCδ-CF stably expressing N27 cells with the use of ViraPower^{TM} lentiviral expression system; however, generation of a PKCδ-CF stably expressing N27 cell line was unsuccessful after many attempts. N27 cells were either refractory to PKCδ-CF or quickly died several days after application of the selection antibiotic, blasticidin. This also suggests that PKCδ-CF itself is toxic and could induce cell death by itself.

DISCUSSION

In the present study, we investigated the downstream events after proteolytic cleavage of PKCδ in dieldrin induced apoptosis of dopaminergic neuronal cells. We demonstrated that

the full-length PKCδ was first cleaved in the cytoplasm and the activated cleaved fragments of PKCδ subsequently translocated into the nucleus. By employing the NLS deletion mutant (PKCδ-ΔNLS) and cleavage resistant mutant of PKCδ (PKCδ-CRM), we showed that the proteolytic activation of full-length PKCδ and nuclear translocation of activated cleaved PKCδ are both necessary for PKCδ's pro-apoptotic function in dieldrin-induced apoptosis of dopaminergic neuronal cells. Furthermore, we also demonstrated that the activated cleaved fragments of PKCδ, after nuclear translocation, mediate Ser14 phosphorylation of histone H2B. The caspase-3 inhibitors Z-DEVD-FMK, PKCδ-CRM, PKCδ-ΔNLS, and PKCδ-DN all inhibit Ser14 phosphorylation of H2B, while PKCδ-CF itself can directly induce Ser14 phosphorylation of H2B and apoptosis. Our study suggests that proteolytically activated PKCδ translocates to the nucleus and mediates Ser14 phosphorylation of histone H2B in neurotoxin-induced apoptotic death of dopaminergic neuronal cells.

Proteolytic activation of PKCδ is associated with its nuclear translocation in apoptotic cells. Depending on the cell type and apoptotic stimuli, the nuclear translocation of PKCδ either precedes (Blass et al., 2002; DeVries et al., 2002) or follows (Cross et al., 2000; Scheel-Toellner et al., 1999) its proteolytic activation in apoptotic cells. The early translocation of the full-length PKCδ to the nucleus before its proteolytic activation has been suggested to regulate the mitochondrial mediated apoptotic pathway and subsequent activation of caspase-3 (DeVries et al., 2002). In etoposide induced apoptotic glioma cells, proteolytic activation of PKCδ occurred in the nucleus after full-length PKCδ was translocated to the nucleus. The inhibition of nuclear translocation of the full-length PKCδ blocked caspase-3 activation and cleavage (Blass et al., 2002). Early nuclear translocation of

the full-length PKCδ is also implicated in early nuclear events to regulate the mitochondrial mediated apoptotic pathway in apoptotic C5 rat parotid salivary acinar cells (DeVries et al., 2002). In contrast, the late translocation of the activated cleaved PKCδ to the nucleus (after its proteolytic activation) is more often implicated as a direct effector to accelerate the apoptotic process by facilitating caspase-3 mediated cleavage of nuclear substrates, like lamin B (Cross et al., 2000) or inactivating survival mechanisms in apoptotic cells (Bharti et al., 1998).

In dieldrin-induced apoptotic dopaminergic neuronal cells, we demonstrated here that full-length PKCδ is first cleaved in the cytoplasm and only the activated cleaved fragments of PKCδ subsequently translocate to the nucleus. By employing the cleavage resistant mutant (PKCδ-CRM) and NLS deletion mutant (PKCδ-ΔNLS), we have further shown that the nuclear translocation of activated cleaved PKCδ was necessary for its function in dieldrin-induced apoptosis of dopaminergic neuronal cells. In addition, although few studies reported that the allosteric activation of full-length PKCδ by TPA treatment promoted the cytochrome C release and apoptosis (Majumder et al., 2000), our results show that allosteric activation of full-length PKCδ by treatment with TPA or a PKCδ specific activator, bistratene A, induces differentiation of dopaminergic neuronal cells, but not apoptotic death. By employing the cleavage resistant mutant of PKCδ (PKCδ-CRM), we further demonstrate that proteolytic activation of PKCδ is required for its pro-apoptotic function in dieldrin induced apoptosis of dopaminergic neuronal cells. Since many other studies have reported that activation of the full-length PKCδ by lipids mediates signal transduction in a range of normal physiological processes, our study suggests that proteolytic activation is the favorable mode for PKCδ's

activation and pro-apoptotic function in apoptotic dopaminergic neuronal cells. Our study further provides insight for the design of better inhibitors that specifically inhibit the proteolytic activation of PKCδ, and target only the activated cleaved fragments of PKCδ for protection against neurotoxin induced apoptosis in dopaminergic neuronal cells.

The downstream nuclear events following nuclear translocation of PKCδ in apoptosis have just begun to be explored as more and more nuclear targets of PKCδ have recently been identified. In DNA damage-induced apoptosis, the PKCδ catalytic fragments phosphorylate the catalytic subunit of DNA dependent protein kinase (DNA-PK) (Bharti et al., 1998), inhibiting the function of DNA-PK to form complexes with DNA and to phosphorylate its downstream target, p53 (Ferri and Kroemer, 2001). PKCδ was also found to interact with hRad9, a member of the human DNA damage sensor family to regulate interaction of hRad9 with Bcl-2 and the hRad9-mediated apoptotic response to DNA damage (Yoshida et al., 2003). PKCδ also phosphorylates transcriptional factors, including p73 (Ren et al., 2002) and STAT1 (DeVries et al., 2004), and regulates gene expression in apoptosis. PKCδ not only regulates the apoptotic signal, but also directly accelerates the collapse of nuclear structure in apoptotic cells. It was shown that PKCδ can phosphorylate lamin B, which is one of the major structural proteins involved in the assembly of the nuclear envelope (Cross et al., 2000). The phosphorylation of lamin B increases its susceptibility to caspase mediated cleavage, eventually leading to the disassembly of nuclear lamina.

Phosphorylation of histone H2B at Ser14 has been ubiquitously found in apoptotic cells in diverse species ranging from frogs to humans (Cheung et al., 2003). The H2B phosphorylation and amino-terminal tail of H2B (de la Barre et al., 2001), but not other

histones, are essential for chromatin condensation, one of the hallmarks of apoptotic cells. Mammalian sterile twenty 1 (Mst1) kinase has been identified as responsible for Ser14 phosphorylation of H2B (Cheung et al., 2003). Interestingly, Mst1 kinase also undergoes caspse-3 mediated proteolytic activation, and activated cleaved fragments of Mst1 kinase also translocate to the nucleus (Graves et al., 1998; Ura et al., 2001). In dopaminergic neuronal cells, we demonstrated that dieldrin exposure induces Ser14 phosphorylation of H2B, and activated PKCδ recovered from N27 cells exposed to dieldrin can phosphorylate H2B *in vitro* in a caspase-3 dependent manner. We further showed that the PKCδ catalytic fragment (PKCδ-CF) itself induces phosphorylation of H2B. These results suggest that other than Mst1, activated cleaved fragments of PKCδ also mediate phosphorylation of H2B directly by itself or indirectly by phosphorylating downstream kinases in apoptotic dopaminergic neuronal cells. During preparation of our manuscript, a recent study also reported that PKCδ mediates phosphorylation of H2B (Mecklenbrauker et al., 2004).

In conclusion, we demonstrate that the activated cleaved fragments of PKCδ translocate to the nucleus after proteolytic activation. We also show that proteolytic activation of the full-length PKCδ and nuclear translocation of the activated cleaved PKCδ are both necessary for its function in dieldrin-induced apoptosis of dopaminergic neuronal cells. In addition, the nuclear active PKCδ mediates phosphorylation of H2B and accelerates the apoptotic process in dopaminergic neuronal cells. Understanding the detailed mechanisms of PKCδ activity in neurotoxin-induced apoptosis of dopaminergic neuronal cells provides insight for drug design to protect dopaminergic neurons against neurotoxin induced degeneration.

Figure 1: Subcellular localization of activated caspase-3 in dopaminergic neuronal cells following dieldrin exposure.

(A) Immunoblot of cleaved caspase-3 in cytosolic and nuclear fractions of N27 cells following dieldrin exposure. After treatment with dieldrin (60 μM) for up to 3 hr in serum-free medium, cytosolic and nuclear fractions of N27 cells were prepared and separated on 15% SDS-PAGE. Cleaved (activated) caspase-3 was then detected on the immunoblots with the use of specific anti-cleaved caspase-3 antibody. Immunoblot of LDH and lamin B was also performed on separate gels for relative purity of cytosolic and nuclear fractions. (B) Immunostaining of cleaved caspase-3 in dopaminergic neuronal cells following dieldrin (60 μM) exposure for 1 hr in serum-free medium. After treatment, cells were fixed and stained with anti-cleaved-caspase-3 antibody. The immunoreactivity of cleaved caspase-3 was visualized by Alexa488 conjugated secondary antibody (green fluorescence). The cells were observed under an LCS/NT confocal microscopy system (Bar = 10 μm). Experiments were repeated three times and representative images are presented.

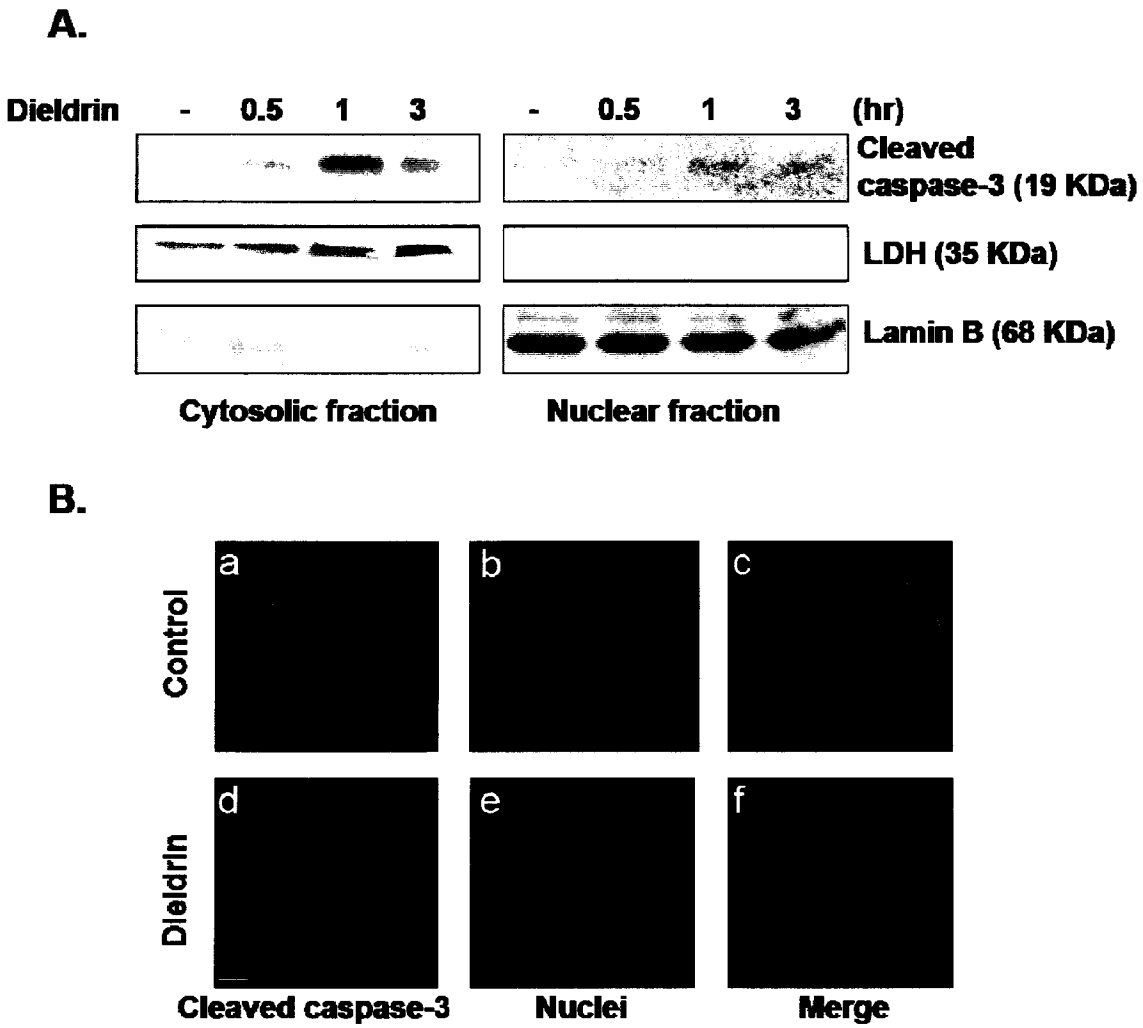
A.
Dieldrin
-
0.5
1
3
-
0.5
1
3
(hr)
Cleaved caspase-3 (19 KDa)
LDH (35 KDa)
Lamin B (68 KDa)
Cytosolic fraction
Nuclear fraction
B.
Control
Dieldrin
a
b
c
d
e
f
Cleaved caspase-3
Nuclei
Merge

Figure 2: Dieldrin exposure induces PKCδ cleavage without changing its expression in N27 cells

(A) Cleaved fragments of PKCδ (38-41kDs) were induced in N27 cells following dieldrin exposure. (B) Dieldrin exposure also induced the generation of cleaved fragments of PARP (85KD) in N27 cells. N27 cells were treated with 60 μM dieldrin for up to 3 hr in serum-free medium. Cells were then lysed and the lysate was used for Western blot analysis to detect both the PKCδ and PARP cleavage. To confirm equal protein loading in Western blots, the membranes were reprobed with β-actin antibody. (C) Amplification plot of quantitative RT-PCR of PKCδ mRNA in N27 cells following dieldrin exposure. (D) Relative quantity of PKCδ mRNA copies in N27 cells following dieldrin exposure. N27 cells were treated with 60 μM dieldrin for up to 3 hr in serum-free medium. Cells were then lysed and total RNA was isolated with TRIZOL reagent and converted to cDNA. The PCR reaction was then set up by mixing 50 ng cDNA, rat PKCδ TaqMan expression assay reagent as well as 2x PCR master mix in a 96-well plate. The PCR reaction was performed in a Mx4000 multiplex Quantitative PCR system (Stratagene, La Jolla, CA). To ensure that equal amounts of RNA were used in the PCR reaction, 18s ribosome RNA (18s rRNA) was used as an endogenous control. The relative quantity of PKCδ mRNA was calculated based on the formula $2^{-(\Delta Ct\ PKC\delta\text{-}\Delta Ct\ 18s\ rRNA)}$ (Ct: threshold of cycle), and the control was used as a calibrator for comparison with other samples. The Ct value was determined by software installed on the Mx4000 multiplex Quantitative PCR system. The data represent the mean ± SEM from three separate experiments in triplicate.

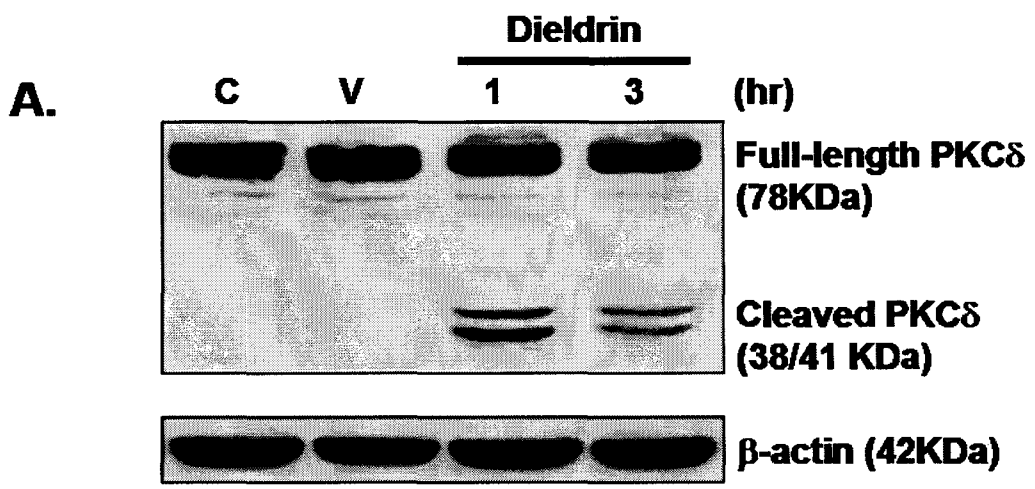
A.
Dieldrin
C
V
1
3
(hr)
Full-length PKCδ
(78KDa)
Cleaved PKCδ
(38/41 KDa)
β-actin (42KDa)

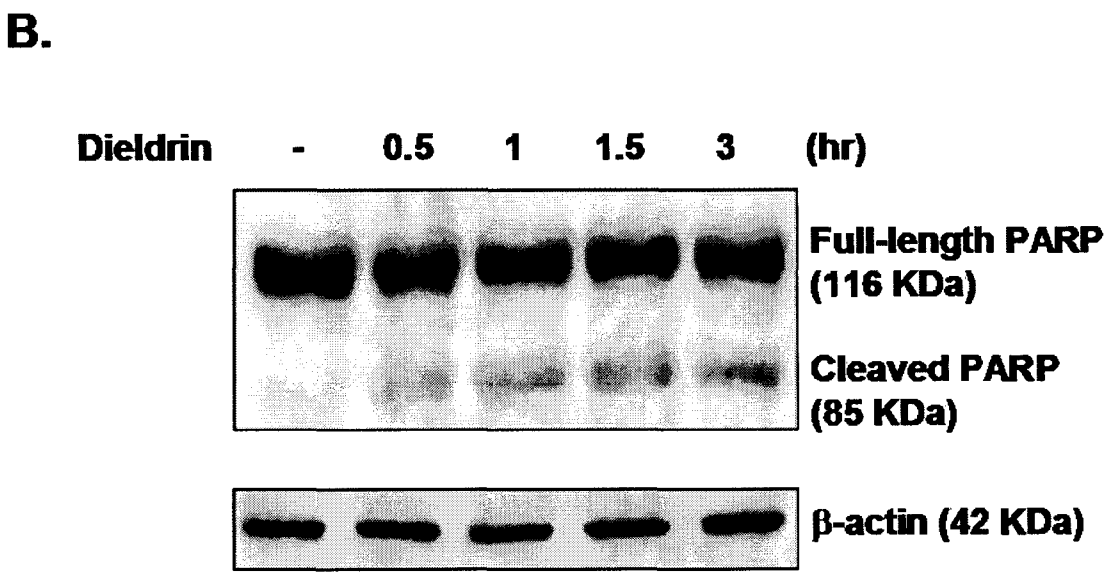
B.
Dieldrin
-
0.5
1
1.5
3
(hr)
Full-length PARP
(116 KDa)
Cleaved PARP
(85 KDa)
β-actin (42 KDa)

C.

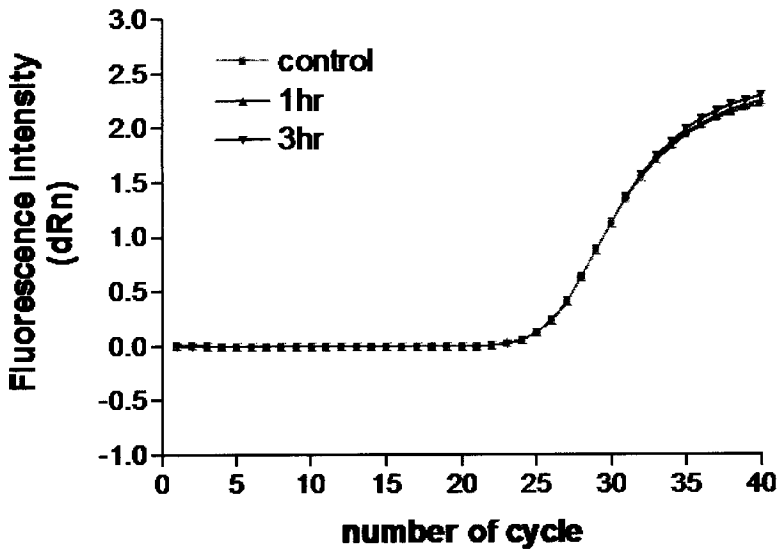
3.0
2.5
2.0
1.5
1.0
0.5
0.0
-0.5
-1.0
Fluorescence Intensity (dRn)
control
1hr
3hr
0
5
10
15
20
25
30
35
40
number of cycle

D.

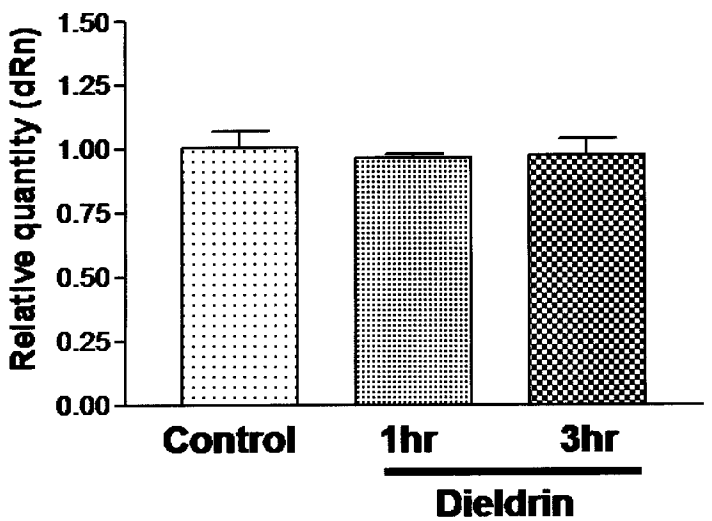
1.50
1.25
1.00
0.75
0.50
0.25
0.00
Relative quantity (dRn)
Control
1hr
3hr
Dieldrin

Figure 3: Dieldrin exposure induces nuclear translocation of cleaved fragments of PKCδ in N27 cells

(A) Nuclear accumulation of PKCδ immunoreactivity in N27 cells following dieldrin exposure. After dieldrin (60 μM) treatment for 1 hr, N27 cells were fixed and stained with anti-PKCδ antibody (1:1000). The PKCδ was visualized then by Alex488 conjugated secondary antibody (1:2000) and images were taken under TCS/NT confocal microscopy (B). Dieldrin exposure induced nuclear translocation of cleaved fragments of PKCδ in N27 cells. (C) Co-treatment of N27 cells with Z-DEVD-FMK reduced dieldrin induced PKCδ cleavage and nuclear translocation of cleaved fragments of PKCδ. Cells were treated with dieldrin (60 μM) alone or co-treated with Z-DEVD-FMK (50 μM or 100 μM) and dieldrin (60 μM) for up to 3 hr. Cytosolic and nuclear fractions were then prepared and separated on 10% SDS-PAGE. Cleaved fragments of PCKδ were then detected on both immunoblots with the use of anti-PKCδ antibody. (D) Nuclear localization of overexpressed PKCδ-CF in the N27 cells. Immunostaining of V5 was performed 24 hr after transfection. Immunoreactivity of V5 was visualized by Cy3 conjugated anti-mouse secondary antibody (1:2000). Nuclei were counterstained by Hoechst 33342. Cells were observed under a LCS/NT confocal microscopy system (Bar = 10 μm).

A.

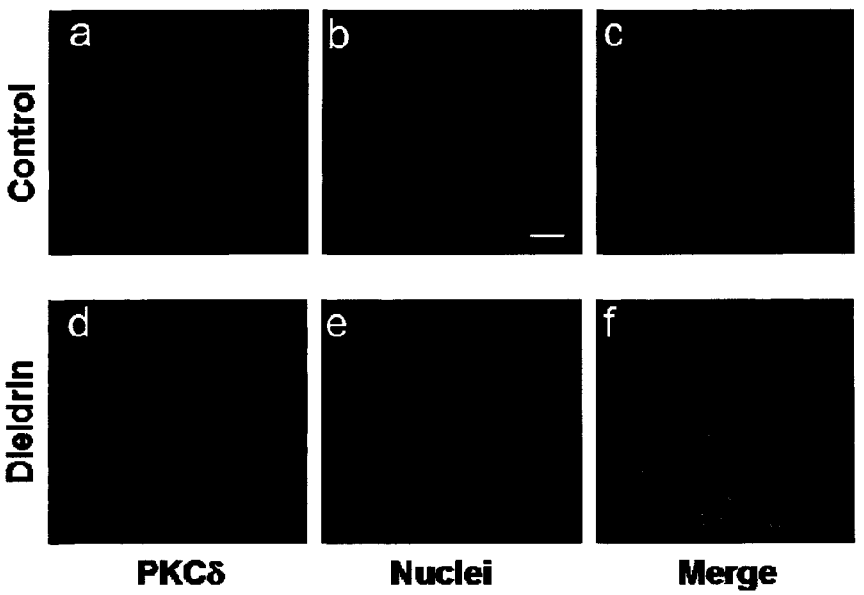
a
b
c
Control
d
e
f
Dieldrin
PKCδ
Nuclei
Merge

B.

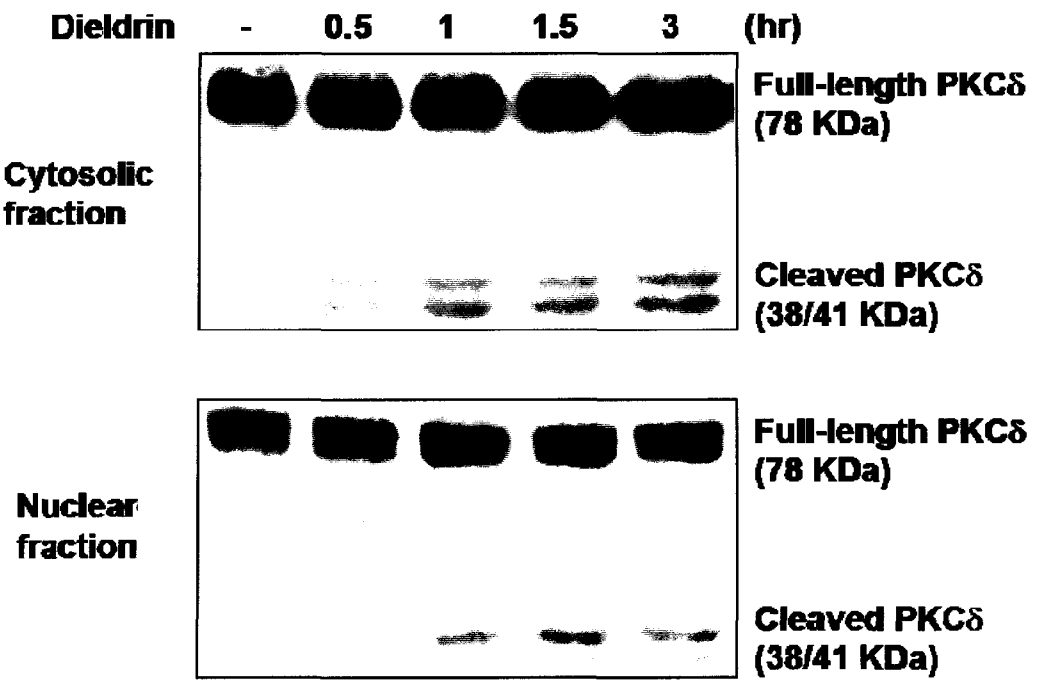
Dieldrin
-
0.5
1
1.5
3
(hr)
Cytosolic fraction
Full-length PKCδ (78 KDa)
Cleaved PKCδ (38/41 KDa)
Nuclear fraction
Full-length PKCδ (78 KDa)
Cleaved PKCδ (38/41 KDa)

C.

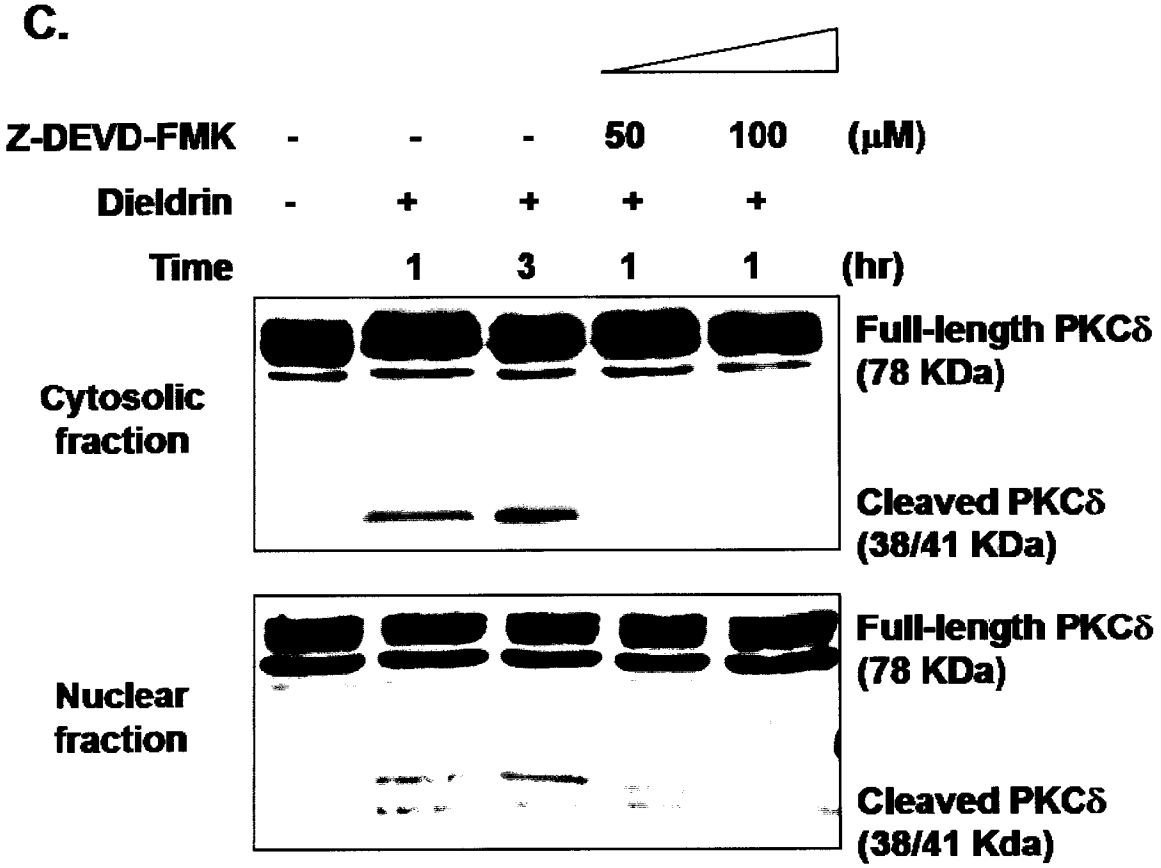
Z-DEVD-FMK - - - 50 100 (μM)
Dieldrin - + + + +
Time 1 3 1 1 (hr)
Cytosolic fraction
Full-length PKCδ (78 KDa)
Cleaved PKCδ (38/41 KDa)
Nuclear fraction
Full-length PKCδ (78 KDa)
Cleaved PKCδ (38/41 Kda)

D.

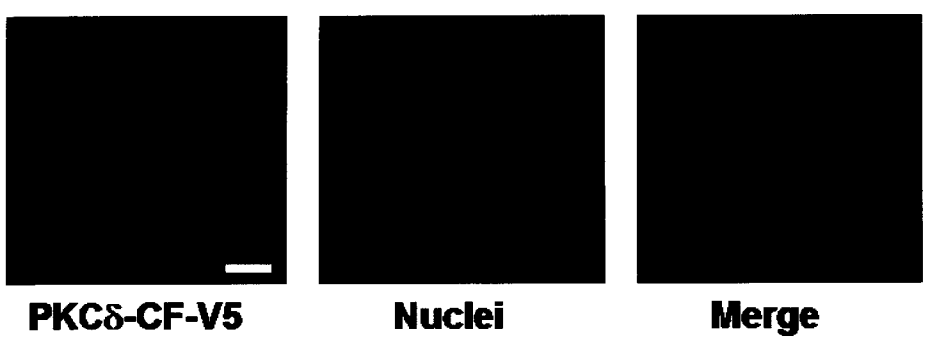
PKCδ-CF-V5
Nuclei
Merge

Figure 4: Cleavage resistant mutant of PKCδ (PKCδ-CRM) abolishes dieldrin induced proteolytic activation of PKCδ and protects cells from dieldrin induced apoptosis in N27 cells.

(A) Stable expression of PKCδ-CRM in dopaminergic neuronal (N27) cells. A ViraPower Lentiviral gene expression system (Invitrogen, Inc. Carlsbad, CA) was employed for generation of a PKCδ-CRM expressing cell line. PKCδ-CRM stably expressing cells were maintained in normal medium supplemented with 10 μg/ml blasticidin. To identify PKCδ-CRM expressing cells, cells were fixed and stained with anti-V5 antibody (1:1000) and Cy3-conjugated secondary anti-mouse antibody (1:2000). Cells were observed under a Nikon inverted fluorescence microscope (Model TE-2000U). (B) Dieldrin induced PKCδ cleavage was abolished in PKCδ-CRM expressing cells. Control cells and PKCδ-CRM expressing cells were treated with dieldrin (60 μM) alone or co-treated with Z-DEVD-FMK (50 μM) and dieldrin (60 μM) for 1 hr. The cells were lysed and whole cell lysate was used for Western blot analysis to detect the PKCδ cleavage. Membrane was reprobed with anti-V5 antibody (1:5000) to ensure abundant PKCδ-CRM was expressed only in the PKCδ-CRM expressing cell line. (C) Dieldrin exposure induced PKCδ kinase activity was attenuated in PKCδ-CRM stably expressing N27 cells. The cells were lysed and PKCδ was first immunoprecipitated and an *in vitro* kinase assay was performed. Significance of difference in kinase activity was compared to untreated control cells. (D) PKCδ-CRM protects against dieldrin induced apoptosis in N27 cells. Significance of difference in DNA fragmentation was compared to untreated control cells. The data represent the mean ± SEM from two separate experiments in triplicate (*, $p<0.05$; ***, $p<0.001$; N=6).

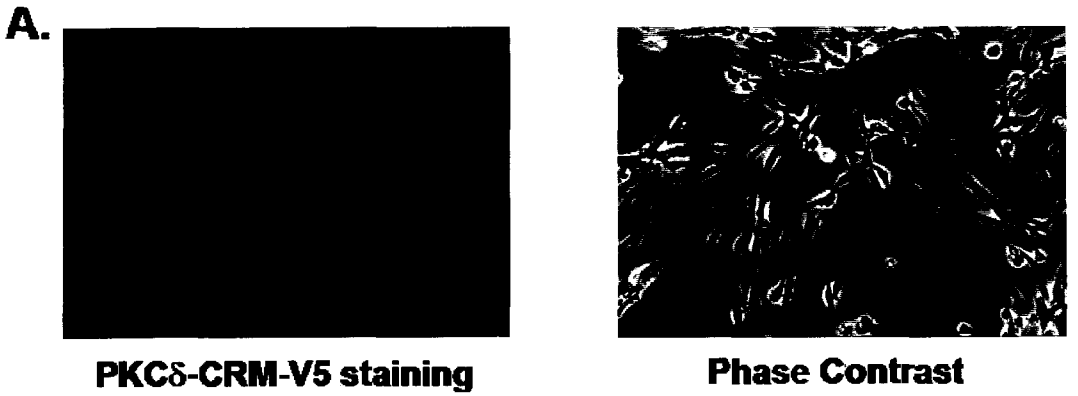
A.
PKCδ-CRM-V5 staining
Phase Contrast

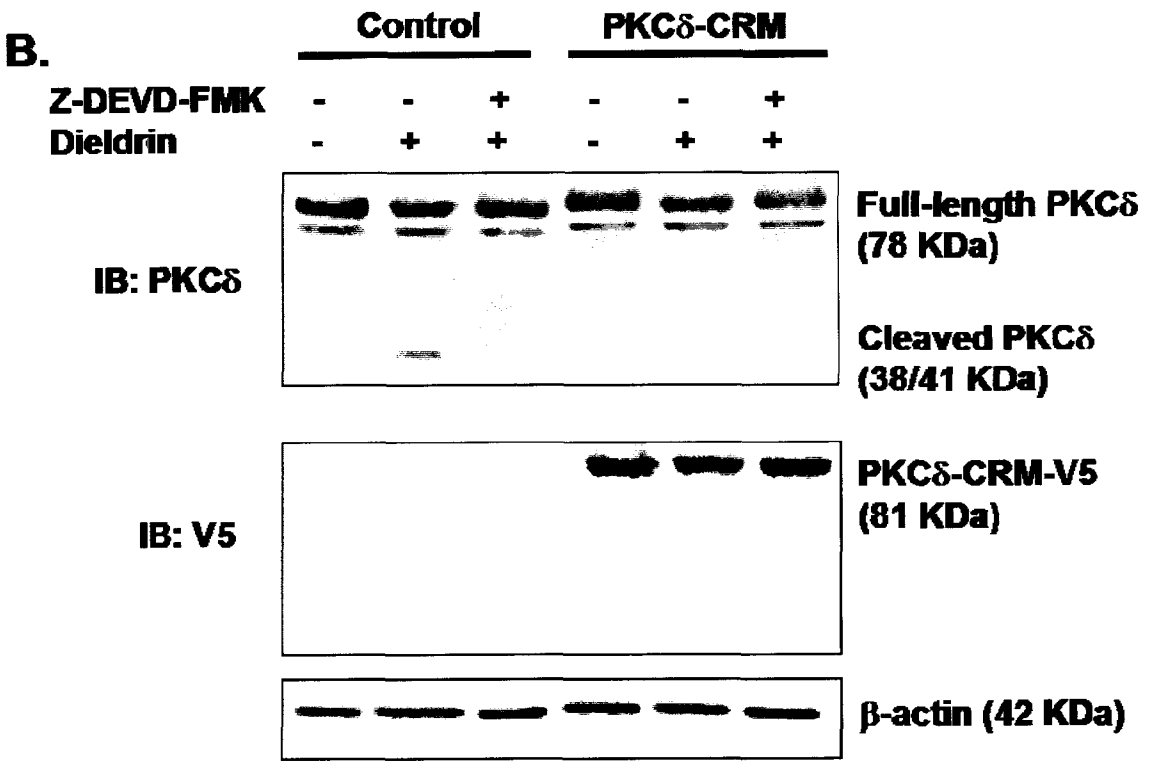
B.
Control
PKCδ-CRM
Z-DEVD-FMK - - + - - +
Dieldrin - + + - + +
IB: PKCδ
Full-length PKCδ (78 KDa)
Cleaved PKCδ (38/41 KDa)
IB: V5
PKCδ-CRM-V5 (81 KDa)
β-actin (42 KDa)

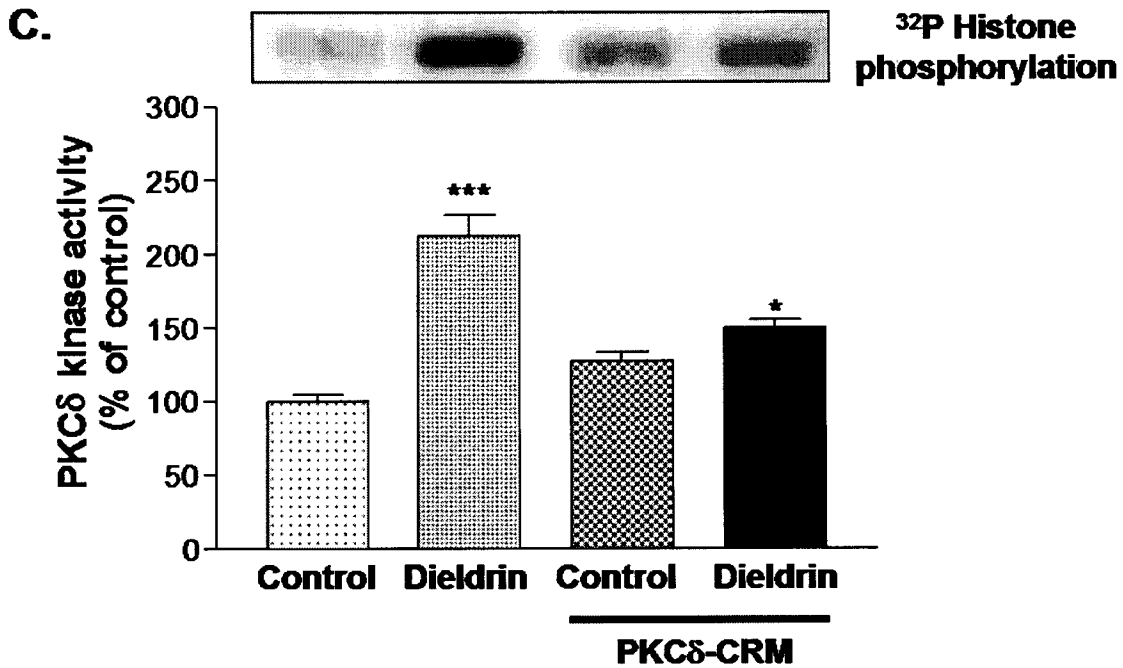
C.
32P Histone phosphorylation
PKCδ kinase activity (% of control)
300
250
200
150
100
50
0
***
*
Control
Dieldrin
Control
Dieldrin
PKCδ-CRM

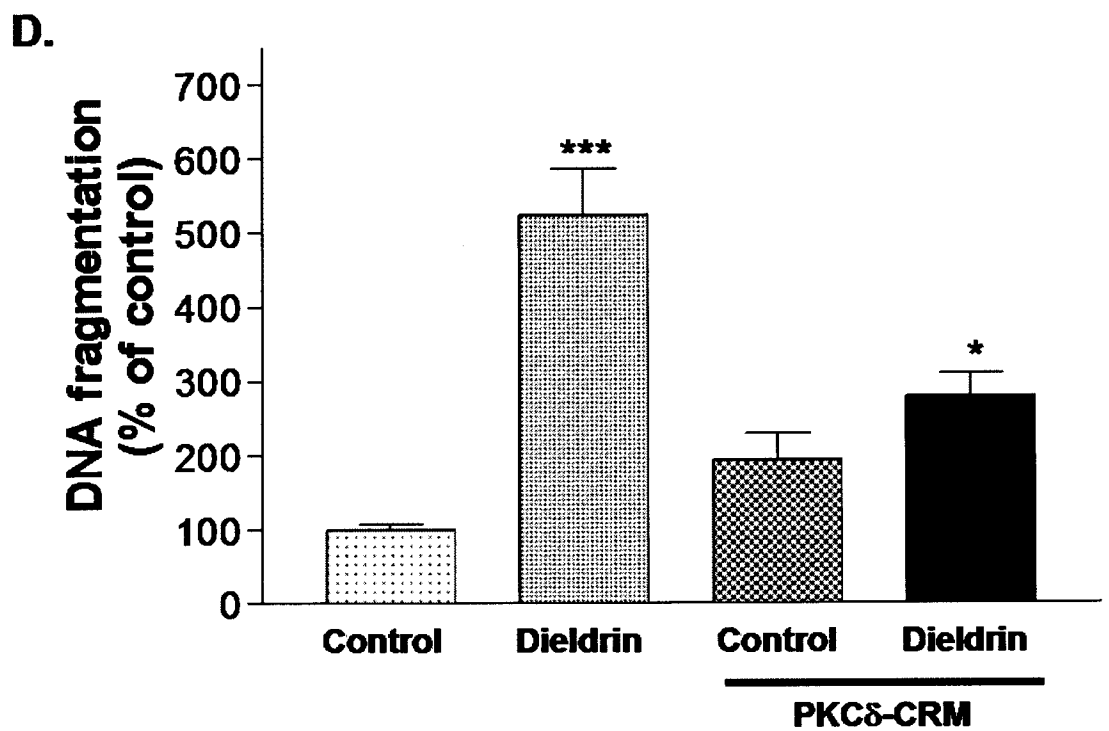
D.
DNA fragmentation (% of control)
700
600
500
400
300
200
100
0
***
*
Control
Dieldrin
Control
Dieldrin
PKCδ-CRM

Figure 5: Lipid-mediated activation of full-length PKCδ induces the differentiation of N27 cells but not apoptotic death.

(A) Plasma membrane translocation of PKCδ and differentiation of N27 cells were induced by bistratene A or TPA treatment. N27 cells were treated with 100 nM bistratene A or TPA for 30 min. PKCδ immunostaining was then performed to visualize its subcellular distribution and cellular morphological changes. Stained cells were observed under confocal microscopy (Bar = 10 μm). (B) TPA and Bistratene A treatment didn't induce PKCδ cleavage in N27 cells. N27 cells were treated with 100 nM TPA or Bis A for 30 min and whole cell lysates were isolated. (C) Apoptotic death was not induced in N27 cells following bistratene A or TPA treatment. After treatment with 100 nM bistratene A or TPA for 30 min, N27 cells were lysed for DNA fragmentation assay. The data represent the mean ± SEM from two separate experiments in triplicate (N=6).

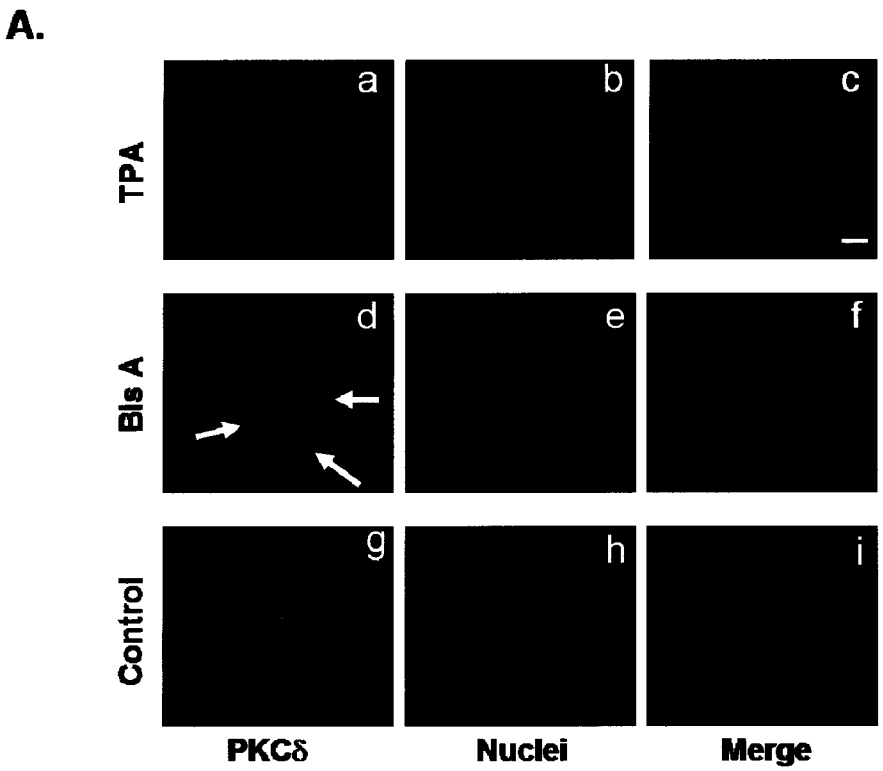
A.
a
b
c
TPA
d
e
f
Bis A
g
h
i
Control
PKCδ
Nuclei
Merge

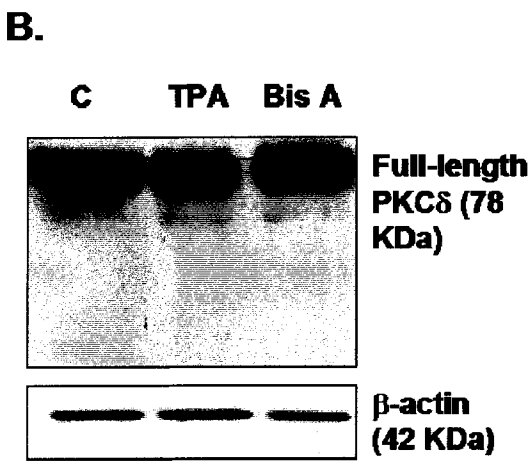
B.
C
TPA
Bis A
Full-length PKCδ (78 KDa)
β-actin (42 KDa)

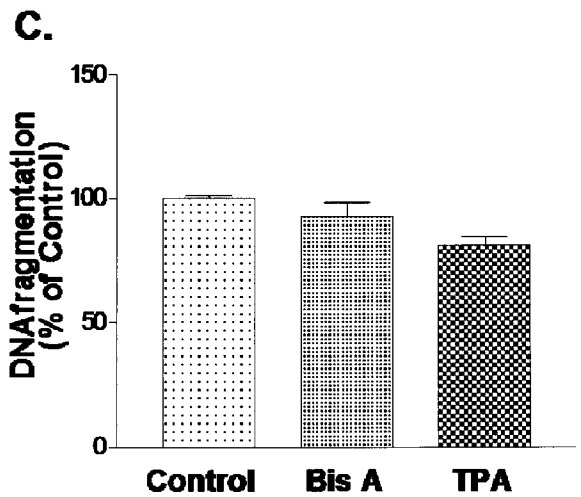
C.
DNAfragmentation (% of Control)
150
100
50
0
Control
Bis A
TPA

Figure 6: Blockade of nuclear localization of cleaved fragments of PKCδ protects N27 cells from dieldrin induced apoptosis.

(A) Schematic representation of primary structure of PKCδ-WT, PKCδ-CRM, and PKCδ-ΔNLS. The V5 tag locates at the C-terminal of the fused protein. (B) Subcellular localization of PKCδ-WT, PKCδ-ΔNLS, and PKCδ-CRM in N27 cells following dieldrin exposure. PKCδ-WT and PKCδ-ΔNLS stably expressing N27 cell lines were also established via ViraPower Lentiviral gene expression system (Invitrogen, Inc. Carlsbad, CA). After dieldrin (60 μM) exposure for 1 hr, subcellular distribution of PKCδ-WT, PKCδ-ΔNLS, and PKCδ-CRM was determined by immunostaining of the C-terminal V5 tag (Bar = 10 μm). (C) Exclusion of PKCδ from the nucleus significantly abolished dieldrin induced apoptosis in N27 cells. Vector control (LacZ), PKCδ-WT, and PKCδ-ΔNLS stably expressing N27 cells were exposed to dieldrin for 1 hr and cells were then lysed for the DNA fragmentation assay. Significance of difference in DNA fragmentation was compared to untreated vector control cells. The data represent the mean $\pm$ SEM from two separate experiments in triplicate (***, $p<0.001$; N=6).

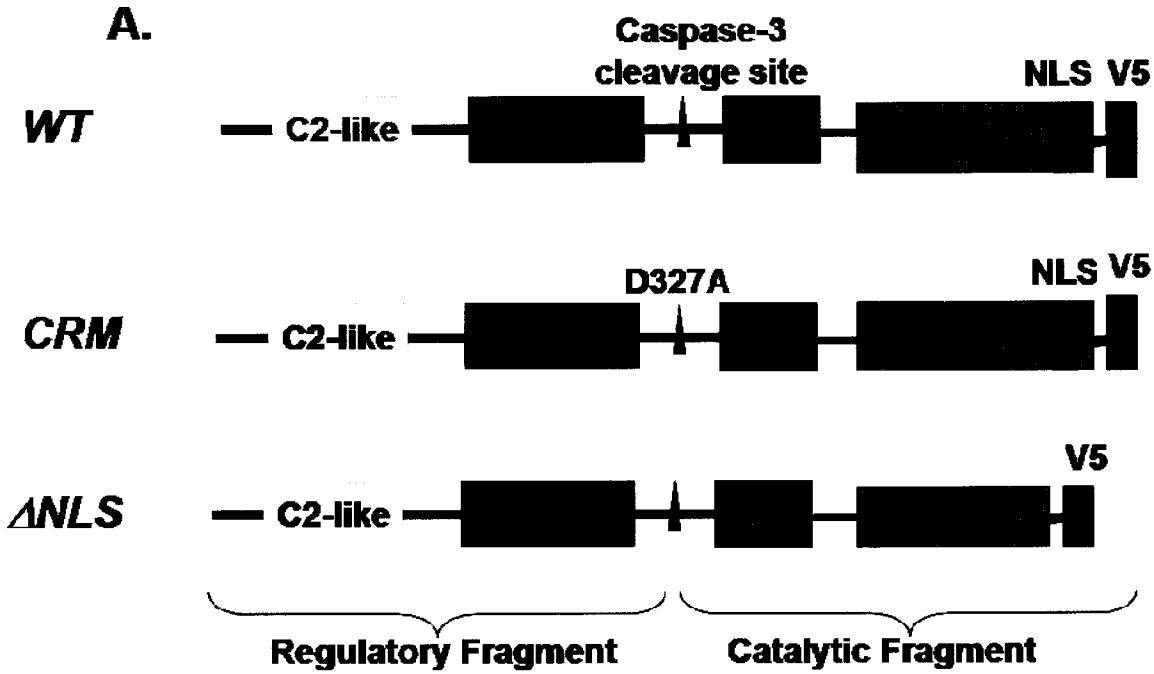
A.
Caspase-3
cleavage site
NLS V5
WT
C2-like
D327A
NLS V5
CRM
C2-like
V5
ΔNLS
C2-like
Regulatory Fragment
Catalytic Fragment

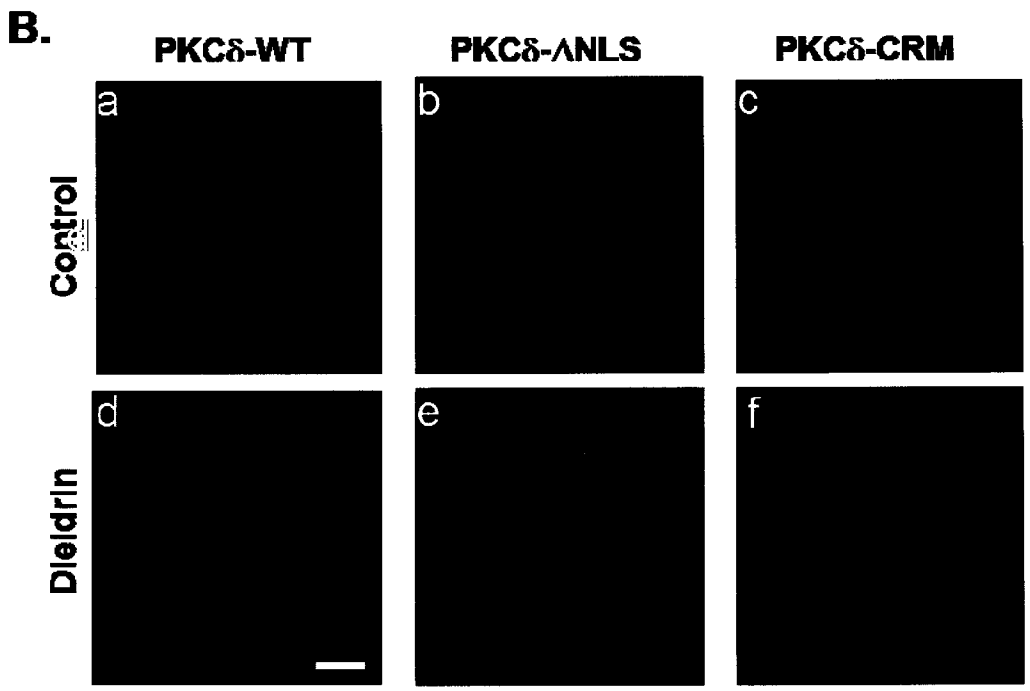
B.
PKCδ-WT
PKCδ-ΔNLS
PKCδ-CRM
Control
Dieldrin
a
b
c
d
e
f

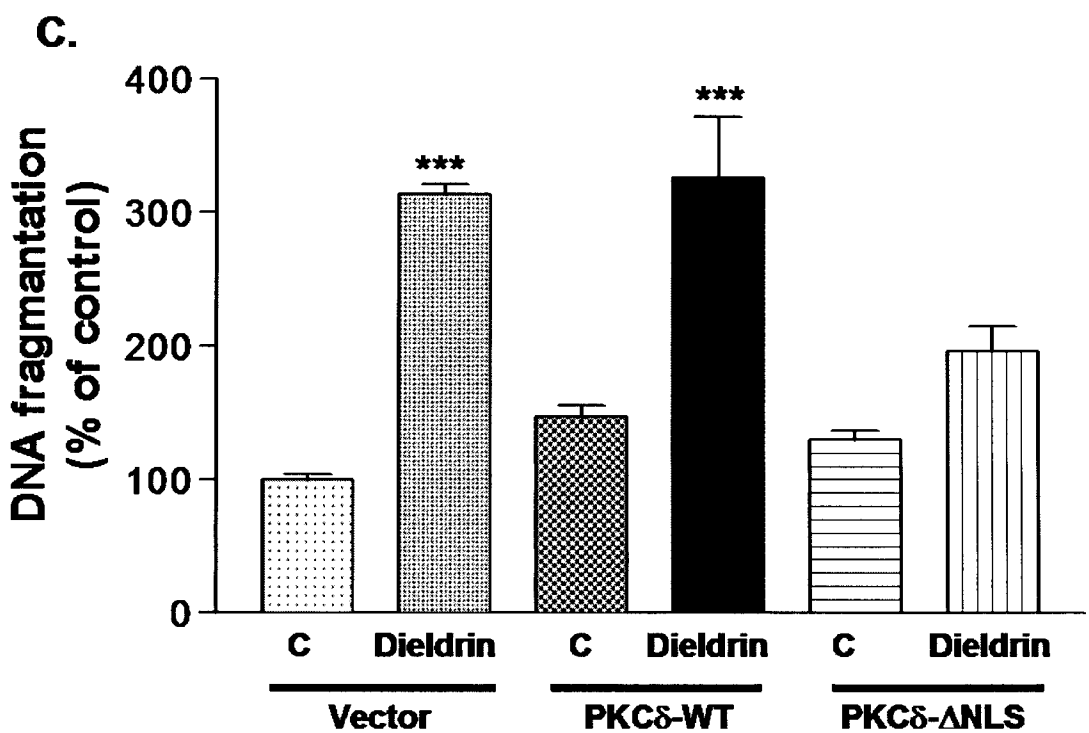
C.
DNA fragmantation
(% of control)
400
300
200
100
0
***
***
C
Dieldrin
C
Dieldrin
C
Dieldrin
Vector
PKCδ-WT
PKCδ-ΔNLS

Figure 7: Cleaved fragments of PKCδ mediate Ser14 phosphorylation of histone H2B in dieldrin induced apoptotic N27 cells.

(A) *In situ* detection of Ser14 phosphorylated H2B in dieldrin induced apoptotic cells. After dieldrin exposure (60 μM) for 1 hr, N27 cells were fixed and stained with Anti-phospho-histone H2B (Ser14) antibody (1:1000) and Alex488 conjugated anti-rabbit secondary antibody (1:2000). Apoptotic nuclei were also shown by counterstaining of nuclei with Hoechst 33342. Cells were observed under a Nikon inverted fluorescence microscope (Model TE-2000U). (B) Dieldrin induced Ser14 phosphorylation of H2B was caspase-3 dependent. (C) *In vitro* phosphorylation of H2B by PKCδ was caspase-3 dependent. Cells were treated with dieldrin (60 μM) alone for up to 3 hr or co-treated with Z-DEVD-FMK (50 μM) and dieldrin (60 μM) for 1 hr. To detect Ser14 phosphorylation of H2B, histone mixtures were then isolated from the nuclear fraction of cells and separated by 15% SDS-PAGE for immunoblot analysis. For the kinase assay, PKCδ was immunoprecipitated from nuclear lysate of cells and an *in vitro* kinase assay was performed with purified H2B as substrate. (D) PKCδ-CRM, PKCδ-DN, and PKCδ-ΔNLS blocked dieldrin-induced Ser14 phosphorylation of Histone H2B. Double immunostaining of V5 and Ser14 phosphorylated H2B was performed after dieldrin treatment for 1 hr. Nuclei were also counterstained by Hoechst 33342. Cells were observed under a Nikon inverted fluorescence microscope (Model TE-2000U). Experiments were repeated three times and representative images are presented.

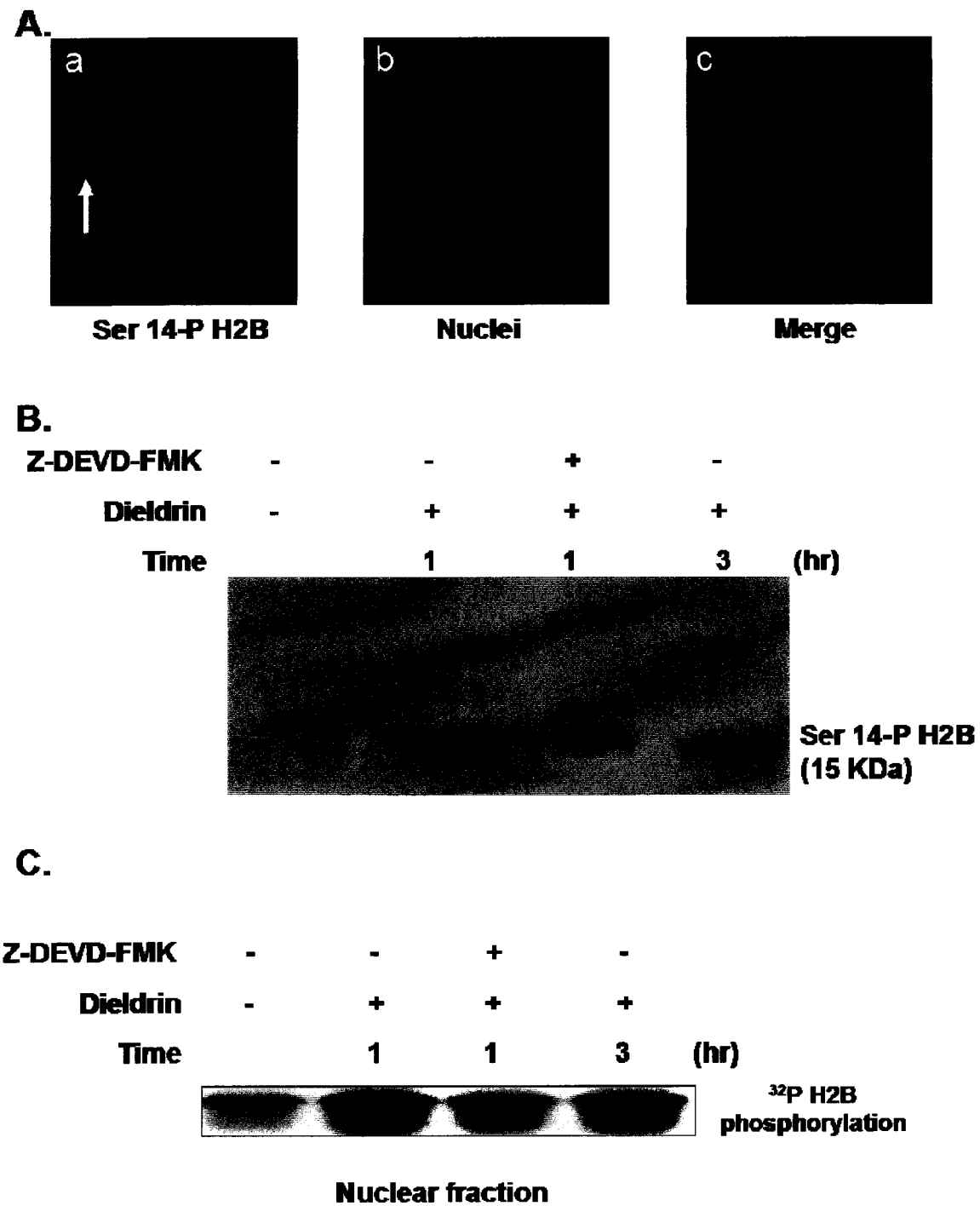
A.
a
b
c
Ser 14-P H2B
Nuclei
Merge
B.
Z-DEVD-FMK - - + -
Dieldrin - + + +
Time 1 1 3 (hr)
Ser 14-P H2B
(15 KDa)
C.
Z-DEVD-FMK - - + -
Dieldrin - + + +
Time 1 1 3 (hr)
32P H2B
phosphorylation
Nuclear fraction

D.

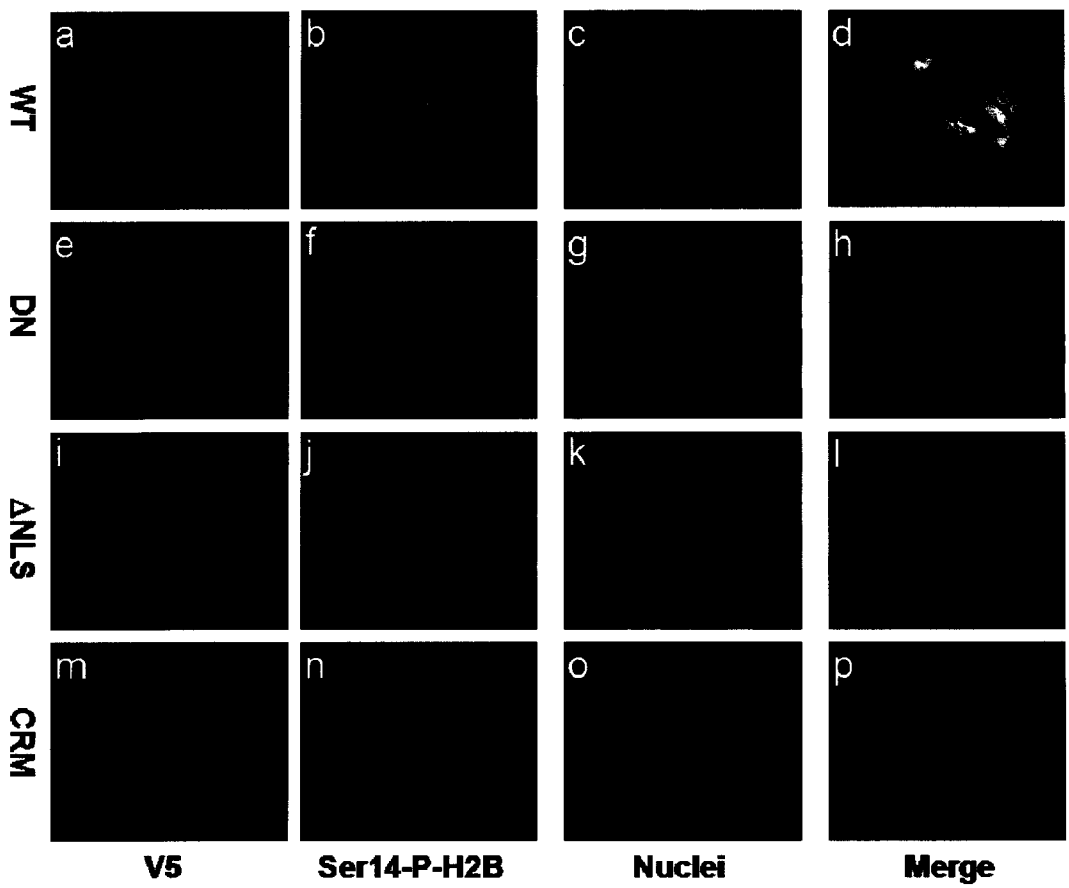

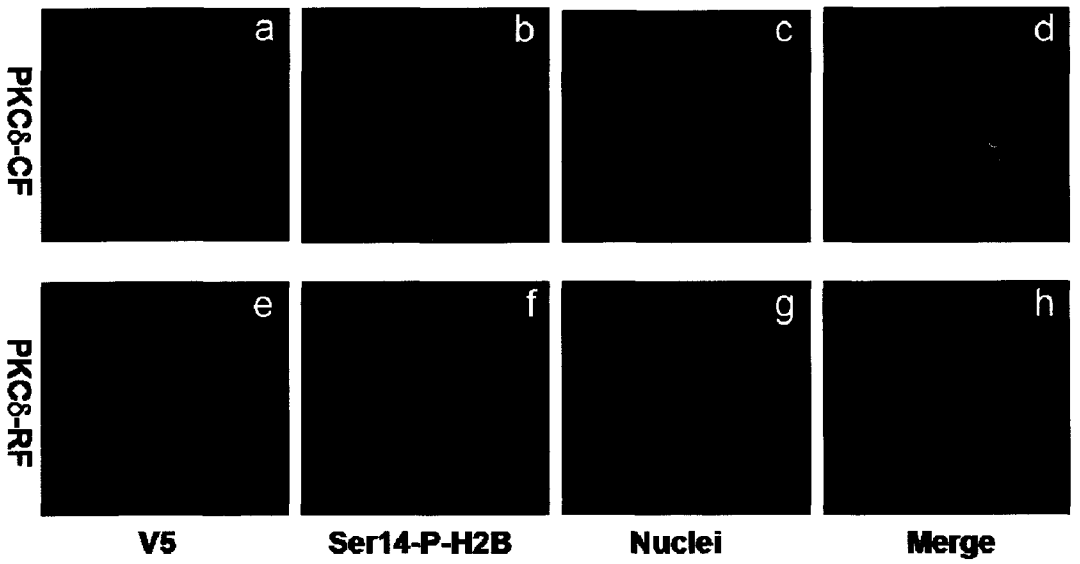

Figure 8: Catalytic fragment of PKCδ (PKCδ-CF) directly induces Ser14 phosphorylation of H2B.

PKCδ-CF and PKCδ-RF were introduced into N27 cells by electroporation. Double immunostaining of V5 and Ser14 phosphorylated H2B was then performed 48 hr after transfection. Immunoreactivity of V5 and Ser14 phosphorylated H2B was visualized by Cy3 conjugated anti-mouse secondary antibody (1:2000) or Alex488 conjugated anti-rabbit secondary antibody (1:2000), respectively. Nuclei were counterstained with Hoechst 33342. Cells were observed under a Nikon inverted fluorescence microscope (Model TE-2000U).

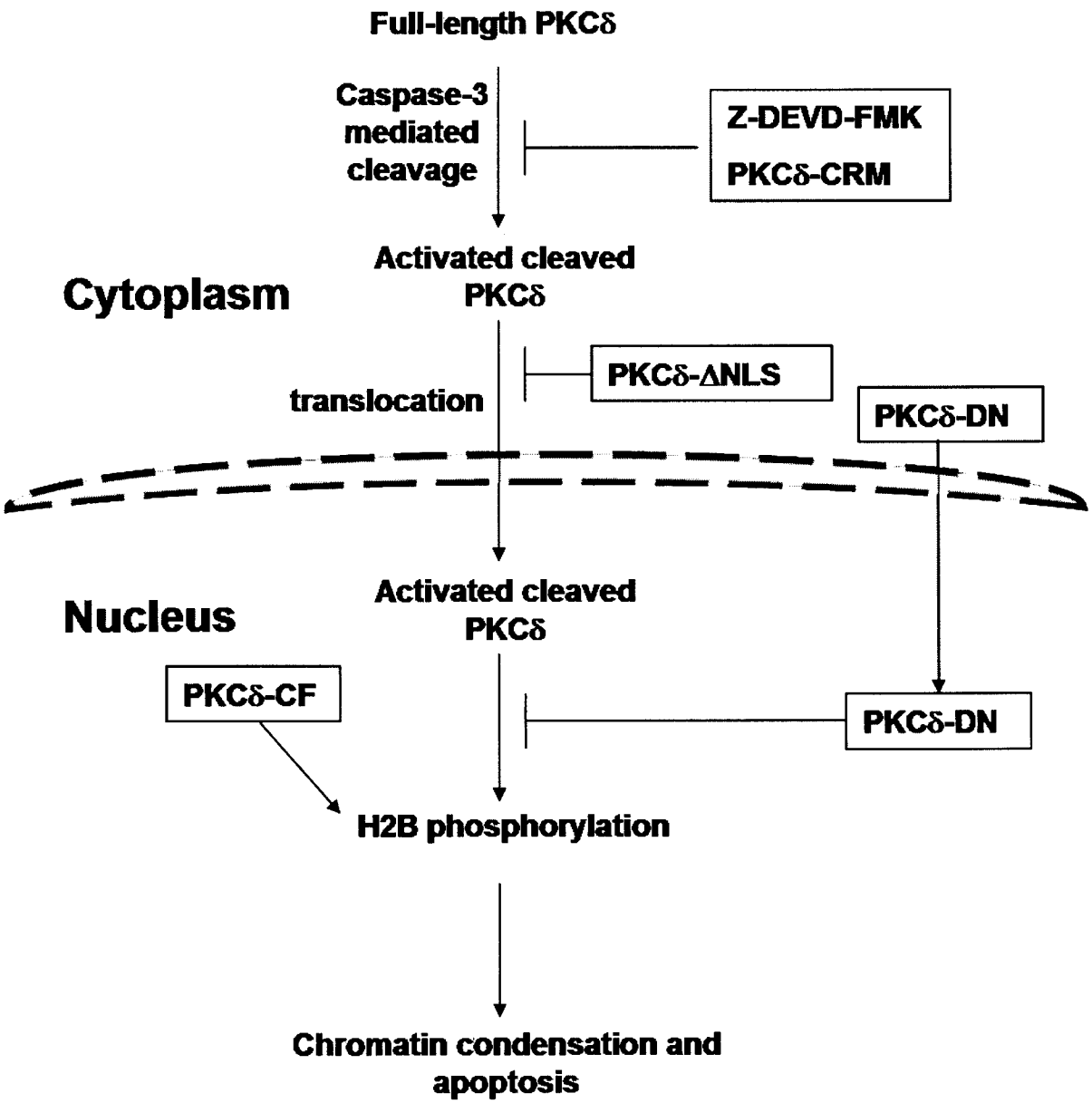

Figure 9: Proposed integrated mechanisms of PKCδ in dieldrin-induced apoptotic death of dopaminergic neuronal (N27) cells.

REFERENCES

Adams, F.S., La Rosa, F.G., Kumar, S., Edwards-Prasad, J., Kentroti, S., Vernadakis, A., Freed, C.R., Prasad, K.N., 1996. Characterization and transplantation of two neuronal cell lines with dopaminergic properties. Neurochem Res. 21,619-27.

Ajiro, K., 2000. Histone H2B phosphorylation in mammalian apoptotic cells. An association with DNA fragmentation. J Biol Chem. 275,439-43.

Anantharam, V., Kitazawa, M., Wagner, J., Kaul, S., Kanthasamy, A.G., 2002. Caspase-3-dependent proteolytic cleavage of protein kinase Cdelta is essential for oxidative stress-mediated dopaminergic cell death after exposure to methylcyclopentadienyl manganese tricarbonyl. J Neurosci. 22,1738-51.

Beal, M.F., 2002. Oxidatively modified proteins in aging and disease. Free Radic Biol Med. 32,797-803.

Betarbet, R., Sherer, T.B., Greenamyre, J.T., 2002. Animal models of Parkinson's disease. Bioessays. 24,308-18.

Betarbet, R., Sherer, T.B., MacKenzie, G., Garcia-Osuna, M., Panov, A.V., Greenamyre, J.T., 2000. Chronic systemic pesticide exposure reproduces features of Parkinson's disease. Nat Neurosci. 3,1301-6.

Bharti, A., Kraeft, S.K., Gounder, M., Pandey, P., Jin, S., Yuan, Z.M., Lees-Miller, S.P., Weichselbaum, R., Weaver, D., Chen, L.B., Kufe, D., Kharbanda, S., 1998. Inactivation of DNA-dependent protein kinase by protein kinase Cdelta: implications for apoptosis. Mol Cell Biol. 18,6719-28.

Blass, M., Kronfeld, I., Kazimirsky, G., Blumberg, P.M., Brodie, C., 2002. Tyrosine phosphorylation of protein kinase Cdelta is essential for its apoptotic effect in response to etoposide. Mol Cell Biol. 22,182-95.

Brodie, C., Blumberg, P.M., 2003. Regulation of cell apoptosis by protein kinase c delta. Apoptosis. 8,19-27.

Bustin, S.A., 2000. Absolute quantification of mRNA using real-time reverse transcription polymerase chain reaction assays. J Mol Endocrinol. 25,169-93.

Bustin, S.A., 2002. Quantification of mRNA using real-time reverse transcription PCR (RT-PCR): trends and problems. J Mol Endocrinol. 29,23-39.

Chen, Y.R., Meyer, C.F., Ahmed, B., Yao, Z., Tan, T.H., 1999. Caspase-mediated cleavage and functional changes of hematopoietic progenitor kinase 1 (HPK1). Oncogene. 18,7370-7.

Cheung, W.L., Ajiro, K., Samejima, K., Kloc, M., Cheung, P., Mizzen, C.A., Beeser, A., Etkin, L.D., Chernoff, J., Earnshaw, W.C., Allis, C.D., 2003. Apoptotic phosphorylation of histone H2B is mediated by mammalian sterile twenty kinase. Cell. 113,507-17.

Coleman, M.L., Sahai, E.A., Yeo, M., Bosch, M., Dewar, A., Olson, M.F., 2001. Membrane blebbing during apoptosis results from caspase-mediated activation of ROCK I. Nat Cell Biol. 3,339-45.

Corrigan, F.M., Murray, L., Wyatt, C.L., Shore, R.F., 1998. Diorthosubstituted polychlorinated biphenyls in caudate nucleus in Parkinson's disease. Exp Neurol. 150,339-42.

Cross, T., Griffiths, G., Deacon, E., Sallis, R., Gough, M., Watters, D., Lord, J.M., 2000. PKC-delta is an apoptotic lamin kinase. Oncogene. 19,2331-7.

Datta, R., Kojima, H., Yoshida, K., Kufe, D., 1997. Caspase-3-mediated cleavage of protein kinase C theta in induction of apoptosis. J Biol Chem. 272,20317-20.

Dauer, W., Przedborski, S., 2003. Parkinson's disease: mechanisms and models. Neuron. 39,889-909.

Dawson, T.M., Dawson, V.L., 2003. Molecular pathways of neurodegeneration in Parkinson's disease. Science. 302,819-22.

de la Barre, A.E., Angelov, D., Molla, A., Dimitrov, S., 2001. The N-terminus of histone H2B, but not that of histone H3 or its phosphorylation, is essential for chromosome condensation. Embo J. 20,6383-93.

de Souza, P.M., Lindsay, M.A., 2004. Mammalian Sterile20-like kinase 1 and the regulation of apoptosis. Biochem Soc Trans. 32,485-8.

DeVries, T.A., Kalkofen, R.L., Matassa, A.A., Reyland, M.E., 2004. Protein kinase Cdelta regulates apoptosis via activation of STAT1. J Biol Chem. 279,45603-12.

DeVries, T.A., Neville, M.C., Reyland, M.E., 2002. Nuclear import of PKCdelta is required for apoptosis: identification of a novel nuclear import sequence. Embo J. 21,6050-60.

Emoto, Y., Manome, Y., Meinhardt, G., Kisaki, H., Kharbanda, S., Robertson, M., Ghayur, T., Wong, W.W., Kamen, R., Weichselbaum, R., et al., 1995. Proteolytic activation of protein kinase C delta by an ICE-like protease in apoptotic cells. Embo J. 14,6148-56.

Ferri, K.F., Kroemer, G., 2001. Organelle-specific initiation of cell death pathways. Nat Cell Biol. 3,E255-63.

Fleming, L., Mann, J.B., Bean, J., Briggle, T., Sanchez-Ramos, J.R., 1994. Parkinson's disease and brain levels of organochlorine pesticides. Ann Neurol. 36,100-3.

Frey, M.R., Clark, J.A., Leontieva, O., Uronis, J.M., Black, A.R., Black, J.D., 2000. Protein kinase C signaling mediates a program of cell cycle withdrawal in the intestinal epithelium. J Cell Biol. 151,763-78.

Frey, M.R., Leontieva, O., Watters, D.J., Black, J.D., 2001. Stimulation of protein kinase C-dependent and -independent signaling pathways by bistratene A in intestinal epithelial cells. Biochem Pharmacol. 61,1093-100.

Ghayur, T., Hugunin, M., Talanian, R.V., Ratnofsky, S., Quinlan, C., Emoto, Y., Pandey, P., Datta, R., Huang, Y., Kharbanda, S., Allen, H., Kamen, R., Wong, W., Kufe, D., 1996. Proteolytic activation of protein kinase C delta by an ICE/CED 3-like protease induces characteristics of apoptosis. J Exp Med. 184,2399-404.

Giasson, B.I., Lee, V.M., 2000. A new link between pesticides and Parkinson's disease. Nat Neurosci. 3,1227-8.

Graves, J.D., Gotoh, Y., Draves, K.E., Ambrose, D., Han, D.K., Wright, M., Chernoff, J., Clark, E.A., Krebs, E.G., 1998. Caspase-mediated activation and induction of apoptosis by the mammalian Ste20-like kinase Mst1. Embo J. 17,2224-34.

Greenamyre, J.T., Hastings, T.G., 2004. Biomedicine. Parkinson's--divergent causes, convergent mechanisms. Science. 304,1120-2.

Greenamyre, J.T., Sherer, T.B., Betarbet, R., Panov, A.V., 2001. Complex I and Parkinson's disease. IUBMB Life. 52,135-41.

Hartmann, A., Hunot, S., Michel, P.P., Muriel, M.P., Vyas, S., Faucheux, B.A., Mouatt-Prigent, A., Turmel, H., Srinivasan, A., Ruberg, M., Evan, G.I., Agid, Y., Hirsch,

E.C., 2000. Caspase-3: A vulnerability factor and final effector in apoptotic death of dopaminergic neurons in Parkinson's disease. Proc Natl Acad Sci U S A. 97,2875-80.

Hartmann, A., Troadec, J.D., Hunot, S., Kikly, K., Faucheux, B.A., Mouatt-Prigent, A., Ruberg, M., Agid, Y., Hirsch, E.C., 2001. Caspase-8 is an effector in apoptotic death of dopaminergic neurons in Parkinson's disease, but pathway inhibition results in neuronal necrosis. J Neurosci. 21,2247-55.

Heinz, G.H., Hill, E.F., Contrera, J.F., 1980. Dopamine and norepinephrine depletion in ring doves fed DDE, dieldrin, and Aroclor 1254. Toxicol Appl Pharmacol. 53,75-82.

Huang, C.Y., Wu, Y.M., Hsu, C.Y., Lee, W.S., Lai, M.D., Lu, T.J., Huang, C.L., Leu, T.H., Shih, H.M., Fang, H.I., Robinson, D.R., Kung, H.J., Yuan, C.J., 2002. Caspase activation of mammalian sterile 20-like kinase 3 (Mst3). Nuclear translocation and induction of apoptosis. J Biol Chem. 277,34367-74.

Jakobi, R., 2004. Subcellular targeting regulates the function of caspase-activated protein kinases in apoptosis. Drug Resist Updat. 7,11-7.

Jakobi, R., McCarthy, C.C., Koeppel, M.A., Stringer, D.K., 2003. Caspase-activated PAK-2 is regulated by subcellular targeting and proteasomal degradation. J Biol Chem. 278,38675-85.

Jenner, P., 1998. Oxidative mechanisms in nigral cell death in Parkinson's disease. Mov Disord. 13 Suppl 1,24-34.

Jenner, P., 2001. Parkinson's disease, pesticides and mitochondrial dysfunction. Trends Neurosci. 24,245-7.

Jenner, P., 2003. Oxidative stress in Parkinson's disease. Ann Neurol. 53 Suppl 3,S26-36; discussion S36-8.

Kanthasamy, A.G., Kitazawa, M., Kanthasamy, A., Anantharam, V., 2003. Role of proteolytic activation of protein kinase Cdelta in oxidative stress-induced apoptosis. Antioxid Redox Signal. 5,609-20.

Kaul, S., Kanthasamy, A., Kitazawa, M., Anantharam, V., Kanthasamy, A.G., 2003. Caspase-3 dependent proteolytic activation of protein kinase C delta mediates and regulates 1-methyl-4-phenylpyridinium (MPP+)-induced apoptotic cell death in dopaminergic cells: relevance to oxidative stress in dopaminergic degeneration. Eur J Neurosci. 18,1387-401.

Kikkawa, U., Matsuzaki, H., Yamamoto, T., 2002. Protein Kinase Cdelta (PKCdelta): Activation Mechanisms and Functions. J Biochem (Tokyo). 132,831-9.

Kitazawa, M., Anantharam, V., Kanthasamy, A.G., 2001. Dieldrin-induced oxidative stress and neurochemical changes contribute to apoptopic cell death in dopaminergic cells. Free Radic Biol Med. 31,1473-85.

Kitazawa, M., Anantharam, V., Kanthasamy, A.G., 2003. Dieldrin induces apoptosis by promoting caspase-3-dependent proteolytic cleavage of protein kinase Cdelta in dopaminergic cells: relevance to oxidative stress and dopaminergic degeneration. Neuroscience. 119,945-964.

Kitazawa, M., Wagner, J.R., Kirby, M.L., Anantharam, V., Kanthasamy, A.G., 2002. Oxidative stress and mitochondrial-mediated apoptosis in dopaminergic cells exposed to methylcyclopentadienyl manganese tricarbonyl. J Pharmacol Exp Ther. 302,26-35.

Langston, J.W., Langston, E.B., Irwin, I., 1984. MPTP-induced parkinsonism in human and non-human primates--clinical and experimental aspects. Acta Neurol Scand Suppl. 100,49-54.

Lee, N., MacDonald, H., Reinhard, C., Halenbeck, R., Roulston, A., Shi, T., Williams, L.T., 1997. Activation of hPAK65 by caspase cleavage induces some of the morphological and biochemical changes of apoptosis. Proc Natl Acad Sci U S A. 94,13642-7.

Leverrier, S., Vallentin, A., Joubert, D., 2002. Positive feedback of protein kinase C proteolytic activation during apoptosis. Biochem J. 368,905-13.

Majumder, P.K., Pandey, P., Sun, X., Cheng, K., Datta, R., Saxena, S., Kharbanda, S., Kufe, D., 2000. Mitochondrial translocation of protein kinase C delta in phorbol ester-induced cytochrome c release and apoptosis. J Biol Chem. 275,21793-6.

McCormack, A.L., Thiruchelvam, M., Manning-Bog, A.B., Thiffault, C., Langston, J.W., Cory-Slechta, D.A., Di Monte, D.A., 2002. Environmental risk factors and Parkinson's disease: selective degeneration of nigral dopaminergic neurons caused by the herbicide paraquat. Neurobiol Dis. 10,119-27.

Mecklenbrauker, I., Kalled, S.L., Leitges, M., Mackay, F., Tarakhovsky, A., 2004. Regulation of B-cell survival by BAFF-dependent PKCdelta-mediated nuclear signalling. Nature. 431,456-61.

Murriel, C.L., Churchill, E., Inagaki, K., Szweda, L.I., Mochly-Rosen, D., 2004. Protein kinase Cdelta activation induces apoptosis in response to cardiac ischemia and reperfusion damage: a mechanism involving BAD and the mitochondria. J Biol Chem. 279,47985-91.

Newton, A.C., 2003. Regulation of the ABC kinases by phosphorylation: protein kinase C as a paradigm. Biochem J. 370,361-71.

Nishizuka, Y., 1992. Intracellular signaling by hydrolysis of phospholipids and activation of protein kinase C. Science. 258,607-14.

Prasad, K.N., Clarkson, E.D., La Rosa, F.G., Edwards-Prasad, J., Freed, C.R., 1998. Efficacy of grafted immortalized dopamine neurons in an animal model of parkinsonism: a review. Mol Genet Metab. 65,1-9.

Ren, J., Datta, R., Shioya, H., Li, Y., Oki, E., Biedermann, V., Bharti, A., Kufe, D., 2002. p73beta is regulated by protein kinase Cdelta catalytic fragment generated in the apoptotic response to DNA damage. J Biol Chem. 277,33758-65.

Reyland, M.E., Anderson, S.M., Matassa, A.A., Barzen, K.A., Quissell, D.O., 1999. Protein kinase C delta is essential for etoposide-induced apoptosis in salivary gland acinar cells. J Biol Chem. 274,19115-23.

Sabourin, L.A., Tamai, K., Seale, P., Wagner, J., Rudnicki, M.A., 2000. Caspase 3 cleavage of the Ste20-related kinase SLK releases and activates an apoptosis-inducing kinase domain and an actin-disassembling region. Mol Cell Biol. 20,684-96.

Scheel-Toellner, D., Pilling, D., Akbar, A.N., Hardie, D., Lombardi, G., Salmon, M., Lord, J.M., 1999. Inhibition of T cell apoptosis by IFN-beta rapidly reverses nuclear translocation of protein kinase C-delta. Eur J Immunol. 29,2603-12.

Seidler, A., Hellenbrand, W., Robra, B.P., Vieregge, P., Nischan, P., Joerg, J., Oertel, W.H., Ulm, G., Schneider, E., 1996. Possible environmental, occupational, and other etiologic factors for Parkinson's disease: a case-control study in Germany. Neurology. 46,1275-84.

Sharma, R.P., Winn, D.S., Low, J.B., 1976. Toxic, neurochemical and behavioral effects of dieldrin exposure in mallard ducks. Arch Environ Contam Toxicol. 5,43-53.

Shen, J., 2004. Protein kinases linked to the pathogenesis of Parkinson's disease. Neuron. 44,575-7.

Sitailo, L.A., Tibudan, S.S., Denning, M.F., 2004. Bax activation and induction of apoptosis in human keratinocytes by the protein kinase C delta catalytic domain. J Invest Dermatol. 123,434-43.

Smith, G.C., d'Adda di Fagagna, F., Lakin, N.D., Jackson, S.P., 1999. Cleavage and inactivation of ATM during apoptosis. Mol Cell Biol. 19,6076-84.

Takahashi, M., Mukai, H., Toshimori, M., Miyamoto, M., Ono, Y., 1998. Proteolytic activation of PKN by caspase-3 or related protease during apoptosis. Proc Natl Acad Sci U S A. 95,11566-71.

Tanner, C.M., Langston, J.W., 1990. Do environmental toxins cause Parkinson's disease? A critical review. Neurology. 40,suppl 17-30; discussion 30-1.

Teruel, M.N., Meyer, T., 2000. Translocation and reversible localization of signaling proteins: a dynamic future for signal transduction. Cell. 103,181-4.

Tewari, M., Quan, L.T., O'Rourke, K., Desnoyers, S., Zeng, Z., Beidler, D.R., Poirier, G.G., Salvesen, G.S., Dixit, V.M., 1995. Yama/CPP32 beta, a mammalian homolog of CED-3, is a CrmA-inhibitable protease that cleaves the death substrate poly(ADP-ribose) polymerase. Cell. 81,801-9.

Toker, A., 1998. Signaling through protein kinase C. Front Biosci. 3,D1134-47.

Tomiyoshi, G., Horita, Y., Nishita, M., Ohashi, K., Mizuno, K., 2004. Caspase-mediated cleavage and activation of LIM-kinase 1 and its role in apoptotic membrane blebbing. Genes Cells. 9,591-600.

Ura, S., Masuyama, N., Graves, J.D., Gotoh, Y., 2001. Caspase cleavage of MST1 promotes nuclear translocation and chromatin condensation. Proc Natl Acad Sci U S A. 98,10148-53.

Vila, M., Przedborski, S., 2003. Targeting programmed cell death in neurodegenerative diseases. Nat Rev Neurosci. 4,365-75.

Wagner, S.R., Greene, F.E., 1978. Dieldrin-induced alterations in biogenic amine content of rat brain. Toxicol Appl Pharmacol. 43,45-55.

Wichmann, T., DeLong, M.R., 2003. Pathophysiology of Parkinson's disease: the MPTP primate model of the human disorder. Ann N Y Acad Sci. 991,199-213.

Widmann, C., Gerwins, P., Johnson, N.L., Jarpe, M.B., Johnson, G.L., 1998a. MEK kinase 1, a substrate for DEVD-directed caspases, is involved in genotoxin-induced apoptosis. Mol Cell Biol. 18,2416-29.

Widmann, C., Gibson, S., Johnson, G.L., 1998b. Caspase-dependent cleavage of signaling proteins during apoptosis. A turn-off mechanism for anti-apoptotic signals. J Biol Chem. 273,7141-7.

Yang, Y., Kaul, S., Zhang, D., Anantharam, V., Kanthasamy, A.G., 2004. Suppression of caspase-3-dependent proteolytic activation of protein kinase C delta by small interfering RNA prevents MPP+-induced dopaminergic degeneration. Mol Cell Neurosci. 25,406-21.

Yoshida, K., Wang, H.G., Miki, Y., Kufe, D., 2003. Protein kinase Cdelta is responsible for constitutive and DNA damage-induced phosphorylation of Rad9. Embo J. 22,1431-41.

CHAPTER IV: NUCLEAR LOCALIZATION OF PKCδ IS REGULATED BY PROXIMITY OF N-TERMINAL C2-LIKE DOMAIN TO THE C-TERMINAL NUCLEAR LOCALIZATION SIGNAL (NLS)

A paper submitted to Proceedings of National Academy of Sciences

Yongjie Yang, Huajun Jin, Vellareddy Anantharam, Anumantha Kanthasamy

ABSTRACT

PKCδ belongs to the novel PKC subfamily that contains a Ca^{2+}-insensitive C2-like domain followed by a lipid-binding C1 domain in its N-terminal regulatory moiety. Although a functional nuclear localization signal (NLS) has been identified in the C-terminal of PKCδ, it primarily localizes in the cytosol. The mechanisms by which PKCδ is retained in the cytosol and by which the nuclear/cytosolic trafficking of PKCδ is regulated are not known. In the present study, we demonstrated that the N- and the C-terminals of PKCδ are in close proximity in the tertiary structure by fluorescence resonance energy transfer (FRET). FRET analysis of N-terminal CFP-FRET and C-terminal YFP FRET of PKCδ gives rise to a significant FRET signal. Furthermore, by employing the C1 or C2-like domain deletion mutants of PKCδ (PKCδ-ΔC1 or PKCδ-ΔC2), we show that deletion of the C2-like domain, but not the C1 domain, induces a strong nuclear localization of PKCδ. The exogenously expressed catalytic fragment of PKCδ (PKCδ-CF) also primarily localizes to the nucleus.

Sequence analysis of the C2-like domain revealed a possible leucine-rich nuclear export signal (NES); however, the C2-like domain is not sensitive to the nuclear export inhibitor leptomycin B, suggesting that this leucine-rich motif is not a functional NES. Moreover, the C2-like domain alone was fused to the N-terminal of a NES mutated form of Rev protein, the RNA binding protein of Equine Infectious Anemia Virus (EIAV), to generate the Rev chimera. Interestingly, the Rev chimera with the C2-like domain is still primarily localized in the nucleus. Together, our studies suggest that the N-terminal C2-like domain regulates the subcellular localization of PKCδ by masking the C-terminal NLS through the position obstacle in the tertiary structure, but not by employing NES or interacting with anchoring proteins.

INTRODUCTION

Protein kinase C (PKC) is one of the major cellular signal transducers that mediates and regulates signals involved in a range of cellular processes, including cell growth, differentiation, apoptosis, neurotransmitter release, and carcinogenesis (Newton, 2003; Spitaler and Cantrell, 2004). All PKC family members share a highly conserved C-terminal catalytic moiety containing the kinase core; however, their regulatory moiety varies dramatically in composition and organization. The function of PKC, as observed in most of protein A, B, and C kinases, is primarily regulated by its regulatory moiety (Newton, 2003). Two key regulation roles of the regulatory moiety in PKC have been identified so far: the regulation of kinase membrane targeting through the C1 and C2 domains and the regulation of kinase activity through the pseudosubstrate.

As a member of the novel PKC (nPKC) subfamily (δ, ε, η, θ), PKCδ contains a Ca^{2+}-insensitive C2-like domain followed by a pseudosubstrate that normally binds to the catalytic site of the kinase core to inactivate the kinase (Orr et al., 1992) and a lipid-binding C1 domain in the N-terminal regulatory moiety. The C1 domain is a small globular structure (~8 KDa) that contains binding sites for small lipid molecules, including diacylglycerol (DAG), phorbol esters, and non-hydrolysable analogues of the endogenous ligand (Newton, 1995; Zhang et al., 1995). Recent studies have further characterized that the C1 domain can be divided into two sub-domains: C1A and C1B. These two sub-domains in different PKC isoforms preferentially bind to different lipid molecules (Bogi et al., 1999; Toker, 1998). In PKCδ, C1B is primarily responsible for the binding of DAG (Szallasi et al., 1996). The binding of lipid molecules to the C1 domain recruits PKCδ to the membrane and promotes a remarkably high affinity interaction between PKCδ and the membrane. This membrane interaction provides the energy to promote the conformational change which results in the release of pseudosubstrate from the catalytic site and activation of the kinase (Toker, 1998). In the conventional PKC (cRKC) subfamily (α, βI, βII, and γ), the lipid-mediated translocation and activation of kinase is through the synergic action of both the C1 and C2 domains. The C2 domain in cPKC provides a binding site for anionic phospholipids and Ca^{2+} (Nalefski and Falke, 1996; Newton and Johnson, 1998; Ponting and Parker, 1996), and together with the binding of lipid to the C1 domain promotes the high affinity interaction of cPKC with the membrane and subsequent activation of kinase.

Unlike the conserved C1 domain whose function in the regulation of the kinase core has been well characterized, the function of the C2-like domain in PKCδ, as well as in all

other nPKC isoforms, is not fully understood. In particular, the C2-like domain is incapable of binding to Ca^{2+}, and therefore loses the response to the Ca^{2+} signal though it shares significant homology with the C2 domain in cPKC (Newton, 1995). The crystallized structure of the C2-like domain from PKCδ (Pappa et al., 1998) and PKCε (Ochoa et al., 2001) suggests that it can still interact with the membrane by binding to phospholipids (phosphatidic acid and phosphatidylserine) in a Ca^{2+} independent manner. Pepio, A.M et al. showed that phosphorylation of Ser36 in the C2-like domain of Apl II, an nPKC isoform from Aplysia, increases the binding to phosphatidylserine and induces more efficient translocation of kinase to the membranes (Pepio and Sossin, 2001). The C2-like domain of PKCδ also mediates direct interaction with filamentous actin (F-actin) in neutrophils to regulate the migration of neutrophils in host-defense mechanisms against invading pathogens (Lopez-Lluch et al., 2001), as well as with non-smooth muscle F-actin in airway epithelial cells (Liedtke et al., 2003; Smallwood et al., 2005).

The function of PKCδ in the cell is closely associated with its subcellular localization. The precise localization is always the premise for kinase to receive upstream signals and transduce them downstream (Teruel and Meyer, 2000). Lipid-mediated translocation of PKCδ to the membrane allows PKCδ to effectively respond to the second messengers produced from different receptors (Nishizuka, 1992). PKCδ also translocates to the mitochondria, Golgi, endoplasmic reticulum (ER), and the nucleus in response to other stimuli (Brodie and Blumberg, 2003). However, the mechanisms that regulate the subcellular localization of PKCδ are poorly understood. Although it has been speculated that the isoform-specific localization of PKC is controlled by specific anchoring proteins (Mochly-

Rosen and Gordon, 1998; Newton, 1997; Newton and Johnson, 1998), like receptors for activated C kinase (RACK), very little information is known about the interaction of PKC isoforms with different anchoring proteins. Recently, a functional nuclear localization signal (NLS) has been identified in the C-terminal of PKCδ that induces PKCδ translocation to the nucleus in response to apoptotic stimuli (DeVries et al., 2002). This NLS alone can also localize GFP to the nucleus. Other studies also observed that the exogenously expressed catalytic fragment of PKCδ itself is primarily localized in the nucleus (Blass et al., 2002; DeVries et al., 2002). Interestingly, though PKCδ contains the functional NLS at the C-terminal of the kinase core that drives kinase into the nucleus in response to stimuli, PKCδ primarily localizes in the cytosol rather than the nucleus in a variety of normal cells. On the other hand, the nuclear export signal (NES) has been identified only in the atypical PKC (aPKC) isoforms (λ and ζ) (Perander et al., 2001), but not in all other cPKC and nPKC isoforms. The mechanisms that retain PKCδ in the cytosol and regulate the nuclear/cytosolic trafficking of PKCδ in normal cells are not clear.

From the primary structure of PKCδ, the pseudosubstrate at the middle of the regulatory moiety and kinase core at the catalytic moiety are distant from each other (Newton and Johnson, 1998). However, the pseudosubstrate constantly binds to the kinase core in normal cells to keep the kinase inactive. In order to do that, the primary structure of PKCδ has to be properly folded to form a specific conformation that brings the pseudosubstrate and the kinase core closer for their interaction in the tertiary structure. Although the structure of full-length PKCδ has not been crystallized, the fold of primary structure certainly brings the regulatory and catalytic moieties together. Since the C2-like domain is at the beginning of the

regulatory moiety and the NLS is located at the C-terminal of the kinase core, the fold of the primary structure may bring the C2-like domain closer to the NLS, which may implicate a role of the C2-like domain in the regulation of subcellular localization of PKCδ. In the present study, we investigate the mechanisms that regulate the cytosolic localization of PKCδ. We demonstrate that the C2-like domain retains PKCδ in the cytosol by directly masking the NLS through the close proximity of the N-terminal to the C-terminal in the tertiary structure, rather than by binding to potential anchoring proteins or employing functional NES.

MATERIALS AND METHODS

Cell culture and treatment

The immortalized rat mesencephalic dopaminergic neuronal (N27) cell line was a kind gift from Dr. Kedar N. Prasad, University of Colorado Health Sciences Center (Denver, CO) (Prasad et al., 1998). N27 cells were grown in RPMI 1640 medium containing 10% fetal bovine serum, 2 mM L-glutamine, 50 units penicillin, and 50 μg/ml streptomycin. Cells were grown in a humidified atmosphere of 5% CO_2 at 37^0C as previously described. For dieldrin treatment, dieldrin was prepared in DMSO and cells were exposed to serum-free RPMI medium containing dieldrin (final concentration 100 μM) for up to 1 hr. For leptomycin B (LMB) treatment, LMB was dissolved in ethanol and cells were exposed to normal growth medium containing LMB (final concentration 0.5-5 ng/ml) for up to 30 min.

Cell transfection

Transient transfection of N27 cells was performed by lipid or electroporation mediated approaches. For lipid-mediated transfection, lipofectamine 2000 from Invitrogen (Carlsbad, CA) was used. Briefly, cells ($0.7\text{-}0.8x10^6$) were plated in 35 mm glass bottom dishes (MatTek Corporation, Ashland, MA). After 16-24 hr, 4 μg plasmid as well as 10 μl lipofectomine 2000 were first diluted in 250 μl Opti-MEM medium, separately. After 5 min, diluted plasmid was mixed with diluted lipofectamine 2000 and incubated for another 20 min for DNA-lipid complex formation. The DNA-lipid complex was then added into a glass bottom dish. After 16-24 hr, cells were directly observed under TCS/NT confocal microscopy. For electroporation, a nucleofector kit for adherent cell transfection from Amaxa biosystems (Cologne, Germany) was employed. Briefly, cultured N27 cells were trypsinized and spun down. About $1\text{-}2x10^6$ cells were resuspended with 100 μl nucleofector solution mixed with 2 μg plasmid and transferred into a cuvette. The cuvette was then put in a nucleofector device (Amaxa biosystems, Cologne, Germany) for electroporation. After electroporation, cells were transferred to a 6-well plate and incubated at 37^0C.

Preparation of constructs

Full-length mouse PKCδ (mPKCδ) cDNA was amplified from pGFP-PKCδ (a kind gift from Dr. Reyland at University of Colorado Health Sciences Center, Denver, CO) (DeVries et al., 2002) by using the following primer pairs that contain Hind III and BamH I sites at each end. Forward primer: 5' atatatataagcttatggcacccttcctgcgc 3'; reverse primer: 5' atatatatggatccaatgtccaggaattgctcaaa 3'. The PCR product was digested with Hind III/BamH I and then cloned into Hind III/BamH I sites of pEYFP-N1 or pECFP-C1 (Clontech, Palo Alto,

CA) to generate the pEYFPδ or pECFPδ. pEYFPδ was then subjected to Xho I/Xba I digestion to digest out the fragment containing mPKCδ together with EYFP. This fragment was subcloned into Xho I/Xba I site of pECFP-C1 to generate the pFRETδ construct.

For the preparation of expression vectors containing PKCδ-WT (wild type), PKCδ-ΔC2 (C2-like domain deletion mutant), PKCδ-ΔNLS (nuclear localization signal deletion mutant), and PKCδ-CF (catalytic fragment), 14-2035bp, 428-2035bp, 14-1843bp, and 995-2035bp of mPKCδ cDNA was amplified individually with the following primer pairs. For PKCδ-WT: 5' caccatggcacccttcctgcgc 3' (F), 5' aatgtccaggaattgctcaaac 3' (R); for PKCδ-ΔC2: 5' caccatgtttccaaccatgaaccgtcgt 3' (F), 5' aatgtccaggaattgctcaaac 3' (R); for PKCδ-ΔNLS: 5' caccatggcacccttcctgcgc 3' (F), 5' ctccaggagggaccagtt 3' (R); for PKCδ-CF: 5' caccatgaacaacgggacctatggcaa 3' (F), 5' aatgtccaggaattgctcaaac 3' (R). To prepare PKCδ-ΔC1 (C1 domain deletion mutant), the C2-like domain and catalytic fragment (CF) was first amplified with the following primer pairs. For the C2-like domain: 5' caccatggcacccttcctgcgc 3' (F) and 5' atatatatgaattcctttgcctcctcctcacta 3' (R); for CF: 5' atcccagacgaattcaacaacgggacc 3' (F) and 5' aatgtccaggaattgctcaaac 3' (R). These two PCR fragments were then ligated after EcoR I digestion and purification. The ligation reaction was used as template for amplification with the following primer pairs: 5' caccatggcacccttcctgcgc 3' (F) and 5' aatgtccaggaattgctcaaac 3' (R). All PCR reactions were performed with *pfu* DNA polymerase to ensure the fidelity of amplification. All PCR products were directly subcloned into the V5-tagged (at the C-terminal) expression vector pLenti/TOPO from Invitrogen, Inc. (Carlsbad, CA) to generate pLenti/PKCδ-WT, pLenti/PKCδ-ΔC2, pLenti/PKCδ-ΔC1, pLenti/PKCδ-ΔNLS, and pLenti/PKCδ-CF.

Plasmids pEGFP-Rev and pEGFP-RDM4 (nuclear export signal deletion mutant of Rev) were kind gifts from Dr. Susan Carpenter (Iowa State University, Ames, IA). To prepare pEGFP-C2RDM4, the C2-like domain of PKCδ was first amplified with the following primer pairs that contain a Hind III and EcoR I site at each end. Forward primer: 5' atatatataagcttatggcacccttcctgcgc 3'; reverse primer: 5' atatatatgaattcctttgcctcctcctcacta 3'. The PCR product was digested with Hind III/EcoR I and cloned into Hind III/EcoR I sites of pEGFP-RDM4 to generate the pEGFP-C2RDM4. All constructs were confirmed by sequencing.

Establishment of PKCδ-ΔC2, PKCδ-ΔC1, PKCδ-ΔNLS, and PKCδ-WT stably expressing N27 cell lines

A ViraPower Lentiviral gene expression system from Invitrogen (Carlsbad, CA) was used to generate PKCδ-ΔC2, PKCδ-ΔC1, PKCδ-ΔNLS, and PKCδ-WT stably expressing N27 cell lines. To produce lentivirus, pLenti6/PKCδ-ΔC2, pLenti/PKCδ-ΔC1, pLenti/PKCδ-ΔNLS or pLenti/PKCδ-WT as well as supporting plasmids (provided with the kit) were co-transfected into human 293FT cells with the use of lipofectamine 2000 as described in the instruction of the kit. The lentivirus particles in the medium were collected by centrifuging at 3000 rpm for 15 min 48-72 hr post-transfection. To generate a stably expressing cell line, lentivirus containing individual pLenti/PKCδ-ΔC2, pLenti/PKCδ-ΔC1, pLenti/PKCδ-ΔNLS or pLenti/PKCδ-WT as well as polybrene (6 μg/ml) was added into cultured N27 cells (2X 10^5) for 24 hr and replaced with fresh medium. Positive N27 cells were selected by keeping blasticidin (10 μg/ml) in the medium for up to 2 weeks. PKCδ-ΔC2, PKCδ-ΔC1, PKCδ-

ΔNLS, or PKCδ-WT expressing N27 cells were identified by immunostaining of the C-terminal V5 tag.

Preparation of whole cell homogenates

After dieldrin treatment or electroporation, the N27 cells were harvested with trypsin/EDTA and spun at 200xg for 5 min. Cell pellets were then washed twice with ice-cold PBS and resuspended in 200 μl of homogenization buffer (pH 8.0, 20 mM Tris, 10 mM EGTA, 2 mM EDTA, 2 mM DTT, 0.5% Triton X-100 and 1:100 dilution of protease inhibitor). After incubation on ice for 5 min, the cell lysates were centrifuged for 30 min at 14,000xg at 4^0C and supernatants were collected as whole cell lysates.

Immunoblotting

An equal amount of protein was loaded in each lane and separated on SDS-polyacrylamide gel as described previously (Yang et al., 2004). Proteins were then transferred to nitrocellulose membrane by electro-blotting overnight (4°C, 25 V). Non-specific binding sites were blocked by treating the nitrocellulose membranes with 5% non-fat dry milk TBST solution (10 mM Tris, 150 mM NaCl, and 0.1% Tween 20) for 1 hr. The nitrocellulose membranes were then incubated with primary antibodies (1:1000) for 1 hr at RT. The primary antibody treatment was followed by treatment with secondary HRP-conjugated anti-rabbit or anti-mouse antibody (1:2000) for 1 hr at RT. Secondary antibody-bound proteins were detected using an ECL chemiluminescence kit (Amersham). To confirm equal protein loading, blots were reprobed with β-actin antibody (1:5000). Gel photographs were analyzed with a Kodak image station (Model 1000R, Rochester, New York).

Immunostaining

Immunostaining of the V5 tag was performed in PKCδ-WT, PKCδ-ΔC1, PKCδ-ΔC2 and PKCδ-ΔNLS expressing cells, as well as in PKCδ-CF transiently transfected N27 cells. Cells cultured on poly L-lysine coated glass cover slips were gently washed with PBS twice, fixed in 4% paraformaldehyde, washed for 3x7 min with PBS, permeabilized, and blocked with blocking reagent (0.4% BSA, 5% goat serum, and 0.2% Triton-X 100 in PBS) for 20 min. Cells were then incubated with anti-V5 mouse antibody (1:1000 in blocking reagent) overnight at 4°C and then washed for 3x7 min with PBS. The V5 tag was visualized by incubation with Cy3-conjugated goat anti-mouse secondary antibody (1:2000 in PBS) at RT for 90 min. After PBS wash, Hoechst 33342 was added to stain the cell nuclei at RT for 3 min. Finally, cells were washed twice in PBS and mounted on a slide with antifade mounting medium. The cells were observed under TCS/NT confocal systems (Leica, Bannockburn, IL). All images were processed in MetaMorph 5.07 (Downingtown, PA).

Live cell imaging

Cells were first transfected with plasmid. After 24 hr, transfected cells cultured in glass bottom dishes (MatTek Corporation, Ashland, MA) were observed by inverted confocal microscopy. To observe the *in vivo* FRET, cells were excited by Argon laser line at 458 nm and image was acquired by using an LP515 emission filter. For ECFP, cells were excited by Argon laser line at 458 nm and image was acquired by using a 475±66 emission filter. For EYFP, cells were excited by Argon laser line at 488 nm and image was acquired by using an LP515 emission filter. For transmitted light images, cells were excited by Krypton laser line at 568 nm through a 488/568 double dichroic excitation filter and image was acquired by

using a 490±40 emission filter. For time-lapse acquisition of image, FRET, CFP, and YFP images were acquired every 5 min for up to 60 min. For visualization of pEGFP-Rev, pEGFP-RDM4, and pEGFP-C2RDM4, N27 cells cultured in glass bottom dishes were first transfected with plasmid. After 24 hr, Hoechst 33342 was added to the dish and incubated at RT for 15 min. The dishes were washed several times with 1x PBS and replaced with normal growth medium. The cells were then observed under confocal microscopy. The EGFP fluorescence was excited by Argon laser line at 488 nm and image was acquired by using a BP525/50 emission filter. All images were acquired by a TCS/NT confocal system controlled by TCS NT software (Leica, Bannockburn, IL) and processed in MetaMorph 5.07 from Universal Imaging (Downingtown, PA).

RESULTS AND DISCUSSION

Design and characterization of PKCδ-FRET

To test whether the N-terminal is in close proximity to the C-terminal in the tertiary PKCδ structure, the hybrid protein PKCδ-FRET was designed and genetically engineered. The PKCδ-FRET is composed of ECFP fused to the N-terminal, followed by the full-length mouse PKCδ cDNA, and EYFP fused to the C-terminal (Figure 1A). The ECFP-PKCδ and PKCδ-EYFP were also constructed as a negative control for PKCδ-FRET. Because of the nature of FRET, in the PKCδ-FRET, resonance energy transfer from ECFP to EYFP can be observed when the N-terminal is in close proximity to the C-terminal in the tertiary structure (Figure 1A). When PKCδ undergoes caspase-3 mediated cleavage, the close proximity of

the N-terminal to the C-terminal is disrupted, as the regulatory fragment is separated from the catalytic fragment (Emoto et al., 1995; Kanthasamy et al., 2003). Because the ECFP and EYFP are not covalently linked, resonance energy transfer from ECFP to EYFP can no longer be observed. Similar FRET systems have been successfully demonstrated in the proteolysis of Bid protein (Onuki et al., 2002) and in monitoring of caspase-3 activity in apoptosis (Lee and Segal, 2004; Wang et al., 2005). The resonance energy transfer from ECFP to EYFP in hybrid protein PKCδ-FRET was directly visualized by employing the confocal microscopy system. Live N27 cells transfected with pFRETδ were excited with an Argon laser line at 458 nm, and emission was monitored by using either a 475±66 (ECFP) or LP515 (EYFP) emission filter. The *in vivo* ECFP fluorescence or fluorescence transferred from ECFP to EYFP (FRET) was observed (Figure 1Bb&c), as well as the EYFP fluorescence when excited with 488 nm (Figure 1Ba). In contrast, when cells transfected with pEYFPδ were excited with 458 nm and emission was monitored by using either a 475±66 or LP515 emission filter, no fluorescence was observed (Figure 1Be&f), while fluorescence of EYFP was observed with excitation at 488 nm and emission at LP515nm (Figure 1Bd). Similarly, no EYFP and FRET fluorescence was observed in cells expressing pECFPδ with excitation at 488nm and emission at LP515 (Figure 1Bg&i), while the ECFP fluorescence was observed with excitation at 458 nm and emission at 475±66 (Figure 1Bh).

Although the structure of full PKCδ has not been successfully crystallized, many attempts to elucidate the structure of PKC have suggested that regulatory and catalytic moieties of PKC are close to each other, and the full protein is tightly compacted and globularly shaped (Newton and Johnson, 1998). The tight binding of pseudosubstrate to the

kinase core in the tertiary structure of PKC also suggests that the regulatory and catalytic moieties must be properly folded. By using FRET, we determined that the N- and C-terminal of PKCδ are in close proximity in the tertiary structure. Since the C2-like domain is located at the beginning of the N-terminal and NLS is located at the very end of the C-terminal kinase core, the close proximity of the N- and C-terminals suggests that the C2-like domain is very close to the NLS in the tertiary structure. In order to mediate the nuclear translocation of protein, the NLS must be recognized and must bind with the nuclear import receptor (Kaffman and O'Shea, 1999). The close proximity of the C2-like domain to the NLS may provide a position obstacle for the recognition and binding of the NLS with the nuclear import receptor, further inhibiting the nuclear localization of PKCδ.

Proteolytic cleavage of PKCδ abolishes FRET *in vivo*

PKCδ has been identified as one of the downstream targets of activated caspase-3 in apoptotic cells (Brodie and Blumberg, 2003; Emoto et al., 1995). We first examined PKCδ cleavage in dopaminergic neuronal cells exposed to the neurotoxin dieldrin (100 μM) for up to 60 min. Anti-PKCδ antibody that recognizes the C-terminal epitope was employed. As shown in Figure 2A, cleaved PKCδ was detected starting from 30 min and increased up to 60 min following dieldrin exposure. The caspase-3 cleavage site of PKCδ has been mapped on the hinge region that connects the regulatory and the catalytic moieties (Emoto et al., 1995); therefore, the cleavage of PKCδ completely separates regulatory and catalytic fragments. To test whether the separation of regulatory and catalytic fragments by cleavage disrupts the close proximity of the N- to C-terminal in the tertiary structure of PKCδ, N27 cells

transfected with pFRETδ were treated with dieldrin (100 μM) for up to 60 min. During the treatment, live cells were excited with an Argon laser line at 458 nm and emission was monitored by using either a 475±66 or LP515 emission filter, and the *in vivo* CFP fluorescence or fluorescence transferred from ECFP to EYFP (FRET) was recorded every 5 min. The ratio of ECFP/EYFP was calculated to represent the FRET efficiency (Violin et al., 2003). When the close proximity of the N- to C-terminal is disrupted, resonance energy transfer from ECFP to EYFP is abolished. Therefore, the ECFP/EYFP ratio increases as more ECFP fluorescence is emitted and less EYFP fluorescence is transferred from ECFP. As shown in Figure 2Ba, the ECFP/EYFP ratio showed no significant change over time, though the value at each time point fluctuated up and down in control N27 cells. In contrast, the ECFP/EYFP ratio gradually increased over time in dieldrin-treated N27 cells, indicating that the close proximity of the N- to C-terminal was partially disrupted during the period of dieldrin treatment. Rapid increases in the ECFP/EYFP ratio were also observed from 15 min to 20 min and from 45 min to 60 min, suggesting that disruption of the close proximity of the N- to C-terminal was intensive during that period of time. The time period of the two rapid decreases in FRET efficiency matches closely with the time point that cleaved PKCδ appeared (Figure 2A), which indicates that the separation of the regulatory and the catalytic fragments by cleavage disrupts the close proximity of the N- to C-terminal.

To demonstrate that the hybrid protein PKCδ-FRET indeed undergoes proteolytic cleavage, the N27 cells transfected with pFRETδ were treated with dieldrin (100 μM) for up to 60 min. Cells were lysed and subjected to immunoblot analysis by using anti-GFP antibody. As shown in Figure 2C, hybrid protein PKCδ-FRET was cleaved and the cleaved CF-YFP/RF-CFP was detected at 60 min following dieldrin exposure. Since antibody

specifically detecting the catalytic fragment of PCKδ is currently unavailable, the localization change of the catalytic fragment of PKCδ in N27 cells following dieldrin exposure cannot be directly explored. Thus, we transiently transfected the catalytic fragment of PKCδ (PKCδ-CF) into N27 cells in order to examine the localization of the catalytic fragment of PKCδ. Immunostaining of the C-terminal V5 tag and counterstaining of the nucleus were performed 24 hr post transfection. As shown in Figure 2D, PKCδ-CF revealed by V5 immunoreactivity primarily localizes in the nucleus.

These results suggest that there is no covalent link between regulatory and catalytic moieties. The separation of the regulatory and catalytic moieties by proteolytic cleavage disrupts the close proximity of the N- to C-terminal and abolishes the FRET. We also demonstrate that the catalytic fragment of PKCδ, by itself, primarily localizes in the nucleus, which is consistent with previous studies (Blass et al., 2002; DeVries et al., 2002). The primary nuclear localization of PKCδ-CF indicates that the recognition of the NLS by the nuclear import receptor is not inhibited and the catalytic fragment itself does not contain a functional NES to transport PKCδ-CF out of the nucleus.

Deletion of the C2-like domain leads to nuclear localization of PKCδ

A functional nuclear localization signal (NLS) has been identified at the C-terminal (611-623) of the kinase core in PKCδ (DeVries et al., 2002). Nuclear translocation of PKCδ was inhibited with mutated NLS. Also, the NLS alone localizes GFP in the nucleus. Interestingly, though PKCδ contains the C-terminal NLS, it is mainly distributed in the cytosol in cells. We demonstrated that the N-terminal is in close proximity to the C-terminal

in the tertiary structure of PKCδ, and PKCδ-CF primarily localizes to the nucleus. The regulatory moiety is probably involved in the regulation of the nuclear localization of PKCδ.

We next investigated the involvement of the regulatory moiety in the regulation of nuclear localization of PKCδ. Expression vectors that express wild-type PKCδ (PKCδ-WT), the C1 or C2-like domain deletion mutant (PKCδ-ΔC1 or PKCδ-ΔC2), or the NLS deletion mutant (PKCδ-ΔNLS) were first constructed. The schematic representation of these constructs is shown in Figure 3A. The PKCδ-WT, PKCδ-ΔC1, PKCδ-ΔC2, and PKCδ-ΔNLS stably expressing N27 cells were then generated by using the ViraPower Lentiviral gene expression system from Invitrogen, Inc. (Carlsbad, CA). V5 immunostaining and nucleus counterstaining were performed to investigate the subcellular distribution of wild type and mutated PKCδ protein. As shown in Figure 3B, PKCδ-WT revealed by V5 immunoreactivity was primarily localized in the cytosol, though a little was in the nucleus (Figure 3Bc). In the PKCδ-ΔNLS expressing cells, the PKCδ-ΔNLS was completely excluded from the nucleus as expected (Figure 3Bf). Strikingly, PKCδ-ΔC2 was primarily localized in the nucleus, with only very light V5 immunoreactivity observed in the cytosol (Figure 3Bl), while PKCδ-ΔC1 was still primarily localized in the cytosol (Figure 3Bi). The dramatic shift in V5 immunoreactivity from the cytosol to the nucleus in PKCδ-WT and PKCδ-ΔC2 strongly suggests that the C2-like domain is involved in the regulation of the nuclear localization of PKCδ.

Since the C2-like domain is located at the beginning of the N-terminal regulatory moiety, and we demonstrated above that the N-terminal is in close proximity to the C-terminal, the C2-like domain might regulate the nuclear localization of PKCδ by

preoccupying the position near the NLS to block the potential contact of the nuclear import receptor to the NLS. This likely results in the inhibition of the nuclear import of PKCδ and the normal primary cytosolic localization of PKCδ. Although the C1 domain could also be in close proximity to the NLS in the tertiary structure and block the contact of NLS with the nuclear import receptor, the deletion of the C1 domain did not result in the shift of PKCδ localization from the cytosol to the nucleus. When the C2-like domain is deleted or the whole regulatory fragment is removed by cleavage, the position obstacle effect of the C2-like domain to the NLS disappears, leading to the exposure of the NLS to the nuclear import receptor and resulting in the import of PKCδ into the nucleus. It is also possible, though, that the C2-like domain contains a functional nuclear export signal (NES) to export PKCδ out of the nucleus, causing the primary cytosolic localization of PKCδ. The C2-like domain might also interact with anchoring proteins of PKC and inhibit the nuclear import of PKCδ, which also induces the primary cytosolic localization of PKCδ.

C2-like domain does not contain CRM1-dependent nuclear export signal (NES)

Similar to the nuclear import, nuclear export of protein is also regulated by the recognition of the nuclear export signal (NES) by its receptor (Kaffman and O'Shea, 1999). Although new NES and corresponding receptors are being identified, the leucine-rich NES and its receptor CRM1 is the major and currently most characterized nuclear export pathway in yeast and mammalian cells (Fornerod et al., 1997; Fukuda et al., 1997; Stade et al., 1997). To investigate whether the C2-like domain contains leucine-rich NES, the leucine-rich motif in the C2-like domain (1-138) was first predicted by using the NETNES 1.1 Server (la Cour

et al., 2004). NETNES is specifically designed for the prediction of leucine-rich NES in eukaryotic proteins. As shown in Figure 4A, no particular motif has an NES score close to or higher than the NES threshold, suggesting that the putative leucine-rich NES was not found in the C2-like domain. However, we did notice that the sequence from 108-116 contained two leucines and gained an NES score. This motif was then aligned with several validated leucine-rich NES in human immunodeficiency virus type 1 (HIV-1) Rev protein (Fischer et al., 1995), mitogen-activated protein kinase (Fukuda et al., 1996), phospholipase C-δ1 (PLCδ1) (Yamaga et al., 1999), cAMP-dependent protein kinase inhibitor (PKI) (Wen et al., 1995) as well as two atypical PKC isoforms ζ and λ (Perander et al., 2001). The alignment is shown in Figure 4B. The C2-like domain contains only two conserved leucines at the first and third position, but not the second and fourth leucines shared by all other NES. In addition, it contains a hydrophilic cysteine instead of hydrophobic leucine or isoleucine at the fourth conserved leucine position. The fourth leucine at the C-terminal has been shown to be critical for the function of NES (Perander et al., 2001). The point mutation of this leucine abolished the functional nuclear export signal in atypical PKC and caused the accumulation of atypical PKC in the nucleus. The lack of sequence homology of the 108-116 region of the C2-like domain with other validated leucine-rich NES, especially the lack of the fourth leucine, makes it incapable of functioning as a leucine-rich NES.

It has been well characterized that the leucine-rich NES is specifically recognized by its receptor CRM1 in the nuclear export process. This CRM1 mediated nuclear export pathway can be effectively inhibited by the fungicide leptomycin B (LMB) through the covalent binding of LMB to a cysteine of CRM1 (Fornerod et al., 1997; Kudo et al., 1999). The potent and specific inhibition of LMB in the CRM1 mediated pathway provides an

excellent tool for the validation of the leucine-rich NES. To further determine if the C2-like domain contains the leucine-rich NES, PKCδ-WT stably expressing N27 cells were treated with LMB (0.5 ng/ml) for up to 30 min. As shown in Figure 4C, LMB did not induce change in the subcellular distribution of PKCδ-WT, as revealed by V5 immunoreactivity. Cells were also treated with ethanol (0.1%) as a vehicle control because LMB was prepared in ethanol. Ethanol itself also did not change the subcellular localization of PKCδ-WT. We also tested a serial combination of LMB concentrations (up to 5 ng/ml) and exposure times (up to 60 min), but no change in subcellular localization of PKCδ-WT was observed under these conditions. The insensitivity of the C2-like domain to LMB further demonstrates that it does not contain a leucine-rich nuclear export signal.

C2-like domain cannot retain the NES deleted Rev in the cytosol

We determined above that the C2-like domain does not contain the classical leucine-rich NES. Next, we tried to determine whether the C2-like domain retains PKCδ in cytosol by employing other types of NES or by interacting with anchoring proteins. To test this, we engineered a C2-like domain as a heterogeneous protein that contains functional NLS but not NES. The functional NLS allows protein importing to the nucleus after synthesis in the cytosol. A NES deleted form of Equine Infectious Anemia Virus (EIAV) Rev protein was employed as the heterogeneous protein because it contains functional NLS and is small in size (23KDa) (Belshan et al., 1998). Rev is a RNA-binding protein of EIAV that contains functional NLS and NES to shuttle itself between the cytosol and nucleus (Fischer et al.,

1995). The deletion of its NES results in the retention of Rev in the nucleus (Belshan et al., 1998).

We first obtained pEGFP-Rev-WT and pEGFP-RDM4 (kind gifts of Dr. Susan Carpenter) that express the N-terminal fused wild type Rev or NES deleted form of Rev, respectively. The C2-like domain of PKCδ was then engineered into the pEGFP-RDM4 to generate the pEGFP-C2RDM4. The schematic presentation of the primary structure of these constructs is presented at Figure 5A. Subcellular localization of these proteins was then visualized by EGFP fluorescence and nucleus staining. In pEGFP-Rev-WT transfected N27 cells, EGFP-Rev-WT showed mixed subcellular localization, as shown in previous studies (Belshan et al., 1998; Belshan et al., 2000). In some cells, EGFP-Rev-WT was mainly localized in the cytosol, but in other cells it was primarily localized in the nucleus. A representative image of the cytosolic localization of EGFP-Rev-WT in N27 cells is shown in Figure 5Ba. However, in pEGFP-RDM4 transfected N27 cells, as shown in Figure 5Bd, EGFP-RDM4 uniformly showed strong nuclear localization in all transfected cells because of the deletion of the functional NES. In pEGFP-C2RDM4 transfected N27 cells, strong nuclear localization of EGFP-C2RDM4 was also uniformly observed in all transfected cells, though a little EGFP fluorescence was also observed in the cytosol (Figure 5Bg). The nucleus was visualized by Hoechst 33342 staining. These results clearly demonstrate that the C2-like domain alone is not capable of compensating for the function of the Rev NES. The failure of the C2-like domain alone to retain Rev chimera in the cytosol indicates that the C2-like domain alone does not contain NES to export the Rev chimera out of the nucleus, nor does it interact with anchoring proteins to retain the Rev chimera in the cytosol in N27 cells.

CONCLUSIONS

In summary, we demonstrate that the C2-like domain at the N-terminal of the regulatory moiety regulates the nuclear localization of PKCδ (Figure 6). We first show that the N-and C-terminals of PKCδ are in close proximity in the tertiary structure, which is disrupted by caspase-3 mediated cleavage. The cleavage of PKCδ or the deletion of the C2-like domain, which both remove the C2-like domain from the NLS, leads to the primary nuclear localization of the kinase. Our results also show that the C2-like domain is not capable of retaining a heterogeneous protein in the cytosol. The C2-like domain regulates the nuclear localization of PKCδ through the position obstacle effect of the C2-like domain, by masking the NLS and blocking the recognition of the nuclear import receptor to the NLS. Our model suggests that the NLS can be kept incompetent in normal situations. A specific signal, like cleavage, can make NLS competent to be recognized by the nuclear import receptor for further nuclear translocation and downstream signaling. The maintenance of competency of the NLS provides a new and distinct mechanism for kinases to self-regulate their subcellular localization and function.

Figure 1: Illustration of FRET system in PKCδ.

(A) Schematic diagram of the FRET system in PKCδ. ECFP and EYFP were fused into the N-terminal and C-terminal of PKCδ, respectively, to generate the PKCδ-FRET hybrid protein. This FRET system is described in detail in the text. (B) Fluorescent and transmitted light images for CFP, YFP, and FRET in live N27 cells. Plasmid pCFPδ, pYFPδ, and pFRETδ were transfected into N27 cells by using lipofectamine 2000. Cells cultured in glass bottom dishes were directly observed by using the TCS/NT confocal system. The detailed procedures for acquisition of images are described in the materials and methods (Bar = 10 μm).

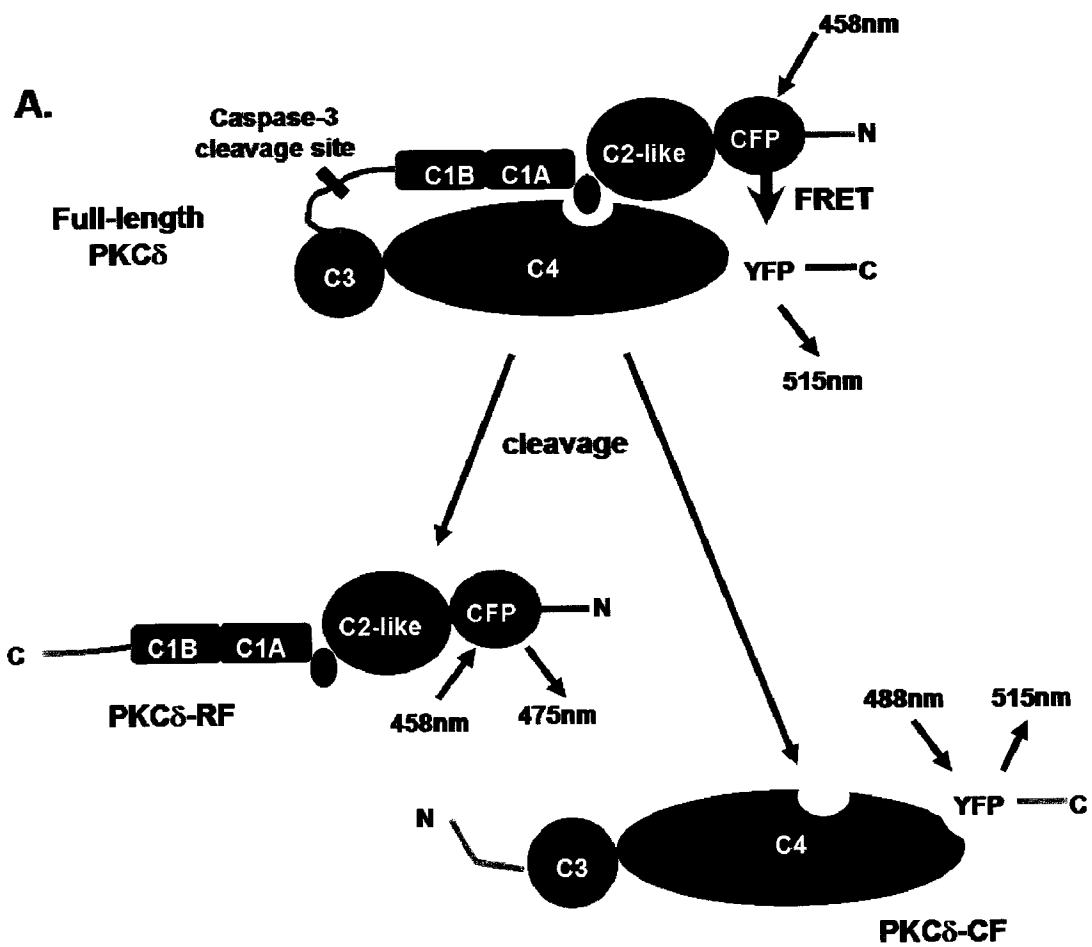
A.
Caspase-3
cleavage site
C1B
C1A
C2-like
CFP
N
FRET
Full-length
PKCδ
C3
C4
YFP
C
515nm
458nm
cleavage
C2-like
CFP
N
C
C1B
C1A
PKCδ-RF
458nm
475nm
488nm
515nm
YFP
C
N
C3
C4
PKCδ-CF

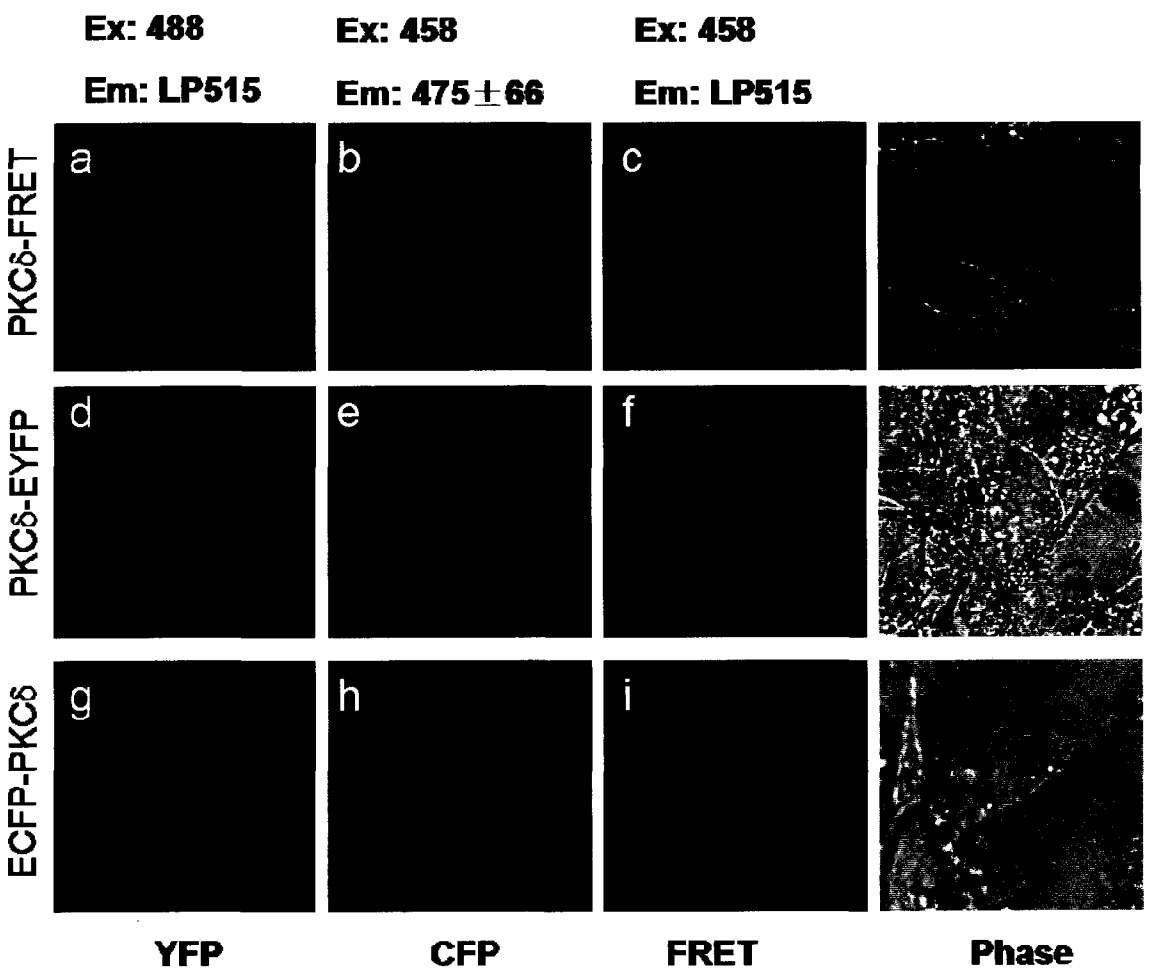
Ex: 488
Em: LP515
Ex: 458
Em: 475±66
Ex: 458
Em: LP515
PKCδ-FRET
PKCδ-EYFP
ECFP-PKCδ
a
b
c
d
e
f
g
h
i
YFP
CFP
FRET
Phase

Figure 2: Separation of regulatory fragment from catalytic fragment of PKCδ by cleavage abolishes FRET.

(A) Dieldrin treatment induces PKCδ cleavage in N27 cells. N27 cells were treated with dieldrin (100 μM) in serum-free medium for up to 60 min. Cell homogenates were prepared and separated by 10% SDS-PAGE. PKCδ cleavage was then detected by using anti-PKCδ-antibody that recognizes a C-terminal epitope. (B) Time-lapse recording of FRET signal in control and dieldrin-treated N27 cells. N27 cells were first transfected with pFRETδ for 24 hr and treated with dieldrin (100 μM) for up to 60 min. During the treatment, the CFP, YFP, and FRET images were acquired every 5 min by using the corresponding excitation laser wavelength and emission filter set. The intensity of CFP and FRET at each time point was measured in Metamorph 5.07. The intensity ratio of CFP/YFP was calculated and plotted in Prism 3.0. (C) Cleavage of PKCδ-FRET was indeed induced in pFRETδ transfected N27 cells following dieldrin exposure. To get the higher transfection efficiency, pFRETδ was transfected into N27 cells by electroporation. After 24 hr, cells were lysed and whole cell lysates were separated by 7.5% SDS-PAGE. The cleavage of PKCδ-FRET was detected by using anti-GFP antibody. (D) Nuclear localization of the catalytic fragment of PKCδ (PKCδ-CF). PKCδ-CF was transiently transfected into N27 cells. The localization of PKCδ-CF was visualized by immunostaining of the V5 tag (Bar = 10 μm).

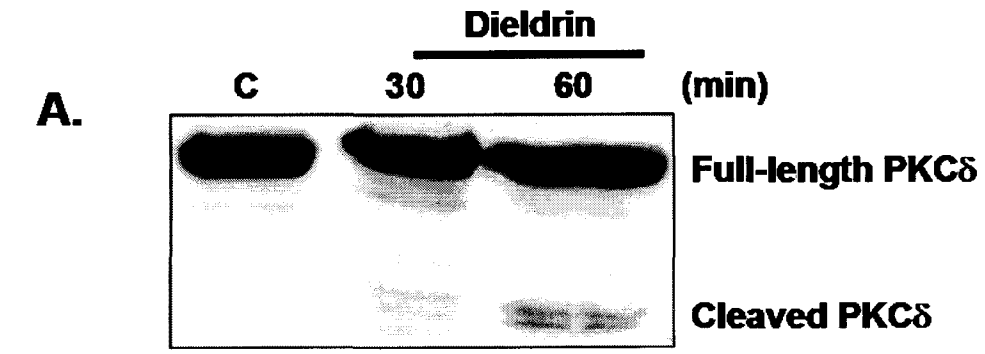
A.
Dieldrin
C
30
60
(min)
Full-length PKCδ
Cleaved PKCδ

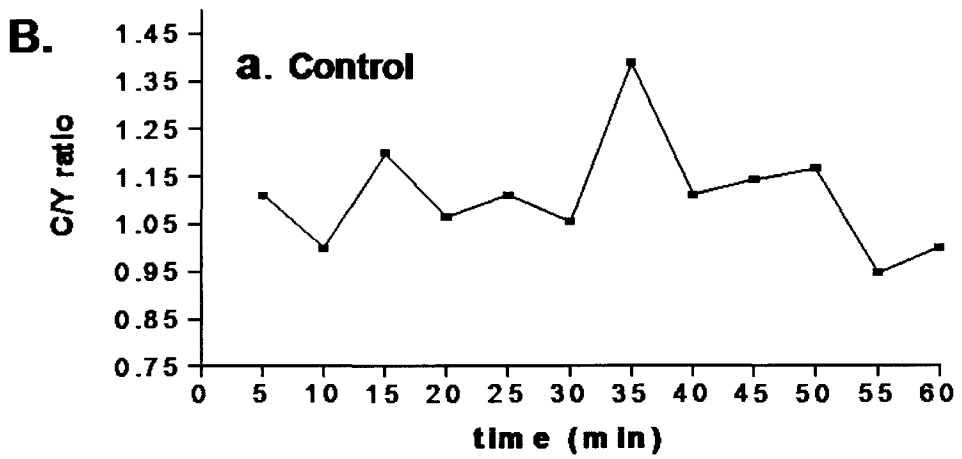
B.
a. Control
C/Y ratio
1.45
1.35
1.25
1.15
1.05
0.95
0.85
0.75
0 5 10 15 20 25 30 35 40 45 50 55 60
time (min)

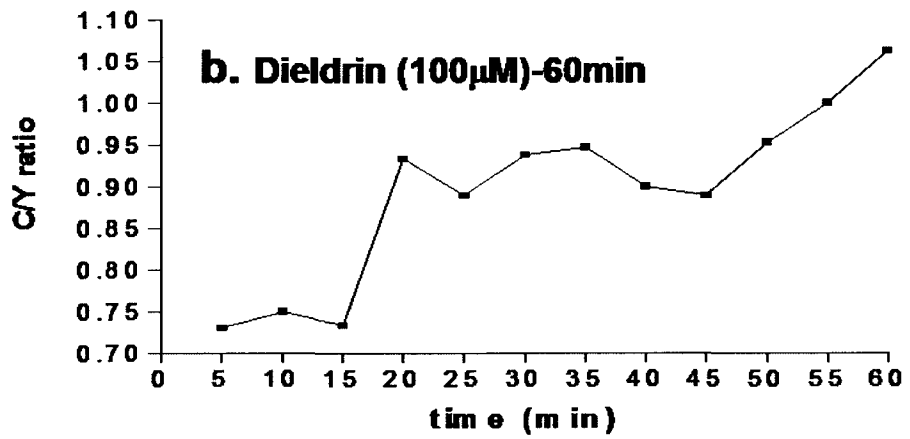
b. Dieldrin (100μM)-60min
C/Y ratio
1.10
1.05
1.00
0.95
0.90
0.85
0.80
0.75
0.70
0 5 10 15 20 25 30 35 40 45 50 55 60
time (min)

C.

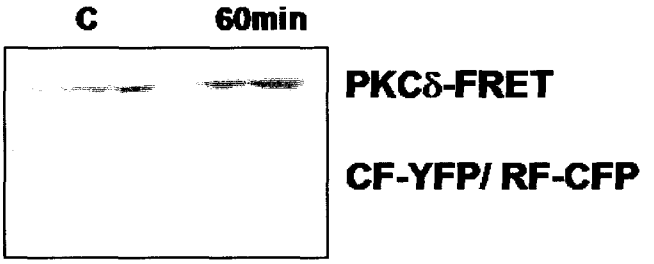

D.

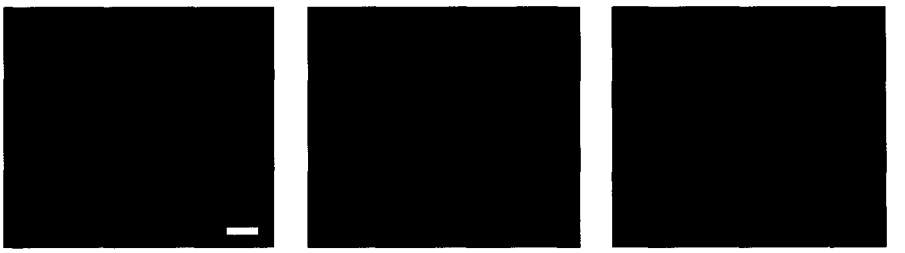

Figure 3: Deletion of C2-like but not C1 domain in PKCδ induced nuclear localization of PCKδ.

(A) Schematic representation of PKCδ-WT, PKCδ-ΔC1, PKCδ-ΔC2, and PKCδ-ΔNLS. Generation of these constructs is described in detail in the materials and methods. (B) Subcellular localization of PKCδ-WT, PKCδ-ΔC1, PKCδ-ΔC2, and PKCδ-ΔNLS in N27 cells. PKCδ-WT, PKCδ-ΔC1, PKCδ-ΔC2, and PKCδ-ΔNLS stably expressing N27 cells were generated via the ViraPower Lentiviral gene expression system (Invitrogen, Inc. Carlsbad, CA). Cells were then fixed, and immunostaining of the V5 tag was performed. To visualize the V5 tag, Cy3-conjugated secondary antibody was used. Subcellular localization of PKCδ-WT, PKCδ-ΔC1, PKCδ-ΔC2, and PKCδ-ΔNLS was revealed by immunoreactivity of the V5 tag. Nuclei were counterstained by Hoechst 33342. Stained cells were observed under a TCS/NT confocal system and all images were processed in Metamorph 5.07 (Bar = 10 μm).

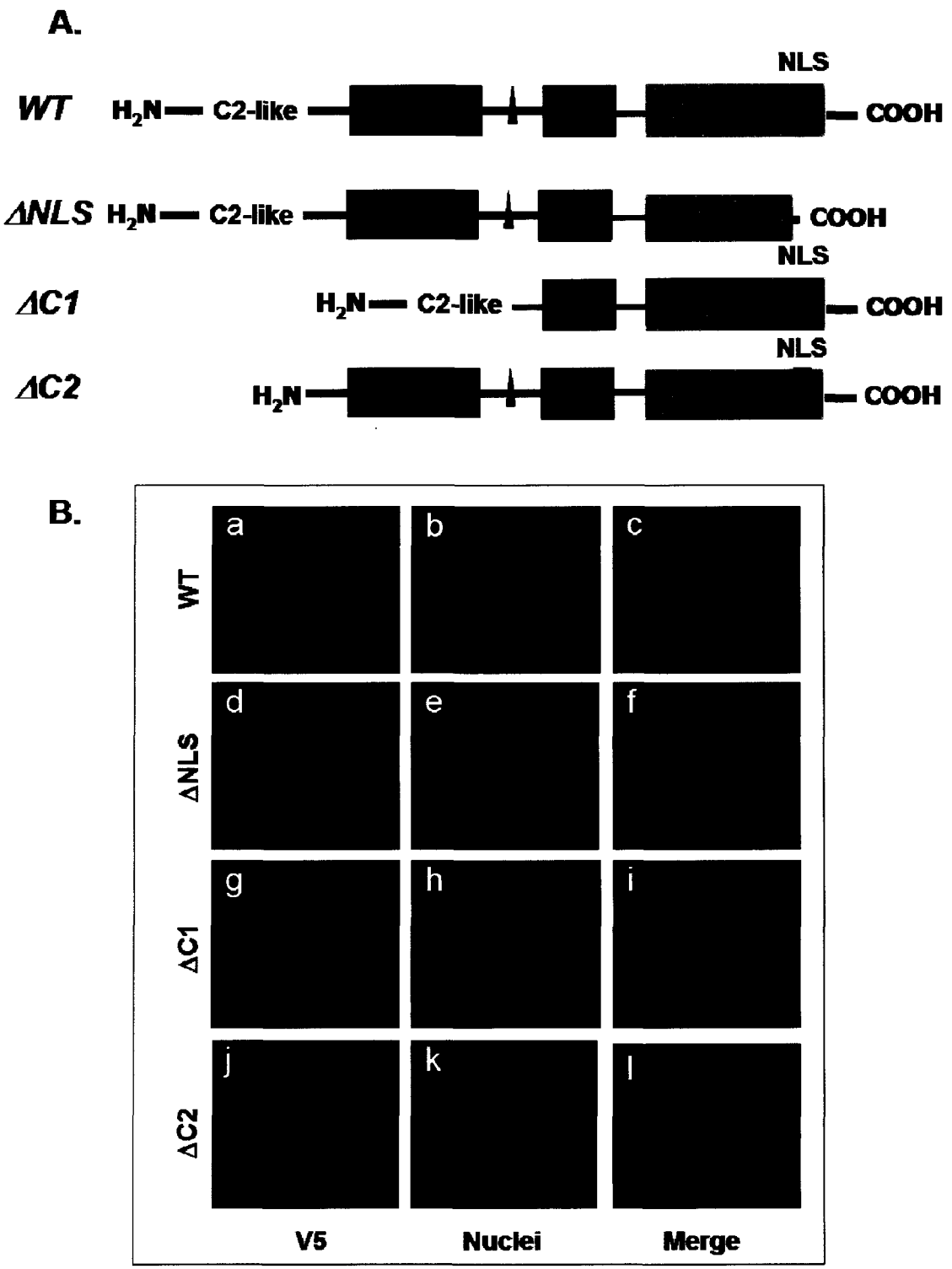
A.
NLS
WT
H2N
C2-like
COOH
ΔNLS
H2N
C2-like
COOH
NLS
ΔC1
H2N
C2-like
COOH
NLS
ΔC2
H2N
COOH
B.
WT
ΔNLS
ΔC1
ΔC2
a
b
c
d
e
f
g
h
i
j
k
l
V5
Nuclei
Merge

Figure 4: C2-like domain of PKCδ does not contain leucine-rich nuclear export signal (NES).

(A) Analysis of the leucine-rich NES motif in the C2-like domain of PKCδ. The amino acid sequence (1-138) of the C2-like domain was uploaded to the NETNES 1.1 server (http://www.cbs.dtu.dk/services/NetNES/) and we performed NES motif prediction. (B) Alignment of the leucine-rich motif in the C2-like domain of PKCδ with a validated NES motif from Rev, MEK, PLCδ1, PKI as well as two atypical PKC isoforms ζ and λ. The NES motifs from different proteins were directly aligned with the leucine-rich motif (108-118) of the C2-like domain in ClustalW 1.8 (http://searchlauncher.bcm.tmc.edu/multi-align/multi-align.html). (C) Leucine-rich motif in the C2-like domain is not sensitive to the nuclear export inhibitor leptomycin B (LMB). Leptomycin B stock (500 ng/ml) was prepared in ethanol. PKCδ-WT stably expressing cells were treated with ethanol (0.1%) alone as a vehicle control or with LMB (0.5 ng/ml) for 5 min, and immunostaining of the V5 tag was performed. The immunoreactivity of the V5 tag was visualized by using Cy3-conjugated secondary antibody. Subcellular localization of PKCδ-WT was revealed by immunoreactivity of the V5 tag. Nuclei were counterstained with Hoechst 33342. Stained cells were observed under a TCS/NT confocal system and all images were processed in Metamorph 5.07 (Bar = 10 μm).

A.

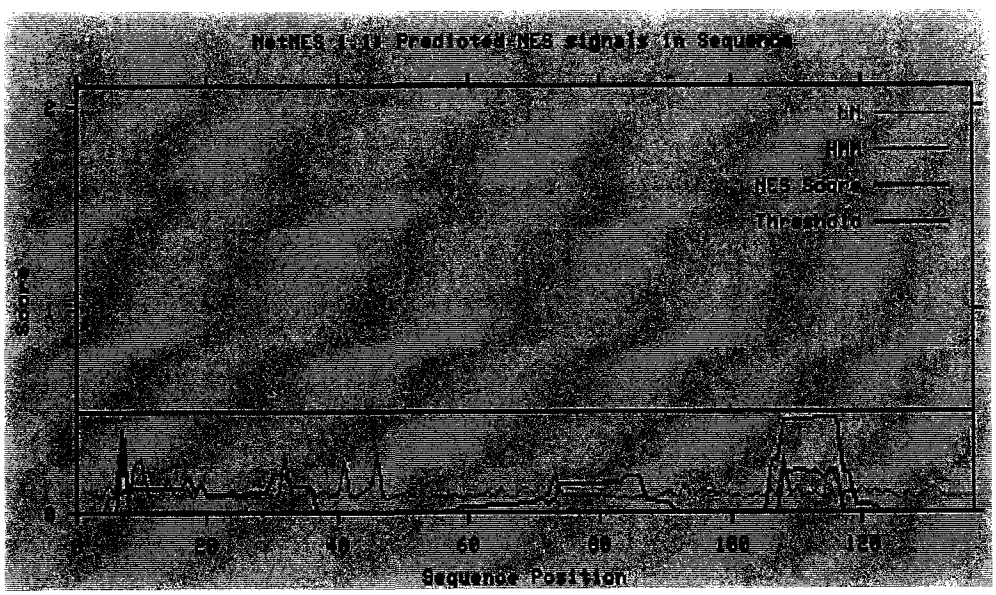

B.

atypical PKC	Lamda	1	--SLGLQDPDLL
	Zeta	1	--GLGLQDPDLI
	PKI	1	ELALKLACLDIN
	PLC	1	ELKDFLKELNIQ
	Rev	1	-QLPPLERLTLD
	MEK	1	ALQKKLEELELD
	C2-domain	1	-LQPQAKVLMCV

1 2 3 4

C.

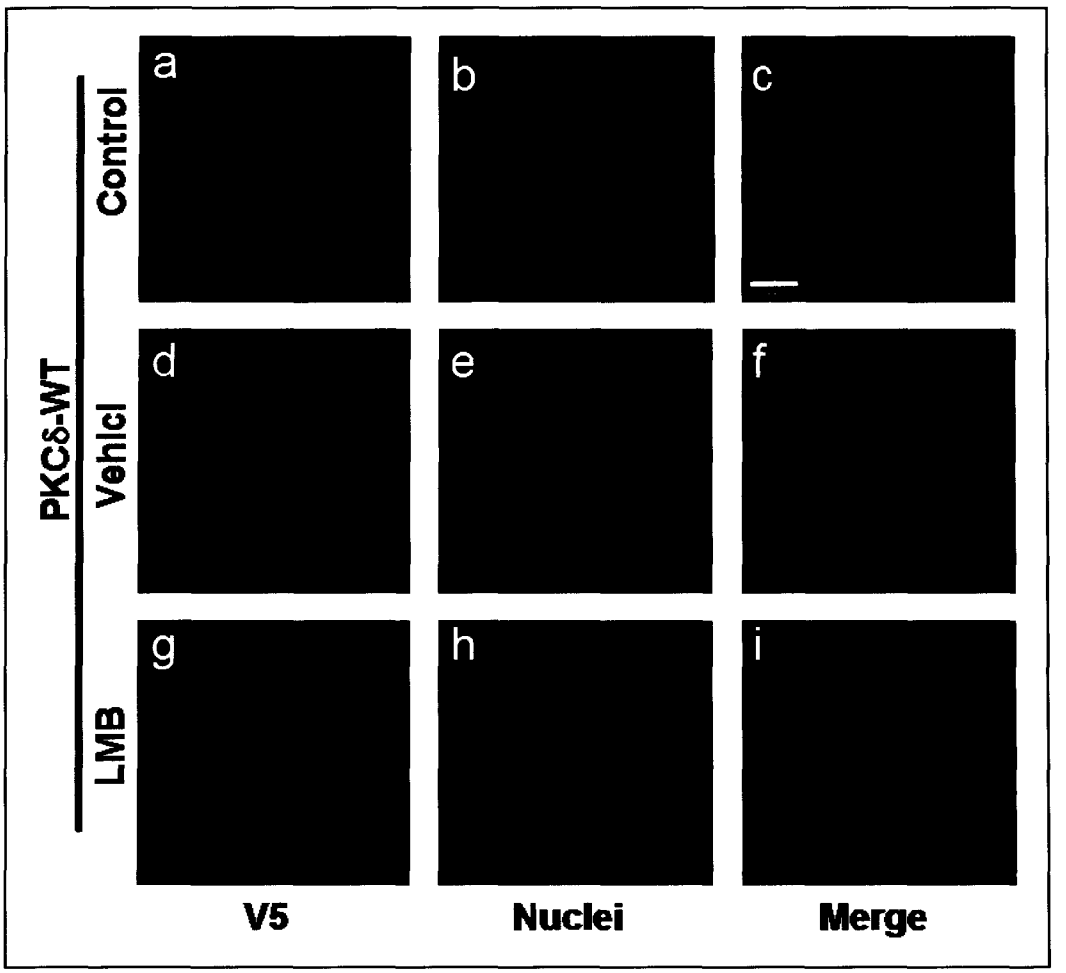

Figure 5: Incapacity of C2-like domain to retain NES deleted form of Rev in the cytoplasm.

(A) Schematic representation of the primary structures of EGFP-Rev-WT, EGFP-RDM4, and EGFP-C2RDM4. All functional domains are illustrated as boxes in different colors. (B) Subcellular localization of EGFP-Rev-WT, EGFP-RDM4, and EGFP-C2RDM4 in N27 cells. EGFP-Rev-WT, EGFP-RDM4, and EGFP-C2RDM4 were transfected into N27 cells cultured in glass bottom culture dishes. About 24 hr post-transfection, Hoechst 33342 was added to culture dishes and incubated at RT for 15 min. The culture dishes were then washed with 1xPBS three times and replaced with normal culture medium. To observe the EGFP fluorescence from live cells, cells in culture dishes were then directly observed by confocal microscopy and all images were processed in Metamorph (Bar = 10 μm).

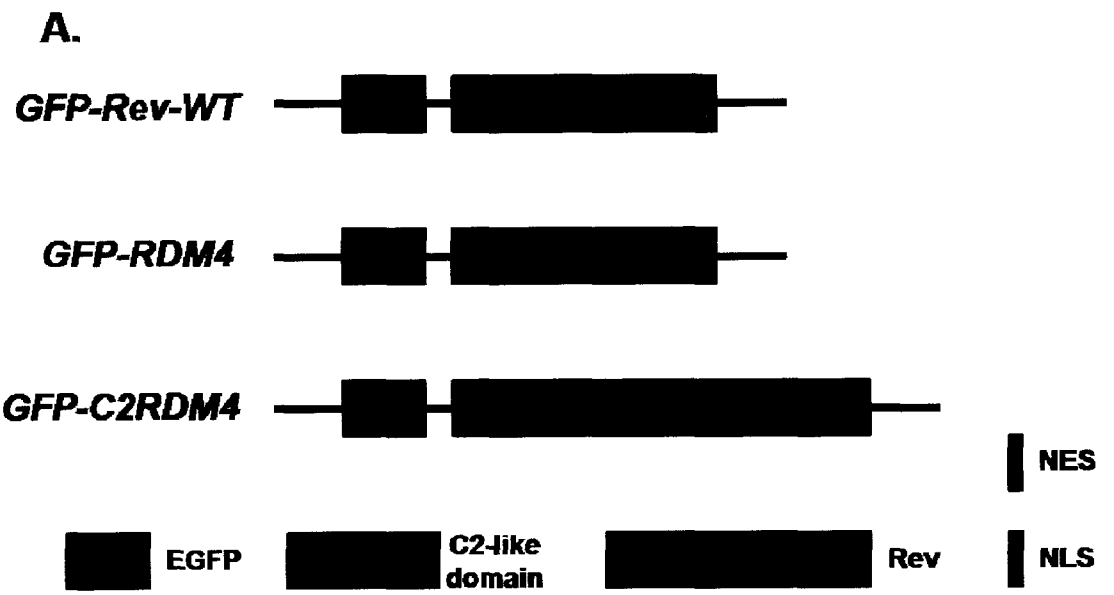
A.
GFP-Rev-WT
GFP-RDM4
GFP-C2RDM4
NES
EGFP
C2-like domain
Rev
NLS

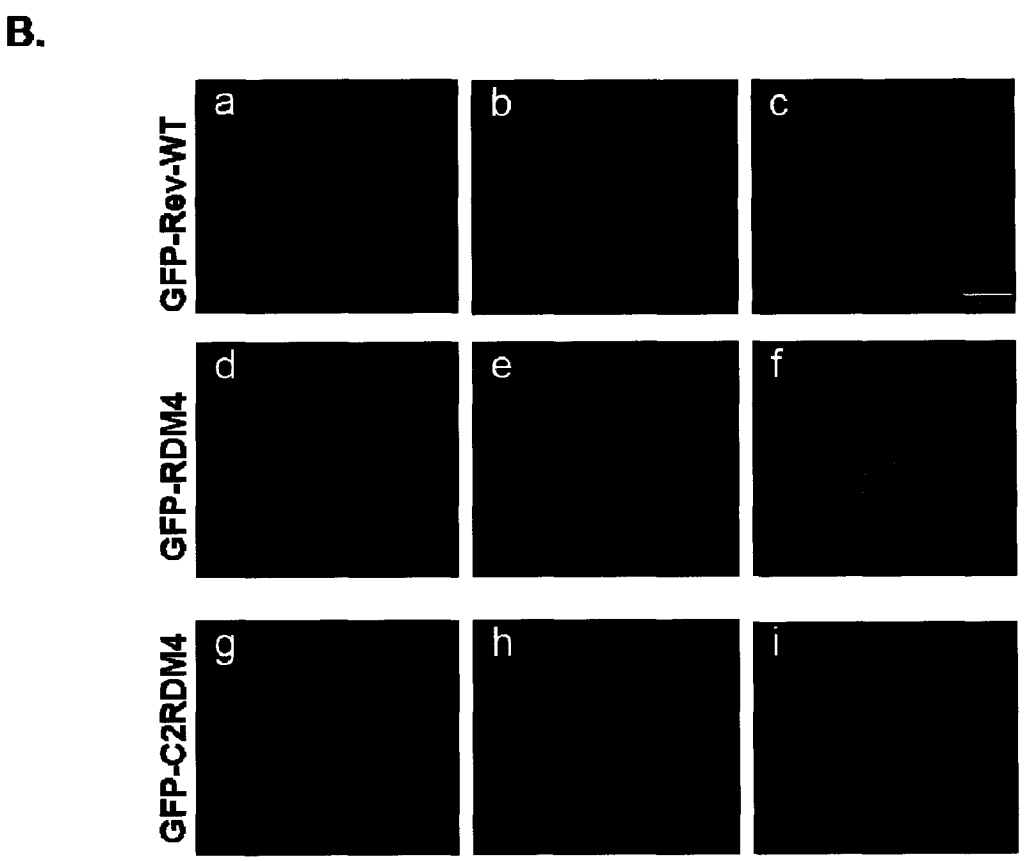
B.
GFP-Rev-WT
GFP-RDM4
GFP-C2RDM4
a
b
c
d
e
f
g
h
i

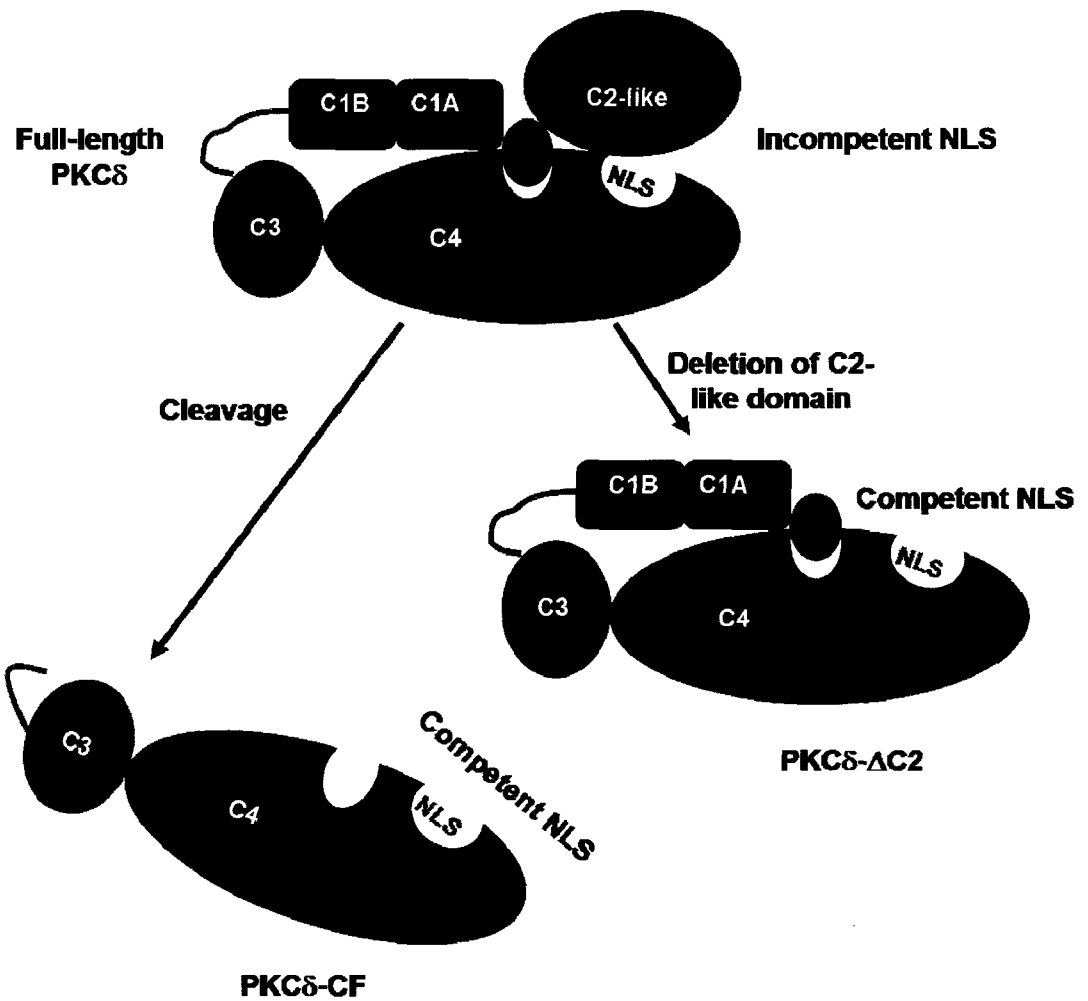

Figure 6: Regulation role of C2-like domain to the nuclear localization of PCKδ

REFERENCES

Belshan, M., Harris, M.E., Shoemaker, A.E., Hope, T.J., Carpenter, S., 1998. Biological characterization of Rev variation in equine infectious anemia virus. J Virol. 72,4421-6.

Belshan, M., Park, G.S., Bilodeau, P., Stoltzfus, C.M., Carpenter, S., 2000. Binding of equine infectious anemia virus rev to an exon splicing enhancer mediates alternative splicing and nuclear export of viral mRNAs. Mol Cell Biol. 20,3550-7.

Blass, M., Kronfeld, I., Kazimirsky, G., Blumberg, P.M., Brodie, C., 2002. Tyrosine phosphorylation of protein kinase Cdelta is essential for its apoptotic effect in response to etoposide. Mol Cell Biol. 22,182-95.

Bogi, K., Lorenzo, P.S., Acs, P., Szallasi, Z., Wagner, G.S., Blumberg, P.M., 1999. Comparison of the roles of the C1a and C1b domains of protein kinase C alpha in ligand induced translocation in NIH 3T3 cells. FEBS Lett. 456,27-30.

Brodie, C., Blumberg, P.M., 2003. Regulation of cell apoptosis by protein kinase c delta. Apoptosis. 8,19-27.

DeVries, T.A., Neville, M.C., Reyland, M.E., 2002. Nuclear import of PKCdelta is required for apoptosis: identification of a novel nuclear import sequence. Embo J. 21,6050-60.

Emoto, Y., Manome, Y., Meinhardt, G., Kisaki, H., Kharbanda, S., Robertson, M., Ghayur, T., Wong, W.W., Kamen, R., Weichselbaum, R., et al., 1995. Proteolytic activation of protein kinase C delta by an ICE-like protease in apoptotic cells. Embo J. 14,6148-56.

Fischer, U., Huber, J., Boelens, W.C., Mattaj, I.W., Luhrmann, R., 1995. The HIV-1 Rev activation domain is a nuclear export signal that accesses an export pathway used by specific cellular RNAs. Cell. 82,475-83.

Fornerod, M., Ohno, M., Yoshida, M., Mattaj, I.W., 1997. CRM1 is an export receptor for leucine-rich nuclear export signals. Cell. 90,1051-60.

Fukuda, M., Asano, S., Nakamura, T., Adachi, M., Yoshida, M., Yanagida, M., Nishida, E., 1997. CRM1 is responsible for intracellular transport mediated by the nuclear export signal. Nature. 390,308-11.

Fukuda, M., Gotoh, I., Gotoh, Y., Nishida, E., 1996. Cytoplasmic localization of mitogen-activated protein kinase kinase directed by its NH2-terminal, leucine-rich short amino acid sequence, which acts as a nuclear export signal. J Biol Chem. 271,20024-8.

Kaffman, A., O'Shea, E.K., 1999. Regulation of nuclear localization: a key to a door. Annu Rev Cell Dev Biol. 15,291-339.

Kanthasamy, A.G., Kitazawa, M., Kanthasamy, A., Anantharam, V., 2003. Role of proteolytic activation of protein kinase Cdelta in oxidative stress-induced apoptosis. Antioxid Redox Signal. 5,609-20.

Kudo, N., Matsumori, N., Taoka, H., Fujiwara, D., Schreiner, E.P., Wolff, B., Yoshida, M., Horinouchi, S., 1999. Leptomycin B inactivates CRM1/exportin 1 by covalent modification at a cysteine residue in the central conserved region. Proc Natl Acad Sci U S A. 96,9112-7.

la Cour, T., Kiemer, L., Molgaard, A., Gupta, R., Skriver, K., Brunak, S., 2004. Analysis and prediction of leucine-rich nuclear export signals. Protein Eng Des Sel. 17,527-36.

Lee, P., Segal, M.S., 2004. Real-time analysis of apoptosis in vivo. Methods Cell Biol. 75,343-54.

Liedtke, C.M., Hubbard, M., Wang, X., 2003. Stability of actin cytoskeleton and PKC-delta binding to actin regulate NKCC1 function in airway epithelial cells. Am J Physiol Cell Physiol. 284,C487-96.

Lopez-Lluch, G., Bird, M.M., Canas, B., Godovac-Zimmerman, J., Ridley, A., Segal, A.W., Dekker, L.V., 2001. Protein kinase C-delta C2-like domain is a binding site for actin and enables actin redistribution in neutrophils. Biochem J. 357,39-47.

Mochly-Rosen, D., Gordon, A.S., 1998. Anchoring proteins for protein kinase C: a means for isozyme selectivity. Faseb J. 12,35-42.

Nalefski, E.A., Falke, J.J., 1996. The C2 domain calcium-binding motif: structural and functional diversity. Protein Sci. 5,2375-90.

Newton, A.C., 1995. Protein kinase C. Seeing two domains. Curr Biol. 5,973-6.

Newton, A.C., 1997. Regulation of protein kinase C. Curr Opin Cell Biol. 9,161-7.

Newton, A.C., 2003. Regulation of the ABC kinases by phosphorylation: protein kinase C as a paradigm. Biochem J. 370,361-71.

Newton, A.C., Johnson, J.E., 1998. Protein kinase C: a paradigm for regulation of protein function by two membrane-targeting modules. Biochim Biophys Acta. 1376,155-72.

Nishizuka, Y., 1992. Intracellular signaling by hydrolysis of phospholipids and activation of protein kinase C. Science. 258,607-14.

Ochoa, W.F., Garcia-Garcia, J., Fita, I., Corbalan-Garcia, S., Verdaguer, N., Gomez-Fernandez, J.C., 2001. Structure of the C2 domain from novel protein kinase Cepsilon. A membrane binding model for Ca(2+)-independent C2 domains. J Mol Biol. 311,837-49.

Onuki, R., Nagasaki, A., Kawasaki, H., Baba, T., Uyeda, T.Q., Taira, K., 2002. Confirmation by FRET in individual living cells of the absence of significant amyloid beta - mediated caspase 8 activation. Proc Natl Acad Sci U S A. 99,14716-21.

Orr, J.W., Keranen, L.M., Newton, A.C., 1992. Reversible exposure of the pseudosubstrate domain of protein kinase C by phosphatidylserine and diacylglycerol. J Biol Chem. 267,15263-6.

Pappa, H., Murray-Rust, J., Dekker, L.V., Parker, P.J., McDonald, N.Q., 1998. Crystal structure of the C2 domain from protein kinase C-delta. Structure. 6,885-94.

Pepio, A.M., Sossin, W.S., 2001. Membrane translocation of novel protein kinase Cs is regulated by phosphorylation of the C2 domain. J Biol Chem. 276,3846-55.

Perander, M., Bjorkoy, G., Johansen, T., 2001. Nuclear import and export signals enable rapid nucleocytoplasmic shuttling of the atypical protein kinase C lambda. J Biol Chem. 276,13015-24.

Ponting, C.P., Parker, P.J., 1996. Extending the C2 domain family: C2s in PKCs delta, epsilon, eta, theta, phospholipases, GAPs, and perforin. Protein Sci. 5,162-6.

Prasad, K.N., Clarkson, E.D., La Rosa, F.G., Edwards-Prasad, J., Freed, C.R., 1998. Efficacy of grafted immortalized dopamine neurons in an animal model of parkinsonism: a review. Mol Genet Metab. 65,1-9.

Smallwood, N.D., Hausman, B.S., Wang, X., Liedtke, C.M., 2005. Involvement of NH2 terminus of PKC-{delta} in binding to F-actin during activation of Calu-3 airway epithelial NKCC1. Am J Physiol Cell Physiol. 288,C906-12.

Spitaler, M., Cantrell, D.A., 2004. Protein kinase C and beyond. Nat Immunol. 5,785-90.

Stade, K., Ford, C.S., Guthrie, C., Weis, K., 1997. Exportin 1 (Crm1p) is an essential nuclear export factor. Cell. 90,1041-50.

Szallasi, Z., Bogi, K., Gohari, S., Biro, T., Acs, P., Blumberg, P.M., 1996. Non-equivalent roles for the first and second zinc fingers of protein kinase Cdelta. Effect of their mutation on phorbol ester-induced translocation in NIH 3T3 cells. J Biol Chem. 271,18299-301.

Teruel, M.N., Meyer, T., 2000. Translocation and reversible localization of signaling proteins: a dynamic future for signal transduction. Cell. 103,181-4.

Toker, A., 1998. Signaling through protein kinase C. Front Biosci. 3,D1134-47.

Violin, J.D., Zhang, J., Tsien, R.Y., Newton, A.C., 2003. A genetically encoded fluorescent reporter reveals oscillatory phosphorylation by protein kinase C. J Cell Biol. 161,899-909.

Wang, F., Chen, T.S., Xing, D., Wang, J.J., Wu, Y.X., 2005. Measuring dynamics of caspase-3 activity in living cells using FRET technique during apoptosis induced by high fluence low-power laser irradiation. Lasers Surg Med. 36,2-7.

Wen, W., Taylor, S.S., Meinkoth, J.L., 1995. The expression and intracellular distribution of the heat-stable protein kinase inhibitor is cell cycle regulated. J Biol Chem. 270,2041-6.

Yamaga, M., Fujii, M., Kamata, H., Hirata, H., Yagisawa, H., 1999. Phospholipase C-delta1 contains a functional nuclear export signal sequence. J Biol Chem. 274,28537-41.

Yang, Y., Kaul, S., Zhang, D., Anantharam, V., Kanthasamy, A.G., 2004. Suppression of caspase-3-dependent proteolytic activation of protein kinase C delta by small

interfering RNA prevents MPP+-induced dopaminergic degeneration. Mol Cell Neurosci. 25,406-21.

Zhang, G., Kazanietz, M.G., Blumberg, P.M., Hurley, J.H., 1995. Crystal structure of the cys2 activator-binding domain of protein kinase C delta in complex with phorbol ester. Cell. 81,917-24.

CHAPTER V: SELECTIVE EXPRESSION OF OXIDATIVE-STRESS SENSITIVE KINASE PROTEIN KINASE C DELTA (PKCδ) CONTRIBUTES TO THE VULNERABILITY OF NIGRAL DOPAMINERGIC NEURONS TO MPP^+-INDUCED DEGENERATION

A paper submitted to the Journal of Neuroscience

Yongjie Yang, Latchoumycandane Calivarathan, Danhui Zhang, Siddharth Kaul, Vellareddy Anantharam, Anumantha Kanthasamy

ABSTRACT

Protein kinase C delta (PKCδ) has been shown to be an oxidative stress sensitive kinase that promotes neurotoxin-induced apoptotic death of dopaminergic neuronal cells. In the present study, we determined the relative expression levels of PKC isoforms, including PKCα, PKCβI, PKCδ, PKCε, PKCθ, and PKCζ in the substantia nigra (SN), striatum (St), and cortex (Ctx) regions of rodent brains. By employing immunostaining, immunoblot, and quantitative RT-PCR, selective expression of PKCδ, but not of other PKC isoforms, was found in the nigral dopaminergic neurons. Co-localization of abundant PKCδ with tyrosine hydroxylase (TH) in the cytoplasm of nigral dopaminergic neurons was also observed. We further demonstrated that PKCδ is proteolytically activated in the substantia nigra region of the mouse brain. The blockade of proteolytic cleavage of endogenous PKCδ by the cleavage

resistant mutant of PKCδ (PKCδ-CRM) not only protects dopaminergic neuronal (N27) cells from MPP^+-induced apoptotic death, but also protects primary dopaminergic neurons from MPP^+-induced degeneration. Moreover, the catalytic fragment of PKCδ (PKCδ-CF), but not the regulatory fragment of PKCδ (PKCδ-RF), can directly induce the degeneration of primary dopaminergic neurons. Finally, we demonstrated that the number of nigral dopaminergic neurons and the striatum dopamine level are significantly higher in PKCδ-/- mice than in PKCδ +/+ mice after administration of MPTP. Taken together, our studies suggest that abundant PKCδ is one of the inherent factors that contribute to the vulnerability of nigral dopaminergic neurons to MPP^+-induced degeneration by its proteolytic activation.

INTRODUCTION

The severe degeneration of substantia nigra pars compacta (SNc) dopaminergic neurons in Parkinson's disease (PD) causes depletion of the neurotransmitter dopamine in the striatum, and subsequently changes the neuronal circuitry controlling voluntary movement and induces the development of hyperkinesia symptoms, including tremors, bradykinesia, and postural instability. The degeneration of dopaminergic neurons in PD is strikingly selective, i.e., dopaminergic neurons located in the SNc region are selectively degenerated, though degeneration of noradrenergic neurons at the locus coeruleus, serotonergic neurons at the raphe, and cholinergic neurons at the nucleus basalis of meynert, dorsal motor nucleus of vagus, and cerebral cortex are also observed (Dauer and Przedborski, 2003). MPTP, a mitochondrial complex I inhibitor, induces rapid development of an irreversible PD-like

syndrome in humans and primates (Langston et al., 1984; Albanese et al., 1993); the development of MPTP cell culture and animal models of PD paves the path to investigate the mechanism of dopaminergic neuronal degeneration.

Extensive studies have suggested that oxidative stress is one of the major upstream events that contributes to the cell death process of the SNc dopaminergic neurons in PD (Cassarino et al., 1997; Greenamyre et al., 2001; Jenner, 2003). Examination of postmortem PD brains has revealed that the SNc region has a higher level of oxidative stress, as indicated by the level of lipid peroxidation and protein or DNA oxidation (Dexter et al., 1989; Floor and Wetzel, 1998; Jenner, 1998). Dopaminergic neurons are particularly susceptible to oxidative stress, as their neurotransmitter dopamine can be oxidized to generate toxic dopamine-quinone species, superoxide radicals, and hydrogen peroxide (Graham, 1978; Lotharius and Brundin, 2002). Oxidative stress induced by MPTP or its active form MPP^+ (Cassarino et al., 1997; Dauer and Przedborski, 2003; Kaul et al., 2003), as a result of mitochondrial complex I inhibition, has also been shown to trigger a series of apoptotic cascades, including cytochrome c release (Cassarino et al., 1999), caspase activation (Hartmann et al., 2000; Hartmann et al., 2001; Viswanath et al., 2001), and apoptotic cell death in numerous cell culture and animal PD models. However, downstream events of caspase-3 activation induced by oxidative stress in dopaminergic neurons have not been fully characterized.

Protein kinase C is one of the major cellular signal transducers involved in various cellular functions. The PKC family includes 11 isoforms, which are classified mainly into three subgroups based on their dependence upon diacylglycerol (DAG) and Ca^{2+} for activation (Newton, 2003). The conventional PKC isoforms (α, βI, βII, and γ) require DAG

and Ca^{2+} for activation, the novel PKC isoforms (δ, ε, η, and θ) require DAG but not Ca^{2+} for activation and the atypical PKCs (PKC ζ, λ, and ι) require neither Ca^{2+} nor DAG for activation. Interestingly, a substantial body of evidence has demonstrated that PKCδ can be proteolytically activated by caspase-3 and promote apoptotic cell death in non-neuronal and neuronal cells (Brodie and Blumberg, 2003; Kitazawa et al., 2003; Yang et al., 2004), although most of the PKC isoforms have anti-apoptotic properties in the cells (Gutcher et al., 2003). Our previous studies have also shown that hydrogen peroxide-induced oxidative stress also induces caspase-3 dependent proteolytic activation of PKCδ in dopaminergic neuronal cells (manuscript under review), suggesting that PKCδ might be an important downstream modulator mediating oxidative stress-induced apoptotic death of dopaminergic neurons. Although several expression surveys of PKC isoforms in the central nervous system have found that PKCδ is highly expressed in the thalamus, septal nuclei, and purkinje cells in the posterior cerebellum (Barmack et al., 2000; Naik et al., 2000), the expression of PKCδ in the SNc dopaminergic neurons has not been investigated.

Previously, we demonstrated that protein kinase C delta (PKCδ) is proteolytically activated by caspase-3 and contributes to the induction of apoptotic death of dopaminergic neuronal cells by various neurotoxins (Kaul et al., 2003; Kitazawa et al., 2003; Yang et al., 2004). Herein, we examined the expression of PKC isoforms in different regions of brain, including the nigral dopaminergic neurons, and investigated the role of proteolytic activation of PKCδ in MPP^+-induced degeneration of nigral dopaminergic neurons in primary mesencephalic neuronal cultures and in the substantia nigra region of mice brains.

MATERIALS AND METHODS

Materials

MPP^+, protease cocktail, ATP, protein-A-sepharose, and anti-β-actin antibody were obtained from Sigma-Aldrich (St. Louis, MO). Antibodies to PKCδ, α, and βI were purchased from Santa Cruz Biotechnology, Inc. (Santa Cruz, CA). Anti-GAD-6 antibody was obtained from the University of Iowa hybridoma facility. TaqMan Rat PKCδ, Mouse PKCδ, ε, and θ, the 18s ribosome RNA expression assay kit, and PCR master mix were purchased from Applied Biosystems (Foster City, CA). Anti-rabbit and anti-mouse secondary antibodies and the ECL chemiluminescence kit were purchased from Amersham Pharmacia Biotech. (Piscataway, NJ). Alexa 488 conjugated anti-rabbit secondary antibody and Hoechst 33342 were purchased from Molecular Probes, Inc. (Eugene, OR). Cy3 conjugated anti-mouse secondary antibody was obtained from Jackson Laboratory (Bar Harbor, Maine) The Cell Death Detection ELISA plus Assay Kit was purchased from Roche Molecular Biochemicals (Indianapolis, IN). [γ-^{32}P] ATP was purchased from Perkin Elmer Life Science Products (Boston, MA). The Bradford protein assay kit was purchased from Bio-Rad Laboratories (Hercules, CA). Brilliant SYBR green QPCR reagent, Brilliant QPCR reagent, and *Pfu* DNA polymerase were purchased from Stratagene (La Jolla, CA). SuperScript III first-strand synthesis system, TRIZOL reagent, ViraPower™ lentiviral expression system, RPMI, fetal bovine serum, L-glutamine, blasticidin, penicillin, streptomycin, and gentamycin were purchased from Invitrogen, Inc. (Carlsbad, CA). Primers were synthesized in IDT (Coralville, IA).

Animals

All male C57 black mice (12-16 weeks old) used in the experiments were maintained in the College of Veterinary Medicine Animal Care Facility of Iowa State University under standard laboratory conditions with water and food available *ad libitum*. PKCδ-/- mice were a kind gift from Prof. Keiichi Nakayama (Kyushu University, Fukuoka, Japan) (Miyamoto et al., 2002). All experimental procedures involving mice have been approved by the Iowa State University Institutional Animal Care and Use Committee.

Cell culture

The immortalized rat mesencephalic dopaminergic neuronal cell line (N27) was a gift from Dr. Kedar N. Prasad (University of Colorado Health Sciences Center, Denver, CO) (Prasad et al., 1998). N27 cells were grown in RPMI 1640 medium containing 10% FBS, 2 mM L-glutamine, 50 units penicillin, and 50 μg/ml streptomycin. Cells were maintained in a humidified atmosphere of 5% CO_2 at 37^0C, and 4-5 day old cells were used for the experiments. For MPP^+ treatment, N27 cells and PKCδ-CRM stably expressing N27 cells were treated with 300 μM MPP^+ for 36 hr in serum-containing medium.

Primary mesencephalic neuronal culture

Primary mesencephalic neuronal cultures were prepared from the ventral mesencephalon of gestational 15-17 day old rat embryos as described previously (Yang et al., 2004). Briefly, midbrain tissues were maintained in ice-chilled dissection solution (HBS supplemented with 200 units/ml penicillin/streptomycin, 10 mM $MgCl_2$, 7 mM pH 7.3 Hepes, and 2 mM L-glutamine) during the dissection. The tissue was collected by centrifugation at

80 g for 5 min and then treated with Trypsin/EDTA for 20-30 min at 37^0C. Trypsin was removed by centrifugation and digested tissues were resuspended in culture medium I (DMEM supplemented with 10% FBS). The digested tissues were further separated by pipetting to obtain the homogenous suspension. The cells were counted and plated at equal density (0.5 x 10^6 cells) on cover slips pre-coated with poly-L-lysine and laminin in 6-well plates. After 24 hr, culture medium I was replaced with culture medium II (Neurobasal-A medium, supplemented with 0.2% insulin, 0.2% transferring, 5% FBS, 2% B-27 supplement, 2 mM GlutaMAX I, 1 μg/ml gentamycin, and 5 μM cytosine arabinoside). The cells were maintained in a humidified CO_2 incubator (5% CO_2, 37°C). Half of the culture medium was replaced every 2 days. Approximately 6-7 day old cultures were used for experiments.

MPTP administration to mice

MPTP dissolved in ddH_2O was administered using an acute dosing regimen of 30 mg/kg intraperitoneally every day for five doses. Control animals were treated with an equal volume of ddH_2O. All animals were sacrificed the day after the last injection. Experimental groups included MPTP-treated PKCδ+/+ mice (n=12) and their control (n=12) and MPTP-treated PKCδ-/- mice (n=12) and their control (n=12).

Immunoblotting

Different regions of brain, including cortex, striatum, and substantia nigra, were first dissected. To prepare the tissue homogenate, brain tissues were homogenized with a mini homogenizer in lysis buffer (pH 8.0, 20 mM Tris-Cl, 10 mM EGTA, 2 mM EDTA, 2 mM DTT, 0.5% Triton X-100, and 1:100 dilution of protease inhibitor). For cell homogenate

preparation, N27 cells ($10x10^6$) were harvested with trypsin/EDTA and spun at 200xg for 5 min. Cell pellets were then washed twice with ice-chilled PBS and resuspended in 200 µl of lysis buffer. After incubation on ice for 5 min, the lysates were centrifuged for 30 min at 14,000xg at 4^0C and supernatants were collected as whole lysates. Equal amounts of protein (20-30 µg) were loaded in each lane and separated on a 10% SDS-polyacrylamide gel. Proteins were then transferred to nitrocellulose membrane by electro-blotting overnight (4°C, 25 V). Non-specific binding sites were blocked by treating the nitrocellulose membranes with 5% non-fat dry milk TBST solution (10 mM Tris, 150 mM NaCl, and 0.1% Tween 20) for 1 hr. The nitrocellulose membranes were then incubated with primary antibodies (1:1000) for 1 hr at RT. The primary antibody treatment was followed by treatment with secondary HRP-conjugated anti-rabbit or anti-mouse IgG (1:2000) for 1 hr at RT. Secondary antibody-bound proteins were detected using an ECL chemiluminescence kit (Amersham Biosciences). Gel photographs and densitometric analysis were performed with a Kodak image station (Model 1000R, Rochester, New York).

RNA preparation and quantitative real time RT-PCR

Total RNA was prepared from N27 cells or from different regions of rodent (mouse and rat) brains. N27 cells ($1x10^6$) were first collected by centrifugation and washed with PBS. For rodent brain tissue samples, different regions of brain (striatum, cortex, substantia nigra) were dissected and frozen in liquid nitrogen. The absolute RNA RT-PCR miniprep kit (Stratagene, La Jolla, CA) was used for RNA preparation. Briefly, the cell pellet or brain tissue (20 mg) was resuspended in lysis buffer (from the kit). Brain tissue was further homogenized with the mini homogenizer. The homogenate was loaded on the spin column

(from the kit) for the enrichment of RNA in the column. DNase solution (from the kit) was added to the column for the degradation of the remaining DNA. After washing with low-salt buffer, RNA retained on the membrane was eluted out with elution buffer. Total RNA was reversely transcribed into cDNA using the SuperScript III first-strand synthesis system (Invitrogen, Inc., Carlsbad, CA) as described in the kit instructions. For quantitative RT-PCR (QRT-PCR) of rodent PKCδ, PKCε, and PKCθ, a TaqMan expression assay kit was used. About 50 ng cDNA was mixed with TaqMan primer and probe, as well as 2x QPCR master mix to set up the reaction (50 μl). For QRT-PCR of mouse PKCβI and PKCζ, specific primers were designed and SYBR green reagent was employed. Primers used for PKCβI were forward: 5' ttctggaagcagttgagctt 3'; reverse: 5' agtgccaaatgtcattcttca 3'; and for PKCζ, forward: 5' cagatcacagatgactatgg 3'; reverse: 5' gagattgctctgtctagaag 3'. About 50 ng cDNA was mixed with primer (100 nM), reference dye (30 nM), and Brilliant SYBR green QPCR master mix to set up the reaction (50 μl). 18s ribosome RNA (rRNA) was used as an endogenous control for both TaqMan and SYBR green based QRT-PCR. For each sample, triplicates were run on the same plate. All PCR reactions were performed and data were analyzed in a Mx4000 multiplex Quantitative PCR system (Stratagene, La Jolla, CA).

Preparation of constructs

PKCδ-CRM (cleavage resistant mutant), PKCδ-CF (catalytic fragment), and PKCδ-RF (regulatory fragment) expression plasmids were prepared. To prepare PKCδ-CF and PKCδ-RF, 995-2035 bp or 14-982 bp of mouse PKCδ (gi: 6755081) cDNA were first amplified from pGFP-PKCδ (a kind gift of Dr. Reyland at University of Colorado) (DeVries

et al., 2002) with the following primer pairs, respectively. For PKCδ-CF: forward primer: 5' caccatgaacaacgggacctatggcaa 3'; reverse primer: 5' aatgtccaggaattgctcaaac 3'; for PKCδ-RF: forward primer: 5' caccatggcacccttcctgcgc 3'; reverse primer: 5' actcccagagacttctggctt 3'. To prepare PKCδ-CRM, full-length mouse PKCδ cDNA with a point mutation at 993(A-C) that abolishes the caspase-3 cleavage site of PKCδ was amplified with pGFP-PKCδ$^{D\text{-}A327}$ (a kind gift of Dr. Reyland at University of Colorado) as template. The primer pairs used were: forward primer: 5' caccatggcacccttcctgcgc 3'; reverse primer: 5' aatgtccaggaattgctcaaac 3'. All PCR reactions were performed with *Pfu* DNA polymerase to maintain the fidelity of the sequence. All PCR products were directly cloned in-frame into the V5-tagged expression vector (at the C terminal) pLenti/TOPO from Invitrogen to get pLenti/PKCδ-CRM, pLenti/PKCδ-CF, and pLenti/PKCδ-RF. All positive clones were confirmed by sequencing.

Establishment of PKCδ-CRM stably expressing N27 cell line

The ViraPower Lentiviral gene expression system from Invitrogen (Carlsbad, CA) was employed for the establishment of the PKCδ-CRM stably expressing N27 cell line. To produce lentiviral particles, pLenti/PKCδ-CRM, as well as supporting plasmids (provided by the kit) were co-transfected into human 293FT cells with the use of lipofectamine 2000, as described in the instruction of the kit. The lentiviral particles in the medium were then collected by centrifuging at 3000 rpm for 15 min at 48-72 hr post-transfection. To generate the PKCδ-CRM stably expressing cell line, lentiviral particles containing pLenti/PKCδ-CRM and polybrene (6 μg/ml) were added into cultured N27 cells ($2x10^5$). After 24 hr, lentiviral particles were replaced with fresh medium. Positive N27 cells were selected by keeping

blasticidin (10 μg/ml) in medium for up to 2 weeks. PKCδ-CRM expressing N27 cells were identified by immunostaining of the C-terminal V5 epitope.

Transient transfection of primary neuronal cultures

Transient transfection of primary neuronal cultures was performed by electroporation. A Rat Neuron Nucleofector kit from Amaxa biosystems (Cologne, Germany) was employed. Briefly, about 1-2x10^6 cells were resuspended with 100 μl nucleofector solution mixed with 2 μg plasmid (pLenti/PKCδ-CRM, pLenti/PKCδ-CF, or pLenti/PKCδ-RF) and transferred into a cuvette. The cuvette was then put in a nucleofector device (Amaxa biosystems, Cologne, Germany) for electroporation. After electroporation, cells were gently transferred to a 6-well plate and incubated at 37^0C.

Immunocytochemistry

Double immunostaining of TH and PKCδ, GAD and PKCδ, and TH and V5 was performed sequentially in primary neuronal cultures. Primary neuronal cultures grown on the poly-L-lysine and laminin coated cover slips were first fixed in 4% paraformaldehyde, then permeabilized and blocked with blocking reagent (0.4% BSA, 5% goat serum, and 0.2% Triton-X 100 in PBS) for 20 min. Cells were then incubated with one of the primary antibodies (mouse anti-TH, mouse anti-GAD, or rabbit anti-TH, 1:1000 in blocking reagent) overnight at 4°C and then washed 4x8 min with PBS. Immunoreactivity was visualized by incubation with Alexa 488-conjugated goat anti-rabbit secondary antibody or Cy3-conjugated goat anti-mouse secondary antibody (1:2000 in PBS) at RT for 90 min. After the wash, cells were incubated with second primary antibodies (rabbit anti-PKCδ or mouse anti-

V5) and the second secondary antibodies. After another 4x8 min PBS wash, Hoechst 33342 (final concentration of 10 μg/ml in PBS) was added to stain the cell nuclei at RT for 3 min. Finally, cells were mounted on a slide with antifade mounting medium. The cells were observed under a TCS/NT confocal microscopy system (Leica, Bannockburn, IL). All images were processed in MetaMorph 5.07 from Universal imaging (Downingtown, PA).

Immunohistochemistry

Control and MPTP-treated mice were perfused by the intracardiac route with 5% sucrose, followed by 4% paraformaldehyde in PBS. The mice were kept for 2 hr and then decapitated. The brains of mice were then removed and immersed for 48 hr in 4% paraformaldehyde for fixation. Nigral and striatal cortical sections (25 μm in thickness) were then prepared with a cryostat. Double immunostaining of TH and PKCδ was then performed sequentially. The sections were rinsed with PBS containing 0.1% Triton-X (PBS-T), followed by incubation with mouse anti-TH antibody (1:1000) in PBS-T containing 10% goat serum overnight at 4°C with continuous shaking. The sections were washed three times with PBS and incubated with Cy3-conjugated goat anti-mouse secondary antibody (1:2000) at RT for 2 hr. The staining of PKCδ was then followed using the same procedure, but with the Alexa 488-conjugated goat anti-rabbit secondary antibody. All sections were washed and mounted on a slide. Mounted sections were observed under a TCS/NT confocal microscopy system (Leica, Bannockburn, IL). All images were processed in MetaMorph 5.07 from Universal Imaging (Downingtown, PA).

Immunoprecipitation kinase assay

PKCδ enzymatic activity was assayed using an immunoprecipitation kinase assay as previously described (Anantharam et al., 2002). Protein (100-200 μg) extracted from the substantia nigra of control and MPTP-treated mice was immunoprecipitated overnight at 4°C using 2 μg of anti-PKCδ antibody. The immunoprecipitates were then incubated with protein-A–sepharose for 1 hr at 4°C. The protein-A bound antigen-antibody complexes were then washed 3 times with lysis buffer, 3 times with kinase buffer (40 mM Tris, pH 7.4, 20 mM $MgCl_2$, 20 μM ATP, and 2.5 mM $CaCl_2$), and resuspended in 20 μl of kinase buffer. Reactions were started by adding 20 μl of reaction buffer containing 0.4 mg Histone H1 and 5 μCi of [γ-^{32}P] ATP (3,000 Ci/mM) to the immunoprecipitated samples and incubated for 10 min at 30°C. SDS gel loading buffer (2X) was then added to terminate the reaction, the samples were boiled for 5 min, and the products were separated on a 12% SDS-PAGE gel. The phosphorylated histone bands were detected using a Personal Molecular Imager (FX model, Bio-Rad) and quantified using Quantity One 4.2.0 software (Bio-Rad, Hercules, CA).

Striatal dopamine and DOPAC measurement

The mice were sacrificed the day after the last MPTP treatment. Both striata were rapidly dissected with the use of a brain slicer and tissue puncher on ice-chilled glass plates. The striata were frozen at -70^{0}C immediately after dissection. For the measurement of dopamine and its metabolites, the striata were then thawed and resuspended in 0.1 M ice-chilled perchloric acid (PCA). The resuspensions were sonicated and centrifuged. Aliquots were taken for protein quantification with the Bradford assay kit. Other aliquots were used

for the measurement of dopamine and its metabolites by HPLC with electrochemical detection. Concentrations of dopamine and DOPAC are expressed as pmol/mg protein.

Quantification assay for DNA fragmentation

DNA fragmentation was measured using a recently developed Cell Death Detection ELISA plus Assay Kit (Molecular Biochemicals, Indianapolis, IN). Briefly, cells were spun down at 200xg for 5 min and washed twice with 1X PBS. Cells were then incubated with a lysis buffer (supplied with the kit) at RT. After 30 min, samples were centrifuged and 20 µl aliquots of the supernatant were then dispensed into streptavidin-coated 96 well microtiter plates followed by addition of 80 µl of HRP-conjugated antibody cocktail, and incubated for 2 hr at RT with mild shaking. After incubation, unbound components were removed by washing with the incubation buffer supplied with the kit. The nucleosomes retained by the antibody cocktail in the immunocomplex were quantified spectrophotometrically with ABTS as an HRP substrate. Measurements were made at 405 nm and 490 nm using a SpectroMax 190 spectrophotometer (Molecular Devices, Sunnyvale, CA). The difference in absorbance between OD405 and OD490 nm was used to measure the actual DNA fragmentation level.

Data analysis

Data analysis was performed using Prism 3.0 software (GraphPad Software, San Diego, CA). DNA fragmentation, QRT-PCR, the number of TH positive neurons and their neuronal processes, and dopamine content were first analyzed using one-way ANOVA. Bonferroni's post-test was then performed to compare all groups, and differences with

$p<0.05$ were considered significant. To analyze the PKCδ kinase enzymatic activity results, the paired t-test was used.

RESULTS

Selectively high expression of PKCδ protein in dopaminergic neurons of substantia nigra (SN)

PKCδ has been shown to be proteolytically activated under oxidative stress conditions in dopaminergic neuronal cells; however, the expression level and subcellular localization of PKCδ have not been investigated in dopaminergic neurons. Double immunostaining of PKCδ with tyrosine hydroxylase (TH) or GABA decarboxylase (GAD) was first performed in rat primary mesencephalic neuronal cultures that contain a mixture of dopaminergic and GABAergic neurons. TH and GAD serve as markers for dopaminergic and GABAergic neurons, respectively. As shown in Figure 1Aa, clear immunoreactivity of PKCδ was seen in dopaminergic neurons identified by positive TH immunostaining; PKCδ was seen mostly in the cytoplasm and neuronal processes that co-localize with TH (Figure 1Ad). In contrast, only very weak immunoreactivity of PKCδ was observed in the cytoplasm and neuronal processes of GABAergic neurons identified by positive GAD immunostaining. This result suggests that PKCδ is more abundant in the dopaminergic neurons than in GABAergic neurons. To verify this observation *in vivo*, double immunostaining of PKCδ with TH or GAD was then performed in the substantia nigra (SN) and striatum sections of mouse brain. As shown in Figure 1B, immunoreactivity of PKCδ in the substantia nigra brain section is

consistently intense, appearing only in the dopaminergic neurons identified by positive TH staining and also co-localizing very well with TH in the cytoplasm. In the striatum section, although some PKCδ immunostaining signals were also seen in GABAergic neurons identified by positive GAD staining and nucleus staining, these signals were not quite distinct from the background. A survey of the expression level of different PKC isoforms in substantia nigra was further examined by immunoblot and was compared to that in cortex and striatum of the mouse brain. Based on the availability and quality of antibodies against different PKC isoforms, immunoblots of PKCα, PKCβI, and PKCδ were made (Figure 1C). Consistent with the immunostaining results, the immunoblot of PKCδ also shows that the substantia nigra has the highest protein level of PKCδ as compared to the cortex and striatum. However, the PKCα protein level is almost the same in the three regions, and the PKCβI protein level is lower in the substantia nigra region as compared to the cortex and striatum regions. The membrane was reprobed with β-actin antibody to ensure equal loading. Taken together, these results consistently demonstrate that nigral dopaminergic neurons in mice have a selectively higher expression of PKCδ.

Selectively high level of PKCδ mRNA in the substantia nigra

To establish the correlation between the protein and mRNA levels of different PKC isoforms we next determined the mRNA levels of different PKC isoforms, including PKCδ, in the cortex (Ctx), striatum (St), and substantia nigra (SN) regions of mice brains, which were first carefully and precisely dissected. Total RNA was then prepared and converted into cDNA. For mouse PKCδ, PKCε, and PKCθ, pre-designed TaqMan probes from Applied

Biosystems were employed for quantitative real time PCR (QRT-PCR). Because pre-designed TaqMan probes are not available for mouse PKCβI and PKCζ, the SYBR green dye based QRT-PCR method was used. 18s Ribosome RNA (18s rRNA) was used as an endogenous control to equalize the amount of RNA used in QRT-PCR. The real-time amplification plot of PKCδ from the Ctx, St, and SN is shown in Figure 2A. The Ct (threshold of cycle) value of amplification from SN cDNA is significantly lower than that in Ctx and St cDNA, indicating that the number of PKCδ mRNA copies in the SN is much higher than that in the Ctx and St. By using Ctx PKCδ Ct as the calibrator, the relative quantity of PKCδ mRNA among the three regions was calculated from the formula $2^{-(\Delta Ct\ PKC\delta - \Delta Ct\ 18s\ rRNA)}$ and presented in Figure 2B. The number of PKCδ mRNA copies in the SN is 30-fold greater than that in the Ctx, and 2-fold greater than that in the St. Similar results were also found in rat: the number of PKCδ mRNA copies in the SN is about 5-fold more than that in the St and Ctx regions (Figure 4A). The relative quantity of several other PKC isoform mRNAs among the SN, Ctx, and St regions was also determined (Ctx as the calibrator). As shown in Figure 2C, the relative quantity of PKCβI and PKCε mRNA among the three regions is: SN < St < Ctx, while the relative quantity of PKCθ mRNA is: Ctx < SN < St. Both SN and St regions have similar levels of PKCζ mRNA, which are higher than the level in the Ctx. We also attempted to determine the quantity of PKCα mRNA in the three regions. Since a pre-designed TaqMan probe for PKCα is unavailable, specific primers for PKCα were designed in order to use the SYBR green based QRT-PCR method; however, these primers failed to give good amplification and resulted in high background disturbance. Nevertheless, none of these PKC isoforms surveyed have more abundant mRNA in the SN

region, suggesting that PKCδ is a unique kinase in the PKC family with a selectively high level of mRNA in the SN region.

Proteolytic activation of PKCδ in nigral dopaminergic neurons of mice

The classic Parkinsonian toxin MPP^+ has been shown to induce oxidative stress and caspase activation in numerous *in vitro* and *in vivo* models of PD (Hartmann et al., 2000; Lee et al., 2000; Hartmann et al., 2001; Jenner, 2003). Our previous studies further demonstrated that PKCδ is proteolytically activated in a caspase-3 dependent manner, followed by MPP^+-induced oxidative stress, and contributes to MPP^+-induced apoptotic death of dopaminergic neuronal cells (Kaul et al., 2003). To examine whether MPP^+ also induces proteolytic activation of PKCδ in nigral dopaminergic neurons *in vivo*, mice were administered 30 mg/kg MPTP for 5d and the substantia nigra region was dissected. Dissected SN was then homogenized and proteins were separated by 10% SDS-PAGE. Anti-PKCδ antibody from Santa Cruz Biotechnology (Santa Cruz, CA) that recognizes the C-terminal epitope of PKCδ was employed for the detection of both native and cleaved PKCδ fragments. As shown in Figure 3A, cleaved PKCδ fragments (41/38KDa) were detected from whole tissue lysates of the SN region from MPTP treated mice. To demonstrate that proteolytic cleavage of PKCδ occurs in dopaminergic neurons, the presence of tyrosine hydroxylase (TH) was also examined and a clear TH band was detected on the immunoblot. The membrane was also reprobed with anti-β-actin antibody to equalize the protein loaded on the gel. After observing the proteolytic cleavage of PKCδ, we next examined the PKCδ kinase activity following MPTP administration. PKCδ was immunoprecipitated from whole lysate of the SN region in

control and MPTP treated mice and was evaluated in an *in vitro* kinase assay. As shown in Figure 3B, MPTP administration increases PKCδ kinase activity to 220% in comparison to untreated control mice, indicating that PKCδ is indeed proteolytically activated in mice administered MPTP.

Cleavage resistant mutant of PKCδ (PKCδ-CRM) attenuates MPP^+-induced proteolytic cleavage of PKCδ in N27 cells and protects N27 cells from MPP^+-induced apoptotic death

RNAi mediated genetic loss-of-function analysis of PKCδ has demonstrated a promotional role of PKCδ in MPP^+-induced degeneration of dopaminergic neurons in rat primary mesencephalic neuronal cultures (Yang et al., 2004). To determine whether the proteolytic cleavage of PKCδ is essential for its promotional role in MPP^+-induced degeneration of dopaminergic neurons, PKCδ cleavage was blocked by using the cleavage resistant mutant of PKCδ (PKCδ-CRM), and MPP^+-induced apoptotic death of dopaminergic neuronal (N27) cells was examined. Dopaminergic neuronal (N27) cells were derived from rat mesencephalic dopaminergic neurons and established as an *in vitro* model of PD (Adams et al., 1996; Prasad et al., 1998). The expression level of PKCδ in N27 cells is comparable to the selectively high expression level of PKCδ in the SN region of rodent brain; thus, N27 cells are a relevant and valid *in vitro* model of PD with regard to the expression level of PKCδ. The expression level of PKCδ in dopaminergic neuronal (N27) cells was determined by the TaqMan probe based QRT-PCR method, and relative abundance of PKCδ mRNA in N27 cells was compared to that in the Ctx, St, and SN regions of rat brain (Ctx as the

calibrator). As shown in Figure 4A, the relative amounts of PKCδ mRNA in the three regions of rat brain are similar to those observed in mouse brain regions, i.e., SN > St > Ctx. The number of PKCδ mRNA copies in N27 cells is comparable to that in the SN region and is also significantly higher than that in the Ctx and St regions of rat brain. A stable N27 cell line that overexpresses PKCδ-CRM was generated via the ViraPower^{TM} lentiviral expression system from Invitrogen. PKCδ-CRM contains a point mutation (D327A) in its caspase-3 recognition and cleavage motif which abolishes the cleavage of PKCδ by activated caspase-3 (Ghayur et al., 1996). As shown in Figure 4B, PKCδ cleavage was induced in the control cells at the 36 hr time point following MPP^+ exposure; however, cleavage of PKCδ was significantly abolished at the 36 hr time point following MPP^+ exposure in the PKCδ-CRM stably expressing N27 cells. The membrane was reprobed with anti-V5 antibody to show the expression of exogenous PKCδ-CRM in PKCδ-CRM stably expressing N27 cells. The detailed mechanism of the dominant-negative effect of PKCδ-CRM in MPP^+-induced cleavage of endogenous PKCδ is still under investigation. Some preliminary results suggest that overexpressed PKCδ-CRM can down-regulate the expression of endogenous PKCδ, as shown by RT-PCR (data not shown). The overexpressed PKCδ-CRM might also inhibit the feedback loop between PKCδ and caspase-3, resulting in the inhibition of continuous activation of caspase-3. Alternatively, the overexpressed PKCδ-CRM may simply out compete endogenous PKCδ for activated caspase-3, thus leaving endogenous PKCδ intact.

We next examined whether inhibition of caspase-3 mediated proteolytic cleavage of endogenous PKCδ by PKCδ-CRM protects N27 cells against MPP^+-induced apoptotic cell death. In control cells, MPP^+ exposure for 42 hr induced an approximate 110% increase in

the DNA fragmentation level compared to untreated control cells; however, only a 30% increase in the DNA fragmentation level was induced in the PKCδ-CRM stably expressing N27 cells following MPP^+ exposure for 42 hr in comparison to untreated control cells (Figure 4C). The overexpression of PKCδ-CRM did not induce any DNA fragmentation (data presented in another manuscript). These results clearly show that the caspase-3 mediated proteolytic cleavage of PKCδ following MPP^+ exposure is required for PKCδ's pro-apoptotic function in MPP^+-induced apoptotic death of dopaminergic neuronal cells.

Cleavage resistant mutant of PKCδ (PKCδ-CRM) protects primary dopaminergic neurons from MPP^+-induced degeneration

We next tested whether PKCδ-CRM also protects primary dopaminergic neurons against MPP^+-induced degeneration. Rat primary mesencephalic neuronal cultures were first transfected with pLenti/PKCδ-CRM by electroporation and then exposed to 10 μM MPP^+ for 48 hr. Because of the presence of the V5 epitope in the C-terminal of pLenti/PCKδ-CRM, double immunostaining of TH and V5 was performed to identify dopaminergic neurons and the expression of exogenous PKCδ-CRM in dopaminergic neurons. The morphology of TH positive neurons among different groups is presented in Figure 5A. This particular dopaminergic neuron is intact and has long, multiple-branched neuronal processes in control cells, as revealed by TH immunoreactivity. Treatment with 10 μM MPP^+ for 48 hr substantially decreased the neuronal processes and induced shrinkage of the cell body. However, the same MPP^+ treatment did not cause any significant degeneration of dopaminergic neurons in pLenti/PKCδ-CRM transfected primary neuronal cultures. The

morphology of this TH positive neuron is also intact with long, multiple-branched neuronal processes. The expression of PKCδ-CRM in TH positive neurons was revealed by V5 immunoreactivity (Figure 5B), and this particular TH positive neuron also has normal morphology following treatment with 10 μM MPP^+ for 48 hr. Expressed PKCδ-CRM is primarily localized in the cytoplasm, where it co-localizes with TH (Figure 5B). This is consistent with the results in Figure 1.

The detection of clear V5 immunoreactivity in TH positive neurons indicates PKCδ-CRM was indeed transfected into dopaminergic neurons. The transfection efficiency of PKCδ-CRM into TH positive neurons is 55%, as calculated from the number of total TH positive neurons and the number of TH and V5 double positive neurons. The TH positive neurons and their neuronal processes were employed to evaluate the effect of PKCδ-CRM on MPP^+-induced degeneration of dopaminergic neurons, since quantification of TH positive neurons is considered to be a reliable method of determining MPP^+-induced dopaminergic toxicity in primary mesencephalic cultures (Choi et al., 1999; Callier et al., 2002). After counting the number of TH positive neurons and measuring their neuronal processes in multiple fields (about 5000 cells in each group), the effect of PKCδ-CRM on MPP^+-induced degeneration of dopaminergic neurons was quantified and presented in Figure 5C&D. Treatment with 10 μM MPP^+ for 48 hr substantially decreased the number of TH positive neurons by over 80% as compared to untreated control cells (Fig. 5C). However, MPP^+-induced loss of TH^+ neurons was significantly reduced to 20% in PKCδ-CRM-transfected primary neuronal cultures, demonstrating a significant neuroprotective effect of PKCδ-CRM. PKCδ-CRM not only protects the number of TH positive neurons, but also protects the

neuronal processes of TH positive neurons from MPP^+-induced degeneration. As shown in Figure 5D, 10 μM MPP^+ exposure for 48 hr causes 83% loss of neuronal processes in TH positive neurons as compared to the control; however, only a 20% loss of neuronal processes in TH positive neurons was found in PKCδ-CRM-transfected primary neuronal cultures. Together, these results demonstrate that inhibition of endogenous PKCδ cleavage by PKCδ-CRM significantly protects dopaminergic neurons from MPP^+-induced degeneration.

Catalytic fragment of PKCδ (PKCδ-CF) directly induces degeneration of primary dopaminergic neurons

Proteolytic cleavage of PKCδ removes the pseudosubstrate bound to the catalytic site, leading to the persistent activation of the kinase (Emoto et al., 1995). The proteolytic activation of PKCδ has been associated with apoptotic death induced by various stimuli in different cells (Brodie and Blumberg, 2003; Kanthasamy et al., 2003). The exogenously introduced PKCδ-CF has also been shown to directly induce apoptosis in some cells (DeVries et al., 2002). However, whether PKCδ-CF directly induces the degeneration of dopaminergic neurons in primary neuronal cultures is not known. pLenti/PKCδ-CF expressing the catalytic fragment of PKCδ (PKCδ-CF) was directly transfected into the rat primary neuronal cultures by electroporation. pLenti/PKCδ-RF, which expresses the regulatory fragment of PKCδ (PKCδ-RF), was also transfected into the primary neuronal culture to serve as control for PKCδ-CF. Double immunostaining of TH and V5 was performed at 48 hr post-transfection to evaluate the degeneration of dopaminergic neurons and examine the expression of PKCδ-CF or PKCδ-RF in primary dopaminergic neurons.

neuronal processes of TH positive neurons from MPP^+-induced degeneration. As shown in Figure 5D, 10 μM MPP^+ exposure for 48 hr causes 83% loss of neuronal processes in TH positive neurons as compared to the control; however, only a 20% loss of neuronal processes in TH positive neurons was found in PKCδ-CRM-transfected primary neuronal cultures. Together, these results demonstrate that inhibition of endogenous PKCδ cleavage by PKCδ-CRM significantly protects dopaminergic neurons from MPP^+-induced degeneration.

Catalytic fragment of PKCδ (PKCδ-CF) directly induces degeneration of primary dopaminergic neurons

Proteolytic cleavage of PKCδ removes the pseudosubstrate bound to the catalytic site, leading to the persistent activation of the kinase (Emoto et al., 1995). The proteolytic activation of PKCδ has been associated with apoptotic death induced by various stimuli in different cells (Brodie and Blumberg, 2003; Kanthasamy et al., 2003). The exogenously introduced PKCδ-CF has also been shown to directly induce apoptosis in some cells (DeVries et al., 2002). However, whether PKCδ-CF directly induces the degeneration of dopaminergic neurons in primary neuronal cultures is not known. pLenti/PKCδ-CF expressing the catalytic fragment of PKCδ (PKCδ-CF) was directly transfected into the rat primary neuronal cultures by electroporation. pLenti/PKCδ-RF, which expresses the regulatory fragment of PKCδ (PKCδ-RF), was also transfected into the primary neuronal culture to serve as control for PKCδ-CF. Double immunostaining of TH and V5 was performed at 48 hr post-transfection to evaluate the degeneration of dopaminergic neurons and examine the expression of PKCδ-CF or PKCδ-RF in primary dopaminergic neurons.

Representative TH positive neurons expressing either PKCδ-CF or PKCδ-RF were presented in Figure 6A. Neurons expressing PKCδ-RF have normal morphology and extended neuronal processes; however, TH positive neurons that express PKCδ-CF have a shrunken cell body and very short neuronal processes, similar to the morphology of the degenerated dopaminergic neuron induced by MPP^+ (Figure 5A). To quantify the effect of PKCδ-CF on the degeneration of dopaminergic neurons, the number of TH positive neurons was counted in multiple fields among different groups (about 5000 cells observed in each group). Quantitative analysis of the number of TH positive neurons in PKCδ-CF and PKCδ-RF transfected primary neuronal cultures is presented in Figure 6B. The number of TH positive neurons was only slightly less (10%) in PKCδ-RF transfected primary neuronal cultures than in control cells, while the number of TH positive neurons in PKCδ-CF transfected primary neuronal cultures was dramatically less (60%) than in control cells. These results clearly demonstrate that PKCδ-CF itself is toxic and directly induces degeneration of dopaminergic neurons in rat primary neuronal cultures.

DISCUSSION

In the present study, we investigated the expression level of different PKC isoforms in the cortex, striatum, and substantia nigra regions of rodent brains and demonstrated that the substantia nigra region of rodent brains has a higher level of PKCδ protein and mRNA as compared to that in the cortex and striatum regions. To our knowledge, this is the first report investigating the expression level of PKC isoforms in the substantia nigral dopaminergic

neurons of rodent brains. Our results also demonstrate, for the first time, that administration of the Parkinsonian toxin MPTP to mice induces *in vivo* proteolytic activation of PKCδ in the substantia nigra region. By employing PKCδ-/- mice, the cleavage resistant mutant of PKCδ (PKCδ-CRM), and the catalytic fragment of PKCδ (PKCδ-CF), our studies clearly suggest that proteolytic activation of PKCδ is an essential downstream event in the degenerative process in nigral dopaminergic neurons in the MPTP mouse model of Parkinson's disease.

The Parkinsonian toxin MPTP has been shown to be a potent mitochondrial complex I inhibitor (Fritz et al., 1985; Singer et al., 1988; Marini et al., 1989). In the brain, MPTP is metabolized to its active form, MPP^+, and selectively accumulates in dopaminergic neurons through the dopamine transporter (DAT) (Uhl et al., 1985; Mayer et al., 1986). The MPP^+-induced inhibition of mitochondrial complex I leads to the massive production of reactive oxygen species (ROS) (Cassarino et al., 1997), which subsequently initiates a series of apoptotic events, including mitochondrial dysfunction, cytochrome C release, and activation of the major effector caspase, caspase-3, in dopaminergic neurons (Kaul et al., 2003; Vila and Przedborski, 2003). Recent *in vitro* studies further characterized that PKCδ is proteolytically activated by caspase-3 in dopaminergic neuronal cells exposed to MPP^+ (Kaul et al., 2003). PKCδ contains the caspase-3 cleavage motif located at the hinge region that connects the regulatory and catalytic fragments of PKCδ. The proteolytic cleavage of PKCδ by caspase-3 separates the inhibitory regulatory fragment from the catalytic fragment, thus persistently activating the kinase (Emoto et al., 1995; Reyland et al., 1999). The kinase active catalytic fragment of PKCδ itself is sufficient to induce cell death, as indicated by our previous study (manuscript under review) as well as several other studies (DeVries et al.,

2002; Ren et al., 2002; Basu, 2003). By employing the cleavage resistant mutant of PKCδ (PKCδ-CRM) that abolishes the caspase-3 cleavage motif by point mutation D327A (DeVries et al., 2002)), we demonstrated that proteolytic cleavage of PKCδ is an essential downstream event in MPP^+-induced degeneration of nigral dopaminergic neurons. In addition, we also showed that the exogenous expression of the kinase active catalytic fragment PKCδ-CF, but not the regulatory fragment PKCδ-RF, directly induces the degeneration of dopaminergic neurons.

Although the pathology of Parkinson's disease has been well characterized, we still do not know why nigral dopaminergic neurons are most severely degenerated in PD. Many studies have suggested that dopaminergic neurons are particularly susceptible to oxidative stress (Lotharius and Brundin, 2002), and the metabolism of the specific neurotransmitter dopamine generates many toxic free radicals, including dopamine-quinone species, superoxide radicals, and hydrogen peroxide in the cytosol of dopaminergic neurons (Graham, 1978). Redox active Fe^{2+}, which contributes to the generation of hydroxyl radicals, was also selectively elevated in the SNc region of PD brains (Sofic et al., 1991; Jellinger, 2000), partially due to the enrichment of Fe^{2+} by neuromelanin (NM) which is selectively localized in nigral dopaminergic neurons (Good et al., 1992; Zecca et al., 1994; Zecca et al., 2003). On the other hand, although genetic mutations of several genes, including α-synuclein, Parkin, UCHL1, DJ-1, PINK1, and LRRK2, have been implicated in the pathogenesis of familial PD patients (Dawson and Dawson, 2003; Shen, 2004), it is not clear how nigral dopaminergic neurons are selectively affected by the loss of function of these genes.

Our studies showed that the oxidative stress sensitive pro-apoptotic kinase PKCδ is selectively abundant in nigral dopaminergic neurons. Because proteolytic cleavage of PKCδ is mediated by activated caspase-3, various apoptotic stresses, including oxidative stress, that trigger the mitochondrial dependent intrinsic pathway can activate caspase-3 and induce subsequent proteolytic cleavage of PKCδ. Thus, the selective abundance of PKCδ in nigral dopaminergic neurons could significantly increase cellular vulnerability due to the potentially easier and enhanced generation of pro-apoptotic cleaved activated fragments of PKCδ, and greatly facilitate oxidative stress-induced degeneration of nigral dopaminergic neurons. We also determined the expression level of other representative PKC isoforms, but found a relatively lower expression level of these isoforms, particularly PKCε and PKCβI, in nigral dopaminergic neurons. Interestingly, most studies indicate that PKCβI and PKCε are predominantly anti-apoptotic PKC kinases (Gutcher et al., 2003). The relatively lower expression level of anti-apoptotic PKC isoforms and the higher expression level of pro-apoptotic PKCδ in nigral dopaminergic neurons suggest that the expression level of these PKC isoforms potentially contributes to the susceptibility of nigral dopaminergic neurons in Parkinson's disease.

Interestingly, abundant levels of PKCδ were also found to co-localize with TH, the rate-limiting enzyme in dopamine synthesis. TH is a substrate of various serine/threonine protein kinases, including cAMP-dependent protein kinase A (PKA) (Lovenberg et al., 1975), cGMP-dependent protein kinase G (PKG) (Roskoski et al., 1987), protein kinase C (PKC) (Albert et al., 1984), Ca^{2+}-calmodulin dependent protein kinase II (CaMKII) (Vulliet et al., 1984), extracellular signal-related kinase (ERK1/2) (Sutherland et al., 1993), and the recently

identified cyclin-dependent protein kinase 5 (Cdk5) (Moy and Tsai, 2004). Phosphorylation status of TH is closely associated with its activity and the synthesis of dopamine in dopaminergic neurons (Dunkley et al., 2004). Studies are underway to elucidate the interaction of PKCδ with TH and the potential regulatory role of PKCδ in TH phosphorylation and activity.

In summary, we demonstrate that MPTP administration induces *in vivo* proteolytic activation of PKCδ in nigral dopaminergic neurons, and proteolytic activation of PKCδ is an essential downstream event following caspase-3 activation in MPTP-induced degeneration of nigral dopaminergic neurons. Our studies suggest that the characterization of downstream apoptotic molecules in experimental models of PD is important to better understand the pathogenesis of this neurodegenerative disorder.

Figure 1: Selectively high expression of PKCδ protein in nigral dopaminergic neurons

(A) Immunostaining of PKCδ in dopaminergic and GABAergic neurons in rat primary mesencephalic neuronal cultures. (B) Immunostaining of PKCδ in dopaminergic and GABAergic neurons in brain sections of mice substantia nigra (SN) and striatum (St). Double immunostaining of PKCδ with TH or GAD in primary neuronal cultures or brain sections was performed sequentially. Mouse anti-TH, mouse anti-GAD antibody (1:1000) and rabbit anti-PKCδ antibody (1:1000) were used. Stained cells and sections were observed under a TCS/NT confocal microscopy system (Leica, Bannockburn, IL). (C) Protein level of PKC isoforms in cortex (Ctx), substantia nigra (SN), and striatum (St) of mice brains. Whole tissue lysates were prepared after Ctx, SN, and St regions were carefully dissected and separated by 10% SDS-PAGE.

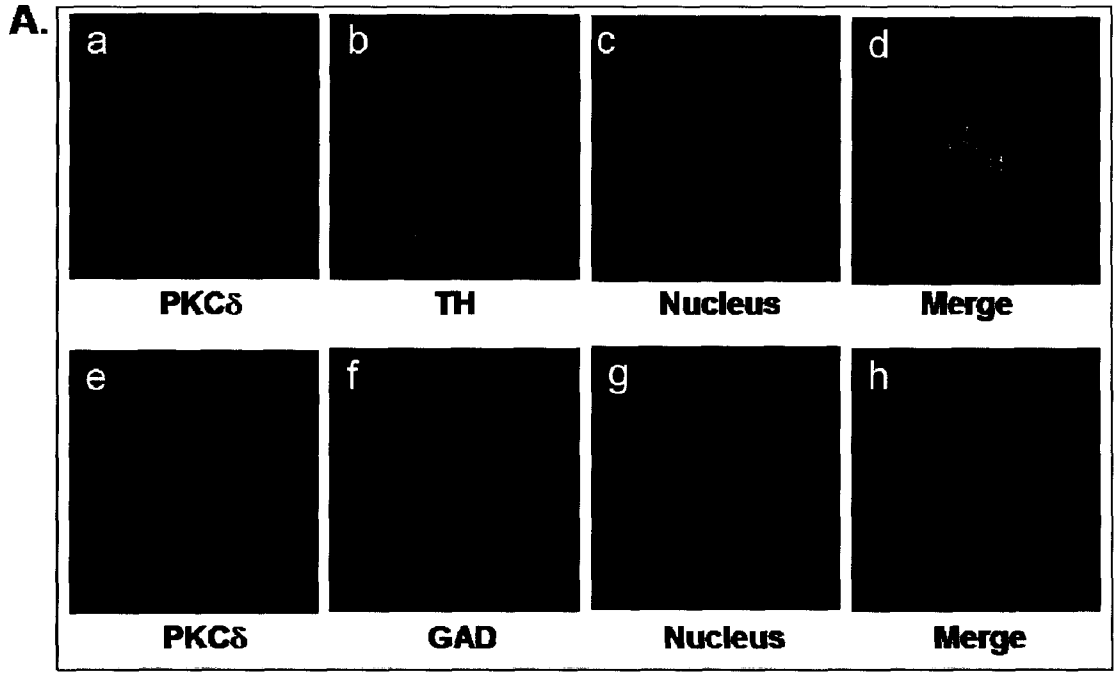
A.
a
b
c
d
PKCδ
TH
Nucleus
Merge
e
f
g
h
PKCδ
GAD
Nucleus
Merge

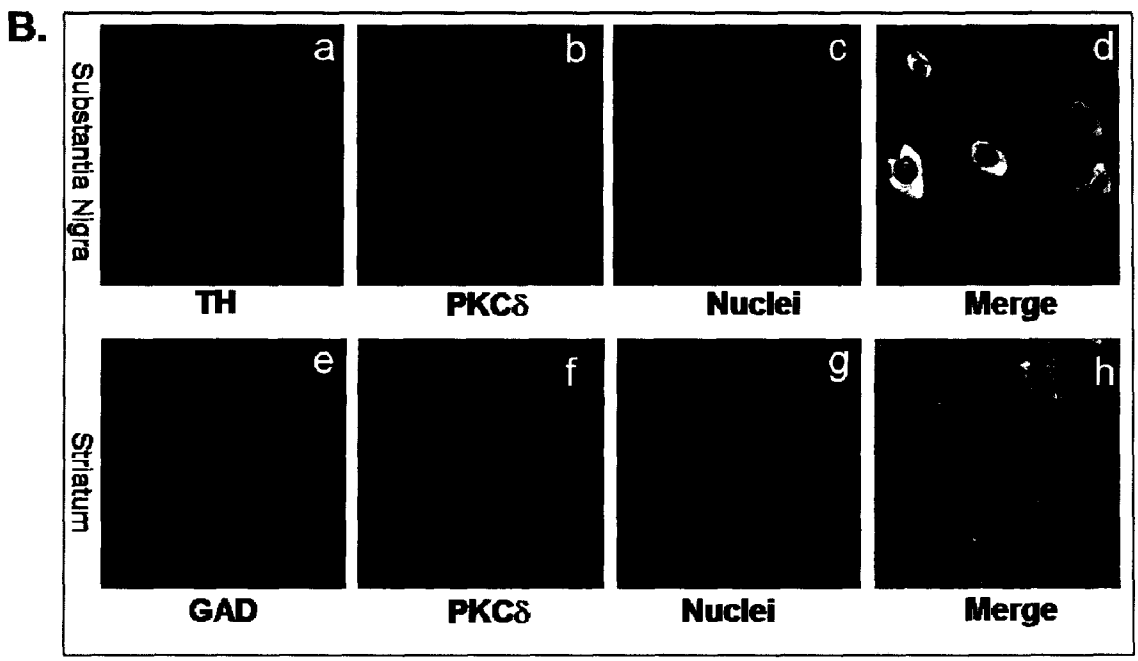
B.
Substantia Nigra
a
b
c
d
TH
PKCδ
Nuclei
Merge
Striatum
e
f
g
h
GAD
PKCδ
Nuclei
Merge

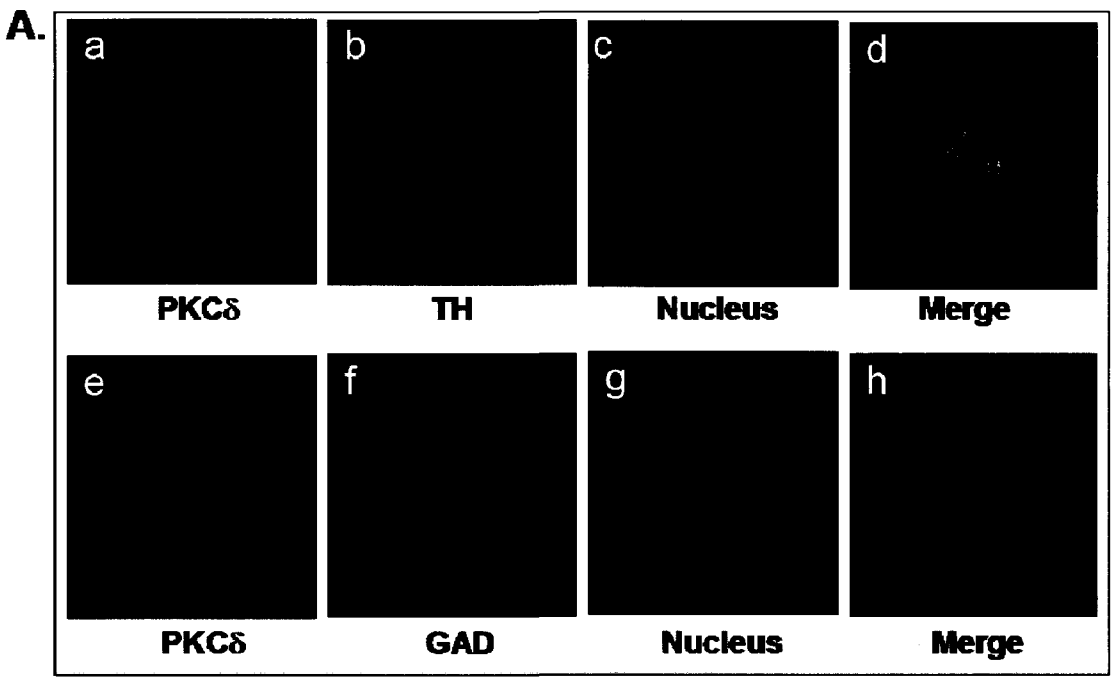
A.
a
b
c
d
PKCδ
TH
Nucleus
Merge
e
f
g
h
PKCδ
GAD
Nucleus
Merge

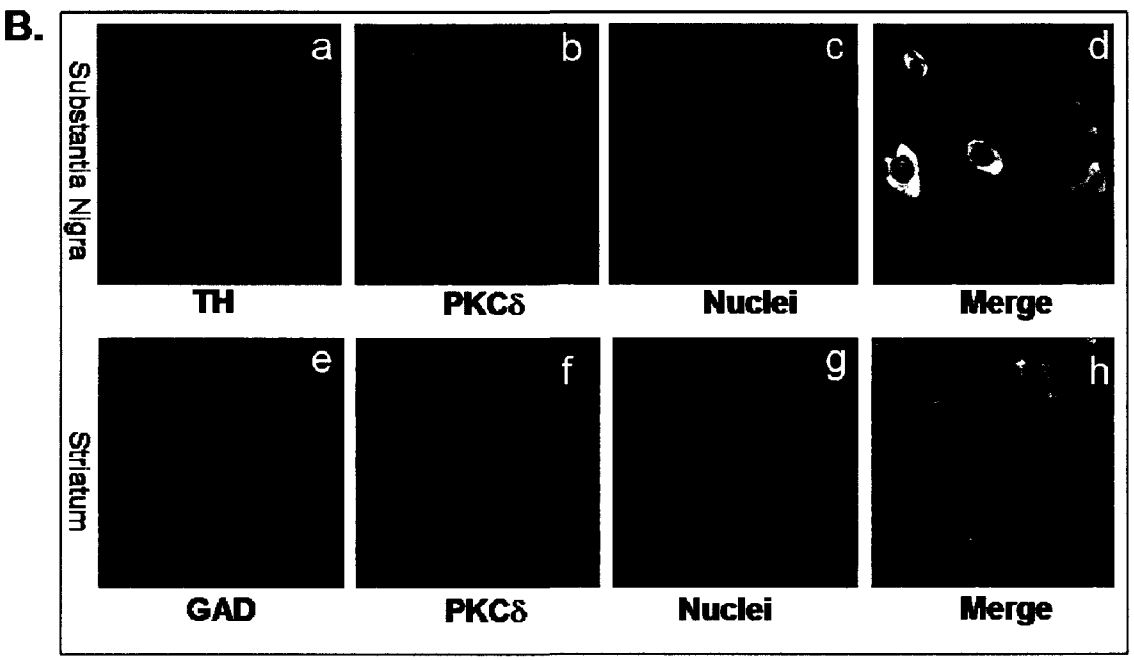
B.
Substantia Nigra
a
b
c
d
TH
PKCδ
Nuclei
Merge
Striatum
e
f
g
h
GAD
PKCδ
Nuclei
Merge

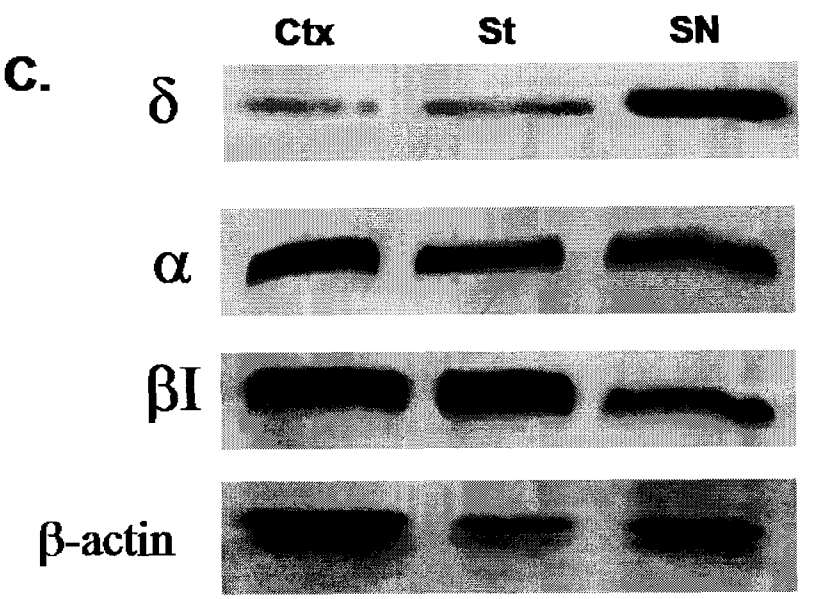
C.
Ctx
St
SN
δ
α
βI
β-actin

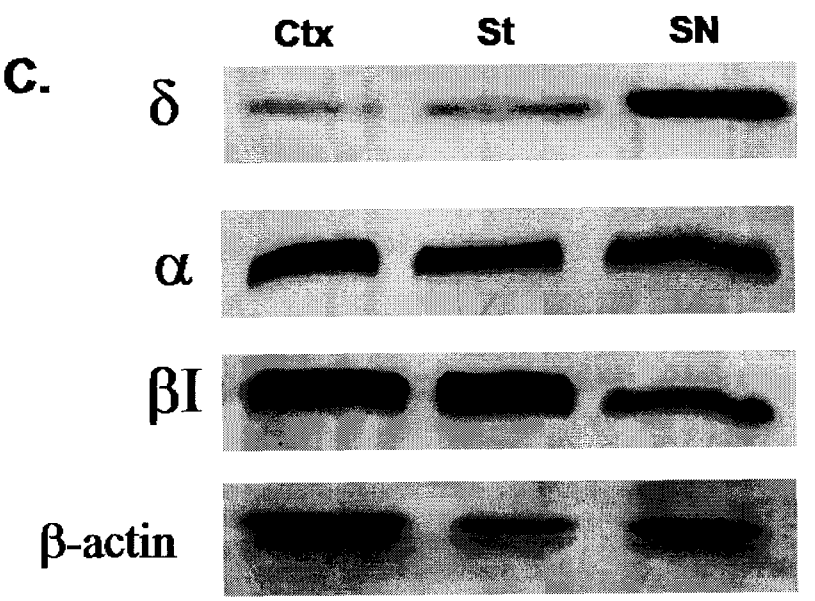
C.
Ctx
St
SN
δ
α
βI
β-actin

Figure 2: Relative quantity of the mRNA level of PKC isoforms in different regions of mice brains

(A) Amplification plot of PKCδ mRNA among SN (red), St (blue), and Ctx (green) regions of mice brains. (B) Relative PKCδ mRNA level among SN, St, and Ctx regions of mice brains. (C) Relative PKCβI, PKCε, PKCθ, and PKCζ mRNA levels among SN, St, and Ctx regions of mice brains. Total RNA extracted from the SN, St, and Ctx regions of mice brains was converted into cDNA. For the QRT-PCR of PKCδ, PKCε, and PKCθ, a TaqMan probe based method was used; for the QRT-PCR of PKCβI and PKCζ, a SYBR green based method was used. 18s Ribosome RNA (18s rRNA) was employed as an endogenous control to normalize the RNA used in QRT-PCR. The relative PKC isoform mRNA levels among the SN, St, and Ctx regions were calculated from the formula $2^{-(\Delta Ct\ PKC\delta - \Delta Ct\ 18s\ rRNA)}$ and the Ct value in the cortex was always used as the calibrator. The data represent the mean $\pm$ SEM from two separate experiments in triplicate (*, $p<0.05$; ***, $p<0.001$; N=6).

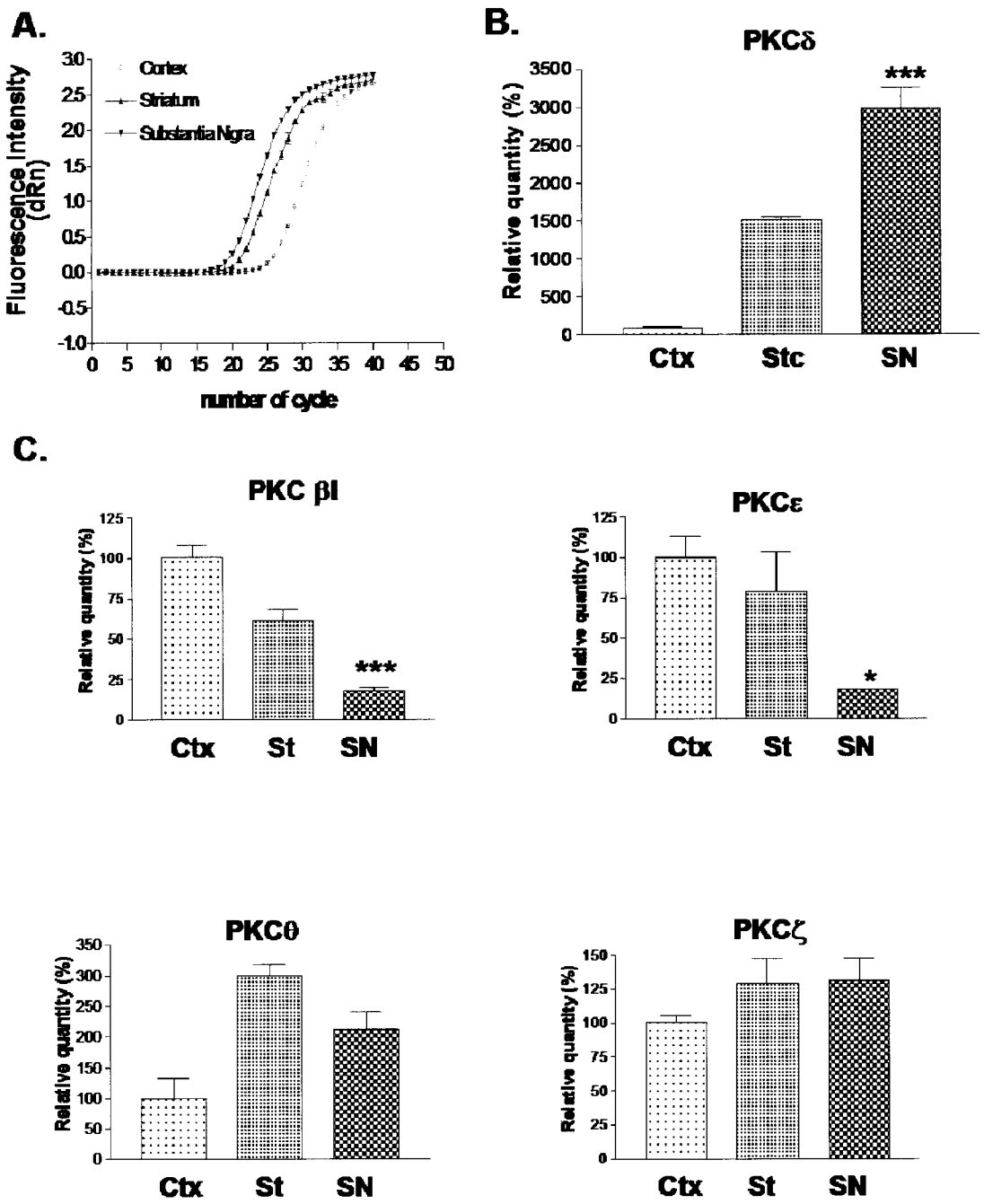
A.
Cortex
Striatum
Substantia Nigra
Fluorescence Intensity (dRn)
number of cycle
B.
PKCδ
Relative quantity (%)
***
Ctx
Stc
SN
C.
PKC βI
Relative quantity (%)
***
Ctx
St
SN
PKCε
Relative quantity (%)
*
Ctx
St
SN
PKCθ
Relative quantity (%)
Ctx
St
SN
PKCζ
Relative quantity (%)
Ctx
St
SN

Figure 3: MPTP administration induces proteolytic activation of PKCδ in the substantia nigra region of mice brains

(A) Proteolytic cleavage of PKCδ in the substantia nigra region of mice brains following MPTP administration for 5d. (B) Increased PKCδ kinase activity in the substantia nigra region of mice brains following MPTP administration for 5d. MPTP was administered at a dose of 30 mg/kg intraperitoneally to mice (n=6) every day for five doses. Control mice (n=6) were treated with an equal volume of ddH_2O. All animals were sacrificed the day after the last injection. The data represent the mean $\pm$ SEM from two separate experiments in triplicate (**, $p<0.01$; N=6).

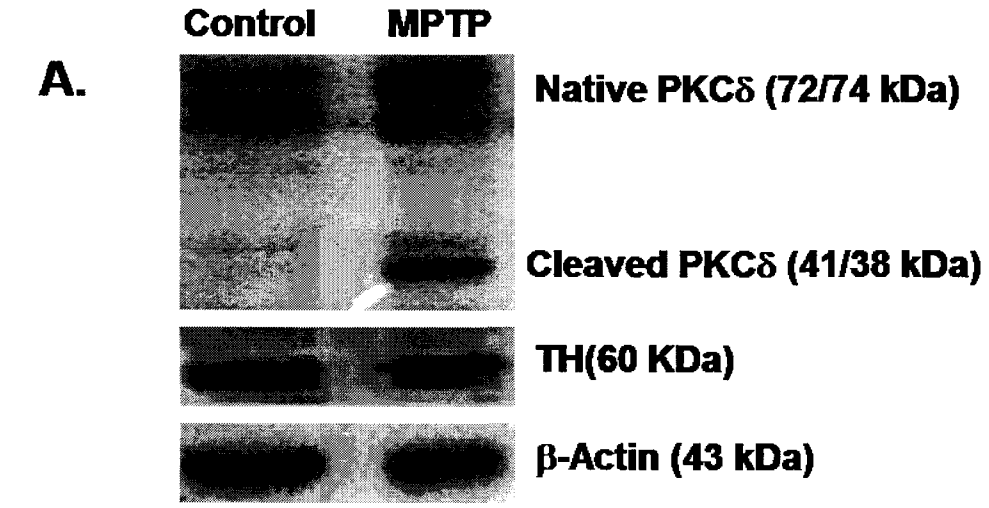
A.
Control
MPTP
Native PKCδ (72/74 kDa)
Cleaved PKCδ (41/38 kDa)
TH(60 KDa)
β-Actin (43 kDa)

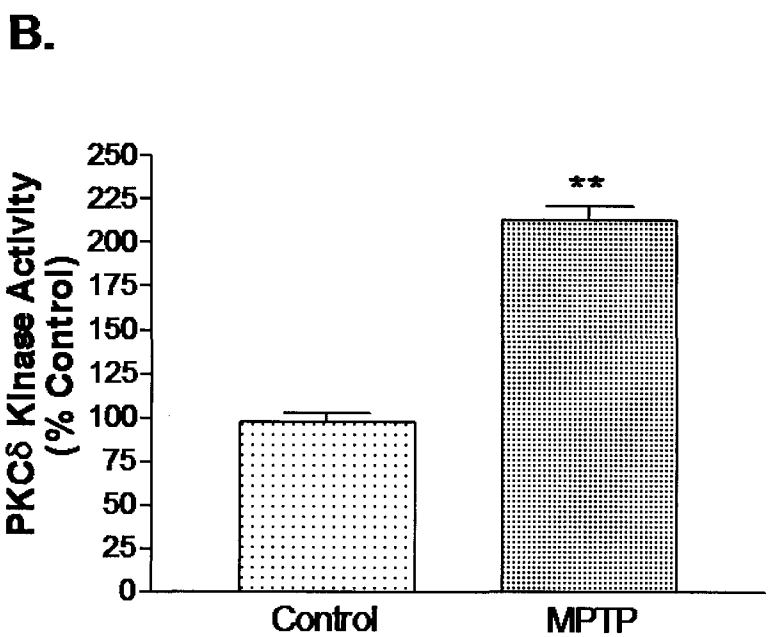
B.
PKCδ Kinase Activity
(% Control)
250
225
200
175
150
125
100
75
50
25
0
**
Control
MPTP

Figure 4: Cleavage resistant mutant of PKCδ (PKCδ-CRM) protects N27 cells from MPP^+-induced apoptotic death

(A) Relative quantity of PKCδ mRNA in N27 cells and in the SN, St, and Ctx regions of rat brains. The TaqMan based QRT-PCR method (rat PKCδ expression assay kit) was employed and 18s rRNA was used as an endogenous control. For comparison of the relative PKCδ mRNA levels, the Ct value of the Ctx sample was used as the calibrator. (B) MPP^+-induced PKCδ cleavage was abolished in PKCδ-CRM stably expressing cells. Control cells and PKCδ-CRM stably expressing cells were treated with 300 μM MPP^+ for 36 hr. The cells were lysed and whole cell lysate was used for immunoblot analysis to detect the PKCδ cleavage. The membrane was reprobed with anti-V5 antibody (1:5000) to ensure the expression of PKCδ-CRM in the PKCδ-CRM stably expressing N27 cell line. (C) PKCδ-CRM protects against MPP^+-induced apoptotic death in N27 cells. The data represent the mean $\pm$ SEM from two separate experiments in triplicate (*, $p<0.05$; ***, $p<0.001$; N=6).

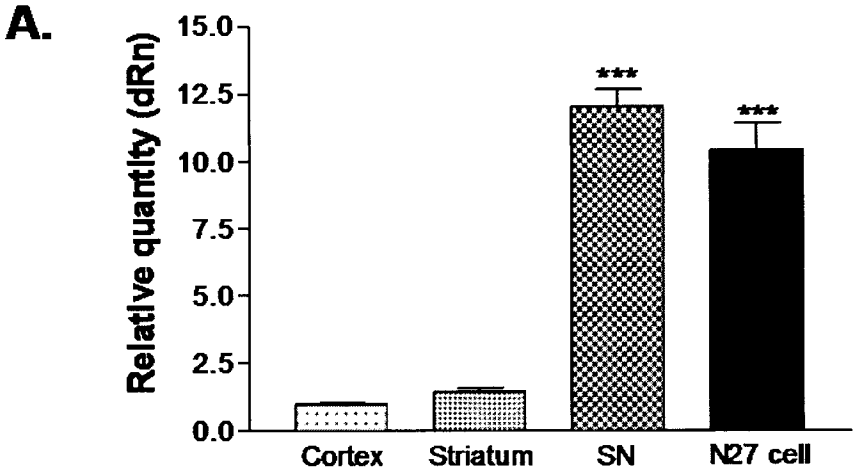
A.
Relative quantity (dRn)
15.0
12.5
10.0
7.5
5.0
2.5
0.0
***
***
Cortex
Striatum
SN
N27 cell

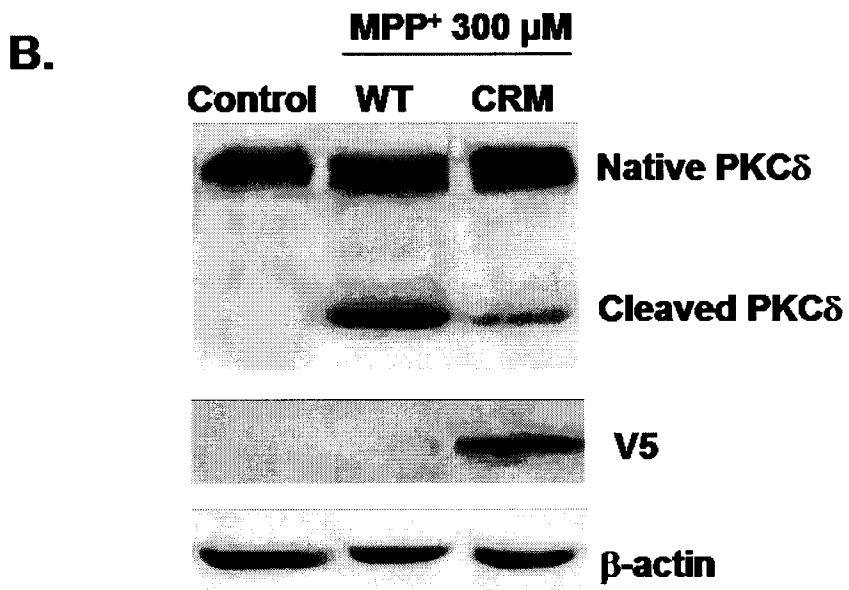
B.
MPP+ 300 μM
Control
WT
CRM
Native PKCδ
Cleaved PKCδ
V5
β-actin

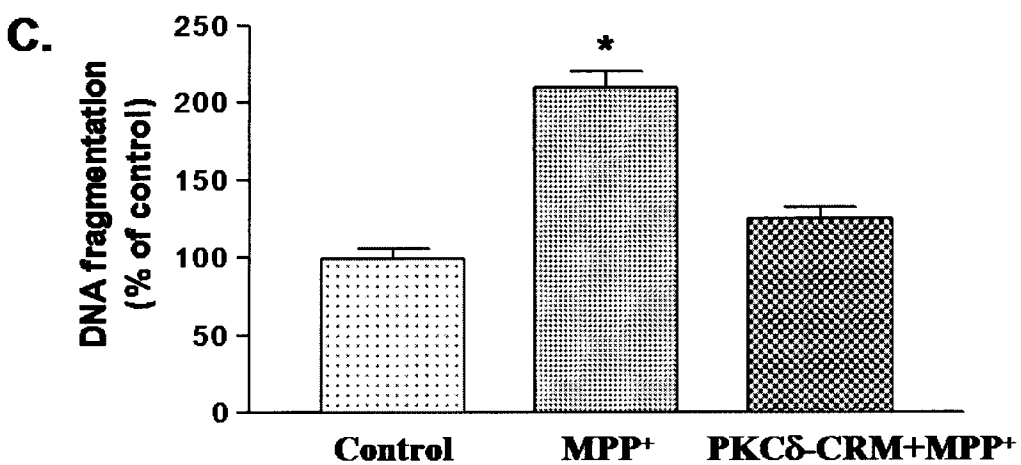
C.
DNA fragmentation
(% of control)
250
200
150
100
50
0
*
Control
MPP+
PKCδ-CRM+MPP+

Figure 5: Cleavage resistant mutant of PKCδ (PKCδ-CRM) protects primary dopaminergic neurons from MPP^+-induced apoptotic death

(A) Morphology of representative TH positive neurons from MPP^+-treated groups with or without pre-transfection of PKCδ-CRM, and control group. Cells were observed under a Nikon inverted fluorescence microscope (Model TE-2000U). (B) Expression of PKCδ-CRM in the TH positive neurons of rat primary mesencephalic neuronal cultures. At 24 hr post-transfection of PKCδ-CRM, primary neuronal cultures were treated with 10 μM MPP^+ for another 48 hr. Double immunostaining of TH (rabbit anti-TH antibody) and V5 (mouse anti-V5 antibody) was performed sequentially after treatment. Cells were observed under a TCS/NT confocal microscopy system (Leica, Bannockburn, IL). (C) Quantitative analysis of the number of TH positive neurons following PKCδ-CRM transfection and MPP^+ treatment. (D) Quantitative analysis of the neuronal processes of TH positive neurons following PKCδ-CRM transfection and MPP^+ treatment. After PKCδ-CRM transfection, cells were exposed to 10 μM MPP^+ for 48 hr and then TH positive neurons were identified using anti-TH antibody exposure. The number of TH positive neurons was counted in multiple fields (total 5000 cells) and their neuronal processes were measured in MetaMorph 5.07. Data represent the mean $\pm$ SEM from two separate experiments in triplicate (***, $p<0.001$; N=6).

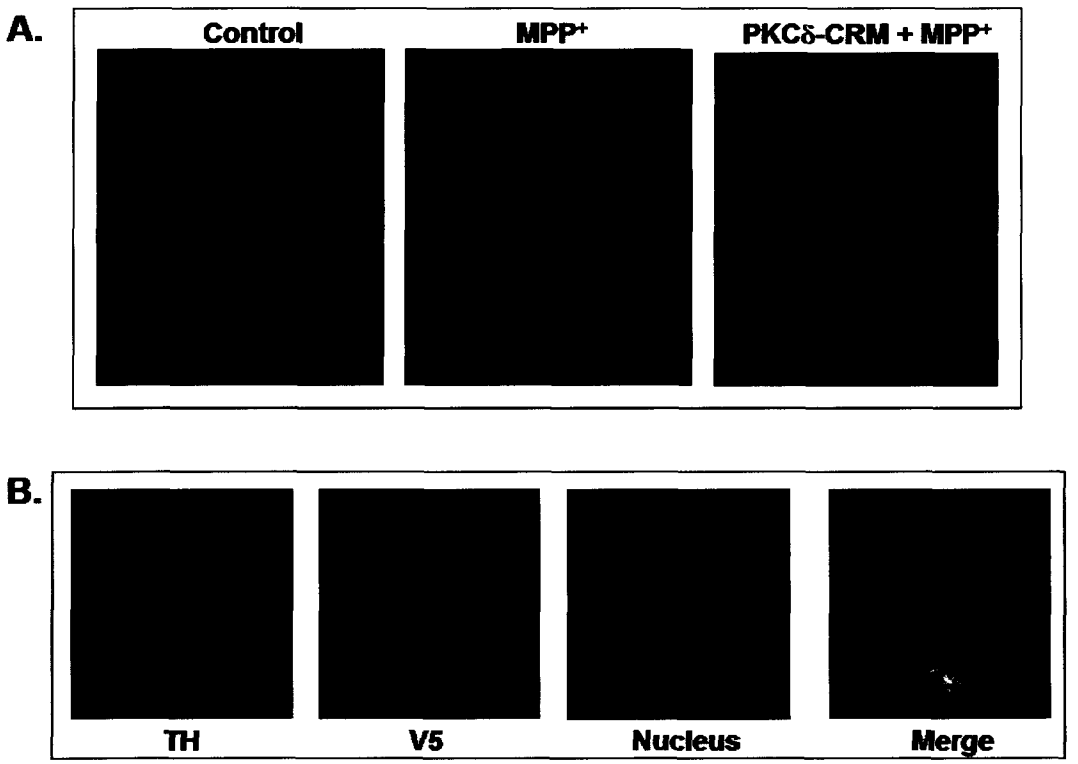
A.
Control
MPP+
PKCδ-CRM + MPP+
B.
TH
V5
Nucleus
Merge
C.
TH positive neurons (% of control)
120
100
80
60
40
20
0
***
Control
MPP+
PKCδ-CRM+MPP
D.
Length of neurites (% of control)
140
120
100
80
60
40
20
0
***
Control
MPP+
PKCδ-CRM+MPP

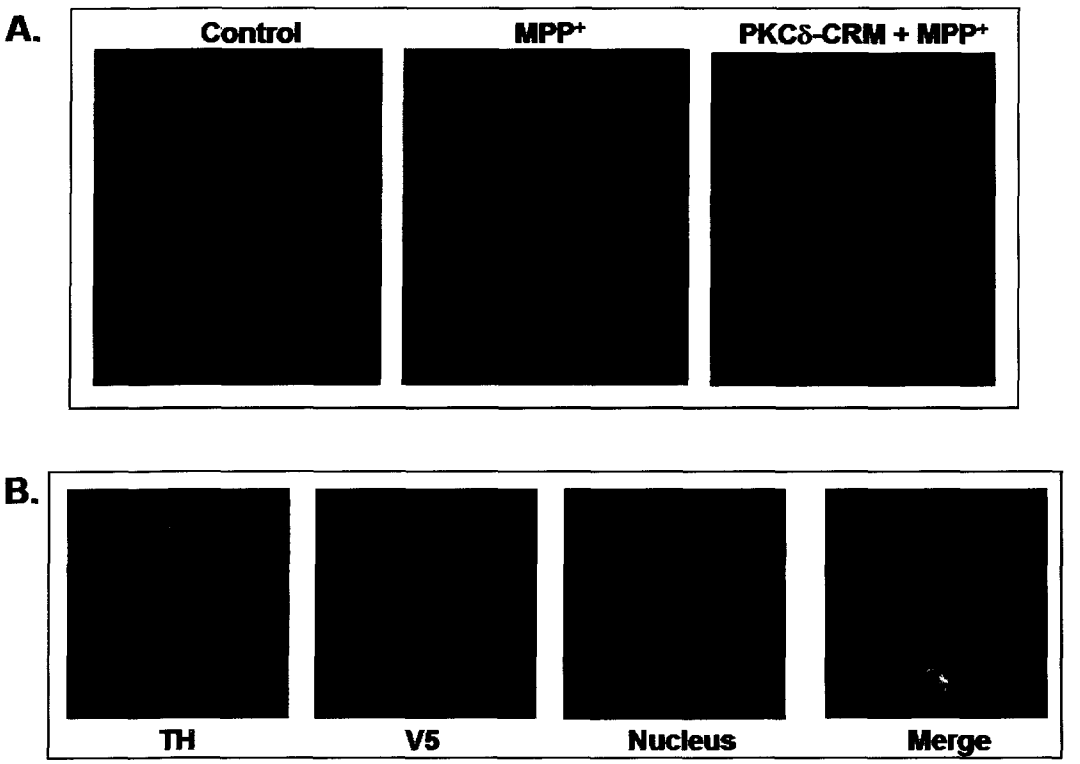
A.
Control
MPP+
PKCδ-CRM + MPP+
B.
TH
V5
Nucleus
Merge
C.
TH positive neurons (% of control)
120
100
80
60
40
20
0
***
Control
MPP+
PKCδ-CRM+MPP
D.
Length of neurites (% of control)
140
120
100
80
60
40
20
0
***
Control
MPP+
PKCδ-CRM+MPP

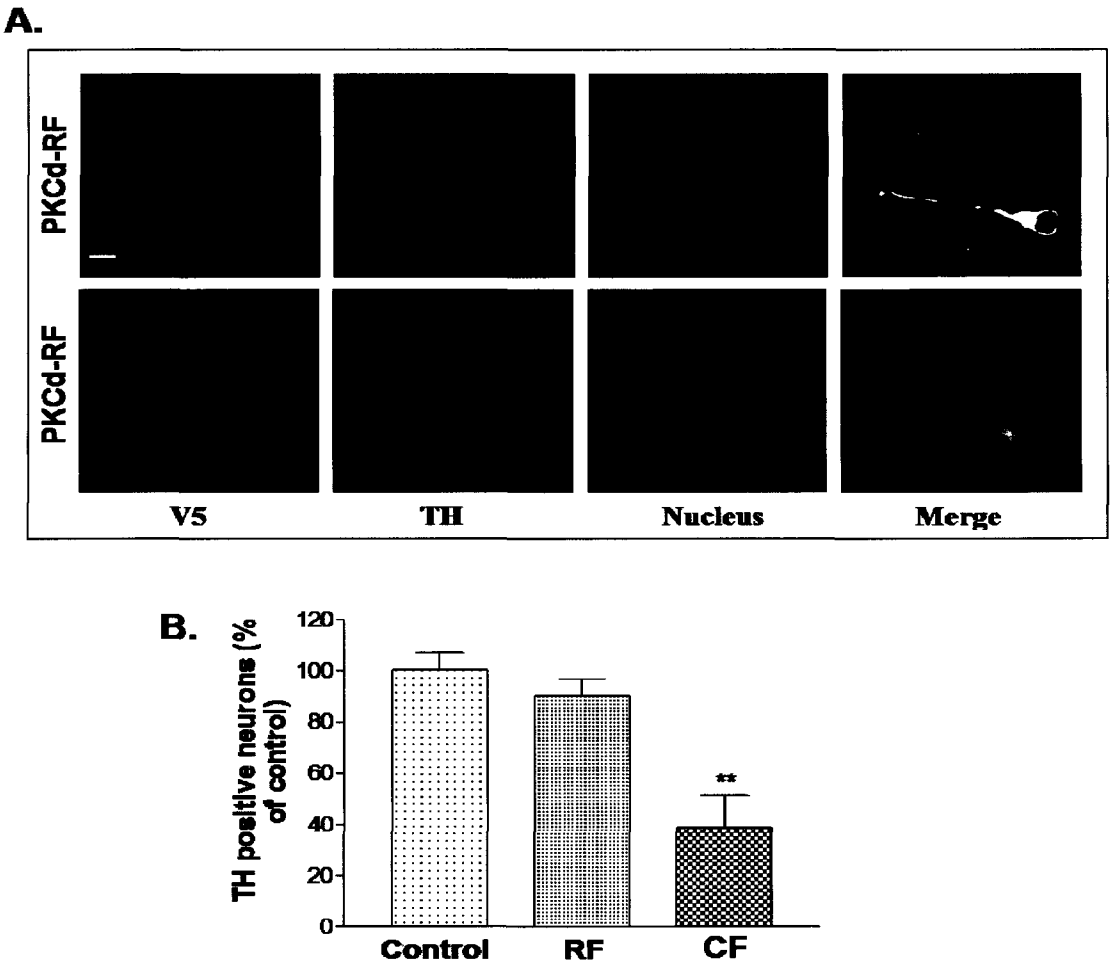

Figure 6: Catalytic fragment of PKCδ (PKCδ-CF) directly induces the degeneration of dopaminergic neurons in rat primary neuronal cultures

(A) Morphology of representative TH positive neurons in PKCδ-RF or PKCδ-CF transfected primary neuronal cultures. (B) Quantitative analysis of the number of TH positive neurons following PKCδ-CF or PKCδ-RF transfection. Double immunostaining of TH (rabbit anti-TH antibody) and V5 (mouse anti-V5 antibody) was performed 48 hr post-transfection of PKCδ-CF or PKCδ-RF. Cells were observed under a TCS/NT confocal microscopy system (Leica, Bannockburn, IL). Data represent the mean $\pm$ SEM from two separate experiments in triplicate (**, $p<0.01$; N=6).

REFERENCES

Adams, F.S., La Rosa, F.G., Kumar, S., Edwards-Prasad, J., Kentroti, S., Vernadakis, A., Freed, C.R., Prasad, K.N., 1996. Characterization and transplantation of two neuronal cell lines with dopaminergic properties. Neurochem Res. 21,619-27.

Anantharam, V., Kitazawa, M., Wagner, J., Kaul, S., Kanthasamy, A.G., 2002. Caspase-3-dependent proteolytic cleavage of protein kinase Cdelta is essential for oxidative stress-mediated dopaminergic cell death after exposure to methylcyclopentadienyl manganese tricarbonyl. J Neurosci. 22,1738-51.

Barmack, N.H., Qian, Z., Yoshimura, J., 2000. Regional and cellular distribution of protein kinase C in rat cerebellar Purkinje cells. J Comp Neurol. 427,235-54.

Basu, A., 2003. Involvement of protein kinase C-delta in DNA damage-induced apoptosis. J Cell Mol Med. 7,341-50.

Beal, M.F., 2002. Oxidatively modified proteins in aging and disease. Free Radic Biol Med. 32,797-803.

Brodie, C., Blumberg, P.M., 2003. Regulation of cell apoptosis by protein kinase c delta. Apoptosis. 8,19-27.

Callier, S., Le Saux, M., Lhiaubet, A.M., Di Paolo, T., Rostene, W., Pelaprat, D., 2002. Evaluation of the protective effect of oestradiol against toxicity induced by 6-hydroxydopamine and 1-methyl-4-phenylpyridinium ion (Mpp+) towards dopaminergic mesencephalic neurones in primary culture. J Neurochem. 80,307-16.

Carlsson, A., Fornstedt, B., 1991. Possible mechanisms underlying the special vulnerability of dopaminergic neurons. Acta Neurol Scand Suppl. 136,16-8.

Choi, W.S., Canzoniero, L.M., Sensi, S.L., O'Malley, K.L., Gwag, B.J., Sohn, S., Kim, J.E., Oh, T.H., Lee, E.B., Oh, Y.J., 1999. Characterization of MPP(+)-induced cell death in a dopaminergic neuronal cell line: role of macromolecule synthesis, cytosolic calcium, caspase, and Bcl-2-related proteins. Exp Neurol. 159,274-82.

Conway, K.A., Rochet, J.C., Bieganski, R.M., Lansbury, P.T., Jr., 2001. Kinetic stabilization of the alpha-synuclein protofibril by a dopamine-alpha-synuclein adduct. Science. 294,1346-9.

Damier, P., Hirsch, E.C., Agid, Y., Graybiel, A.M., 1999a. The substantia nigra of the human brain. I. Nigrosomes and the nigral matrix, a compartmental organization based on calbindin D(28K) immunohistochemistry. Brain. 122 (Pt 8),1421-36.

Damier, P., Hirsch, E.C., Agid, Y., Graybiel, A.M., 1999b. The substantia nigra of the human brain. II. Patterns of loss of dopamine-containing neurons in Parkinson's disease. Brain. 122 (Pt 8),1437-48.

Damier, P., Hirsch, E.C., Zhang, P., Agid, Y., Javoy-Agid, F., 1993. Glutathione peroxidase, glial cells and Parkinson's disease. Neuroscience. 52,1-6.

Dauer, W., Przedborski, S., 2003. Parkinson's disease: mechanisms and models. Neuron. 39,889-909.

DeVries, T.A., Neville, M.C., Reyland, M.E., 2002. Nuclear import of PKCdelta is required for apoptosis: identification of a novel nuclear import sequence. Embo J. 21,6050-60.

Dexter, D.T., Carter, C.J., Wells, F.R., Javoy-Agid, F., Agid, Y., Lees, A., Jenner, P., Marsden, C.D., 1989. Basal lipid peroxidation in substantia nigra is increased in Parkinson's disease. J Neurochem. 52,381-9.

Dunkley, P.R., Bobrovskaya, L., Graham, M.E., von Nagy-Felsobuki, E.I., Dickson, P.W., 2004. Tyrosine hydroxylase phosphorylation: regulation and consequences. J Neurochem. 91,1025-43.

Emoto, Y., Manome, Y., Meinhardt, G., Kisaki, H., Kharbanda, S., Robertson, M., Ghayur, T., Wong, W.W., Kamen, R., Weichselbaum, R., et al., 1995. Proteolytic activation of protein kinase C delta by an ICE-like protease in apoptotic cells. Embo J. 14,6148-56.

Floor, E., Wetzel, M.G., 1998. Increased protein oxidation in human substantia nigra pars compacta in comparison with basal ganglia and prefrontal cortex measured with an improved dinitrophenylhydrazine assay. J Neurochem. 70,268-75.

Ghayur, T., Hugunin, M., Talanian, R.V., Ratnofsky, S., Quinlan, C., Emoto, Y., Pandey, P., Datta, R., Huang, Y., Kharbanda, S., Allen, H., Kamen, R., Wong, W., Kufe, D., 1996. Proteolytic activation of protein kinase C delta by an ICE/CED 3-like protease induces characteristics of apoptosis. J Exp Med. 184,2399-404.

Giros, B., Jaber, M., Jones, S.R., Wightman, R.M., Caron, M.G., 1996. Hyperlocomotion and indifference to cocaine and amphetamine in mice lacking the dopamine transporter. Nature. 379,606-12.

Gonzalez-Hernandez, T., Barroso-Chinea, P., De La Cruz Muros, I., Del Mar Perez-Delgado, M., Rodriguez, M., 2004. Expression of dopamine and vesicular monoamine transporters and differential vulnerability of mesostriatal dopaminergic neurons. J Comp Neurol. 479,198-215.

Good, P.F., Olanow, C.W., Perl, D.P., 1992. Neuromelanin-containing neurons of the substantia nigra accumulate iron and aluminum in Parkinson's disease: a LAMMA study. Brain Res. 593,343-6.

Graham, D.G., 1978. Oxidative pathways for catecholamines in the genesis of neuromelanin and cytotoxic quinones. Mol Pharmacol. 14,633-43.

Gutcher, I., Webb, P.R., Anderson, N.G., 2003. The isoform-specific regulation of apoptosis by protein kinase C. Cell Mol Life Sci. 60,1061-70.

Halliwell, B., 1992. Reactive oxygen species and the central nervous system. J Neurochem. 59,1609-23.

Hartmann, A., Hunot, S., Michel, P.P., Muriel, M.P., Vyas, S., Faucheux, B.A., Mouatt-Prigent, A., Turmel, H., Srinivasan, A., Ruberg, M., Evan, G.I., Agid, Y., Hirsch, E.C., 2000. Caspase-3: A vulnerability factor and final effector in apoptotic death of dopaminergic neurons in Parkinson's disease. Proc Natl Acad Sci U S A. 97,2875-80.

Hartmann, A., Troadec, J.D., Hunot, S., Kikly, K., Faucheux, B.A., Mouatt-Prigent, A., Ruberg, M., Agid, Y., Hirsch, E.C., 2001. Caspase-8 is an effector in apoptotic death of dopaminergic neurons in Parkinson's disease, but pathway inhibition results in neuronal necrosis. J Neurosci. 21,2247-55.

Hirsch, E.C., Faucheux, B., Damier, P., Mouatt-Prigent, A., Agid, Y., 1997. Neuronal vulnerability in Parkinson's disease. J Neural Transm Suppl. 50,79-88.

Hitri, A., Hurd, Y.L., Wyatt, R.J., Deutsch, S.I., 1994. Molecular, functional and biochemical characteristics of the dopamine transporter: regional differences and clinical relevance. Clin Neuropharmacol. 17,1-22.

Jellinger, K.A., 2000. Cell death mechanisms in Parkinson's disease. J Neural Transm. 107,1-29.

Jenner, P., 1998. Oxidative mechanisms in nigral cell death in Parkinson's disease. Mov Disord. 13 Suppl 1,24-34.

Jenner, P., 2003. Oxidative stress in Parkinson's disease. Ann Neurol. 53 Suppl 3,S26-36; discussion S36-8.

Kanthasamy, A.G., Kitazawa, M., Kanthasamy, A., Anantharam, V., 2003. Role of proteolytic activation of protein kinase Cdelta in oxidative stress-induced apoptosis. Antioxid Redox Signal. 5,609-20.

Kaul, S., Kanthasamy, A., Kitazawa, M., Anantharam, V., Kanthasamy, A.G., 2003. Caspase-3 dependent proteolytic activation of protein kinase C delta mediates and regulates 1-methyl-4-phenylpyridinium (MPP+)-induced apoptotic cell death in dopaminergic cells: relevance to oxidative stress in dopaminergic degeneration. Eur J Neurosci. 18,1387-401.

Kitazawa, M., Anantharam, V., Kanthasamy, A.G., 2003. Dieldrin induces apoptosis by promoting caspase-3-dependent proteolytic cleavage of protein kinase Cdelta in dopaminergic cells: relevance to oxidative stress and dopaminergic degeneration. Neuroscience. 119,945-964.

Korotkova, T.M., Ponomarenko, A.A., Brown, R.E., Haas, H.L., 2004. Functional diversity of ventral midbrain dopamine and GABAergic neurons. Mol Neurobiol. 29,243-59.

Lee, H.S., Park, C.W., Kim, Y.S., 2000. MPP(+) increases the vulnerability to oxidative stress rather than directly mediating oxidative damage in human neuroblastoma cells. Exp Neurol. 165,164-71.

Lotharius, J., Brundin, P., 2002. Pathogenesis of Parkinson's disease: dopamine, vesicles and alpha-synuclein. Nat Rev Neurosci. 3,932-42.

Maker, H.S., Weiss, C., Silides, D.J., Cohen, G., 1981. Coupling of dopamine oxidation (monoamine oxidase activity) to glutathione oxidation via the generation of hydrogen peroxide in rat brain homogenates. J Neurochem. 36,589-93.

Miyamoto, A., Nakayama, K., Imaki, H., Hirose, S., Jiang, Y., Abe, M., Tsukiyama, T., Nagahama, H., Ohno, S., Hatakeyama, S., Nakayama, K.I., 2002. Increased proliferation of B cells and auto-immunity in mice lacking protein kinase Cdelta. Nature. 416,865-9.

Naik, M.U., Benedikz, E., Hernandez, I., Libien, J., Hrabe, J., Valsamis, M., Dow-Edwards, D., Osman, M., Sacktor, T.C., 2000. Distribution of protein kinase Mzeta and the complete protein kinase C isoform family in rat brain. J Comp Neurol. 426,243-58.

Nirenberg, M.J., Chan, J., Liu, Y., Edwards, R.H., Pickel, V.M., 1996. Ultrastructural localization of the vesicular monoamine transporter-2 in midbrain dopaminergic neurons: potential sites for somatodendritic storage and release of dopamine. J Neurosci. 16,4135-45.

Peter, D., Liu, Y., Sternini, C., de Giorgio, R., Brecha, N., Edwards, R.H., 1995. Differential expression of two vesicular monoamine transporters. J Neurosci. 15,6179-88.

Prasad, K.N., Clarkson, E.D., La Rosa, F.G., Edwards-Prasad, J., Freed, C.R., 1998. Efficacy of grafted immortalized dopamine neurons in an animal model of parkinsonism: a review. Mol Genet Metab. 65,1-9.

Ren, J., Datta, R., Shioya, H., Li, Y., Oki, E., Biedermann, V., Bharti, A., Kufe, D., 2002. p73beta is regulated by protein kinase Cdelta catalytic fragment generated in the apoptotic response to DNA damage. J Biol Chem. 277,33758-65.

Riddle, R., Pollock, J.D., 2003. Making connections: the development of mesencephalic dopaminergic neurons. Brain Res Dev Brain Res. 147,3-21.

Sofic, E., Paulus, W., Jellinger, K., Riederer, P., Youdim, M.B., 1991. Selective increase of iron in substantia nigra zona compacta of parkinsonian brains. J Neurochem. 56,978-82.

Storch, A., Ludolph, A.C., Schwarz, J., 2004. Dopamine transporter: involvement in selective dopaminergic neurotoxicity and degeneration. J Neural Transm. 111,1267-86.

Uhl, G.R., 1998. Hypothesis: the role of dopaminergic transporters in selective vulnerability of cells in Parkinson's disease. Ann Neurol. 43,555-60.

Uhl, G.R., Hall, F.S., Sora, I., 2002. Cocaine, reward, movement and monoamine transporters. Mol Psychiatry. 7,21-6.

Yang, Y., Kaul, S., Zhang, D., Anantharam, V., Kanthasamy, A.G., 2004. Suppression of caspase-3-dependent proteolytic activation of protein kinase C delta by small interfering RNA prevents MPP+-induced dopaminergic degeneration. Mol Cell Neurosci. 25,406-21.

Zecca, L., Tampellini, D., Gerlach, M., Riederer, P., Fariello, R.G., Sulzer, D., 2001. Substantia nigra neuromelanin: structure, synthesis, and molecular behaviour. Mol Pathol. 54,414-8.

CHAPTER VI: GENERAL CONCLUSIONS

The major findings of my research described in the dissertation have already been discussed in the discussion sections of each chapter. The overall conclusions derived from these studies and integral mechanisms of PKCδ in neurotoxin-induced apoptotic death of dopaminergic neurons and relevance to the pathogenesis of Parkinson's disease (PD) will be discussed here.

Selectively high expression of oxidative stress sensitive kinase PKCδ contributes to the vulnerability of nigral dopaminergic neurons to neurotoxin-induced degeneration

Nigral dopaminergic neurons are most severely degenerated in Parkinson's disease partially due to the presence of dopamine in these neurons (Carlsson and Fornstedt, 1991; Hirsch et al., 1997). Dopaminergic neurons are persistently exposed to oxidative stress because metabolism of free cytosolic dopamine dramatically increases the generation of ROS. DAT and VMAT2 regulate the level of free cytosolic dopamine, and therefore, have been implicated in the selective vulnerability of dopaminergic neurons (Gonzalez-Hernandez et al., 2004; Uhl, 1998). In addition, other molecules related to oxidative stress, including neuromelanin (NM) and redox active $Fe2^{+}$, are also selectively rich or elevated in nigral dopaminergic neurons (Good et al., 1992; Lotharius and Brundin, 2002; Zecca et al., 2003). In this study, we demonstrated that oxidative stress sensitive kinase PKCδ is selectively abundant in nigral dopaminergic neurons and co-localizes with TH, the rate-limiting enzyme in dopamine synthesis. Ongoing studies in our laboratory have demonstrated that abundant PKCδ normally inhibits TH activity to regulate dopamine synthesis. However, abundant

PKCδ becomes sensitive to neurotoxin-induced oxidative stress and is cleaved by caspase-3 in dopaminergic neuronal cells and in mice. In dopaminergic neuronal cells, we demonstrated that caspase-3 mediated cleavage of PKCδ releases the catalytic fragment of PKCδ (PKCδ-CF), which further translocates to the nucleus. The PKCδ-CF serves as effector and promotes apoptotic death of dopaminergic neuronal cells by mediating the ser14 phosphorylation of histone H2B.

Proteolytic cleavage of PKCδ apparently serves as a switch that converts the physiologically important PKCδ in the regulation of TH activity and dopamine synthesis to a pro-apoptotic kinase promoting degeneration of dopaminergic neurons. Because proteolytic cleavage of PKCδ is mediated by activated caspase-3, various apoptotic stresses, including oxidative stress, which triggers the mitochondrial-dependent intrinsic pathway and subsequent activation of caspse-3, can activate this switch. A certain extent of oxidative stress and other apoptotic stresses are always present in the central nervous system (Halliwell, 1992; Jenner, 2003). The selective abundance of PKCδ could significantly increase the vulnerability of dopaminergic neurons to the same level of insults due to the potentially easier and increased generation of pro-apoptotic cleaved activated fragments of PKCδ.

Regulation of the nuclear localization of PKCδ by regulatory fragments through position obstacle effects in tertiary structure

The function of some serine/threonine protein kinases in cells is closely related to their nuclear/cytoplasmic localization. For example, p21-activated kinase 2 (PAK2) is mainly localized in the cytoplasm and promotes cell survival; however, cleaved PAK2p34 is

localized in the nucleus and promotes cell death (Jakobi, 2004). The nuclear/cytoplasmic localization is mainly regulated by a nucleus localization signal (NLS)/nucleus export signal (NES) mediated nuclear import/export (Kaffman and O'Shea, 1999). NLS but not NES has been identified in the C-terminal of the catalytic fragment of PKCδ (DeVries et al., 2004); however, PKCδ is primarily localized in the cytoplasm in various cell types, including dopaminergic neuronal cells. The regulation of the nuclear localization of PKCδ is unknown. In dopaminergic neuronal cells, we demonstrated that the N- and C-terminals of PKCδ are in close proximity in the tertiary structure by FRET. By employing the C1 or C2-like domain deletion mutant of PKCδ (PKCδ-ΔC1 or PKCδ-ΔC2), we showed that deletion of the C2-like domain, but not the C1 domain, induces strong nuclear localization of PKCδ. Meanwhile, nuclear translocation of activated cleaved fragments of PKCδ generated from caspase-3-mediated proteolytic cleavage in response to neurotoxin exposure has been observed, and the exogenously expressed catalytic fragment of PKCδ (PKCδ-CF) also primarily localizes to the nucleus. Although sequence analysis of the C2-like domain reveals a possible leucine-rich nuclear export signal (NES), the C2-like domain is not sensitive to the nuclear export inhibitor leptomycin B (Fornerod et al., 1997), suggesting that this leucine-rich motif is not a functional NES. Moreover, the human immunodeficiency virus (HIV) Rev chimera protein was generated by fusing the C2-like domain in the N-terminal of a NES deleted form of Rev, the RNA binding protein of HIV, which is still primarily localized in the cytoplasm. Our studies suggest that the N-terminal C2-like domain regulates the subcellular localization of PKCδ by masking the C-terminal NLS through the position obstacle in the tertiary structure, but not by employing NES or interacting with anchoring proteins. Our model is consistent

with the previously proposed tertiary conformation of PKCδ; the pseudosubstrate in the middle of the N-terminal regulatory fragment binds to the catalytic site of the C-terminal catalytic fragment.

The presence of NLS is not sufficient but necessary, as shown in our study, to localize PKCδ into the nucleus. NLS could be normally kept in an incompetent status and converted to competent status in response to certain stimuli. The subcellular localization of kinases is critical for their close proximity to their activator or substrates; thus, the maintenance and regulation of competent status of NLS is important for their functions. In addition, the intra-molecular regulation provides more flexibility for kinases to self-regulate subcellular localization and functions.

In summary, we surveyed the expression of different isoforms of PKC in rodent brains and determined that PKCδ has the highest expression in the SNc dopaminergic neurons in rodent brains. We also characterized the molecular mechanisms of PKCδ in neurotoxin-induced apoptotic death of dopaminergic neuronal cells. Under normal physiological conditions, the highly expressed PKCδ interacts with tyrosine hydroxylase (TH) in dopaminergic neurons. The close proximity of the C2-like domain to the nuclear localization signal (NLS) provides the position obstacle to inhibit the recognition of the nuclear import receptor to the NLS and retains PKCδ in the cytoplasm. However, under stressful conditions, abundant PKCδ was proteolytically cleaved by caspase-3 activated by neurotoxin-induced oxidative stress to release the activated cleaved fragments of PKCδ. The proteolytic cleavage of PCKδ by caspase-3 serves as a switch to convert it from non-apoptotic to pro-apoptotic kinase and makes highly expressed PKCδ a potential inherent

factor for the vulnerability of dopaminergic neurons. The removal of the regulatory fragment from the catalytic fragment by cleavage also exposes the NLS and induces the nuclear translocation of the activated cleaved fragments of PKCδ. In the nucleus, we further demonstrated that activated PKCδ mediated the Ser14 phosphorylation of histone H2B, and the catalytic fragment of PKCδ (PKCδ-CF) itself induced the apoptosis of dopaminergic neuronal cells.

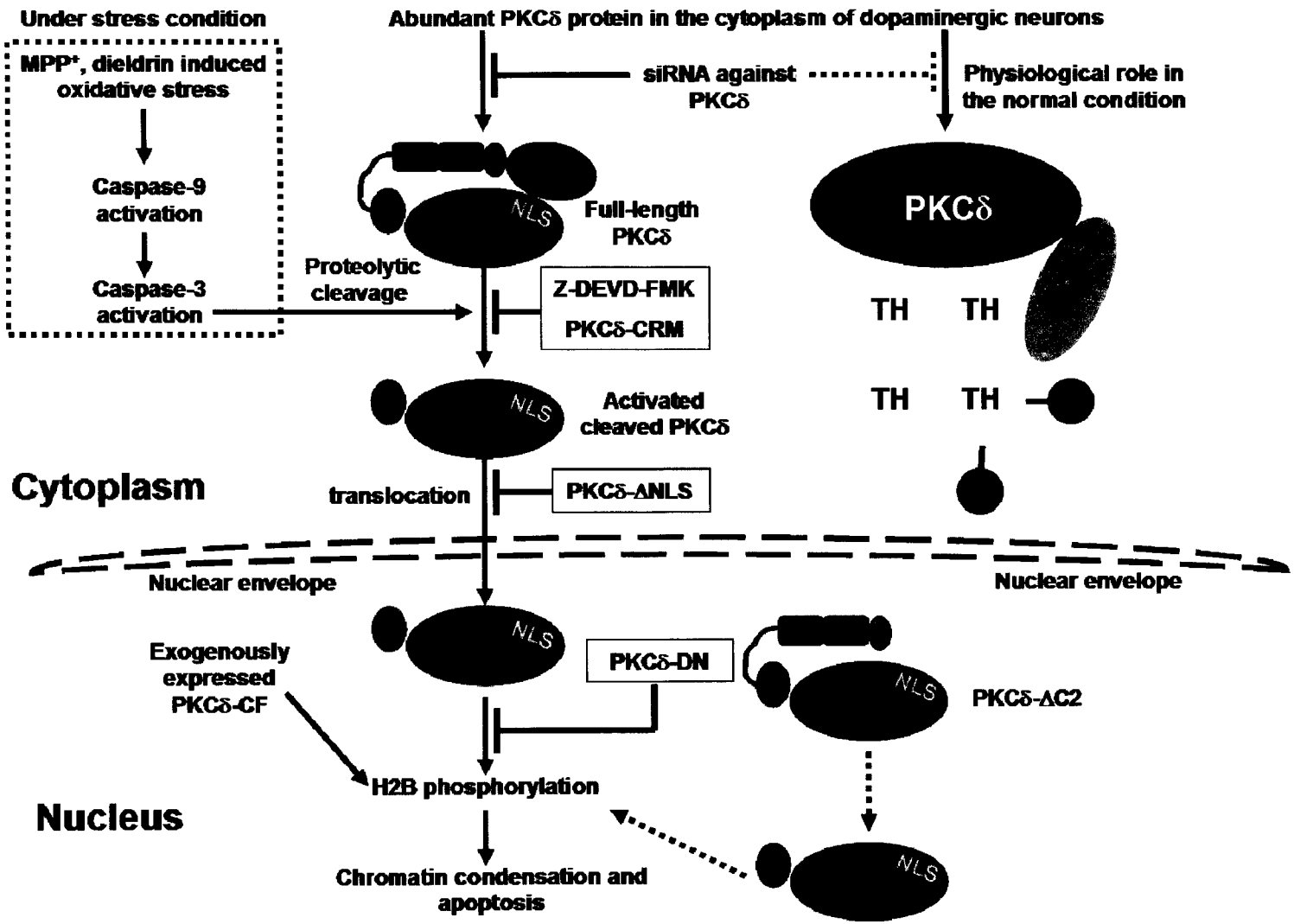

Figure 13. Integral mechanisms of PKCδ in neurotoxin-induced apoptotic death of dopaminergic neurons

LITERATURE CITED

Abeliovich, A., Schmitz, Y., Farinas, I., Choi-Lundberg, D., Ho, W.H., Castillo, P.E., Shinsky, N., Verdugo, J.M., Armanini, M., Ryan, A., Hynes, M., Phillips, H., Sulzer, D., Rosenthal, A., 2000. Mice lacking alpha-synuclein display functional deficits in the nigrostriatal dopamine system. Neuron. 25,239-52.

Ajenjo, N., Canon, E., Sanchez-Perez, I., Matallanas, D., Leon, J., Perona, R., Crespo, P., 2004. Subcellular localization determines the protective effects of activated ERK2 against distinct apoptogenic stimuli in myeloid leukemia cells. J Biol Chem. 279,32813-23.

Ajiro, K., 2000. Histone H2B phosphorylation in mammalian apoptotic cells. An association with DNA fragmentation. J Biol Chem. 275,439-43.

Albert, K.A., Helmer-Matyjek, E., Nairn, A.C., Muller, T.H., Haycock, J.W., Greene, L.A., Goldstein, M., Greengard, P., 1984. Calcium/phospholipid-dependent protein kinase (protein kinase C) phosphorylates and activates tyrosine hydroxylase. Proc Natl Acad Sci U S A. 81,7713-7.

Albin, R.L., Young, A.B., Penney, J.B., 1989. The functional anatomy of basal ganglia disorders. Trends Neurosci. 12,366-75.

Alexander, G.E.C., M. D. Delong, M. R., 1990. Basal ganalia-thalamocortical circuits: parallel substrates for motor, oculomotor, 'prefrontal' and 'limbic' functions. Prog Brain Res. 85,119-146.

Alexi, T., Hefti, F., 1996. Neurotrophin-4/5 selectively protects nigral calbindin-containing neurons in rats with medial forebrain bundle transections. Neuroscience. 72,911-21.

Anantharam, V., Kitazawa, M., Wagner, J., Kaul, S., Kanthasamy, A.G., 2002. Caspase-3-dependent proteolytic cleavage of protein kinase Cdelta is essential for oxidative stress-mediated dopaminergic cell death after exposure to methylcyclopentadienyl manganese tricarbonyl. J Neurosci. 22,1738-51.

Andressen, C., Blumcke, I., Celio, M.R., 1993. Calcium-binding proteins: selective markers of nerve cells. Cell Tissue Res. 271,181-208.

Aravind, L., Dixit, V.M., Koonin, E.V., 2001. Apoptotic molecular machinery: vastly increased complexity in vertebrates revealed by genome comparisons. Science. 291,1279-84.

Baptista, M.J., O'Farrell, C., Daya, S., Ahmad, R., Miller, D.W., Hardy, J., Farrer, M.J., Cookson, M.R., 2003. Co-ordinate transcriptional regulation of dopamine synthesis genes by alpha-synuclein in human neuroblastoma cell lines. J Neurochem. 85,957-68.

Barmack, N.H., Qian, Z., Yoshimura, J., 2000. Regional and cellular distribution of protein kinase C in rat cerebellar Purkinje cells. J Comp Neurol. 427,235-54.

Bartel, D.P., 2004. MicroRNAs: genomics, biogenesis, mechanism, and function. Cell. 116,281-97.

Baulcombe, D., 2002a. RNA silencing. Curr Biol. 12,R82-4.

Baulcombe, D., 2002b. Viral suppression of systemic silencing. Trends Microbiol. 10,306-8.

Beal, M.F., 2002. Oxidatively modified proteins in aging and disease. Free Radic Biol Med. 32,797-803.

Beresford, P.J., Zhang, D., Oh, D.Y., Fan, Z., Greer, E.L., Russo, M.L., Jaju, M., Lieberman, J., 2001. Granzyme A activates an endoplasmic reticulum-associated caspase-

independent nuclease to induce single-stranded DNA nicks. J Biol Chem. 276,43285-93.

Bernstein, E., Caudy, A.A., Hammond, S.M., Hannon, G.J., 2001. Role for a bidentate ribonuclease in the initiation step of RNA interference. Nature. 409,363-6.

Betarbet, R., Sherer, T.B., MacKenzie, G., Garcia-Osuna, M., Panov, A.V., Greenamyre, J.T., 2000. Chronic systemic pesticide exposure reproduces features of Parkinson's disease. Nat Neurosci. 3,1301-6.

Blass, M., Kronfeld, I., Kazimirsky, G., Blumberg, P.M., Brodie, C., 2002. Tyrosine phosphorylation of protein kinase Cdelta is essential for its apoptotic effect in response to etoposide. Mol Cell Biol. 22,182-95.

Blomer, U., Naldini, L., Kafri, T., Trono, D., Verma, I.M., Gage, F.H., 1997. Highly efficient and sustained gene transfer in adult neurons with a lentivirus vector. J Virol. 71,6641-9.

Bonni, A., Brunet, A., West, A.E., Datta, S.R., Takasu, M.A., Greenberg, M.E., 1999. Cell survival promoted by the Ras-MAPK signaling pathway by transcription-dependent and -independent mechanisms. Science. 286,1358-62.

Brenner, S., Malech, H.L., 2003. Current developments in the design of onco-retrovirus and lentivirus vector systems for hematopoietic cell gene therapy. Biochim Biophys Acta. 1640,1-24.

Brodie, C., Blumberg, P.M., 2003. Regulation of cell apoptosis by protein kinase c delta. Apoptosis. 8,19-27.

Brunet, A., Bonni, A., Zigmond, M.J., Lin, M.Z., Juo, P., Hu, L.S., Anderson, M.J., Arden, K.C., Blenis, J., Greenberg, M.E., 1999. Akt promotes cell survival by phosphorylating and inhibiting a Forkhead transcription factor. Cell. 96,857-68.

Bucciantini, M., Giannoni, E., Chiti, F., Baroni, F., Formigli, L., Zurdo, J., Taddei, N., Ramponi, G., Dobson, C.M., Stefani, M., 2002. Inherent toxicity of aggregates implies a common mechanism for protein misfolding diseases. Nature. 416,507-11.

Buendia, B., Santa-Maria, A., Courvalin, J.C., 1999. Caspase-dependent proteolysis of integral and peripheral proteins of nuclear membranes and nuclear pore complex proteins during apoptosis. J Cell Sci. 112 (Pt 11),1743-53.

Cabin, D.E., Shimazu, K., Murphy, D., Cole, N.B., Gottschalk, W., McIlwain, K.L., Orrison, B., Chen, A., Ellis, C.E., Paylor, R., Lu, B., Nussbaum, R.L., 2002. Synaptic vesicle depletion correlates with attenuated synaptic responses to prolonged repetitive stimulation in mice lacking alpha-synuclein. J Neurosci. 22,8797-807.

Cardone, M.H., Roy, N., Stennicke, H.R., Salvesen, G.S., Franke, T.F., Stanbridge, E., Frisch, S., Reed, J.C., 1998. Regulation of cell death protease caspase-9 by phosphorylation. Science. 282,1318-21.

Cardone, M.H., Salvesen, G.S., Widmann, C., Johnson, G., Frisch, S.M., 1997. The regulation of anoikis: MEKK-1 activation requires cleavage by caspases. Cell. 90,315-23.

Carlsson, A., Fornstedt, B., 1991. Possible mechanisms underlying the special vulnerability of dopaminergic neurons. Acta Neurol Scand Suppl. 136,16-8.

Cassarino, D.S., Fall, C.P., Swerdlow, R.H., Smith, T.S., Halvorsen, E.M., Miller, S.W., Parks, J.P., Parker, W.D., Jr., Bennett, J.P., Jr., 1997. Elevated reactive oxygen

species and antioxidant enzyme activities in animal and cellular models of Parkinson's disease. Biochim Biophys Acta. 1362,77-86.

Chen, Y.R., Meyer, C.F., Ahmed, B., Yao, Z., Tan, T.H., 1999. Caspase-mediated cleavage and functional changes of hematopoietic progenitor kinase 1 (HPK1). Oncogene. 18,7370-7.

Cheng, B., Mattson, M.P., 1991. NGF and bFGF protect rat hippocampal and human cortical neurons against hypoglycemic damage by stabilizing calcium homeostasis. Neuron. 7,1031-41.

Cheung, P., Allis, C.D., Sassone-Corsi, P., 2000. Signaling to chromatin through histone modifications. Cell. 103,263-71.

Cheung, W.L., Ajiro, K., Samejima, K., Kloc, M., Cheung, P., Mizzen, C.A., Beeser, A., Etkin, L.D., Chernoff, J., Earnshaw, W.C., Allis, C.D., 2003. Apoptotic phosphorylation of histone H2B is mediated by mammalian sterile twenty kinase. Cell. 113,507-17.

Chinnaiyan, A.M., O'Rourke, K., Tewari, M., Dixit, V.M., 1995. FADD, a novel death domain-containing protein, interacts with the death domain of Fas and initiates apoptosis. Cell. 81,505-12.

Chung, K.K., Zhang, Y., Lim, K.L., Tanaka, Y., Huang, H., Gao, J., Ross, C.A., Dawson, V.L., Dawson, T.M., 2001. Parkin ubiquitinates the alpha-synuclein-interacting protein, synphilin-1: implications for Lewy-body formation in Parkinson disease. Nat Med. 7,1144-50.

Coleman, M.L., Sahai, E.A., Yeo, M., Bosch, M., Dewar, A., Olson, M.F., 2001. Membrane blebbing during apoptosis results from caspase-mediated activation of ROCK I. Nat Cell Biol. 3,339-45.

Connor, J.R., Snyder, B.S., Beard, J.L., Fine, R.E., Mufson, E.J., 1992. Regional distribution of iron and iron-regulatory proteins in the brain in aging and Alzheimer's disease. J Neurosci Res. 31,327-35.

Conway, K.A., Harper, J.D., Lansbury, P.T., Jr., 2000a. Fibrils formed in vitro from alpha-synuclein and two mutant forms linked to Parkinson's disease are typical amyloid. Biochemistry. 39,2552-63.

Conway, K.A., Lee, S.J., Rochet, J.C., Ding, T.T., Harper, J.D., Williamson, R.E., Lansbury, P.T., Jr., 2000b. Accelerated oligomerization by Parkinson's disease linked alpha-synuclein mutants. Ann N Y Acad Sci. 920,42-5.

Conway, K.A., Lee, S.J., Rochet, J.C., Ding, T.T., Williamson, R.E., Lansbury, P.T., Jr., 2000c. Acceleration of oligomerization, not fibrillization, is a shared property of both alpha-synuclein mutations linked to early-onset Parkinson's disease: implications for pathogenesis and therapy. Proc Natl Acad Sci U S A. 97,571-6.

Conway, K.A., Rochet, J.C., Bieganski, R.M., Lansbury, P.T., Jr., 2001. Kinetic stabilization of the alpha-synuclein protofibril by a dopamine-alpha-synuclein adduct. Science. 294,1346-9.

Corrigan, F.M., French, M., Murray, L., 1996. Organochlorine compounds in human brain. Hum Exp Toxicol. 15,262-4.

Craig, N.J., Duran Alonso, M.B., Hawker, K.L., Shiels, P., Glencorse, T.A., Campbell, J.M., Bennett, N.K., Canham, M., Donald, D., Gardiner, M., Gilmore, D.P., MacDonald,

R.J., Maitland, K., McCallion, A.S., Russell, D., Payne, A.P., Sutcliffe, R.G., Davies, R.W., 2001. A candidate gene for human neurodegenerative disorders: a rat PKC gamma mutation causes a Parkinsonian syndrome. Nat Neurosci. 4,1061-2.

Cross, T., Griffiths, G., Deacon, E., Sallis, R., Gough, M., Watters, D., Lord, J.M., 2000a. PKC-delta is an apoptotic lamin kinase. Oncogene. 19,2331-7.

Cross, T.G., Scheel-Toellner, D., Henriquez, N.V., Deacon, E., Salmon, M., Lord, J.M., 2000b. Serine/threonine protein kinases and apoptosis. Exp Cell Res. 256,34-41.

Dalmay, T., Hamilton, A., Rudd, S., Angell, S., Baulcombe, D.C., 2000. An RNA-dependent RNA polymerase gene in Arabidopsis is required for posttranscriptional gene silencing mediated by a transgene but not by a virus. Cell. 101,543-53.

Damier, P., Hirsch, E.C., Agid, Y., Graybiel, A.M., 1999a. The substantia nigra of the human brain. I. Nigrosomes and the nigral matrix, a compartmental organization based on calbindin D(28K) immunohistochemistry. Brain. 122 (Pt 8),1421-36.

Damier, P., Hirsch, E.C., Agid, Y., Graybiel, A.M., 1999b. The substantia nigra of the human brain. II. Patterns of loss of dopamine-containing neurons in Parkinson's disease. Brain. 122 (Pt 8),1437-48.

Damier, P., Hirsch, E.C., Zhang, P., Agid, Y., Javoy-Agid, F., 1993. Glutathione peroxidase, glial cells and Parkinson's disease. Neuroscience. 52,1-6.

Datta, R., Kojima, H., Yoshida, K., Kufe, D., 1997. Caspase-3-mediated cleavage of protein kinase C theta in induction of apoptosis. J Biol Chem. 272,20317-20.

Dauer, W., Przedborski, S., 2003. Parkinson's disease: mechanisms and models. Neuron. 39,889-909.

Davis, R.J., 2000. Signal transduction by the JNK group of MAP kinases. Cell. 103,239-52.

Dawson, T.M., Dawson, V.L., 2003. Molecular pathways of neurodegeneration in Parkinson's disease. Science. 302,819-22.

de Rijk, M.C., Launer, L.J., Berger, K., Breteler, M.M., Dartigues, J.F., Baldereschi, M., Fratiglioni, L., Lobo, A., Martinez-Lage, J., Trenkwalder, C., Hofman, A., 2000. Prevalence of Parkinson's disease in Europe: A collaborative study of population-based cohorts. Neurologic Diseases in the Elderly Research Group. Neurology. 54,S21-3.

de Souza, P.M., Lindsay, M.A., 2004. Mammalian Sterile20-like kinase 1 and the regulation of apoptosis. Biochem Soc Trans. 32,485-8.

DeVries, T.A., Kalkofen, R.L., Matassa, A.A., Reyland, M.E., 2004. Protein kinase Cdelta regulates apoptosis via activation of STAT1. J Biol Chem. 279,45603-12.

DeVries, T.A., Neville, M.C., Reyland, M.E., 2002. Nuclear import of PKCdelta is required for apoptosis: identification of a novel nuclear import sequence. Embo J. 21,6050-60.

Dexter, D.T., Carter, C.J., Wells, F.R., Javoy-Agid, F., Agid, Y., Lees, A., Jenner, P., Marsden, C.D., 1989. Basal lipid peroxidation in substantia nigra is increased in Parkinson's disease. J Neurochem. 52,381-9.

Dickson, D.W., 2002. Dementia with Lewy bodies: neuropathology. J Geriatr Psychiatry Neurol. 15,210-6.

Double, K.L., Ben-Shachar, D., Youdim, M.B., Zecca, L., Riederer, P., Gerlach, M., 2002. Influence of neuromelanin on oxidative pathways within the human substantia nigra. Neurotoxicol Teratol. 24,621-8.

Du, C., Fang, M., Li, Y., Li, L., Wang, X., 2000. Smac, a mitochondrial protein that promotes cytochrome c-dependent caspase activation by eliminating IAP inhibition. Cell. 102,33-42.

Dunkley, P.R., Bobrovskaya, L., Graham, M.E., von Nagy-Felsobuki, E.I., Dickson, P.W., 2004. Tyrosine hydroxylase phosphorylation: regulation and consequences. J Neurochem. 91,1025-43.

Dykxhoorn, D.M., Lieberman, J., 2005. The silent revolution: RNA interference as basic biology, research tool, and therapeutic. Annu Rev Med. 56,401-23.

Dykxhoorn, D.M., Novina, C.D., Sharp, P.A., 2003. Killing the messenger: short RNAs that silence gene expression. Nat Rev Mol Cell Biol. 4,457-67.

Edwards, R.H., 1993. Neural degeneration and the transport of neurotransmitters. Ann Neurol. 34,638-45.

Elbashir, S.M., Harborth, J., Lendeckel, W., Yalcin, A., Weber, K., Tuschl, T., 2001a. Duplexes of 21-nucleotide RNAs mediate RNA interference in cultured mammalian cells. Nature. 411,494-8.

Elbashir, S.M., Martinez, J., Patkaniowska, A., Lendeckel, W., Tuschl, T., 2001b. Functional anatomy of siRNAs for mediating efficient RNAi in Drosophila melanogaster embryo lysate. Embo J. 20,6877-88.

Emoto, Y., Kisaki, H., Manome, Y., Kharbanda, S., Kufe, D., 1996. Activation of protein kinase Cdelta in human myeloid leukemia cells treated with 1-beta-D-arabinofuranosylcytosine. Blood. 87,1990-6.

Emoto, Y., Manome, Y., Meinhardt, G., Kisaki, H., Kharbanda, S., Robertson, M., Ghayur, T., Wong, W.W., Kamen, R., Weichselbaum, R., et al., 1995. Proteolytic activation of protein kinase C delta by an ICE-like protease in apoptotic cells. Embo J. 14,6148-56.

Enari, M., Sakahira, H., Yokoyama, H., Okawa, K., Iwamatsu, A., Nagata, S., 1998. A caspase-activated DNase that degrades DNA during apoptosis, and its inhibitor ICAD. Nature. 391,43-50.

Fan, Z., Beresford, P.J., Oh, D.Y., Zhang, D., Lieberman, J., 2003. Tumor suppressor NM23-H1 is a granzyme A-activated DNase during CTL-mediated apoptosis, and the nucleosome assembly protein SET is its inhibitor. Cell. 112,659-72.

Ferri, K.F., Kroemer, G., 2001. Organelle-specific initiation of cell death pathways. Nat Cell Biol. 3,E255-63.

Fire, A., Xu, S., Montgomery, M.K., Kostas, S.A., Driver, S.E., Mello, C.C., 1998. Potent and specific genetic interference by double-stranded RNA in Caenorhabditis elegans. Nature. 391,806-11.

Fleming, L., Mann, J.B., Bean, J., Briggle, T., Sanchez-Ramos, J.R., 1994. Parkinson's disease and brain levels of organochlorine pesticides. Ann Neurol. 36,100-3.

Floor, E., Wetzel, M.G., 1998. Increased protein oxidation in human substantia nigra pars compacta in comparison with basal ganglia and prefrontal cortex measured with an improved dinitrophenylhydrazine assay. J Neurochem. 70,268-75.

Fornerod, M., Ohno, M., Yoshida, M., Mattaj, I.W., 1997. CRM1 is an export receptor for leucine-rich nuclear export signals. Cell. 90,1051-60.

Forno, L.S., DeLanney, L.E., Irwin, I., Langston, J.W., 1993. Similarities and differences between MPTP-induced parkinsonsim and Parkinson's disease. Neuropathologic considerations. Adv Neurol. 60,600-8.

Fornstedt, B., Rosengren, E., Carlsson, A., 1986. Occurrence and distribution of 5-S-cysteinyl derivatives of dopamine, dopa and dopac in the brains of eight mammalian species. Neuropharmacology. 25,451-4.

Fujiwara, H., Hasegawa, M., Dohmae, N., Kawashima, A., Masliah, E., Goldberg, M.S., Shen, J., Takio, K., Iwatsubo, T., 2002. alpha-Synuclein is phosphorylated in synucleinopathy lesions. Nat Cell Biol. 4,160-4.

Gainetdinov, R.R., Fumagalli, F., Jones, S.R., Caron, M.G., 1997. Dopamine transporter is required for in vivo MPTP neurotoxicity: evidence from mice lacking the transporter. J Neurochem. 69,1322-5.

Gainetdinov, R.R., Fumagalli, F., Wang, Y.M., Jones, S.R., Levey, A.I., Miller, G.W., Caron, M.G., 1998. Increased MPTP neurotoxicity in vesicular monoamine transporter 2 heterozygote knockout mice. J Neurochem. 70,1973-8.

Giasson, B.I., Lee, V.M., 2000. A new link between pesticides and Parkinson's disease. Nat Neurosci. 3,1227-8.

Giasson, B.I., Lee, V.M., 2001. Parkin and the molecular pathways of Parkinson's disease. Neuron. 31,885-8.

Gil, J., Esteban, M., 2000. Induction of apoptosis by the dsRNA-dependent protein kinase (PKR): mechanism of action. Apoptosis. 5,107-14.

Golbe, L.I., Di Iorio, G., Bonavita, V., Miller, D.C., Duvoisin, R.C., 1990. A large kindred with autosomal dominant Parkinson's disease. Ann Neurol. 27,276-82.

Gonzalez-Alegre, P., Miller, V.M., Davidson, B.L., Paulson, H.L., 2003. Toward therapy for DYT1 dystonia: allele-specific silencing of mutant TorsinA. Ann Neurol. 53,781-7.

Gonzalez-Hernandez, T., Barroso-Chinea, P., De La Cruz Muros, I., Del Mar Perez-Delgado, M., Rodriguez, M., 2004. Expression of dopamine and vesicular monoamine transporters and differential vulnerability of mesostriatal dopaminergic neurons. J Comp Neurol. 479,198-215.

Good, P.F., Olanow, C.W., Perl, D.P., 1992. Neuromelanin-containing neurons of the substantia nigra accumulate iron and aluminum in Parkinson's disease: a LAMMA study. Brain Res. 593,343-6.

Gorell, J.M., Johnson, C.C., Rybicki, B.A., Peterson, E.L., Kortsha, G.X., Brown, G.G., Richardson, R.J., 1997. Occupational exposures to metals as risk factors for Parkinson's disease. Neurology. 48,650-8.

Gorell, J.M., Rybicki, B.A., Johnson, C.C., Peterson, E.L., 1999. Smoking and Parkinson's disease: a dose-response relationship. Neurology. 52,115-9.

Graham, D.G., 1978. Oxidative pathways for catecholamines in the genesis of neuromelanin and cytotoxic quinones. Mol Pharmacol. 14,633-43.

Greenamyre, J.T., Sherer, T.B., Betarbet, R., Panov, A.V., 2001. Complex I and Parkinson's disease. IUBMB Life. 52,135-41.

Grutter, M.G., 2000. Caspases: key players in programmed cell death. Curr Opin Struct Biol. 10,649-55.

Gschwendt, M., 1999. Protein kinase C delta. Eur J Biochem. 259,555-64.

Halliwell, B., 1992. Reactive oxygen species and the central nervous system. J Neurochem. 59,1609-23.

Hammond, S.M., Caudy, A.A., Hannon, G.J., 2001. Post-transcriptional gene silencing by double-stranded RNA. Nat Rev Genet. 2,110-9.

Hannon, G.J., 2002. RNA interference. Nature. 418,244-51.

Hardy, J., 2003. The relationship between Lewy body disease, Parkinson's disease, and Alzheimer's disease. Ann N Y Acad Sci. 991,167-70.

Hartmann, A., Hunot, S., Michel, P.P., Muriel, M.P., Vyas, S., Faucheux, B.A., Mouatt-Prigent, A., Turmel, H., Srinivasan, A., Ruberg, M., Evan, G.I., Agid, Y., Hirsch, E.C., 2000. Caspase-3: A vulnerability factor and final effector in apoptotic death of dopaminergic neurons in Parkinson's disease. Proc Natl Acad Sci U S A. 97,2875-80.

Hartmann, A., Michel, P.P., Troadec, J.D., Mouatt-Prigent, A., Faucheux, B.A., Ruberg, M., Agid, Y., Hirsch, E.C., 2001a. Is Bax a mitochondrial mediator in apoptotic death of dopaminergic neurons in Parkinson's disease? J Neurochem. 76,1785-93.

Hartmann, A., Troadec, J.D., Hunot, S., Kikly, K., Faucheux, B.A., Mouatt-Prigent, A., Ruberg, M., Agid, Y., Hirsch, E.C., 2001b. Caspase-8 is an effector in apoptotic death of dopaminergic neurons in Parkinson's disease, but pathway inhibition results in neuronal necrosis. J Neurosci. 21,2247-55.

Hegde, R., Srinivasula, S.M., Zhang, Z., Wassell, R., Mukattash, R., Cilenti, L., DuBois, G., Lazebnik, Y., Zervos, A.S., Fernandes-Alnemri, T., Alnemri, E.S., 2002. Identification of Omi/HtrA2 as a mitochondrial apoptotic serine protease that disrupts inhibitor of apoptosis protein-caspase interaction. J Biol Chem. 277,432-8.

Heinz, G.H., Hill, E.F., Contrera, J.F., 1980. Dopamine and norepinephrine depletion in ring doves fed DDE, dieldrin, and Aroclor 1254. Toxicol Appl Pharmacol. 53,75-82.

Hammond, S.M., Caudy, A.A., Hannon, G.J., 2001. Post-transcriptional gene silencing by double-stranded RNA. Nat Rev Genet. 2,110-9.

Hannon, G.J., 2002. RNA interference. Nature. 418,244-51.

Hardy, J., 2003. The relationship between Lewy body disease, Parkinson's disease, and Alzheimer's disease. Ann N Y Acad Sci. 991,167-70.

Hartmann, A., Hunot, S., Michel, P.P., Muriel, M.P., Vyas, S., Faucheux, B.A., Mouatt-Prigent, A., Turmel, H., Srinivasan, A., Ruberg, M., Evan, G.I., Agid, Y., Hirsch, E.C., 2000. Caspase-3: A vulnerability factor and final effector in apoptotic death of dopaminergic neurons in Parkinson's disease. Proc Natl Acad Sci U S A. 97,2875-80.

Hartmann, A., Michel, P.P., Troadec, J.D., Mouatt-Prigent, A., Faucheux, B.A., Ruberg, M., Agid, Y., Hirsch, E.C., 2001a. Is Bax a mitochondrial mediator in apoptotic death of dopaminergic neurons in Parkinson's disease? J Neurochem. 76,1785-93.

Hartmann, A., Troadec, J.D., Hunot, S., Kikly, K., Faucheux, B.A., Mouatt-Prigent, A., Ruberg, M., Agid, Y., Hirsch, E.C., 2001b. Caspase-8 is an effector in apoptotic death of dopaminergic neurons in Parkinson's disease, but pathway inhibition results in neuronal necrosis. J Neurosci. 21,2247-55.

Hegde, R., Srinivasula, S.M., Zhang, Z., Wassell, R., Mukattash, R., Cilenti, L., DuBois, G., Lazebnik, Y., Zervos, A.S., Fernandes-Alnemri, T., Alnemri, E.S., 2002. Identification of Omi/HtrA2 as a mitochondrial apoptotic serine protease that disrupts inhibitor of apoptosis protein-caspase interaction. J Biol Chem. 277,432-8.

Heinz, G.H., Hill, E.F., Contrera, J.F., 1980. Dopamine and norepinephrine depletion in ring doves fed DDE, dieldrin, and Aroclor 1254. Toxicol Appl Pharmacol. 53,75-82.

Hellenbrand, W., Boeing, H., Robra, B.P., Seidler, A., Vieregge, P., Nischan, P., Joerg, J., Oertel, W.H., Schneider, E., Ulm, G., 1996a. Diet and Parkinson's disease. II: A possible role for the past intake of specific nutrients. Results from a self-administered food-frequency questionnaire in a case-control study. Neurology. 47,644-50.

Hellenbrand, W., Seidler, A., Boeing, H., Robra, B.P., Vieregge, P., Nischan, P., Joerg, J., Oertel, W.H., Schneider, E., Ulm, G., 1996b. Diet and Parkinson's disease. I: A possible role for the past intake of specific foods and food groups. Results from a self-administered food-frequency questionnaire in a case-control study. Neurology. 47,636-43.

Hirsch, E.C., Faucheux, B., Damier, P., Mouatt-Prigent, A., Agid, Y., 1997. Neuronal vulnerability in Parkinson's disease. J Neural Transm Suppl. 50,79-88.

Hitri, A., Hurd, Y.L., Wyatt, R.J., Deutsch, S.I., 1994. Molecular, functional and biochemical characteristics of the dopamine transporter: regional differences and clinical relevance. Clin Neuropharmacol. 17,1-22.

Hodara, R., Norris, E.H., Giasson, B.I., Mishizen-Eberz, A.J., Lynch, D.R., Lee, V.M., Ischiropoulos, H., 2004. Functional consequences of alpha-synuclein tyrosine nitration: diminished binding to lipid vesicles and increased fibril formation. J Biol Chem. 279,47746-53.

Hodgkinson, C.P., Sale, G.J., 2002. Regulation of both PDK1 and the phosphorylation of PKC-zeta and -delta by a C-terminal PRK2 fragment. Biochemistry. 41,561-9.

Holle, L., Hicks, L., Song, W., Holle, E., Wagner, T., Yu, X., 2004. Bcl-2 targeting siRNA expressed by a T7 vector system inhibits human tumor cell growth in vitro. Int J Oncol. 24,615-21.

Hommel, J.D., Sears, R.M., Georgescu, D., Simmons, D.L., DiLeone, R.J., 2003. Local gene knockdown in the brain using viral-mediated RNA interference. Nat Med. 9,1539-44.

Huang, Y., Cheung, L., Rowe, D., Halliday, G., 2004. Genetic contributions to Parkinson's disease. Brain Res Brain Res Rev. 46,44-70.

Imai, Y., Soda, M., Inoue, H., Hattori, N., Mizuno, Y., Takahashi, R., 2001. An unfolded putative transmembrane polypeptide, which can lead to endoplasmic reticulum stress, is a substrate of Parkin. Cell. 105,891-902.

Itoh, T., Horio, T., 2001. DNA-dependent protein kinase catalytic subunit is cleaved during UV-induced apoptosis. J Dermatol Sci. 25,72-7.

Jackson-Lewis, V., Jakowec, M., Burke, R.E., Przedborski, S., 1995. Time course and morphology of dopaminergic neuronal death caused by the neurotoxin 1-methyl-4-phenyl-1,2,3,6-tetrahydropyridine. Neurodegeneration. 4,257-69.

Jakobi, R., 2004. Subcellular targeting regulates the function of caspase-activated protein kinases in apoptosis. Drug Resist Updat. 7,11-7.

Jakobi, R., McCarthy, C.C., Koeppel, M.A., Stringer, D.K., 2003. Caspase-activated PAK-2 is regulated by subcellular targeting and proteasomal degradation. J Biol Chem. 278,38675-85.

Jellinger, K.A., 2000. Cell death mechanisms in Parkinson's disease. J Neural Transm. 107,1-29.

Jenner, P., 1998. Oxidative mechanisms in nigral cell death in Parkinson's disease. Mov Disord. 13 Suppl 1,24-34.

Jenner, P., 2001. Parkinson's disease, pesticides and mitochondrial dysfunction. Trends Neurosci. 24,245-7.

Jenner, P., 2003. Oxidative stress in Parkinson's disease. Ann Neurol. 53 Suppl 3,S26-36; discussion S36-8.

Jeon, H.K., Jin, H.S., Lee, D.H., Choi, W.S., Moon, C.K., Oh, Y.J., Lee, T.H., 2004. Proteome analysis associated with cadmium adaptation in U937 cells: identification of calbindin-D28k as a secondary cadmium-responsive protein that confers resistance to cadmium-induced apoptosis. J Biol Chem. 279,31575-83.

Jiang, X., Kim, H.E., Shu, H., Zhao, Y., Zhang, H., Kofron, J., Donnelly, J., Burns, D., Ng, S.C., Rosenberg, S., Wang, X., 2003. Distinctive roles of PHAP proteins and prothymosin-alpha in a death regulatory pathway. Science. 299,223-6.

Johnson, D.E., 2000. Noncaspase proteases in apoptosis. Leukemia. 14,1695-703.

Jope, R.S., Johnson, G.V., 2004. The glamour and gloom of glycogen synthase kinase-3. Trends Biochem Sci. 29,95-102.

Kadowaki, H., Nishitoh, H., Ichijo, H., 2004. Survival and apoptosis signals in ER stress: the role of protein kinases. J Chem Neuroanat. 28,93-100.

Kaffman, A., O'Shea, E.K., 1999. Regulation of nuclear localization: a key to a door. Annu Rev Cell Dev Biol. 15,291-339.

Kafri, T., Blomer, U., Peterson, D.A., Gage, F.H., Verma, I.M., 1997. Sustained expression of genes delivered directly into liver and muscle by lentiviral vectors. Nat Genet. 17,314-7.

Kandel, E.R., Schwartz, J.H., Jessell, T.M. (2000) Principles of Neural Science: McGraw-Hill.

Kanthasamy, A.G., Kitazawa, M., Kanthasamy, A., Anantharam, V., 2003. Role of proteolytic activation of protein kinase Cdelta in oxidative stress-induced apoptosis. Antioxid Redox Signal. 5,609-20.

Katayama, T., Imaizumi, K., Sato, N., Miyoshi, K., Kudo, T., Hitomi, J., Morihara, T., Yoneda, T., Gomi, F., Mori, Y., Nakano, Y., Takeda, J., Tsuda, T., Itoyama, Y., Murayama, O., Takashima, A., St George-Hyslop, P., Takeda, M., Tohyama, M., 1999. Presenilin-1 mutations downregulate the signalling pathway of the unfolded-protein response. Nat Cell Biol. 1,479-85.

Kaul, S., Kanthasamy, A., Kitazawa, M., Anantharam, V., Kanthasamy, A.G., 2003. Caspase-3 dependent proteolytic activation of protein kinase C delta mediates and regulates 1-methyl-4-phenylpyridinium (MPP+)-induced apoptotic cell death in dopaminergic cells: relevance to oxidative stress in dopaminergic degeneration. Eur J Neurosci. 18,1387-401.

Kikkawa, U., Matsuzaki, H., Yamamoto, T., 2002. Protein Kinase Cdelta (PKCdelta): Activation Mechanisms and Functions. J Biochem (Tokyo). 132,831-9.

Kirik, D., Bjorklund, A., 2003. Modeling CNS neurodegeneration by overexpression of disease-causing proteins using viral vectors. Trends Neurosci. 26,386-92.

Kitazawa, M., Anantharam, V., Kanthasamy, A.G., 2001. Dieldrin-induced oxidative stress and neurochemical changes contribute to apoptopic cell death in dopaminergic cells. Free Radic Biol Med. 31,1473-85.

Kitazawa, M., Anantharam, V., Kanthasamy, A.G., 2003. Dieldrin induces apoptosis by promoting caspase-3-dependent proteolytic cleavage of protein kinase Cdelta in

dopaminergic cells: relevance to oxidative stress and dopaminergic degeneration. Neuroscience. 119,945-964.

Klaidman, L.K., Adams, J.D., Jr., Leung, A.C., Kim, S.S., Cadenas, E., 1993. Redox cycling of MPP+: evidence for a new mechanism involving hydride transfer with xanthine oxidase, aldehyde dehydrogenase, and lipoamide dehydrogenase. Free Radic Biol Med. 15,169-79.

Knaus, U.G., Bokoch, G.M., 1998. The p21Rac/Cdc42-activated kinases (PAKs). Int J Biochem Cell Biol. 30,857-62.

Konishi, H., Tanaka, M., Takemura, Y., Matsuzaki, H., Ono, Y., Kikkawa, U., Nishizuka, Y., 1997. Activation of protein kinase C by tyrosine phosphorylation in response to H2O2. Proc Natl Acad Sci U S A. 94,11233-7.

Konishi, H., Yamauchi, E., Taniguchi, H., Yamamoto, T., Matsuzaki, H., Takemura, Y., Ohmae, K., Kikkawa, U., Nishizuka, Y., 2001. Phosphorylation sites of protein kinase C delta in H2O2-treated cells and its activation by tyrosine kinase in vitro. Proc Natl Acad Sci U S A. 98,6587-92.

Korotkova, T.M., Ponomarenko, A.A., Brown, R.E., Haas, H.L., 2004. Functional diversity of ventral midbrain dopamine and GABAergic neurons. Mol Neurobiol. 29,243-59.

Krishnan, S., Chi, E.Y., Wood, S.J., Kendrick, B.S., Li, C., Garzon-Rodriguez, W., Wypych, J., Randolph, T.W., Narhi, L.O., Biere, A.L., Citron, M., Carpenter, J.F., 2003. Oxidative dimer formation is the critical rate-limiting step for Parkinson's disease alpha-synuclein fibrillogenesis. Biochemistry. 42,829-37.

Kruger, R., Kuhn, W., Muller, T., Woitalla, D., Graeber, M., Kosel, S., Przuntek, H., Epplen, J.T., Schols, L., Riess, O., 1998. Ala30Pro mutation in the gene encoding alpha-synuclein in Parkinson's disease. Nat Genet. 18,106-8.

Kuhn, W., Winkel, R., Woitalla, D., Meves, S., Przuntek, H., Muller, T., 1998. High prevalence of parkinsonism after occupational exposure to lead-sulfate batteries. Neurology. 50,1885-6.

Langston, J.W., Langston, E.B., Irwin, I., 1984. MPTP-induced parkinsonism in human and non-human primates--clinical and experimental aspects. Acta Neurol Scand Suppl. 100,49-54.

Le Good, J.A., Ziegler, W.H., Parekh, D.B., Alessi, D.R., Cohen, P., Parker, P.J., 1998. Protein kinase C isotypes controlled by phosphoinositide 3-kinase through the protein kinase PDK1. Science. 281,2042-5.

Lee, G., Tanaka, M., Park, K., Lee, S.S., Kim, Y.M., Junn, E., Lee, S.H., Mouradian, M.M., 2004. Casein kinase II-mediated phosphorylation regulates alpha-synuclein/synphilin-1 interaction and inclusion body formation. J Biol Chem. 279,6834-9.

Lee, K.K., Ohyama, T., Yajima, N., Tsubuki, S., Yonehara, S., 2001. MST, a physiological caspase substrate, highly sensitizes apoptosis both upstream and downstream of caspase activation. J Biol Chem. 276,19276-85.

Lee, K.K., Yonehara, S., 2002. Phosphorylation and dimerization regulate nucleocytoplasmic shuttling of mammalian STE20-like kinase (MST). J Biol Chem. 277,12351-8.

Lee, N., MacDonald, H., Reinhard, C., Halenbeck, R., Roulston, A., Shi, T., Williams, L.T., 1997. Activation of hPAK65 by caspase cleavage induces some of the morphological and biochemical changes of apoptosis. Proc Natl Acad Sci U S A. 94,13642-7.

Lee, Y., Ahn, C., Han, J., Choi, H., Kim, J., Yim, J., Lee, J., Provost, P., Radmark, O., Kim, S., Kim, V.N., 2003. The nuclear RNase III Drosha initiates microRNA processing. Nature. 425,415-9.

Lee, Y., Jeon, K., Lee, J.T., Kim, S., Kim, V.N., 2002. MicroRNA maturation: stepwise processing and subcellular localization. Embo J. 21,4663-70.

Leibersperger, H., Gschwendt, M., Gernold, M., Marks, F., 1991. Immunological demonstration of a calcium-unresponsive protein kinase C of the delta-type in different species and murine tissues. Predominance in epidermis. J Biol Chem. 266,14778-84.

Leitges, M., Mayr, M., Braun, U., Mayr, U., Li, C., Pfister, G., Ghaffari-Tabrizi, N., Baier, G., Hu, Y., Xu, Q., 2001. Exacerbated vein graft arteriosclerosis in protein kinase Cdelta-null mice. J Clin Invest. 108,1505-12.

Lev, N., Melamed, E., Offen, D., 2003. Apoptosis and Parkinson's disease. Prog Neuropsychopharmacol Biol Psychiatry. 27,245-50.

Leverrier, S., Vallentin, A., Joubert, D., 2002. Positive feedback of protein kinase C proteolytic activation during apoptosis. Biochem J. 368,905-13.

Lewis, D.L., Hagstrom, J.E., Loomis, A.G., Wolff, J.A., Herweijer, H., 2002. Efficient delivery of siRNA for inhibition of gene expression in postnatal mice. Nat Genet. 32,107-8.

Li, L.Y., Luo, X., Wang, X., 2001. Endonuclease G is an apoptotic DNase when released from mitochondria. Nature. 412,95-9.

Li, P., Nijhawan, D., Budihardjo, I., Srinivasula, S.M., Ahmad, M., Alnemri, E.S., Wang, X., 1997. Cytochrome c and dATP-dependent formation of Apaf-1/caspase-9 complex initiates an apoptotic protease cascade. Cell. 91,479-89.

Liang, C.L., Nelson, O., Yazdani, U., Pasbakhsh, P., German, D.C., 2004. Inverse relationship between the contents of neuromelanin pigment and the vesicular monoamine transporter-2: human midbrain dopamine neurons. J Comp Neurol. 473,97-106.

Liang, C.L., Sinton, C.M., Sonsalla, P.K., German, D.C., 1996. Midbrain dopaminergic neurons in the mouse that contain calbindin-D28k exhibit reduced vulnerability to MPTP-induced neurodegeneration. Neurodegeneration. 5,313-8.

Lindersson, E.K., Hojrup, P., Gai, W.P., Locker, D., Martin, D., Jensen, P.H., 2004. alpha-Synuclein filaments bind the transcriptional regulator HMGB-1. Neuroreport. 15,2735-9.

Liu, C.C., Walsh, C.M., Young, J.D., 1995. Perforin: structure and function. Immunol Today. 16,194-201.

Liu, Y., Fallon, L., Lashuel, H.A., Liu, Z., Lansbury, P.T., Jr., 2002. The UCH-L1 gene encodes two opposing enzymatic activities that affect alpha-synuclein degradation and Parkinson's disease susceptibility. Cell. 111,209-18.

Liu, Y., Peter, D., Roghani, A., Schuldiner, S., Prive, G.G., Eisenberg, D., Brecha, N., Edwards, R.H., 1992. A cDNA that suppresses MPP+ toxicity encodes a vesicular amine transporter. Cell. 70,539-51.

Lopiano, L., Chiesa, M., Digilio, G., Giraudo, S., Bergamasco, B., Torre, E., Fasano, M., 2000. Q-band EPR investigations of neuromelanin in control and Parkinson's disease patients. Biochim Biophys Acta. 1500,306-12.

Lotharius, J., Brundin, P., 2002. Pathogenesis of Parkinson's disease: dopamine, vesicles and alpha-synuclein. Nat Rev Neurosci. 3,932-42.

Lovenberg, W., Bruckwick, E.A., Hanbauer, I., 1975. ATP, cyclic AMP, and magnesium increase the affinity of rat striatal tyrosine hydroxylase for its cofactor. Proc Natl Acad Sci U S A. 72,2955-8.

Lucking, C.B., Abbas, N., Durr, A., Bonifati, V., Bonnet, A.M., de Broucker, T., De Michele, G., Wood, N.W., Agid, Y., Brice, A., 1998. Homozygous deletions in parkin gene in European and North African families with autosomal recessive juvenile parkinsonism. The European Consortium on Genetic Susceptibility in Parkinson's Disease and the French Parkinson's Disease Genetics Study Group. Lancet. 352,1355-6.

Majumder, P.K., Pandey, P., Sun, X., Cheng, K., Datta, R., Saxena, S., Kharbanda, S., Kufe, D., 2000. Mitochondrial translocation of protein kinase C delta in phorbol ester-induced cytochrome c release and apoptosis. J Biol Chem. 275,21793-6.

Maker, H.S., Weiss, C., Silides, D.J., Cohen, G., 1981. Coupling of dopamine oxidation (monoamine oxidase activity) to glutathione oxidation via the generation of hydrogen peroxide in rat brain homogenates. J Neurochem. 36,589-93.

Markey, S.P., Johannessen, J.N., Chiueh, C.C., Burns, R.S., Herkenham, M.A., 1984. Intraneuronal generation of a pyridinium metabolite may cause drug-induced parkinsonism. Nature. 311,464-7.

Marsden, C.D., 1990. Parkinson's disease. Lancet. 335,948-52.

Martinez-Martin, P., Gil-Nagel, A., Gracia, L.M., Gomez, J.B., Martinez-Sarries, J., Bermejo, F., 1994. Unified Parkinson's Disease Rating Scale characteristics and structure. The Cooperative Multicentric Group. Mov Disord. 9,76-83.

Matsukawa, J., Matsuzawa, A., Takeda, K., Ichijo, H., 2004. The ASK1-MAP kinase cascades in mammalian stress response. J Biochem (Tokyo). 136,261-5.

Matsuzawa, A., Ichijo, H., 2005. Stress-responsive protein kinases in redox-regulated apoptosis signaling. Antioxid Redox Signal. 7,472-81.

Mattson, M.P., 2000. Apoptosis in neurodegenerative disorders. Nat Rev Mol Cell Biol. 1,120-9.

Maundrell, K., Antonsson, B., Magnenat, E., Camps, M., Muda, M., Chabert, C., Gillieron, C., Boschert, U., Vial-Knecht, E., Martinou, J.C., Arkinstall, S., 1997. Bcl-2 undergoes phosphorylation by c-Jun N-terminal kinase/stress-activated protein kinases in the presence of the constitutively active GTP-binding protein Rac1. J Biol Chem. 272,25238-42.

Mayer, R.A., Kindt, M.V., Heikkila, R.E., 1986. Prevention of the nigrostriatal toxicity of 1-methyl-4-phenyl-1,2,3,6-tetrahydropyridine by inhibitors of 3,4-dihydroxyphenylethylamine transport. J Neurochem. 47,1073-9.

McCaffrey, A.P., Meuse, L., Pham, T.T., Conklin, D.S., Hannon, G.J., Kay, M.A., 2002. RNA interference in adult mice. Nature. 418,38-9.

McCormack, A.L., Thiruchelvam, M., Manning-Bog, A.B., Thiffault, C., Langston, J.W., Cory-Slechta, D.A., Di Monte, D.A., 2002. Environmental risk factors and Parkinson's disease: selective degeneration of nigral dopaminergic neurons caused by the herbicide paraquat. Neurobiol Dis. 10,119-27.

McKeith, I.G., Burn, D.J., Ballard, C.G., Collerton, D., Jaros, E., Morris, C.M., McLaren, A., Perry, E.K., Perry, R., Piggott, M.A., O'Brien, J.T., 2003. Dementia with Lewy bodies. Semin Clin Neuropsychiatry. 8,46-57.

Medema, J.P., Scaffidi, C., Kischkel, F.C., Shevchenko, A., Mann, M., Krammer, P.H., Peter, M.E., 1997. FLICE is activated by association with the CD95 death-inducing signaling complex (DISC). Embo J. 16,2794-804.

Meier, P., Finch, A., Evan, G., 2000. Apoptosis in development. Nature. 407,796-801.

Metzstein, M.M., Stanfield, G.M., Horvitz, H.R., 1998. Genetics of programmed cell death in C. elegans: past, present and future. Trends Genet. 14,410-6.

Miller, G.W., Erickson, J.D., Perez, J.T., Penland, S.N., Mash, D.C., Rye, D.B., Levey, A.I., 1999. Immunochemical analysis of vesicular monoamine transporter (VMAT2) protein in Parkinson's disease. Exp Neurol. 156,138-48.

Miller, V.M., Gouvion, C.M., Davidson, B.L., Paulson, H.L., 2004. Targeting Alzheimer's disease genes with RNA interference: an efficient strategy for silencing mutant alleles. Nucleic Acids Res. 32,661-8.

Miller, V.M., Xia, H., Marrs, G.L., Gouvion, C.M., Lee, G., Davidson, B.L., Paulson, H.L., 2003. Allele-specific silencing of dominant disease genes. Proc Natl Acad Sci U S A. 100,7195-200.

Mittal, V., 2004. Improving the efficiency of RNA interference in mammals. Nat Rev Genet. 5,355-65.

Miyoshi, H., Takahashi, M., Gage, F.H., Verma, I.M., 1997. Stable and efficient gene transfer into the retina using an HIV-based lentiviral vector. Proc Natl Acad Sci U S A. 94,10319-23.

Mochizuki, H., Goto, K., Mori, H., Mizuno, Y., 1996. Histochemical detection of apoptosis in Parkinson's disease. J Neurol Sci. 137,120-3.

Morens, D.M., Grandinetti, A., Reed, D., White, L.R., Ross, G.W., 1995. Cigarette smoking and protection from Parkinson's disease: false association or etiologic clue? Neurology. 45,1041-51.

Moroianu, J., 1999. Nuclear import and export pathways. J Cell Biochem. Suppl 32-33,76-83.

Mourrain, P., Beclin, C., Elmayan, T., Feuerbach, F., Godon, C., Morel, J.B., Jouette, D., Lacombe, A.M., Nikic, S., Picault, N., Remoue, K., Sanial, M., Vo, T.A., Vaucheret, H., 2000. Arabidopsis SGS2 and SGS3 genes are required for posttranscriptional gene silencing and natural virus resistance. Cell. 101,533-42.

Moy, L.Y., Tsai, L.H., 2004. Cyclin-dependent kinase 5 phosphorylates serine 31 of tyrosine hydroxylase and regulates its stability. J Biol Chem. 279,54487-93.

Munch, G., Luth, H.J., Wong, A., Arendt, T., Hirsch, E., Ravid, R., Riederer, P., 2000. Crosslinking of alpha-synuclein by advanced glycation endproducts--an early pathophysiological step in Lewy body formation? J Chem Neuroanat. 20,253-7.

Murriel, C.L., Churchill, E., Inagaki, K., Szweda, L.I., Mochly-Rosen, D., 2004. Protein kinase Cdelta activation induces apoptosis in response to cardiac ischemia and reperfusion damage: a mechanism involving BAD and the mitochondria. J Biol Chem. 279,47985-91.

Nagatsu, T., 1995. Tyrosine hydroxylase: human isoforms, structure and regulation in physiology and pathology. Essays Biochem. 30,15-35.

Naik, M.U., Benedikz, E., Hernandez, I., Libien, J., Hrabe, J., Valsamis, M., Dow-Edwards, D., Osman, M., Sacktor, T.C., 2000. Distribution of protein kinase Mzeta and the complete protein kinase C isoform family in rat brain. J Comp Neurol. 426,243-58.

Newton, A.C., 2003. Regulation of the ABC kinases by phosphorylation: protein kinase C as a paradigm. Biochem J. 370,361-71.

Nicholson, D.W., Thornberry, N.A., 1997. Caspases: killer proteases. Trends Biochem Sci. 22,299-306.

Nijhawan, D., Honarpour, N., Wang, X., 2000. Apoptosis in neural development and disease. Annu Rev Neurosci. 23,73-87.

Nirenberg, M.J., Chan, J., Liu, Y., Edwards, R.H., Pickel, V.M., 1996. Ultrastructural localization of the vesicular monoamine transporter-2 in midbrain dopaminergic neurons: potential sites for somatodendritic storage and release of dopamine. J Neurosci. 16,4135-45.

Nishizuka, Y., 1992. Intracellular signaling by hydrolysis of phospholipids and activation of protein kinase C. Science. 258,607-14.

Nowak, S.J., Corces, V.G., 2004. Phosphorylation of histone H3: a balancing act between chromosome condensation and transcriptional activation. Trends Genet. 20,214-20.

Nykanen, A., Haley, B., Zamore, P.D., 2001. ATP requirements and small interfering RNA structure in the RNA interference pathway. Cell. 107,309-21.

Okochi, M., Walter, J., Koyama, A., Nakajo, S., Baba, M., Iwatsubo, T., Meijer, L., Kahle, P.J., Haass, C., 2000. Constitutive phosphorylation of the Parkinson's disease associated alpha-synuclein. J Biol Chem. 275,390-7.

Olanow, C.W., Tatton, W.G., 1999. Etiology and pathogenesis of Parkinson's disease. Annu Rev Neurosci. 22,123-44.

Orrenius, S., Zhivotovsky, B., Nicotera, P., 2003. Regulation of cell death: the calcium-apoptosis link. Nat Rev Mol Cell Biol. 4,552-65.

Paddison, P.J., Caudy, A.A., Bernstein, E., Hannon, G.J., Conklin, D.S., 2002. Short hairpin RNAs (shRNAs) induce sequence-specific silencing in mammalian cells. Genes Dev. 16,948-58.

Paik, S.R., Shin, H.J., Lee, J.H., Chang, C.S., Kim, J., 1999. Copper(II)-induced self-oligomerization of alpha-synuclein. Biochem J. 340 (Pt 3),821-8.

Parkinson, J., 2002. An essay on the shaking palsy. 1817. J Neuropsychiatry Clin Neurosci. 14,223-36; discussion 222.

Paul, C.P., Good, P.D., Winer, I., Engelke, D.R., 2002. Effective expression of small interfering RNA in human cells. Nat Biotechnol. 20,505-8.

Paviour, D.C., Surtees, R.A., Lees, A.J., 2004. Diagnostic considerations in juvenile parkinsonism. Mov Disord. 19,123-35.

Peter, D., Liu, Y., Sternini, C., de Giorgio, R., Brecha, N., Edwards, R.H., 1995. Differential expression of two vesicular monoamine transporters. J Neurosci. 15,6179-88.

Phiel, C.J., Wilson, C.A., Lee, V.M., Klein, P.S., 2003. GSK-3alpha regulates production of Alzheimer's disease amyloid-beta peptides. Nature. 423,435-9.

Pilas, B., Sarna, T., Kalyanaraman, B., Swartz, H.M., 1988. The effect of melanin on iron associated decomposition of hydrogen peroxide. Free Radic Biol Med. 4,285-93.

Polymeropoulos, M.H., Lavedan, C., Leroy, E., Ide, S.E., Dehejia, A., Dutra, A., Pike, B., Root, H., Rubenstein, J., Boyer, R., Stenroos, E.S., Chandrasekharappa, S.,

Athanassiadou, A., Papapetropoulos, T., Johnson, W.G., Lazzarini, A.M., Duvoisin, R.C., Di Iorio, G., Golbe, L.I., Nussbaum, R.L., 1997. Mutation in the alpha-synuclein gene identified in families with Parkinson's disease. Science. 276,2045-7.

Prehn, J.H., Bindokas, V.P., Marcuccilli, C.J., Krajewski, S., Reed, J.C., Miller, R.J., 1994. Regulation of neuronal Bcl2 protein expression and calcium homeostasis by transforming growth factor type beta confers wide-ranging protection on rat hippocampal neurons. Proc Natl Acad Sci U S A. 91,12599-603.

Przedborski, S., Chen, Q., Vila, M., Giasson, B.I., Djaldatti, R., Vukosavic, S., Souza, J.M., Jackson-Lewis, V., Lee, V.M., Ischiropoulos, H., 2001. Oxidative post-translational modifications of alpha-synuclein in the 1-methyl-4-phenyl-1,2,3,6-tetrahydropyridine (MPTP) mouse model of Parkinson's disease. J Neurochem. 76,637-40.

Przedborski, S., Vila, M., 2003. The 1-methyl-4-phenyl-1,2,3,6-tetrahydropyridine mouse model: a tool to explore the pathogenesis of Parkinson's disease. Ann N Y Acad Sci. 991,189-98.

Rajput, A.H., 1992. Frequency and cause of Parkinson's disease. Can J Neurol Sci. 19,103-7.

Ramsay, R.R., Salach, J.I., Dadgar, J., Singer, T.P., 1986. Inhibition of mitochondrial NADH dehydrogenase by pyridine derivatives and its possible relation to experimental and idiopathic parkinsonism. Biochem Biophys Res Commun. 135,269-75.

Ramsey, A.J., Fitzpatrick, P.F., 2000. Effects of phosphorylation on binding of catecholamines to tyrosine hydroxylase: specificity and thermodynamics. Biochemistry. 39,773-8.

Recchia, A., Debetto, P., Negro, A., Guidolin, D., Skaper, S.D., Giusti, P., 2004. Alpha-synuclein and Parkinson's disease. Faseb J. 18,617-26.

Reynolds, A., Leake, D., Boese, Q., Scaringe, S., Marshall, W.S., Khvorova, A., 2004. Rational siRNA design for RNA interference. Nat Biotechnol. 22,326-30.

Riddle, R., Pollock, J.D., 2003. Making connections: the development of mesencephalic dopaminergic neurons. Brain Res Dev Brain Res. 147,3-21.

Roskoski, R., Jr., Vulliet, P.R., Glass, D.B., 1987. Phosphorylation of tyrosine hydroxylase by cyclic GMP-dependent protein kinase. J Neurochem. 48,840-5.

Rubinson, D.A., Dillon, C.P., Kwiatkowski, A.V., Sievers, C., Yang, L., Kopinja, J., Rooney, D.L., Ihrig, M.M., McManus, M.T., Gertler, F.B., Scott, M.L., Van Parijs, L., 2003. A lentivirus-based system to functionally silence genes in primary mammalian cells, stem cells and transgenic mice by RNA interference. Nat Genet. 33,401-6.

Rudel, T., Bokoch, G.M., 1997. Membrane and morphological changes in apoptotic cells regulated by caspase-mediated activation of PAK2. Science. 276,1571-4.

Sabourin, L.A., Tamai, K., Seale, P., Wagner, J., Rudnicki, M.A., 2000. Caspase 3 cleavage of the Ste20-related kinase SLK releases and activates an apoptosis-inducing kinase domain and an actin-disassembling region. Mol Cell Biol. 20,684-96.

Saigoh, K., Wang, Y.L., Suh, J.G., Yamanishi, T., Sakai, Y., Kiyosawa, H., Harada, T., Ichihara, N., Wakana, S., Kikuchi, T., Wada, K., 1999. Intragenic deletion in the gene encoding ubiquitin carboxy-terminal hydrolase in gad mice. Nat Genet. 23,47-51.

Samii, A., Nutt, J.G., Ransom, B.R., 2004. Parkinson's disease. Lancet. 363,1783-93.

Sanchez-Ramos, J., Facca, A., Basit, A., Song, S., 1998. Toxicity of dieldrin for dopaminergic neurons in mesencephalic cultures. Exp Neurol. 150,263-71.

Sanghera, M.K., Manaye, K., McMahon, A., Sonsalla, P.K., German, D.C., 1997. Dopamine transporter mRNA levels are high in midbrain neurons vulnerable to MPTP. Neuroreport. 8,3327-31.

Saporito, M.S., Thomas, B.A., Scott, R.W., 2000. MPTP activates c-Jun NH(2)-terminal kinase (JNK) and its upstream regulatory kinase MKK4 in nigrostriatal neurons in vivo. J Neurochem. 75,1200-8.

Scheid, M.P., Duronio, V., 1998. Dissociation of cytokine-induced phosphorylation of Bad and activation of PKB/akt: involvement of MEK upstream of Bad phosphorylation. Proc Natl Acad Sci U S A. 95,7439-44.

Schiebel, W., Pelissier, T., Riedel, L., Thalmeir, S., Schiebel, R., Kempe, D., Lottspeich, F., Sanger, H.L., Wassenegger, M., 1998. Isolation of an RNA-directed RNA polymerase-specific cDNA clone from tomato. Plant Cell. 10,2087-101.

Schmitz, I., Walczak, H., Krammer, P.H., Peter, M.E., 1999. Differences between CD95 type I and II cells detected with the CD95 ligand. Cell Death Differ. 6,821-2.

Schramke, V., Allshire, R., 2004. Those interfering little RNAs! Silencing and eliminating chromatin. Curr Opin Genet Dev. 14,174-80.

Schulz, J.B., Lindenau, J., Seyfried, J., Dichgans, J., 2000. Glutathione, oxidative stress and neurodegeneration. Eur J Biochem. 267,4904-11.

Schwarz, D.S., Hutvagner, G., Du, T., Xu, Z., Aronin, N., Zamore, P.D., 2003. Asymmetry in the assembly of the RNAi enzyme complex. Cell. 115,199-208.

Schwarz, D.S., Hutvagner, G., Haley, B., Zamore, P.D., 2002. Evidence that siRNAs function as guides, not primers, in the Drosophila and human RNAi pathways. Mol Cell. 10,537-48.

Sebbagh, M., Renvoize, C., Hamelin, J., Riche, N., Bertoglio, J., Breard, J., 2001. Caspase-3-mediated cleavage of ROCK I induces MLC phosphorylation and apoptotic membrane blebbing. Nat Cell Biol. 3,346-52.

Shamoto-Nagai, M., Maruyama, W., Akao, Y., Osawa, T., Tribl, F., Gerlach, M., Zucca, F.A., Zecca, L., Riederer, P., Naoi, M., 2004. Neuromelanin inhibits enzymatic activity of 26S proteasome in human dopaminergic SH-SY5Y cells. J Neural Transm. 111,1253-65.

Sharma, S.K., Ebadi, M., 2003. Metallothionein attenuates 3-morpholinosydnonimine (SIN-1)-induced oxidative stress in dopaminergic neurons. Antioxid Redox Signal. 5,251-64.

Shastry, B.S., 2001. Parkinson disease: etiology, pathogenesis and future of gene therapy. Neurosci Res. 41,5-12.

Shen, J., 2004. Protein kinases linked to the pathogenesis of Parkinson's disease. Neuron. 44,575-7.

Shimura, H., Schlossmacher, M.G., Hattori, N., Frosch, M.P., Trockenbacher, A., Schneider, R., Mizuno, Y., Kosik, K.S., Selkoe, D.J., 2001. Ubiquitination of a new form of alpha-synuclein by parkin from human brain: implications for Parkinson's disease. Science. 293,263-9.

Sidhu, A., Wersinger, C., Vernier, P., 2004. alpha-Synuclein regulation of the dopaminergic transporter: a possible role in the pathogenesis of Parkinson's disease. FEBS Lett. 565,1-5.

Simon, H.H., Bhatt, L., Gherbassi, D., Sgado, P., Alberi, L., 2003. Midbrain dopaminergic neurons: determination of their developmental fate by transcription factors. Ann N Y Acad Sci. 991,36-47.

Singleton, A.B., Farrer, M., Johnson, J., Singleton, A., Hague, S., Kachergus, J., Hulihan, M., Peuralinna, T., Dutra, A., Nussbaum, R., Lincoln, S., Crawley, A., Hanson, M., Maraganore, D., Adler, C., Cookson, M.R., Muenter, M., Baptista, M., Miller, D., Blancato, J., Hardy, J., Gwinn-Hardy, K., 2003. alpha-Synuclein locus triplication causes Parkinson's disease. Science. 302,841.

Sitailo, L.A., Tibudan, S.S., Denning, M.F., 2004. Bax activation and induction of apoptosis in human keratinocytes by the protein kinase C delta catalytic domain. J Invest Dermatol. 123,434-43.

Smith, M.A., Harris, P.L., Sayre, L.M., Perry, G., 1997. Iron accumulation in Alzheimer disease is a source of redox-generated free radicals. Proc Natl Acad Sci U S A. 94,9866-8.

Sofic, E., Paulus, W., Jellinger, K., Riederer, P., Youdim, M.B., 1991. Selective increase of iron in substantia nigra zona compacta of parkinsonian brains. J Neurochem. 56,978-82.

Song, E., Lee, S.K., Wang, J., Ince, N., Ouyang, N., Min, J., Chen, J., Shankar, P., Lieberman, J., 2003. RNA interference targeting Fas protects mice from fulminant hepatitis. Nat Med. 9,347-51.

Souza, J.M., Giasson, B.I., Chen, Q., Lee, V.M., Ischiropoulos, H., 2000. Dityrosine cross-linking promotes formation of stable alpha -synuclein polymers. Implication of

nitrative and oxidative stress in the pathogenesis of neurodegenerative synucleinopathies. J Biol Chem. 275,18344-9.

Speciale, S.G., 2002. MPTP: insights into parkinsonian neurodegeneration. Neurotoxicol Teratol. 24,607-20.

Speciale, S.G., Liang, C.L., Sonsalla, P.K., Edwards, R.H., German, D.C., 1998. The neurotoxin 1-methyl-4-phenylpyridinium is sequestered within neurons that contain the vesicular monoamine transporter. Neuroscience. 84,1177-85.

Spillantini, M.G., Schmidt, M.L., Lee, V.M., Trojanowski, J.Q., Jakes, R., Goedert, M., 1997. Alpha-synuclein in Lewy bodies. Nature. 388,839-40.

Spitaler, M., Cantrell, D.A., 2004. Protein kinase C and beyond. Nat Immunol. 5,785-90.

Srinivasula, S.M., Hegde, R., Saleh, A., Datta, P., Shiozaki, E., Chai, J., Lee, R.A., Robbins, P.D., Fernandes-Alnemri, T., Shi, Y., Alnemri, E.S., 2001. A conserved XIAP-interaction motif in caspase-9 and Smac/DIABLO regulates caspase activity and apoptosis. Nature. 410,112-6.

Stoothoff, W.H., Johnson, G.V., 2005. Tau phosphorylation: physiological and pathological consequences. Biochim Biophys Acta. 1739,280-97.

Storch, A., Ludolph, A.C., Schwarz, J., 2004. Dopamine transporter: involvement in selective dopaminergic neurotoxicity and degeneration. J Neural Transm. 111,1267-86.

Strasser, A., O'Connor, L., Dixit, V.M., 2000. Apoptosis signaling. Annu Rev Biochem. 69,217-45.

Sui, G., Soohoo, C., Affar el, B., Gay, F., Shi, Y., Forrester, W.C., 2002. A DNA vector-based RNAi technology to suppress gene expression in mammalian cells. Proc Natl Acad Sci U S A. 99,5515-20.

Sulzer, D., Bogulavsky, J., Larsen, K.E., Behr, G., Karatekin, E., Kleinman, M.H., Turro, N., Krantz, D., Edwards, R.H., Greene, L.A., Zecca, L., 2000. Neuromelanin biosynthesis is driven by excess cytosolic catecholamines not accumulated by synaptic vesicles. Proc Natl Acad Sci U S A. 97,11869-74.

Susin, S.A., Zamzami, N., Castedo, M., Hirsch, T., Marchetti, P., Macho, A., Daugas, E., Geuskens, M., Kroemer, G., 1996. Bcl-2 inhibits the mitochondrial release of an apoptogenic protease. J Exp Med. 184,1331-41.

Sutherland, C., Alterio, J., Campbell, D.G., Le Bourdelles, B., Mallet, J., Haavik, J., Cohen, P., 1993. Phosphorylation and activation of human tyrosine hydroxylase in vitro by mitogen-activated protein (MAP) kinase and MAP-kinase-activated kinases 1 and 2. Eur J Biochem. 217,715-22.

Takahashi, M., Mukai, H., Toshimori, M., Miyamoto, M., Ono, Y., 1998. Proteolytic activation of PKN by caspase-3 or related protease during apoptosis. Proc Natl Acad Sci U S A. 95,11566-71.

Takahashi, N., Miner, L.L., Sora, I., Ujike, H., Revay, R.S., Kostic, V., Jackson-Lewis, V., Przedborski, S., Uhl, G.R., 1997. VMAT2 knockout mice: heterozygotes display reduced amphetamine-conditioned reward, enhanced amphetamine locomotion, and enhanced MPTP toxicity. Proc Natl Acad Sci U S A. 94,9938-43.

Takeda, K., Matsuzawa, A., Nishitoh, H., Ichijo, H., 2003. Roles of MAPKKK ASK1 in stress-induced cell death. Cell Struct Funct. 28,23-9.

Tanner, C.M., Ben-Shlomo, Y., 1999. Epidemiology of Parkinson's disease. Adv Neurol. 80,153-9.

Tanner, C.M., Chen, B., Wang, W., Peng, M., Liu, Z., Liang, X., Kao, L.C., Gilley, D.W., Goetz, C.G., Schoenberg, B.S., 1989. Environmental factors and Parkinson's disease: a case-control study in China. Neurology. 39,660-4.

Tanner, C.M., Ottman, R., Goldman, S.M., Ellenberg, J., Chan, P., Mayeux, R., Langston, J.W., 1999. Parkinson disease in twins: an etiologic study. Jama. 281,341-6.

Tatton, W.G., Chalmers-Redman, R., Brown, D., Tatton, N., 2003. Apoptosis in Parkinson's disease: signals for neuronal degradation. Ann Neurol. 53 Suppl 3,S61-70; discussion S70-2.

Teruel, M.N., Meyer, T., 2000. Translocation and reversible localization of signaling proteins: a dynamic future for signal transduction. Cell. 103,181-4.

Tofaris, G.K., Razzaq, A., Ghetti, B., Lilley, K.S., Spillantini, M.G., 2003. Ubiquitination of alpha-synuclein in Lewy bodies is a pathological event not associated with impairment of proteasome function. J Biol Chem. 278,44405-11.

Toker, A., 1998. Signaling through protein kinase C. Front Biosci. 3,D1134-47.

Tomiyoshi, G., Horita, Y., Nishita, M., Ohashi, K., Mizuno, K., 2004. Caspase-mediated cleavage and activation of LIM-kinase 1 and its role in apoptotic membrane blebbing. Genes Cells. 9,591-600.

Tong, X., Liu, B., Dong, Y., Sun, Z., 2000. Cleavage of ATM during radiation-induced apoptosis: caspase-3-like apoptotic protease as a candidate. Int J Radiat Biol. 76,1387-95.

Tournier, C., Hess, P., Yang, D.D., Xu, J., Turner, T.K., Nimnual, A., Bar-Sagi, D., Jones, S.N., Flavell, R.A., Davis, R.J., 2000. Requirement of JNK for stress-induced activation of the cytochrome c-mediated death pathway. Science. 288,870-4.

Uhl, G.R., 1998. Hypothesis: the role of dopaminergic transporters in selective vulnerability of cells in Parkinson's disease. Ann Neurol. 43,555-60.

Uhl, G.R., Javitch, J.A., Snyder, S.H., 1985. Normal MPTP binding in parkinsonian substantial nigra: evidence for extraneuronal toxin conversion in human brain. Lancet. 1,956-7.

Ura, S., Masuyama, N., Graves, J.D., Gotoh, Y., 2001. Caspase cleavage of MST1 promotes nuclear translocation and chromatin condensation. Proc Natl Acad Sci U S A. 98,10148-53.

Urano, F., Wang, X., Bertolotti, A., Zhang, Y., Chung, P., Harding, H.P., Ron, D., 2000. Coupling of stress in the ER to activation of JNK protein kinases by transmembrane protein kinase IRE1. Science. 287,664-6.

Valente, E.M., Abou-Sleiman, P.M., Caputo, V., Muqit, M.M., Harvey, K., Gispert, S., Ali, Z., Del Turco, D., Bentivoglio, A.R., Healy, D.G., Albanese, A., Nussbaum, R., Gonzalez-Maldonado, R., Deller, T., Salvi, S., Cortelli, P., Gilks, W.P., Latchman, D.S., Harvey, R.J., Dallapiccola, B., Auburger, G., Wood, N.W., 2004. Hereditary early-onset Parkinson's disease caused by mutations in PINK1. Science. 304,1158-60.

Vander Heiden, M.G., Thompson, C.B., 1999. Bcl-2 proteins: regulators of apoptosis or of mitochondrial homeostasis? Nat Cell Biol. 1,E209-16.

Vila, M., Jackson-Lewis, V., Vukosavic, S., Djaldetti, R., Liberatore, G., Offen, D., Korsmeyer, S.J., Przedborski, S., 2001. Bax ablation prevents dopaminergic neurodegeneration in the 1-methyl- 4-phenyl-1,2,3,6-tetrahydropyridine mouse model of Parkinson's disease. Proc Natl Acad Sci U S A. 98,2837-42.

Vila, M., Przedborski, S., 2003. Targeting programmed cell death in neurodegenerative diseases. Nat Rev Neurosci. 4,365-75.

Vila, M., Przedborski, S., 2004. Genetic clues to the pathogenesis of Parkinson's disease. Nat Med. 10 Suppl,S58-62.

Viswanath, V., Wu, Y., Boonplueang, R., Chen, S., Stevenson, F.F., Yantiri, F., Yang, L., Beal, M.F., Andersen, J.K., 2001. Caspase-9 activation results in downstream caspase-8 activation and bid cleavage in 1-methyl-4-phenyl-1,2,3,6-tetrahydropyridine-induced Parkinson's disease. J Neurosci. 21,9519-28.

Voinnet, O., Vain, P., Angell, S., Baulcombe, D.C., 1998. Systemic spread of sequence-specific transgene RNA degradation in plants is initiated by localized introduction of ectopic promoterless DNA. Cell. 95,177-87.

Vulliet, P.R., Woodgett, J.R., Cohen, P., 1984. Phosphorylation of tyrosine hydroxylase by calmodulin-dependent multiprotein kinase. J Biol Chem. 259,13680-3.

Wagey, R.T., Krieger, C., 1998. Abnormalities of protein kinases in neurodegenerative diseases. Prog Drug Res. 51,133-83.

Wagner, S.R., Greene, F.E., 1978. Dieldrin-induced alterations in biogenic amine content of rat brain. Toxicol Appl Pharmacol. 43,45-55.

Wang, X., 2001. The expanding role of mitochondria in apoptosis. Genes Dev. 15,2922-33.

Wen, L.P., Fahrni, J.A., Troie, S., Guan, J.L., Orth, K., Rosen, G.D., 1997. Cleavage of focal adhesion kinase by caspases during apoptosis. J Biol Chem. 272,26056-61.

Wetsel, W.C., Khan, W.A., Merchenthaler, I., Rivera, H., Halpern, A.E., Phung, H.M., Negro-Vilar, A., Hannun, Y.A., 1992. Tissue and cellular distribution of the extended family of protein kinase C isoenzymes. J Cell Biol. 117,121-33.

Wichmann, T., DeLong, M.R., 2003. Pathophysiology of Parkinson's disease: the MPTP primate model of the human disorder. Ann N Y Acad Sci. 991,199-213.

Widmann, C., Gerwins, P., Johnson, N.L., Jarpe, M.B., Johnson, G.L., 1998. MEK kinase 1, a substrate for DEVD-directed caspases, is involved in genotoxin-induced apoptosis. Mol Cell Biol. 18,2416-29.

Wilms, H., Rosenstiel, P., Sievers, J., Deuschl, G., Zecca, L., Lucius, R., 2003. Activation of microglia by human neuromelanin is NF-kappaB dependent and involves p38 mitogen-activated protein kinase: implications for Parkinson's disease. Faseb J. 17,500-2.

Winston, W.M., Molodowitch, C., Hunter, C.P., 2002. Systemic RNAi in C. elegans requires the putative transmembrane protein SID-1. Science. 295,2456-9.

Wiznerowicz, M., Trono, D., 2003. Conditional suppression of cellular genes: lentivirus vector-mediated drug-inducible RNA interference. J Virol. 77,8957-61.

Xia, H., Mao, Q., Eliason, S.L., Harper, S.Q., Martins, I.H., Orr, H.T., Paulson, H.L., Yang, L., Kotin, R.M., Davidson, B.L., 2004. RNAi suppresses polyglutamine-induced neurodegeneration in a model of spinocerebellar ataxia. Nat Med. 10,816-20.

Xia, X.G., Harding, T., Weller, M., Bieneman, A., Uney, J.B., Schulz, J.B., 2001. Gene transfer of the JNK interacting protein-1 protects dopaminergic neurons in the MPTP model of Parkinson's disease. Proc Natl Acad Sci U S A. 98,10433-8.

Xie, J., Awad, K.S., Guo, Q., 2005. RNAi knockdown of Par-4 inhibits neurosynaptic degeneration in ALS-linked mice. J Neurochem. 92,59-71.

Yamamoto, K., Ichijo, H., Korsmeyer, S.J., 1999. BCL-2 is phosphorylated and inactivated by an ASK1/Jun N-terminal protein kinase pathway normally activated at G(2)/M. Mol Cell Biol. 19,8469-78.

Yang, Y., Kaul, S., Zhang, D., Anantharam, V., Kanthasamy, A.G., 2004. Suppression of caspase-3-dependent proteolytic activation of protein kinase C delta by small interfering RNA prevents MPP+-induced dopaminergic degeneration. Mol Cell Neurosci. 25,406-21.

Yu, J.Y., DeRuiter, S.L., Turner, D.L., 2002. RNA interference by expression of short-interfering RNAs and hairpin RNAs in mammalian cells. Proc Natl Acad Sci U S A. 99,6047-52.

Yuan, J., Yankner, B.A., 2000. Apoptosis in the nervous system. Nature. 407,802-9.

Zamore, P.D., Tuschl, T., Sharp, P.A., Bartel, D.P., 2000. RNAi: double-stranded RNA directs the ATP-dependent cleavage of mRNA at 21 to 23 nucleotide intervals. Cell. 101,25-33.

Zareba, M., Bober, A., Korytowski, W., Zecca, L., Sarna, T., 1995. The effect of a synthetic neuromelanin on yield of free hydroxyl radicals generated in model systems. Biochim Biophys Acta. 1271,343-8.

Zarranz, J.J., Alegre, J., Gomez-Esteban, J.C., Lezcano, E., Ros, R., Ampuero, I., Vidal, L., Hoenicka, J., Rodriguez, O., Atares, B., Llorens, V., Gomez Tortosa, E., del Ser, T., Munoz, D.G., de Yebenes, J.G., 2004. The new mutation, E46K, of alpha-synuclein causes Parkinson and Lewy body dementia. Ann Neurol. 55,164-73.

Zecca, L., Pietra, R., Goj, C., Mecacci, C., Radice, D., Sabbioni, E., 1994. Iron and other metals in neuromelanin, substantia nigra, and putamen of human brain. J Neurochem. 62,1097-101.

Zecca, L., Shima, T., Stroppolo, A., Goj, C., Battiston, G.A., Gerbasi, R., Sarna, T., Swartz, H.M., 1996. Interaction of neuromelanin and iron in substantia nigra and other areas of human brain. Neuroscience. 73,407-15.

Zecca, L., Tampellini, D., Gerlach, M., Riederer, P., Fariello, R.G., Sulzer, D., 2001. Substantia nigra neuromelanin: structure, synthesis, and molecular behaviour. Mol Pathol. 54,414-8.

Zecca, L., Zucca, F.A., Wilms, H., Sulzer, D., 2003. Neuromelanin of the substantia nigra: a neuronal black hole with protective and toxic characteristics. Trends Neurosci. 26,578-80.

Zemskov, E.A., Jana, N.R., Kurosawa, M., Miyazaki, H., Sakamoto, N., Nekooki, M., Nukina, N., 2003. Pro-apoptotic protein kinase C delta is associated with intranuclear inclusions in a transgenic model of Huntington's disease. J Neurochem. 87,395-406.

Zeng, Y., Cullen, B.R., 2003. Sequence requirements for micro RNA processing and function in human cells. Rna. 9,112-23.

Zeng, Y., Yi, R., Cullen, B.R., 2003. MicroRNAs and small interfering RNAs can inhibit mRNA expression by similar mechanisms. Proc Natl Acad Sci U S A. 100,9779-84.

Zhang, Y., Gao, J., Chung, K.K., Huang, H., Dawson, V.L., Dawson, T.M., 2000. Parkin functions as an E2-dependent ubiquitin- protein ligase and promotes the degradation of the synaptic vesicle-associated protein, CDCrel-1. Proc Natl Acad Sci U S A. 97,13354-9.

Zecca, L., Pietra, R., Goj, C., Mecacci, C., Radice, D., Sabbioni, E., 1994. Iron and other metals in neuromelanin, substantia nigra, and putamen of human brain. J Neurochem. 62,1097-101.

Zecca, L., Shima, T., Stroppolo, A., Goj, C., Battiston, G.A., Gerbasi, R., Sarna, T., Swartz, H.M., 1996. Interaction of neuromelanin and iron in substantia nigra and other areas of human brain. Neuroscience. 73,407-15.

Zecca, L., Tampellini, D., Gerlach, M., Riederer, P., Fariello, R.G., Sulzer, D., 2001. Substantia nigra neuromelanin: structure, synthesis, and molecular behaviour. Mol Pathol. 54,414-8.

Zecca, L., Zucca, F.A., Wilms, H., Sulzer, D., 2003. Neuromelanin of the substantia nigra: a neuronal black hole with protective and toxic characteristics. Trends Neurosci. 26,578-80.

Zemskov, E.A., Jana, N.R., Kurosawa, M., Miyazaki, H., Sakamoto, N., Nekooki, M., Nukina, N., 2003. Pro-apoptotic protein kinase C delta is associated with intranuclear inclusions in a transgenic model of Huntington's disease. J Neurochem. 87,395-406.

Zeng, Y., Cullen, B.R., 2003. Sequence requirements for micro RNA processing and function in human cells. Rna. 9,112-23.

Zeng, Y., Yi, R., Cullen, B.R., 2003. MicroRNAs and small interfering RNAs can inhibit mRNA expression by similar mechanisms. Proc Natl Acad Sci U S A. 100,9779-84.

Zhang, Y., Gao, J., Chung, K.K., Huang, H., Dawson, V.L., Dawson, T.M., 2000. Parkin functions as an E2-dependent ubiquitin- protein ligase and promotes the degradation of the synaptic vesicle-associated protein, CDCrel-1. Proc Natl Acad Sci U S A. 97,13354-9.

Zimprich, A., Biskup, S., Leitner, P., Lichtner, P., Farrer, M., Lincoln, S., Kachergus, J., Hulihan, M., Uitti, R.J., Calne, D.B., Stoessl, A.J., Pfeiffer, R.F., Patenge, N., Carbajal, I.C., Vieregge, P., Asmus, F., Muller-Myhsok, B., Dickson, D.W., Meitinger, T., Strom, T.M., Wszolek, Z.K., Gasser, T., 2004. Mutations in LRRK2 cause autosomal-dominant parkinsonism with pleomorphic pathology. Neuron. 44,601-7.

ACKNOWLEDGEMENTS

I would like to sincerely thank my major professor/advisor Professor Anumantha G. Kanthasamy for providing me a great opportunity in the Iowa State University to pursue my Ph.D. degree and for giving me many important advices throughout my graduate study period. With these advices, I could always keep my research on the right track and have fruitful output in my research. The research experience I had in his laboratory will certainly be influential and help me pave my research path in the future. I would also like to thank my co-major professor/advisor Professor Kristen Johansen, who always gives valuable suggestions about my research. I also want to thank my POS committee members: Drs. Donald S. Sakaguchi, Richard J. Martin, Susan Carpenter for their comments and supports, especially I want to thank Professor Susan Carpenter for providing some Rev constructs and giving valuable inputs about my research in the regulation of nuclear localization of PKCδ.

I would like to acknowledge Drs. Vellareddy Anantharam, Arthi Kanthasamy, Calivarathan Latchoumycandane for their contribution to my research work, and my fellow graduate students Drs. Masashi Kitazawa, Siddarth Kaul, Lalitha Madhaven, and Faneng Sun, Christopher Choi, Huajun Jin, Saminathan Hariharan, and Danhui Zhang, Qi Xu, and rotation students Ruth Wagner, Carlie Peck, Tim Alcon, Kim Petry, Yi Zhang.

I would like to thank DNA sequencing and synthesis facility, Gene chip facility, protein facility, hybridoma facility, and especially Margie Carter from Confocal microscopy facility for her help in the live cell imaging.

I would like to appreciate all BMS staffs, Kim M. Adams, Linda Erickson, Cheryl R. Ervin and William B. Robertson, and coordinator of interdepartmental genetics and

neuroscience programs, Linda M. Wild and Kathryn B. Andre for all the paper work and other help.

Finally, I dedicate my dissertation to my parents, my wife and daughter for their support and understanding. It would certainly have been a harder journey for me to reach this point without their support.